NASA Contractor Report CR 191066

BROAD SPECIFICATION FUELS COMBUSTION TECHNOLOGY PROGRAM - PHASE II

Final Report

R. P:. Lohmann, R. A. Jeroszko, and J. B. Kennedy
Commercial Engine Business
Pratt & Whitney
East Hartford, Conn. 06108

October 1990

Prepared for
Lewis Research Center
Under Contract NAS3–23269

National Aeronautics and
Space Administration

FOREWORD

This report presents the results of an experimental evaluation conducted to assess the potential of using advanced technology combustor concepts to facilitate operation on broadened properties fuels. The program was conducted as Phase II of the Broad Specification Fuels combustion Technology Program under Contract NAS3-23269.

The NASA Project Manager for this contract was Mr. James S. Fear of the Aerothermodynamics and Fuels Division, Lewis Research Center, Cleveland, Ohio, and the Pratt & Whitney Program Manager was Dr. Robert P.Lohmann. The principal investigators were Dr. Lohmann and Mr. Ronald A. Jeroszko at Pratt & Whitney while Mr. Jan B. Kennedy was principal investigator in the parts of the program conducted at United Technologies Research Center.

TABLE OF CONTENTS

TABLE OF CONTENTS (Continued)

SECTION 1.0

SUMMARY

This report presents the results of Phase II of the Broad Specification Fuels Combustion Technology program. The objective of the overall program was to identify and evolve the combustor technology required to accommodate the use of broadened properties fuels in current and future high bypass ratio engines for Conventional Takeoff and Landing (CTOL) aircraft. The specific objective of the Phase II program was to evolve two advanced technology combustor concepts that had been identified in Phase I of the program as offering the potential of operation with broadened properties fuels while meeting exhaust emissions and performance specifications and maintaining acceptable durability characteristics.

The target broadened properties fuel for this program was Experimental Referee Broad Specification fuel, hereafter referred to by the acronym ERBS. This fuel had a hydrogen content of 12.93 percent as opposed to a nominal level of about 13.7 percent in Jet. A. The program goals had been stipulated for a combustor operating on ERBS fuel and included durability and operational characteristics consistent with the reference PW2037 engine combustor when it was operated on Jet A fuel. Further goals included aggressive levels of control of the combustor exit temperature distribution, section pressure loss and combustion efficiency as well as compliance with the then proposed 1984 Environmental Protection Agency standards for emissions and smoke output.

At the conclusion of Phase I, the evaluation of the staged Vorbix combustor; which had been evolved under the NASA/P&W Experimental Clean Combustor and Energy Efficient Engine programs; and the variable geometry combustor were found to provide a degree of flexibility in combustion stoichiometry that offered fundamental advantages in accommodating the use of broadened property fuels. For this reason, variations of these combustor concepts were selected for evaluation in Phase II. While not addressed specifically in the Phase I program, consideration of the use of broadened properties fuels leads to concern over deterioration in thermal stability with increased propensity for carbon deposition in fuel injectors and their supports. The use of duplex and staged fuel system in which parts of the system are not operational at low power levels are of particular concern because of the risk of thermal decomposition of stagnant fuel in the absence of the convective cooling produced by flowing fuel. This situation is avoided in the production PW2037 combustor by incorporating "single pipe" aerating fuel injectors that are operational at all power levels. The variable geometry combustor concept evaluated in Phase II was based on the production PW2037 combustor; including the aerating fuel system; and incorporated externally actuated valves on the front end that varied the quantity of air entering the primary combustion zone. The second advanced technology combustor evaluated in Phase II was an outgrowth of the Vorbix combustor. Designated the Mark IV, this configuration simplified the fuel and air staging of the basic Vorbix combustor while exploiting the same aerothermal concepts. In particular it employed a unique fuel system approach that was intended to achieve the dual combustion zone features of a staged combustor while employing a single pipe fuel injection system.

To accomplish the objectives of the program a reference PW2037 combustor and twenty configurations of the two advanced technology combustor concepts were tested in a rig that incorporated rectangular representations of the appropriate full annular combustor. The critical tests were conducted in a facility capable of providing nonvitiated air at temperatures and combustor inlet Mach numbers consistent with all engine power levels. Engine pressure levels were maintained at all power levels through cruise but were diminished slightly at higher power levels - the reduction being only fifteen percent at simulated takeoff. The fuel for the majority of these tests was ERBS but selected configurations were also evaluated with Jet A and two fuels of lower hydrogen content.

The results of the evaluation of the production PW2037 combustor indicated it was capable of meeting the program goals for emissions of unburned hydrocarbons and carbon monoxide by wide margins with ERBS fuel. The combustor was not designed to meet the program goals for emissions of oxides of nitrogen and in addition, a modest increase of the order of three to five percent, must be anticipated in these emissions if ERBS were substituted for Jet A fuel. The combustor was also demonstrated to marginally meet the program goal for smoke output when operating on ERBS fuel. While the combustor exit temperature distribution of the tested configuration would need additional refinement to meet the program goals, the temperature distribution was shown to be essentially independent of fuel composition. The lean stability characteristics of the PW2037 combustor were not affected adversely by the use of ERBS rather than Jet A. Increased liner temperatures, caused by increased radiant heat load, are an obstacle in accommodating broadened properties fuels. Reductions in liner life of up to 15 percent are projected with the use of ERBS rather than Jet A fuel in the PW2037 combustor on the basis of the liner temperature increments measured in this test.

The evaluation of the variable geometry combustor indicated this concept had the functional capability to shift 30 percent of the combustor air between the primary zone and cooling and intermediate/dilution air apertures in the liner. The combustor exhibited only moderate sensitivity to fuel composition and properties. Over the range of test fuels evaluated the emissions and smoke output and liner temperatures increased moderately with decreasing fuel hydrogen content while there was some evidence that fuel viscosity and volatility was influencing the lean stability characteristics. Fuel composition had no significant effect on the combustor exit temperature distribution. The variable geometry combustor met or exceeded the program goals for section pressure loss, lean stability and combustion efficiency at all power levels above idle. The emissions and smoke output of the variable geometry combustor were generally deficient relative to the program goals but the concept had been subject to a very limited extent of development and its full potential could not be achieved in a program of this scope. However, the fundamental process causing these deficiencies was identified. The variable airflow entered the primary combustion zone through swirlers concentric with the fuel injectors and the control of mixing between these airstreams was the controlling factor. Strong intermixing was required at high power levels while mixing had to be suppressed at low power. The

evaluation of a pair of combustor configurations incorporating features that would induce an extreme of intermixing in each configuration indicated that conceptual refinement of the variable geometry combustor to accomplish this mixing control would offer significant improvements in performance and emissions relative to the program goals. While still somewhat deficient in emissions at idle, this long range variable geometry combustor was projected to meet program goals for combustion efficiency above idle, smoke, lean stability and potential for reduction of oxides of nitrogen while operating on ERBS fuel. Substantial reductions in liner metal temperatures were demonstrated relative to the reference PW2037 combustor. These reductions in liner temperature would more than offset the increments associated with a Jet A to ERBS fuel transition.

The evolution of the Mark IV combustor concept was a process of refinement and optimization of the aerothermal features while the performance improved toward the program goals. At the highest level of maturity achieved in the program the combustor met the program goal for emissions of carbon monoxide when operating on Jet A fuel but became deficient when ERBS fuel was introduced. The unburned hydrocarbon emissions were consistently high at idle, exceeding the program goal by a factor of three and precluding satisfying the program goal of 99 percent combustion efficiency. However, the goal for lean combustion stability at idle was marginally achieved with both Jet A and ERBS fuel.

At high power levels the combustion efficiency goal was exceeded but the performance was not indicative of the intended dual zone mode of combustion. Emissions of oxides of nitrogen and smoke, while demonstrating declines with increasing fuel hydrogen content, were high relative to both the expectations for this concept and the program goals. The liner temperature exhibited only moderate sensitivity to fuel composition but the location and intensity of the peak temperature of the liner varied considerably between configurations implying a strong convective heat transfer mode. The combustor exit temperature distribution also implied that combustion was being restricted to areas close to the liners. Based on these observations it was evident that the fundamental concept of using a single pipe fuel system to produce a staged fuel injection effect was not being achieved. While several variations of the single pipe fuel system were evaluated it became evident that the production of injectors with the desired spray variation characteristics would in itself require an extensive development effort beyond the scope of this program. Consequently, the final configurations evaluated were directed at demonstrating the long range potential of the Mark IV combustor. Since the single pipe fuel system as conceived at the time was incapable of supplying fuel to both the pilot and secondary zones from a single source, a staged fuel system was employed to provide this distribution artificially. When operated in this mode the high power performance was enhanced significantly with the combustor exit temperature distribution near the target and the program goals for smoke and NOx emissions being achieved.

At the conclusion of the program it was evident that both the variable geometry and the Mark IV combustor concepts had been demonstrated as having the potential of accommodating the use of broadened properties fuels while achieving the program goals for emissions, durability and operability. However, both of these advanced technology combustors require refinement at the conceptual level and substantial additional development to evolve them to technical maturity.

SECTION 2.0

TECHNICAL BACKGROUND

2.1 INTRODUCTION

Escalating fuel costs have severely impacted the economics of both commercial and military aircraft operations. The problem has been compounded by a reduction in the quantity of high quality petroleum crude available to produce aviation fuels to current specification. One method of alleviating fuel cost and availability concerns is to modify these specifications to allow the use of lower quality fuels. Another alternative is to accelerate production of synthetic fuels from shale or coal-derived feed stocks to reduce our dependence on uncertain foreign sources and maintain stable fuel prices. However, either of these approaches could lead to variations in the chemical composition and physical properties of the fuel which would have adverse impacts on the operation and maintainability of aircraft engines. Intelligent selection of fuels for the aircraft of the future will require careful cost/benefit analysis which recognizes not only fuel cost and availability but also the impact of increased engine maintenance costs and the expense of developing technology to accommodate the new fuels.

As early as 1974, the National Aeronautics and Space Administration (NASA) recognized this situation and initiated programs to evaluate the effects of changes in fuel composition on the performance, emissions and overall design and operation of aircraft gas turbine combustors. This effort included both in-house investigations and contracted studies such as the Alternate Fuels Addendums to the Experimental Clean Combustor Program (References 1 and 2). This initial evaluation indicated that relaxing the fuel specification to permit higher aromatic levels or lower hydrogen content would have significant impacts on gas turbine combustion systems.

At the time, it seemed most appropriate to coordinate the efforts to evolve fuel-related combustor technology by concentrating on the implications of a single fixed broadened properties fuel. The Jet Aircraft Hydrocarbon Fuels Technology Workshop, convened at NASA-Lewis Research Center in June 1977, provided the basis for identifying this particular fuel (Reference 3). The attendees, including representatives of the petroleum industry, engine and airframe manufacturers, airlines, the military, and NASA, reviewed the experience to date and arrived at a tentative specification for Experimental Referee Broad Specification Fuel, hereafter referred to by the acronym ERBS.

Under Contract NAS3-20802 (Reference 4), Pratt & Whitney conducted a design study to assess the impact of the use of ERBS specification fuel on combustors for current and advanced gas turbine engines for commercial aircraft. This design study identified specific areas where new technology would have to be developed and substantiated to produce combustion systems capable of operating on ERBS specification fuel without compromising the environmental acceptability, performance, durability or reliability of the combustor. The Broad Specification Fuels Combustion Technology Program is directed at this specific objective.

2.2 ERBS FUEL COMPOSITION

In Table 2-1, the specification for ERBS fuel is compared to the specification for Jet A, the fuel currently used for the majority of commercial aircraft operations in the United States. Specifications of this type stipulate only allowable limits on the composition of the fuel. The method of defining these limits differs, most notably in the means of limiting the fractions of aromatics and complex aromatics. The Jet A specification stipulates specific limits on the concentration of these constituents while the ERBS specification uses the hydrogen content of the fuel as the controlling parameter. Hydrogen content provides a characterization of the hydrocarbon composition of the fuel. Since the aromatic compounds have a high ratio of carbon to hydrogen atoms, increasing the aromatic content reduces the hydrogen content. The hydrogen content stipulated in the ERBS specification would permit the aromatic content to be in the range of 30 to 35 percent.

TABLE 2-1

COMPARISON OF SPECIFICATIONS FOR JET A AND ERBS FUEL

	ASTM D 1655 JET A	ERBS
Aromatic Content - % vol	20 max	Report
Hydrogen Content - % wt	--	12.8 ±0.2
Sulphur Mercaptan - % wt	0.003 max	0.003
Sulphur Total - % wt	0.3 max	0.3 max
Nitrogen Total - % wt	--	Report
Naphthalene Content - % vol	3.0 max	Report
Hydrocarbon Compositional Analysis	--	Report
Distillation Temperature - °K (°F)		
Initial Boil Point	--	Report
10 Percent	477 (400) max	477 (400) max
50 Percent	505 (450) max	Report
90 Percent	--	534 (500) min
Final Boil Point	561 (550) max	Report
Residue - % vol	1.5 max	Report
Loss - % vol	1.5 max	Report
Flashpoint - °K (°F)	316 (110) min	316 (110) min
API Gravity	--	Report
Freezing Point - °K (°F)	233 (-40) max	244 (-20) max
Maximum Viscosity - cs	8 @ 253°K (-4°F)	12 @ 249°K (-10°F)
Specific Gravity	0.7753 to 0.8299	Report
Heat of Combustion - MJ/kg (BTU/lb)	42.8 (18,400) min	Report
Thermal Stability:		
JFTOT Breakpoint		
Temperature - °K (°F)	533 (500) min	511 (460) min
Method	Visual Code 3 ΔP = 12	TDR = 13. ΔP = 25

The lower hydrogen content of ERBS fuel is also reflected in the distillation temperature distribution where the high end of the distillation range occurs at higher temperature levels. The decrease in hydrogen content also necessitates an increase in freezing point relative to Jet A -- a factor that affects both fuel storage and pumpability during ground operations and on long duration high altitude flights. The proximity of the fuel temperature to the freezing point has a strong influence on viscosity and deteriorated fuel atomization could compromise cold engine starting. Consequently, both specifications also include a limit on low temperature fuel viscosity. The differences in the maximum allowable breakpoint temperature imply that the thermal stability of ERBS fuel will be poorer than that of Jet A.

These changes in the chemical composition and physical properties of the fuel are expected to have significant impacts on the design and operation of combustors for aircraft gas turbine engines. These impacts are characteristic of all reduced hydrogen content broadened property fuels and include:

- Increased flame luminosity resulting in higher radiant heat transfer to the combustor liner, which will shorten liner life.

- Increased carbon monoxide and unburned hydrocarbon emissions output at low power levels because of poorer fuel atomization and more complex fuel chemistry.

- Increased smoke production and NO_x emissions because of the more complex fuel chemistry.

- More difficult cold starting and altitude relight because of increased fuel viscosity and, in the case of some fuels, reduced volatility. These factors could also impair combustion stability.

- Greater propensity toward carbon deposition on liners, and fuel injector plugging and streaking because of the reduced thermal stability of the fuel.

Under the Broad Specification Fuels Combustion Technology Program, the magnitude of these concerns with use of ERBS fuel rather than Jet A have been investigated. A major effort has been made to define the technology required to resolve these problems with minimal impact on the acceptability of the engine.

2.3 PROGRAM OBJECTIVES AND STRUCTURE

The overall objective of the Broad Specification Fuels Combustion Technology Program has been to identify and conceptually demonstrate the technology required to use broadened properties fuels in current and future high bypass ratio engines for commercial aircraft. Combustor design concepts have been identified which minimize the impact of Experimental Referee Broad Specification (ERBS) fuel on the emissions, performance, durability and operating characteristics of these engines. The data accumulated under this program will provide valuable input to the cost/benefit analysis of broadened properties fuels.

The program was conducted in two phases, both of which involved systematic rig testing of various combustor concepts. Phase I, the results of which are reported in References 5, 6 and 7, consisted of a screening of three different combustor concepts selected to be representative of a wide range of technology from current in-service burners through substantially more advanced configurations with the objective of establishing the potential of each for achieving the program goals. In Phase II, which is the subject of this report, additional combustor rig tests were conducted on two combustor concepts with the objective of refining, optimizing and combining the design features of the most promising concepts identified in Phase I and other advanced combustor technology programs.

A total of thirty-nine combustor configurations were evaluated during the overall program, eighteen in Phase I and twenty-one in Phase II. All configurations were tested on a single lot of fuel meeting the ERBS specification of Table 2-1 and the majority were also evaluated with ASTM specification Jet A fuel. Selected configurations were also evaluated while operating on fuels having even lower hydrogen, or equivalent, higher aromatic content than the ERBS specification to provide a more comprehensive evaluation of the sensitivity to fuel composition.

The three basic combustor concepts selected for evaluation in Phase I consisted of a single stage combustor, representative of current in service technology, a staged Vorbix combustor and a variable geometry combustor. The JT9D-7 was selected as the reference engine for the Phase I program and the single stage production combustor in this engine was selected as the first combustor concept. This selection allowed some of the less complex technological advances, such as fuel injectors with improved atomization and enhanced liner cooling approaches, to be evaluated as a means of accommodating broadened properties fuels. The selection also allowed program results to be compared to in-service engine experience.

The Vorbix combustor was selected as the initial advanced technology combustor concept for evaluation in the Phase I program. This combustor was evolved and demonstrated under the NASA/Pratt & Whitney Aircraft Experimental Clean Combustor Program (References 8, 9 and 10). More recently, a second generation or improved version of this concept was designed and developed under the NASA/Pratt & Whitney Aircraft Energy Efficient Engine Program (References 11 and 12). The Vorbix burner is a staged system with two distinct combustion zones, each serviced by an independent fuel injection system. By operating the combustor on only one zone at low power levels and both zones at high power, the combustor may be optimized at two operating conditions, rather than a single condition. Use of a rich mixture strength in the low power stage produces low carbon monoxide and unburned hydrocarbon emissions at idle. When the two stages are used in combination, a low equivalence ratio can be maintained at high power to minimize NO_x and smoke output. This type of stoichiometry control appears useful in circumventing some of the problems associated with broadened properties fuel. For example, rich primary zone stoichiometry at low power could offset potential deterioration in ignition capability while lean combustion at high power levels could reduce the radiant heat load on the burner liners.

A variable geometry combustor was selected as the third concept for evaluation in Phase I. Studies (References 13 and 14) have indicated that variable geometry combustors, in which moveable gaspath components shift the airflow distribution with operating condition to achieve optimum stoichiometry at all power levels, offer significant advantages in meeting performance and emissions requirements. As in the staged combustor concept, the enhanced control of stoichiometry could be used to advantage in accommodating broadened properties fuels. Because the tests conducted under Phase I were of a screening nature, the test combustor did not incorporate the complexity of mechanically variable air admission apertures. Rather, pairs or sequences of fixed geometry configurations representative of the extremes of airflow distribution in the combustor were tested and the performance of the equivalent variable geometry combustor was synthesized from the composite test results.

At the conclusion of Phase I, it appeared that areas of technology had been identified that could be pursued to adapt the single stage combustor concept to the use of ERBS fuel. These include primarily the evolution of improved fuel injectors offering better atomization of more viscous broadened specification fuels and improved liner cooling approaches to accommodate the higher radiant head loads. However, significant development efforts that would be unique to the particular engine configuration or model would be required to mature this technology. Conversely, the evaluation of the advanced technology staged Vorbix and variable geometry combustors indicated that these concepts, through their ability to provide a degree of flexibility in combustion stoichiometry, offered more extensive and technically more fundamental advantages in accommodating the use of broadened properties fuels. For this reason, variations of these combustors were selected for evaluation in Phase II.

While the JT9D-7 engine served as the reference engine for Phase I of the Broad Specification Fuels Combustion Technology Program, the PW2037 engine was selected as the reference engine for Phase II. The PW2037 is the first of a new generation of advanced technology turbofan engines being developed at Pratt and Whitney. This change in reference engine was made because the two combustor concepts identified above represent advanced technology approaches that are more likely to find application in future engines, such as the PW2037 and its derivatives, than in retrofit to older engine models.

Relative to their counterparts in Phase I, both of the combustors evaluated in this phase incorporated more advanced features. The variable geometry combustor was based on the production PW2037 single stage combustor and incorporated externally actuatable valves on the front end that could vary the quantity of air entering the primary combustion zone.

For several years prior to the initiation of Phase II, Pratt and Whitney had been investigating a new advanced combustor concept (References 15 and 16) that is an outgrowth of the Vorbix combustor evolved under the NASA/PWA Experimental Clean Combustor and Energy Efficient Engine programs. This combustor, designated the Mark IV, simplifies the physical arrangement of the fuel and air staging of the basic Vorbix concept while incorporating features that enhance hot section durability and reduce combustor section pressure loss to improve specific fuel consumption. Since the Mark IV, a logical

outgrowth of the Vorbix combustor evaluated in Phase I, was sufficiently mature in concept and offered unique features consistent with minimizing sensitivity to fuel composition, it was incorporated as the second combustor concept in the Phase II program.

2.4 PROGRAM GOALS

The objective of the Broad Specification Fuels Combustion Technology Program has been to identify and evolve the technology required to operate current and advanced commercial aircraft engines on broadened properties fuels with minimal impact on the performance, emissions, durability and operating characteristics of the engines. To provide guidelines for this program, goals were established for both combustor performance and emissions.

2.4.1 Performance Goals

The following performance goals were established for the combustors when operating on Experimental Referee Broad Specification fuel:

- Combustion efficiency of 99 percent, as defined by emissions measurements, at all operating conditions.
- Combustor section total pressure loss of no more than 6 percent at sea level takeoff with a preference for the lower section loss of the current PW2037 engine.
- Combustor exit temperature pattern factor of 0.25.
- Combustor exit average radial temperature profile consistent with turbine design requirements.
- Liner metal temperatures comparable to those currently obtained with Jet A fuel to maintain liner life.
- Altitude relight and cold starting capability consistent with engine specifications.

2.4.2 Emissions Goals

The emissions goals for the program are those which had been advanced by the Environmental Protection Agency for Class T-2 aircraft engines with thrust levels in excess of 90 kilonewtons (Reference 17) at the time the program was formulated. Using the pressure ratio of the PW2037 engine cycle, these goals are listed in Table 2-2 in terms of the Environmental Protection Agency parameter, which is defined by weighting the emissions indices over the landing and takeoff cycle of Reference 17.

TABLE 2-2

EMISSIONS GOALS FOR COMBUSTORS IN THE PW2037 ENGINE

	Engines Manufactured after January 1, 1981*	Engines Manufactured after January 1, 1984	Engines Certified after January 1, 1984
EPA Parameter (kg/kN)			
Carbon Monoxide	36.1	36.1	25.0
Unburned Hydrocarbon	6.7	6.7	3.3
Oxides of Nitrogen	--	33.1	33.1
Maximum SAE Smoke Number	21	21	21

*Compliance date extended to January 1, 1983

In establishing appropriate goals from these proposed standards, it was evident that combustor concepts or technology evolved from this program would be sufficiently different from the current PW2037 combustor to require recertification. Consequently, the engine would be subject to the requirements on engines certified in the post 1984 time period and the more stringent carbon monoxide and unburned hydrocarbon emissions standards as well as that for oxides of nitrogen would be applicable.

SECTION 3.0

REFERENCE ENGINE AND COMBUSTOR

While the JT9D-7 engine served as the reference engine for Phase I of the Broad Specification Fuels Combustion Technology Program, the PW2037 engine was selected as the reference engine for Phase II of the program. The PW2037 is the first of a new generation of advanced technology turbofan engines that will meet the requirements of a wide spectrum of commercial and military aircraft into the next century. The selection of this engine over the JT9D-7 as a reference for the remainder of the program was motivated by consideration of the technology level of the two combustor concepts that were selected for evaluation under Phase II. Both of these concepts represent advanced technology approaches that are more likely to find application in future engines rather than in retrofit into older existing engines such as the JT9D. This section contains a brief description of the PW2037 engine and detailed information on the mechanical design, performance, and emissions characteristics of the combustor.

3.1 REFERENCE ENGINE DESCRIPTION

The PW2037 is a 37,000 pound thrust, second generation high bypass ratio turbofan engine designed to power modern short to medium range transport aircraft. This engine design evolved from high-bypass-ratio engine technology development programs conducted by Pratt & Whitney Aircraft since 1964 and from the knowledge gained from millions of hours of operating experience with the JT9D engine, the first-generation high bypass-ratio turbofan engine. The initial application of the PW2037 engine was in the Boeing 757 aircraft. Growth versions are being developed for the U.S. Air Force C-17 transport and other potential applications.

Figure 3-1 shows a cross-section of the PW2037 which is a twin-spool, five bearing, axial flow, high bypass-ratio turbofan engine. It incorporates multistage compressors and a fan driven by a multistage reaction turbine designed for operation with fixed area nozzles for primary and fan discharge. The engine employs a single-stage fan while the low-pressure compressor consists of four compression stages. The high-pressure compressor is a twelve-stage compression system with the nine central stages formed on a drum rotor. Bolted to this drum are a disk for the front stage and two disks for the rear stages. Variable geometry is provided in the first five high-pressure compressor stages. A two-stage high-pressure turbine and a five-stage low-pressure turbine are employed. The engine is designed with a fan case mounted accessory drive gearbox. Power is extracted from the high-pressure rotor and transmitted through a tower shaft to the gearbox which provides drive pads for airframe accessories including a starter, an electrical generator, and fluid power pumps.

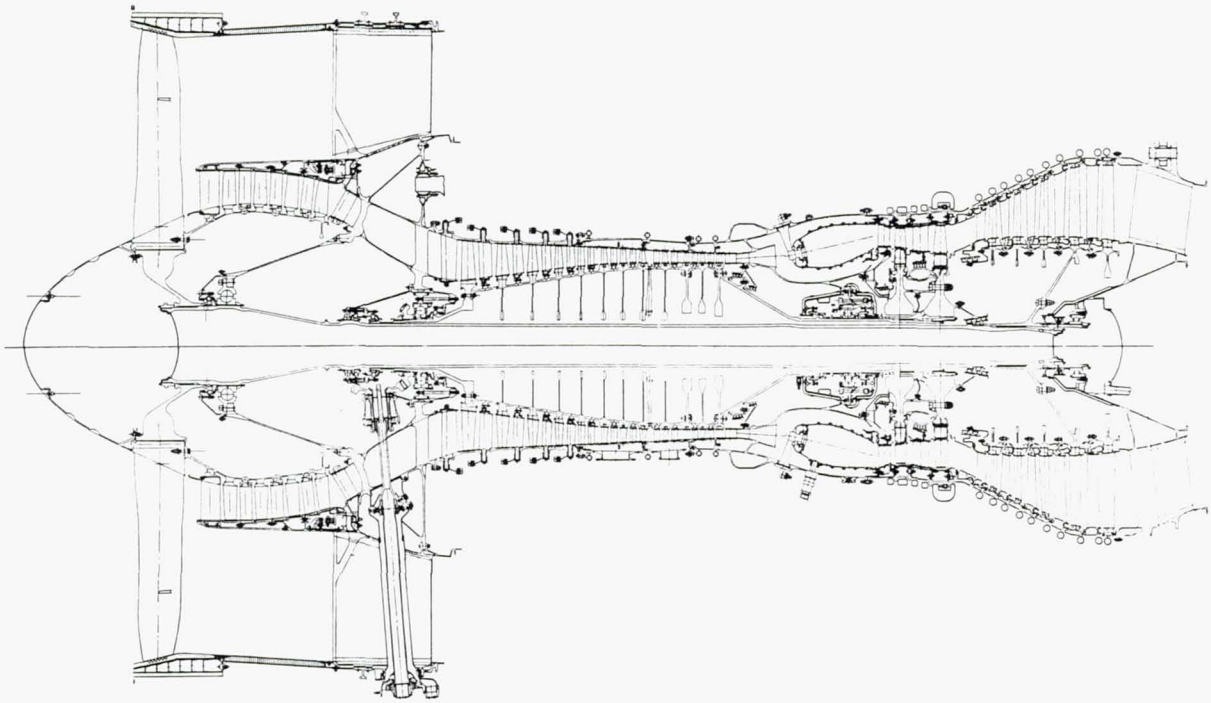

Figure 3-1 Cross Section of the PW2037 Reference Engine.

3.2 REFERENCE COMBUSTOR DESCRIPTION

The combustor in the PW2037 engine also incorporates several unique advanced technology concepts that enhance its durability, operability and performance, relative to the combustors in prior generation engines. Figure 3-2 shows the overall mechanical design of this combustor which is annular with an overall length between the trailing edge of the compressor exit guide vane and the leading edge of the turbine inlet guide vane of 439 mm (17.3 inches). The burning length between the fuel nozzle face and the turbine inlet guide vane leading edge is 229 mm (9 inches). The diffuser section is unique in that 24 struts span the prediffuser. These struts are equal in number to and spaced circumferential between the fuel injectors. This permits the walls of the diffuser to diverge further to enhance airflow feed to the burner shrouds. The burner liner is a single assembly retained by mount pins penetrating the hood with thermal expansion accommodated by slip joints at the downstream end of the liner. The liners are film cooled using an advanced rolled ring louver construction. Relative to conventional sheet metal louvered liners the rolled ring construction offers enhanced structural integrity and more effective film cooling of the liner surfaces.

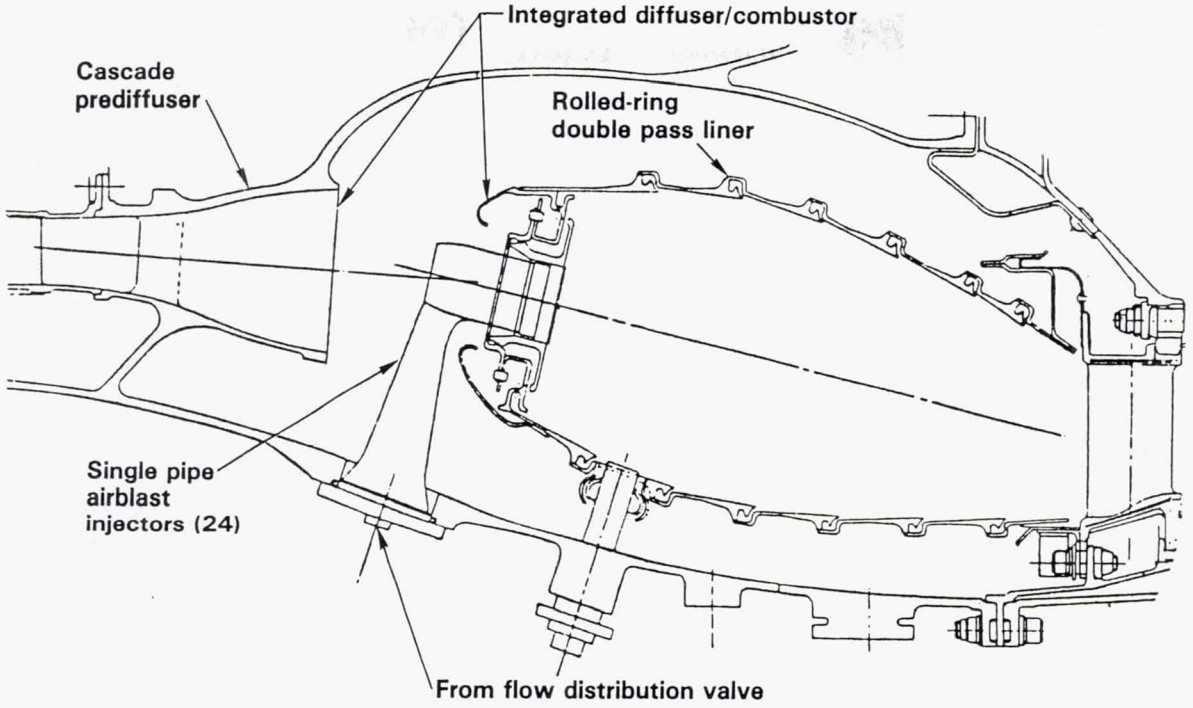

Figure 3-2 Cross Section of PW2037 Combustor.

The combustor incorporates twenty-four single pipe airblast fuel injectors that are externally removable from the engine case. Figure 3-3 shows a cross-section of one of these injectors in which a film of fuel is emitted from an annular orifice and atomized by the concentric swirling airstreams passing through the center of the injector and through the outer air cap. The use of external air rather than hydraulic pressure within the injector to provide the atomization function leads to a much simpler fuel injector configuration. With the metering of the fuel flow occurring in an external distribution valve rather than in the injector proper, small metering passages; that are susceptible to plugging; are eliminated. The single pipe supply system eliminates the risk of carbon deposition in inactive secondary fuel passages at low fuel flow conditions. In combination with effective heatshielding to thermally isolate the fuel passages from the hot compressor discharge air, the single pipe fuel system offers a decided advantage when operating on broadened properties fuels with lower thermal stability.

3.3 REFERENCE COMBUSTOR PERFORMANCE

Table 3-1 lists the critical operating parameters for the PW2037 combustor at the four sea level static conditions of the Environmental Protection Agency landing and takeoff cycle and the maximum cruise aerodynamic design point of the engine. the idle condition is at 7.0 percent of the takeoff thrust. Other critical design parameters for the combustor at the sea level takeoff condition are:

Compressor Exit Axial Mach Number	0.24
Combustor Reference Velocity m/sec (ft/sec)	21.3 (70)
Combustor Section Total Pressure Loss - %	4.2
Combustor Exit Temperature Pattern Factor	0.37

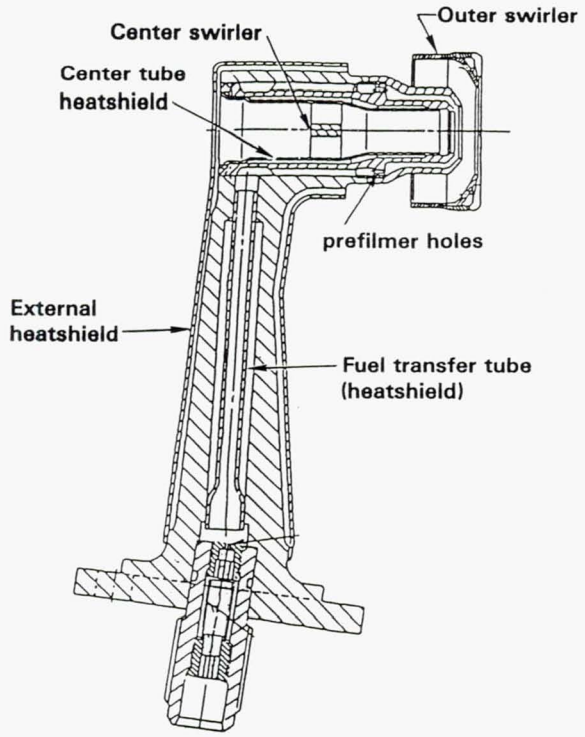

Figure 3-3 Cross Section of PW2037 Fuel Injector.

TABLE 3-1

PW2037 ENGINE COMBUSTOR OPERATING PARAMETERS

Operating Condition	Inlet Total Pressure MPa (psia)	Inlet Total Temperature °K (°F)	Combustor Airflow kg/sec (lb/sec)	Combustor Fuel/Air Ratio
Ground Idle (6.37% Thrust)	0.425 (61.8)	475 (396)	13.63 (30.0)	0.0096
Approach (30% Thrust)	1.076 (156.4)	607 (633)	30.27 (66.6)	0.0134
Climb (85% Thrust)	2.370 (344.3)	758 (905)	56.68 (124.7)	0.0219
Sea Level Takeoff (100% Thrust)	2.721 (395.2)	790 (963)	63.04 (138.7)	0.0241
Max Cruise (9144 m/30,000 ft M = 0.8)	1.409 (204.7)	744 (880)	34.09 (75.0)	0.0209

In addition to meeting the pattern factor requirement, the circumferentially averaged radial profile of the combustor exit temperature distribution must also be consistent with the design gas temperature distribution of the high pressure turbine blades. Figure 3-4 shows the required radial temperature profile.

Figure 3-5 shows the required altitude ignition envelope of the PW2037 engine. The engine must be capable of self starting with the combustor driven only by a windmilling fan and compressor over a substantial fraction of the envelope as shown on the figure. Table 3-2 lists the combustor operating conditions at the lettered points on the upper boundary of the relight envelope as estimated from the characteristics of the PW2037 compressor. As the data of Figure 3-5 indicate, the combustor is capable of ignition at conditions considerably beyond the required envelope.

TABLE 3-2

COMBUSTOR INLET CONDITIONS AT ALTITUDE RELIGHT

Point of Figure 3-5	A	B	C	D
Flight Mach Number	0.40	0.50	0.67	0.88
Altitude - meters (feet)	6100 (20,000)	6100 (20,000)	9150 (30,000)	9150 (30,000)
Combustor Inlet Total Pressure - KPa (psia)	50.0 (7.3)	54.8 (8.0)	40.4 (5.9)	52.7 (7.7)
Combustor Inlet Total Temperature - °K (°F)	264 (16)	275 (36)	267 (21)	297 (76)
Engine Airflow Kg/sec (lb/sec)	0.91 (2.0)	1.45 (3.2)	1.45 (3.2)	2.36 (5.2)
Fuel Flow* Kg/hr (lb/hr)	190.9 (420)	190.9 (420)	190.9 (420)	190.9 (420)

*Minimum fuel flow of PW2037 engine control schedule.

The PW2037 engine specification also requires ground start capability at an ambient temperature of 219°K (-65°F) or the temperature at which the fuel viscosity is 12 centistokes. With Jet A fuel this occurs at an ambient temperature of about 239°K (-30°F). When the engine is cranked at this temperature the combustor inlet total pressure is about 0.11 MPa (16 psia) and the air temperature rise in the compressor is essentially negligible.

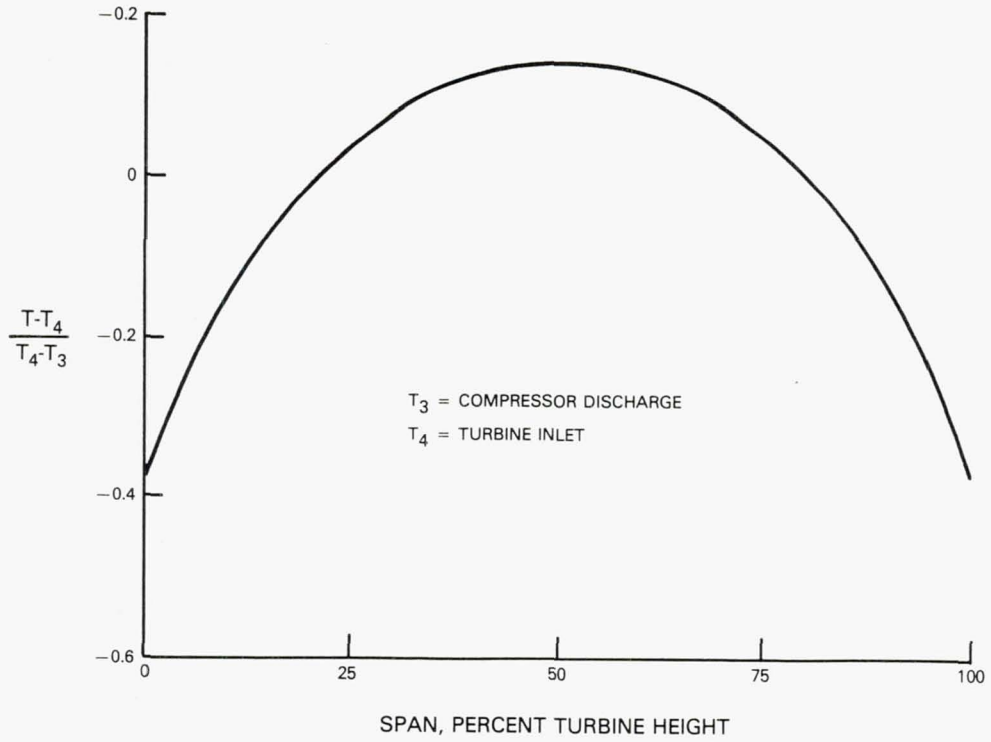

Figure 3-4 Required PW2037 Combustor Exit Average Radial Temperature Profile.

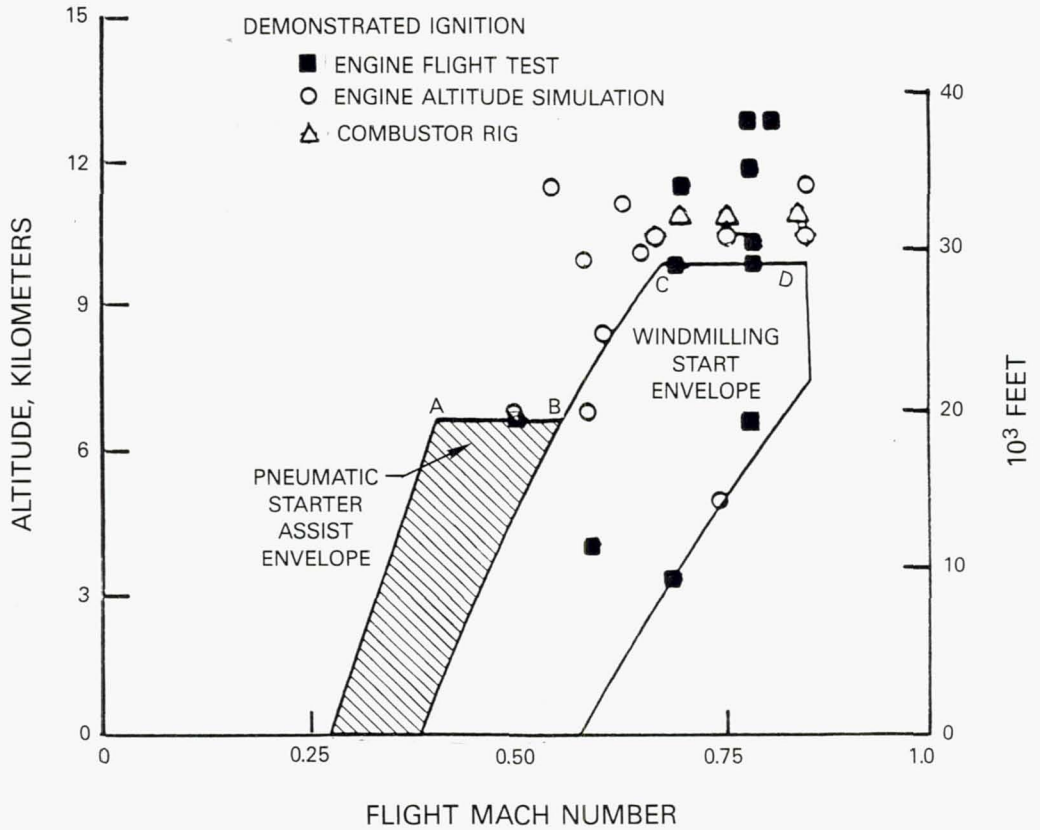

Figure 3-5 Altitude Ignition Envelope of the PW2037 Engine.

3.4 REFERENCE COMBUSTOR EMISSIONS CHARACTERISTICS

As part of the certification process, the emissions characteristics of the PW2037 engine were documented to assure compliance with the latest Environmental Protection Agency regulations (Reference 18) and the International Civil Aviation Organization (ICAO) guidelines (Reference 19). Results for the idle, 30 percent, 85 percent, and 100 percent sea level static thrust power settings are shown in Table 3-3. These power settings correspond to the simulated ground idle, approach, climb, and takeoff conditions specified by the Environmental Protection Agency (EPA) to establish aircraft engine emission standards. The ground idle emissions were obtained at 6.37 percent of rated thrust. The engine was equipped with the Model 2-37-K combustor liner which is the production engine configuration. The data have been corrected to standard day temperature and pressure and to an ambient humidity level of 6.3g H_2O/kg dry air. Jet A fuel was used for the tests. The corresponding values of the Environmental Protection Agency Parameter (EPAP) are also presented in Table 3-3. This parameter combines emission rates at the idle, approach, climb, and takeoff operating modes, integrated over a specific landing/takeoff cycle (Reference 17).

TABLE 3-3

EMISSIONS CHARACTERISTICS OF THE PW2037 COMBUSTOR

	Emission Index gm/kg			
	Carbon Monoxide	Total Unburned Hydrocarbons	Oxides of Nitrogen	SAE Smoke Number
Ground Idle (6.37% Thrust)	23.10	2.26	4.4	--
Approach (30% Thrust)	2.30	0.21	10.3	--
Climb (85% Thrust)	0.41	0.06	24.8	--
Sea Level Takeoff (100% Thrust)	0.40	0.05	31.1	11.8
Max Cruise (M = 0.8 9150m/30,000 ft.)	0.67	0.08	12.2	--
EPA Parameter	32.0	3.16	48.1	--

Notes:

Data for oxides of nitrogen presented as nitrogen dioxide equivalent.

Cruise emissions estimated on the basis of data obtained from sea level operating line.

SECTION 4.0
COMBUSTOR CONCEPTS AND TEST CONFIGURATIONS

The Phase II program was structured around the experimental evaluation of two advanced technology combustor concepts that were selected on the basis of the experience derived in Phase I. These concepts consisted of:

- A variable geometry combustor in which the airflow to the primary combustor zone could be modulated to vary stoichiometry.
- The Mark IV combustor concept which is an outgrowth of the Vorbix combustor evaluated under the NASA/PWA Experimental Clean Combustor and Energy Efficient Engine Programs.

In addition, because of the change from the JT9D-7 of Phase I to the PW2037 as the reference engine for Phase II, one of the test configurations consisted of a combustor representative of that in the PW2037. This configuration established a new baseline of current engine performance capability for referencing the results of the evaluation of the advanced technology concepts.

This section provides a description of the reference PW2037 combustor and the baseline configuration of the variable geometry and Mark IV combustors. The modifications that were incorporated in subsequent configurations of the two advanced technology concepts are also identified and the motivation for these revisions established.

4.1 REFERENCE PW2037 COMBUSTOR

Figure 4-1 shows a photograph of the rectangular sector of the reference PW2037 combustor evaluated in this program, while a cross-section is shown in Figure 4-2. This sector is an early development version of the PW2037 combustor and was used to provide the initial substantiation of the conceptual design of that burner. By incorporating four of the 24 fuel injectors used in the full annular burner it was equivalent to a 60 degree arc section of that burner. Figure 4-2 also shows the airflow distribution in the combustor as determined from the known dimensions, flow characteristics of the apertures in the combustor and the pressure distribution measured in the rig during test. The aperture dimensions and calibrated flow areas of components of this combustor sector and all other configurations evaluated during the Phase II program are listed in Appendix A. The test rig used for evaluation of this sector and the two advanced technology combustor concepts is described in detail in Section 5.2.1. For identification purposes the reference PW2037 combustor was given the designation V-1, i.e. the first of the sequence of variable geometry combustor configurations and the actual variable geometry combustors were designated Configuration V-2 V-3, etc.

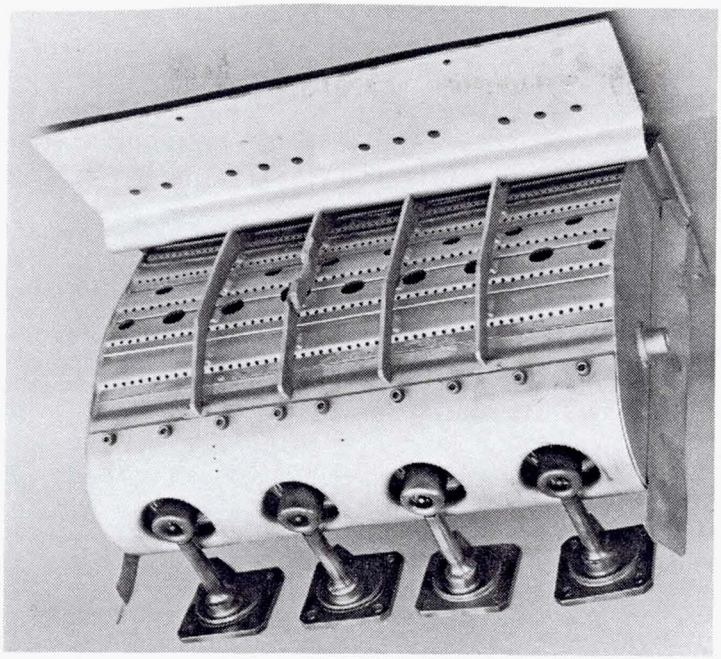

Figure 4-1 Reference PDW2037 Combustor Test Sector.

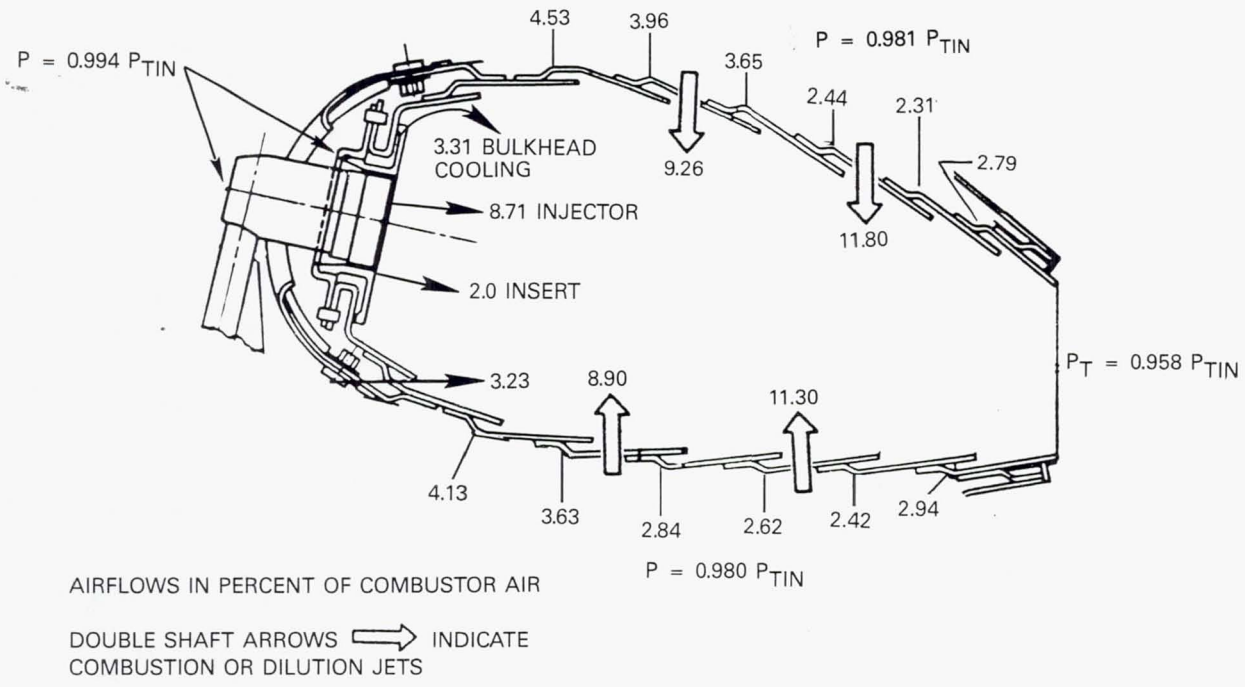

Figure 4-2 Cross Section of the Reference PW2037 Combustor Test Sector With Airflow Distribution.

Being an early developmental prototype of the PW2037 combustor, there were obviously some differences between the test combustor sector and the final production engine combustor shown in Figure 3-2. However, these deviations are relatively minor and the test configuration is sufficiently representative of the production combustor to provide an accurate definition of the fuel property sensitivity of the latter.

As a comparison of the cross-sections of Figure 3-2 and 4-2 indicate, the test burner sector and the production combustor have essentially identical aerothermal configurations. Both have the same 229 mm (9 inch) burning length from fuel injector face to turbine inlet guide vane leading edge. The airblast single pipe fuel injectors used in the test burner are prototypes of the production fuel injectors shown in Figure 3-3. With identical air and fuel passage dimensions, the only differences are in the absence of heat shielding and the use of less rigorous structural design criteria in the support region relative to the production injector.

The construction and aerothermal details of the front end of production and test combustors are also identical in that the airblast fuel injectors are surrounded by an insert ring that accommodates in plane motion of the injector relative to the combustor bulkhead. The insert supports an annular bulkhead heatshield, and cooling air for the bulkhead is fed radially outward relative to the injector centerline from behind the heat shield. The quantities of air passing through the injector and slots in the insert ring in the production combustor are essentially identical to those shown for the test combustor in Figure 4-2 but the production combustor employs more than twice the quantity of bulkhead cooling air of the prototype combustor. This increase was due to cooling revisions made during development to provide adequate long term structural integrity of the bulkhead in the production combustor.

After the prototype combustor sector and its associated rig hardware were fabricated, sizing studies of the PW2037 engine led to a decision to increase the airflow size of the engine by ten percent relative to the earlier engine definitions upon which the combustor rig was based. As a result the radial height of the liner of the production combustor (118.6mm (4.67 inches) at the maximum radial height position) is aboaut 10 percent higher than in the test combustor. While this alters parameters such as fuel injector spacing to bulkhead height ratio, the deviations are small. The effect of the radial height difference was compensated for in setting test rig operating conditions by reducing the rig airflow proportionately relative to the levels of Table 3-1 to maintain the reference velocities and hence residence time in the combustor consistent with those in the production burner.

The production engine combustor incorporates a rolled ring liner that provides more effective film cooling and enhanced structural durability relative to the conventional sheet metal louvered liner used in the test combustors. The sheet metal construction had been selected for economy and ease of modification in the combustor segment rig burner. From the point of view of determining sensitivity to fuel composition, the type of film cooled liner construction is immaterial because the impact of fuel on liner life is

estimated through analytical models from increments in measured liner metal temperature. With the sheet metal louver construction, the test combustor sector uses approximately 45 percent of the combustor airflow for liner cooling, while the production combustor uses only about three quarters of this quantity.

About one-third of this difference is due to the higher surface area to volume ratio of the test combustor brought about by the reduced radial height, while the remainder is attributable to the enhanced film cooling effectiveness of the double pass liner construction and the optimization of cooling air utilization in the production combustor.

The overall stoichiometry history in the test combustor sector is very similar to that in the production engine combustor. As indicated previously, both combustors have essentially identical fuel injector and insert airflow. While the fully optimized schedule of combustion and dilution airflow addition is more gradual in the production combustor, occurring in four stages rather than in the two stages of the prototype combustor sector, the net histories are nearly identical. This should assure similarity of the global combustion process.

On this basis it is apparent that, despite minor aerothermal and construction differences between the PW2037 test combustor sector and the production engine combustor, the test sector should provide an adequate definition of the fuel property sensitivity of the latter and a representative reference for assessing the merits of the advanced technology combustor concepts.

4.2 VARIABLE GEOMETRY COMBUSTOR

The experience derived during the Phase I program, in which the performance characteristics of variable geometry combustors was synthesized by the evaluation of pairs or sequences of fixed geometry combustors, indicated that the enhanced control of stoichiometry could be used to advantage in accommodating broadened properties fuels. Consequently the variable geometry combustor concept was selected for further assessment during the Phase II program and the definition of a responsive combustor with a workable airflow management system was a major objective of this effort.

4.2.1 VARIABLE GEOMETRY COMBUSTOR CONCEPT

Figure 4-3 shows the conceptual definition of the most general type of variable geometry combustor, hereafter referred to as "fully modulated" because the airflow to both the primary combustion zone and the dilution zone can be varied simultaneously. Airflow control is provided by butterfly valves rotating about radial axes in the air supply ducts adjacent to the outer combustor liner. Actuation of these valves diverts air from one combustor zone to the other while holding the overall flow resistance and hence pressure drop across the system reasonably invariant. The fully modulated variable geometry is required to maintain optimum equivalence ratios in the primary combustion zone over the entire engine operating range.

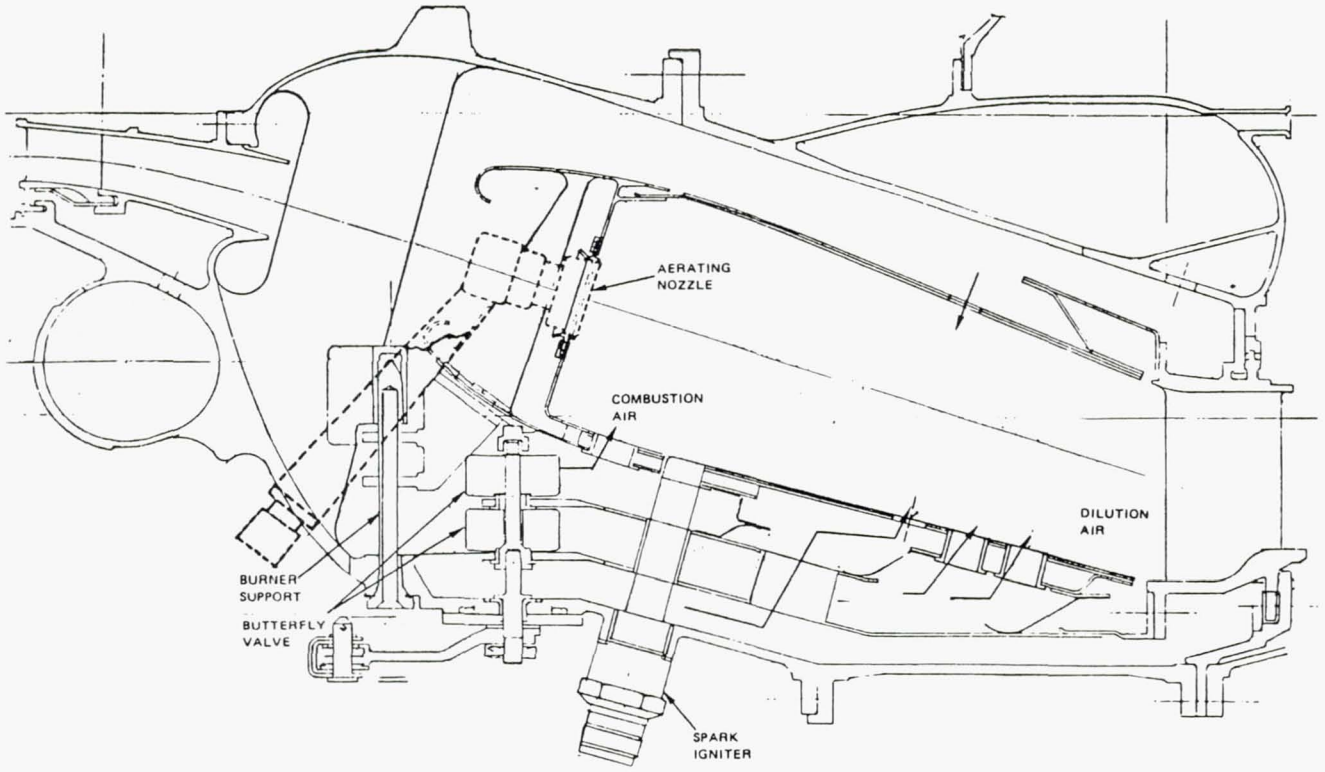

Figure 4-3 Fully Modulating Variable Geometry Concept.

To minimize carbon monoxide and unburned hydrocarbon emissions, the primary combustion zone must operate at an equivalence ratio of about unity at low power levels. At high power levels, a low primary zone equivalence ratio, of the order of 0.5, is required to minimize NO_x emissions, smoke formation and radiant heat transfer to the combustor liner. The airflow shifts needed to achieve these optimum equivalence ratios are rather massive; the primary combustion zone requires about 15 percent of combustor airflow at idle and 65 percent at takeoff of the PW2037 engine cycle.

Other potential advantages of a variable geometry combustor include a simplified fuel system, reduced residence time in the combustor and the possible enhancement of thrust specific fuel consumption. Specifically:

- Variable geometry can be used to enrich the primary zone at ignition and low power altitude operating conditions. This reduces demand on the low flow atomization characteristics of fuel injectors and encourages the use of single pipe injectors. The fuel system could then be simplified relative to duplex injectors or staged fuel systems. This also eliminates the risk of carbon deposition in inactive high power stage injectors, a decided advantage when operating on broadened properties fuels with lower thermal stability.

- Because the primary combustion zone is operated at the optimum equivalence ratios to minimize formation of carbon monoxide at low power and smoke at high power, the residence time required to oxidize these species is reduced. This could lead to decreases in combustor length, reducing the surface area which must be cooled and thereby permitting more of the combustor airflow to be used to control the exit temperature pattern factor and radial profile. The reduced residence time in the shorter combustor would also lead to lower NO_x emissions.

- Through appropriate scheduling of airflow areas with engine power level, variations in the net inlet flow area of the combustor (and hence pressure drop) may be used to advantage. Opening the combustor area at cruise and other intermediate power levels would increase the fraction of engine air passing through the combustor and reduce the turbine cooling air. This would increase turbine efficiency and reduce burner section pressure loss, thus improving thrust specific fuel consumption.

The major disadvantage of a "fully modulating" variable geometry combustor is the increased complexity and cost introduced by the air management system. The airflow shifts between the primary zone and dilution zone of the combustor are massive and must be accomplished without compromising the combustor exit temperature pattern factor or radial profile. The reliability of the airflow management system and its actuation mechanisms will also be of paramount concern and fail safe operation of the combustor must be assured.

Alternative variable geometry concepts that are less complex than the fully modulating combustor of Figure 4-3 are available. One such approach involves modulation of only the airflow entering the primary combustion zone through variable apertures on the front end of the burner. A combustor of this type would probably not have sufficient airflow transfer capability to produce the extremely lean primary zone equivalence ratios required to achieve very low NO_x output at high power and would experience variations in total pressure drop when the system was actuated. However, this approach could be used to establish favorable tradeoffs between low power carbon monoxide and unburned hydrocarbon emissions, enhanced ignition and stability, while reducing liner heat load. It was concluded that the evaluation of a variable geometry combustor based on this design approach would be more consistent with the planned scope and objectives of the Phase II Program.

4.2.2 VARIABLE GEOMETRY COMBUSTOR CONFIGURATION

Figure 4-4 shows the design details of the basic variable geometry combustor concept while Figures 4-5, 4-6 and 4-7 show photographs of the test combustor sector. The variable geometry combustor is a modified version of the basic four injector combustor sector used for the reference PW2037 combustor of Section 4.1. The louvered liner and aft end construction of the PW2037 combustor sector was retained while the bulkhead, and front end components were replaced to incorporate the variable geometry system. The latter consists of means of admitting air into a relatively tightly sealed plenum between the hood and the front bulkhead of the combustor from which it discharges into the primary zone of the burner through a large diameter swirler concentric with the fuel injector in the bulkhead. The air is

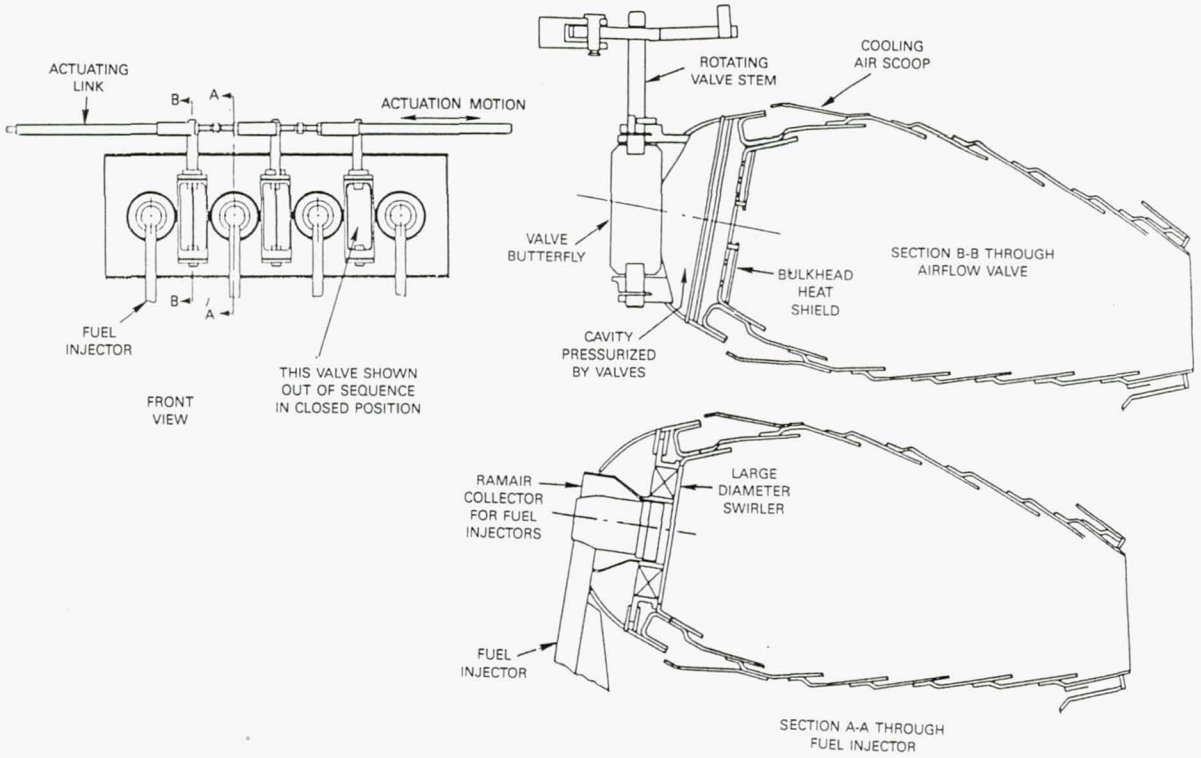

Figure 4-4 Variable Geometry Combustor Configuration.

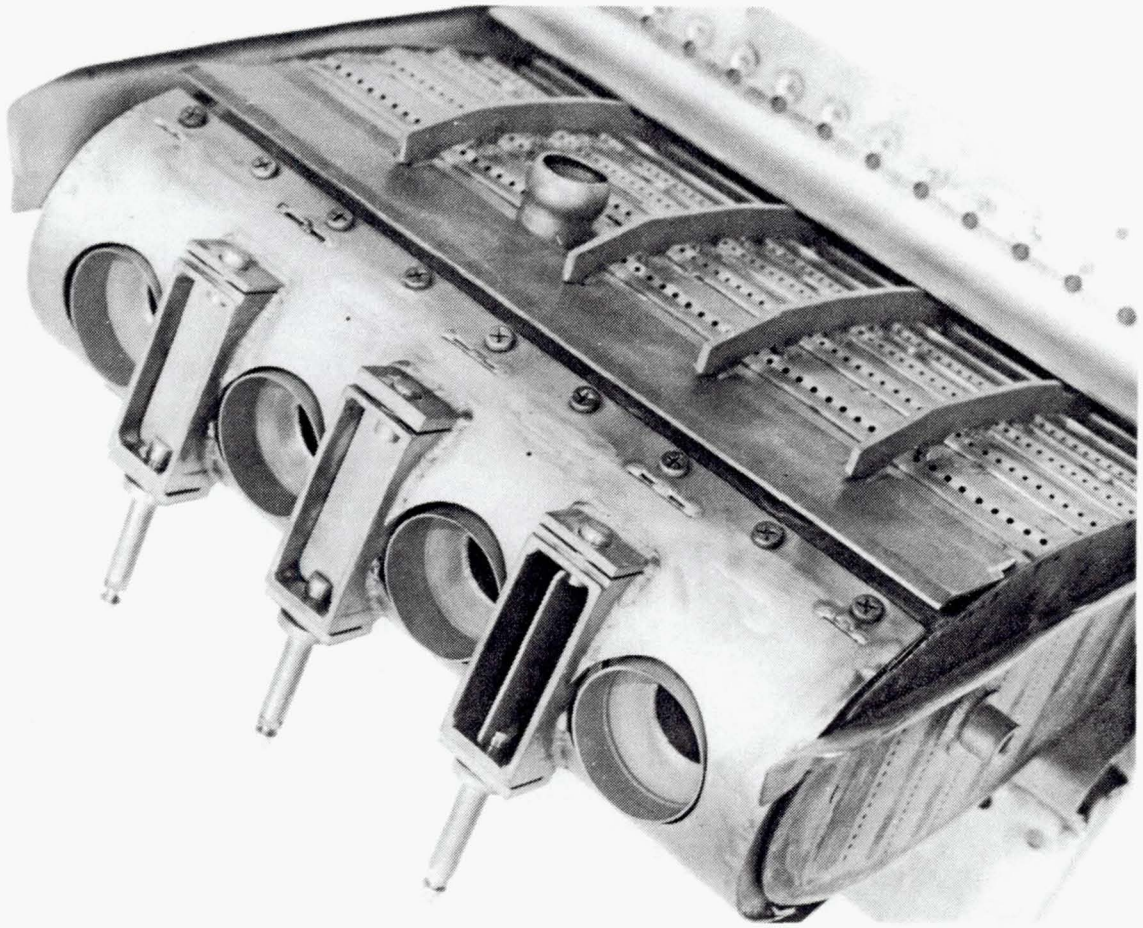

Figure 4-5 Variable Geometry Combusor Sector.

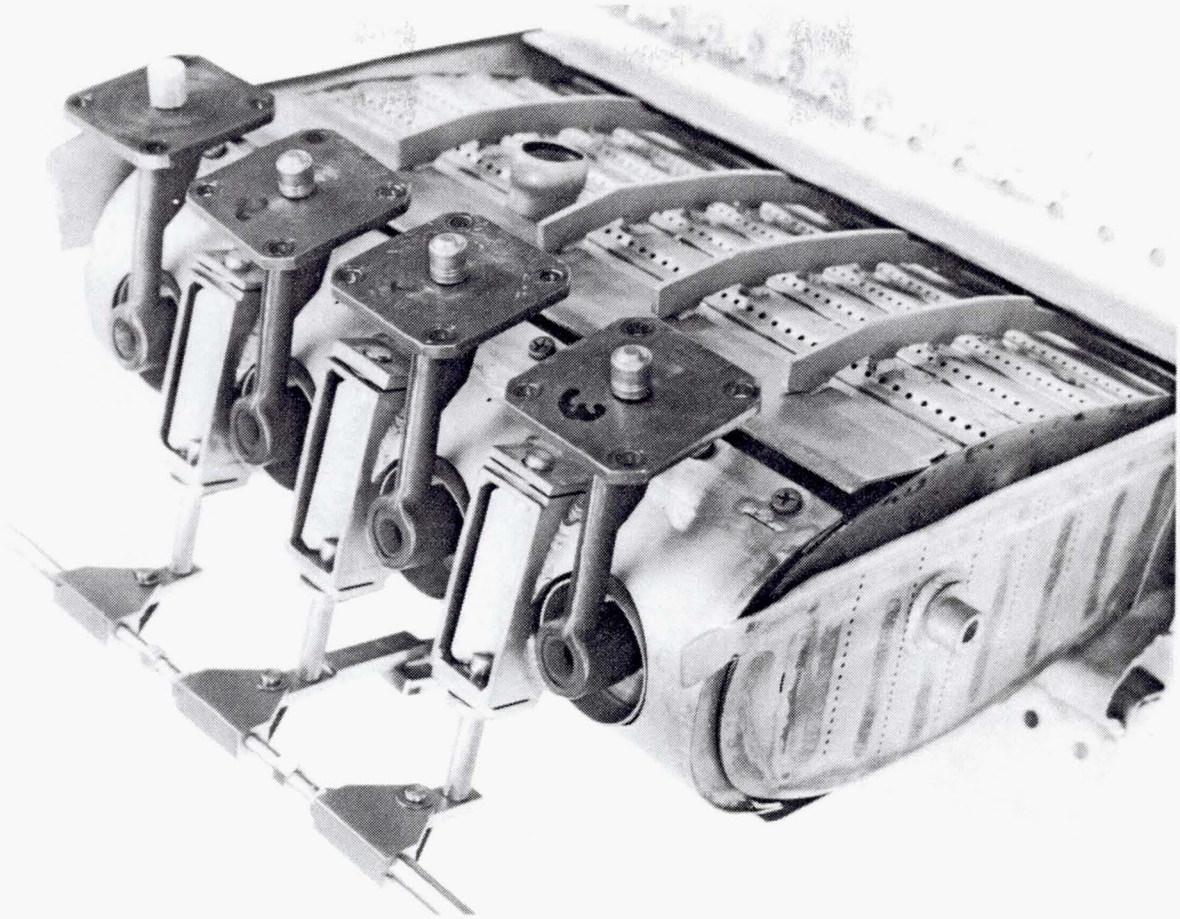

Figure 4-6 Variable Geometry Combustor Sector with Fuel Injectors and Valve Actuating Linkage Installed.

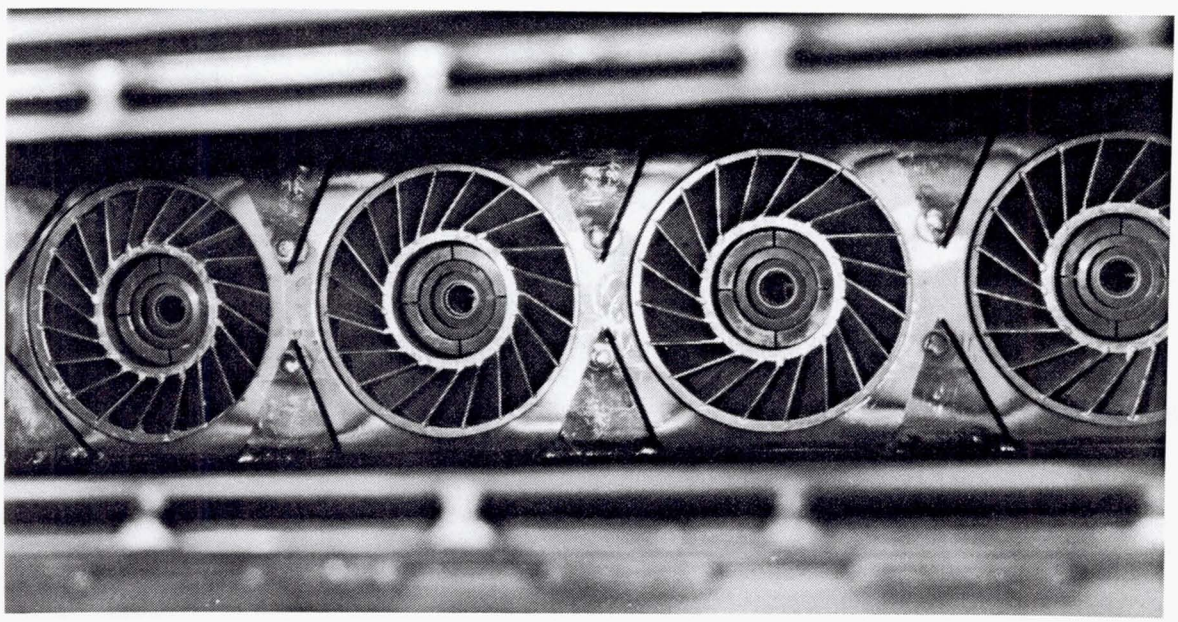

Figure 4-7 Bulkhead of Variable Geometry Combustor Showing Fuel Injectors, Swirlers and Bulkhead Heatshields.

admitted to the plenum through three rectangular inlets positioned on the front of the hood between fuel injectors. Butterfly valves in the inlets with their axes in radial direction provide for modulation of the airflow to the plenum. The individual valves are linked via a transverse drive rod which is actuated from outside the combustor casing. To provide for adequate airflow and pressure drop across the fuel injectors regardless of the variable geometry valve position, extension tubes are employed to capture rammed air upstream of the burner hood. The annular gap between these tubes and the burner hood is minimal consistent with accommodating differential motion between the combustor and the case mounted fuel injectors during operation. However some gap is required to provide a purging airflow through the underhood cavity and cool the vanes of the swirler when the butterfly valves are in the closed position. Features of the valves, their actuation system and the fuel injector extension tubes are shown on Figures 4-5 and 4-6. As shown on Figure 4-2, the cooling air for the bulkhead and the first inner and outer liner louver of the reference PW2037 combustor was provided from air captured under the hood. However, with the hood cavity being used as a conduit for the variable primary zone airflow, the pressure in this compartment varies, dictating an alternative approach to cooling the front end of the combustor. This was accomplished by incorporating air scoops on the second louver panel of both the inner and outer liner. These scoops, one of which is evident on Figure 4-5, extend outboard of the combustor hood contour to capture ram air from the burner shroud to cool the first and second liner louvers. Air from these cavities is also fed into the space formed between the bulkhead exposed to the combustion products in the burner and a false bulkhead about 6.4 mm (0.25 inches) further upstream which retains the swirlers. From this cavity the cooling air is discharged through holes in the bulkhead to impinge on the back face of triangular heat shields and diffuse across the remaining exposed surfaces of the bulkhead. These heatshields and their position relative to the swirlers may be seen in Figure 4-7.

Throughout the design of the variable geometry combustor concept, an effort was made to maintain compatibility with the existing PW2037 combustor so as to minimize the impact of its potential use in an engine application. The fuel injectors in the tests combustor are the same prototypes of the production engine injectors described in Section 4.1. The positioning of these injectors is identical to the reference combustor sector, thereby preserving the 229 mm (9 inch) burning length and the fuel injector mount pad configuration and location on the outer burner case.

A study was also conducted to define the optimum configuration for the actuating mechanism for the variable geometry combustor in the PW2037 engine. In the sector rig, a large and non-flight weight linkage was incorporated outside the primary gaspath. The installation of such a linkage within the engine cases would introduce excessive blockage in the burner shroud. To avoid this blockage, the study indicated that the best approach for actuating the valves would be to extend the radial stem of each valve through the outer burner case and actuate them with an externally mounted unison ring in a construction similar to a variable geometry compressor stator. The PW2037 engine combustor is front mounted with pins at an axial position near the valves so relative motion between the burner hood and the engine case would be minimal and could be accommodated by splines in the valve stem extensions.

Since the fuel injectors employed in the variable geometry combustor concept are the same single pipe aerating injectors used in the PW2037 engine, it would not be necessary to make revisions to the fuel delivery or control system to incorporate this combustor. The study also addressed operation of the variable geometry combustor in a two position, i.e., not continuously modulatable, mode during operation of the engine. Assuming actuation from valve open to closed at a particular engine power level, the overall engine total pressure ratio appears to be the best control parameter. With the electronic fuel control on the PW2037, a solenoid could readily be incorporated in the control system to actuate an external electric, hydraulic or pneumatic driver for the variable geometry linkage.

4.2.3 VARIABLE GEOMETRY COMBUSTOR MODIFICATIONS

A total of seven perturbations of the basic variable geometry combustor concept, designated Configurations V-2 through V-8 were evaluated during the Phase II program. The modifications evaluated consisted of: 1) use of different fuel injectors, 2) changes to the vane angle of the swirlers in the primary zone, 3) the use of deflectors on the primary zone swirlers, and 4) changes to liner combustion/dilution air hole schedules. Table 4-1 lists the details of the seven configurations evaluated and they are described further in the remainder of this section.

TABLE 4-1

VARIABLE GEOMETRY COMBUSTOR TEST CONFIGURATIONS

Configuration Number	Fuel Injector	Primary Zone Swirler Vane Angle	Primary Zone Swirler Deflector	Intermediate Zone Air Admission*
V-2	B	45°	None	None
V-3	A	45°	None	None
V-4	C	45°	None	None
V-5	B	45°	None	13% Wab in Louver 3
V-6	B	30°	Convergent	13% Wab in Louver 3
V-7	B	45°	Divergent	13% Wab in Louver 3
V-8	B	30°	None	13% Wab in Louver 2

* Nominal airflow with valves closed.

Alternative Fuel Injectors

Variations in fuel properties, primarily viscosity but to a lesser extent surface tension and specific gravity, are known to affect the atomization characteristics and spray patterns produced by fuel injectors. Since deterioration of fuel atomization or spray pattern changes could adversely impact several combustor performance parameters, including ignition capability, emissions at lower power and smoke formation at high power, particular emphasis must be placed on fuel injector performance characteristics when considering the use of fuels with non-conventional properties.

When the reference PW2037 combustor sector described in Section 4.1 and its associated rig components were being fabricated, three manufacturers were asked to submit candidate injector configurations for the PW2037 engine, to be screened in this combustor rig. Figure 4-8 shows upstream and downstream views of one of each of these injectors which were designated A, B and C for identification purposes. All three are single pipe aerating injectors designed to the same overall tip diameter and airflow capacity. Injector B is the prototype of the injector, shown in Figure 3-3, that was selected for use in the production PW2037 engine. This prototype injector was also used in the reference PW2037 combustor test sector Configuration V-1. The other injectors differed from Injector B in the details of the internal air passages and geometry of the fuel dispersion region in accordance with the individual manufacturers' design philosophy. When the three different injector configurations were tested in the combustor rig on Jet A fuel under the company sponsored PW2037 development program, significant differences in emissions and smoke output as well as the level and location of maximum liner metal temperatures were observed, implying that the prototype fuel injectors had substantially different atomization and/or spray angle characteristics that might be exploited in optimizing the variable geometry combustor for operation on broadened properties fuels.

To provide a more quantitative characterization of the three prototype injectors with regard to the accommodation of broadened properties fuels, bench spray tests were conducted to measure spray geometry and atomization at conditions simulating operation in the PW2037 engine. The test fuels consisted of Jet A, ERBS and a No. 2 distillate fuel having a viscosity of about 18cs at 250K(-10°F). The results of these tests are reported in detail in Appendix B and a summary is presented in Table 4-2.

TABLE 4-2

SPRAY CHARACTERISTICS OF THE PW2037 PROTOTYPE FUEL INJECTORS

	INJECTOR A			INJECTOR B			INJECTOR C		
FUEL	JET A	ERBS	NO. 2	JET A	ERBS	NO. 2	JET A	ERBS	NO. 2
SAUTER MEAN DIAMETER									
Cold Start	106.8	109.0	107.8	41.3	46.0	45.8	20.9	25.1	25.2
Idle	36.4	45.0	48.7	30.6	32.1	30.2	9.5	12.9	14.8
Takeoff	36.6	41.0	44.3	44.3	39.8	52.5	--	8.0	11.9
PEAK DENSITY DROPLET SIZE									
Cold Start	161.0	173.7	166.5	65.0	65.3	70.0	40.6	47.8	50.3
Idle	86.0	89.5	115.5	46.0	49.0	45.0	30.6	34.5	28.3
Takeoff	98.0	119.0	105.0	105.0	102.0	100.0	1.0	14.5	23.0
SPRAY CONE ANGLE									
Cold Start	51.4	55.8	63.2	48.2	52.3	38.2	54.6	58.4	55.7
Idle	84.8	78.7	78.4	48.4	45.9	48.9	49.3	49.6	53.3
Takeoff	86.7	86.3	85.6	82.1	82.4	82.8	52.9	51.7	54.8

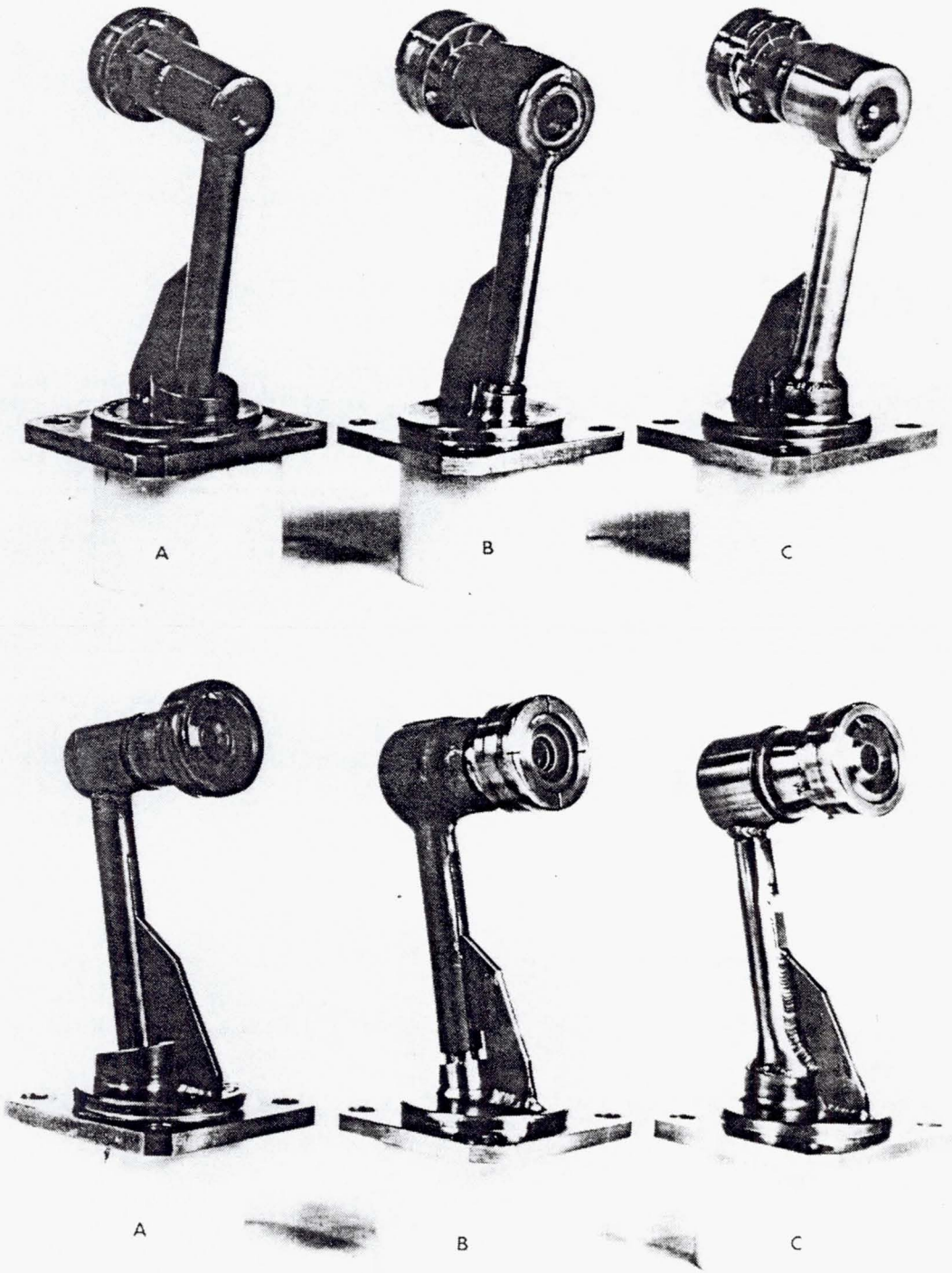

Figure 4-8 Upstream and Downstream Views of Prototype Fuel Injectors Used in Variable Geometry Combustor.

Table 4-2 shows the measured characteristic droplet sizes produced by the three injectors when operating on the different fuels. The Sauter Mean Diameter is the droplet diameter that has the same surface area to volume ratio as the entire spray, while the peak density size is the droplet diameter with the greatest number density in the spray. The data indicate a general trend of progressively increasing droplet size as fuel viscosity increases, i.e., from Jet A to ERBS to the No. 2 fuel. The increases are moderate, in most cases, of the order of 10 percent although increases of 20 to 25 percent were encountered in a few instances. There is also a significant difference in the nominal atomization capability of the injectors. Both characteristic droplet sizes reduced with progression from Injector A to Injector B and then to Injector C.

The spray characterization tests also included measurement of the geometry of the spray produced by the injectors. The results indicated that the spray cone angle and conical width of the spray was relatively insensitive to the fuel used but varied considerably with injector type and engine operating condition. The prototype of the production engine injector, Injector B, produced a compact spray with a total included angle of 48° at start and idle but expanded to 82° at takeoff. This variation appears to be desirable because it would produce a rich central combustion region at low power while the divergent spray at high power would enhance distribution of fuel into the large quantities of air entering through the swirler when the variable geometry valves are open at these conditions. Injector C, which achieved the finest atomization, did not produce this variation of spray angle. The total included angle of the spray produced by this injector remained in the range of 51° to 59° for all combinations of fuel and simulated engine operating condition. Injector A produced a spray angle characteristic similar to the baseline Injector B with the total cone angle increasing from 56° at cold start to 87° at takeoff condition. The combination of a wide spray angle and larger droplet size produced by this injector at takeoff could also be used to advantage in the variable geometry combustor if radial dispersion of fuel into the swirler airflow is found to be a limitation during high power operation.

On the basis of these bench spray evaluations and the prior experience in the company sponsored PW2037 combustor development program, it is evident that the three different prototype injectors each offer unique combinations of performance characteristics that should be evaluated in the variable geometry combustor. Injector B was selected as the reference in view of its use in the production engine combustor and was incorporated in Configuration V-2, and injectors A and C were evaluated in Configurations V-3 and V-4 respectively.

Primary Zone Swirler Vane Angle

The swirl strength of the flow entering the primary combustor zone can have a strong effect on the flow structure in that zone. It influences both the extent and stability of the recirculation in that zone and the mixing or stratification between the swirler discharge flow and the fuel air mixture emanating from the fuel injector. Recognizing its potential as a design parameter, two sets of swirlers were fabricated for use in the primary zone of the variable geometry combustor. The basic swirler, used in the majority of the test configurations, had twenty vanes per swirler set at a 45° angle.

The second set was designed for reduced swirler strength and had thirty vanes set at 30° from the axial direction. The increased blockage of the thirty vanes in the 30° angle swirler offset the higher turning angle of the 45° angle swirler so as to create essentially equal flow capacities. Figure 4-9 shows views of both swirlers from the downstream direction and a view of the 45° swirler from the upstream direction in which the fuel injector ram air capture tube is evident. While the majority of the test configurations incorporated the 45° vane angle swirlers, the 30° vane angle swirlers were used in conjunction with other combustor modifications in Configurations V-6 and V-8 as a means of reducing the outward centrifuging of the swirler discharge flow and promoting its mixing with the central fuel-air jet from the injector.

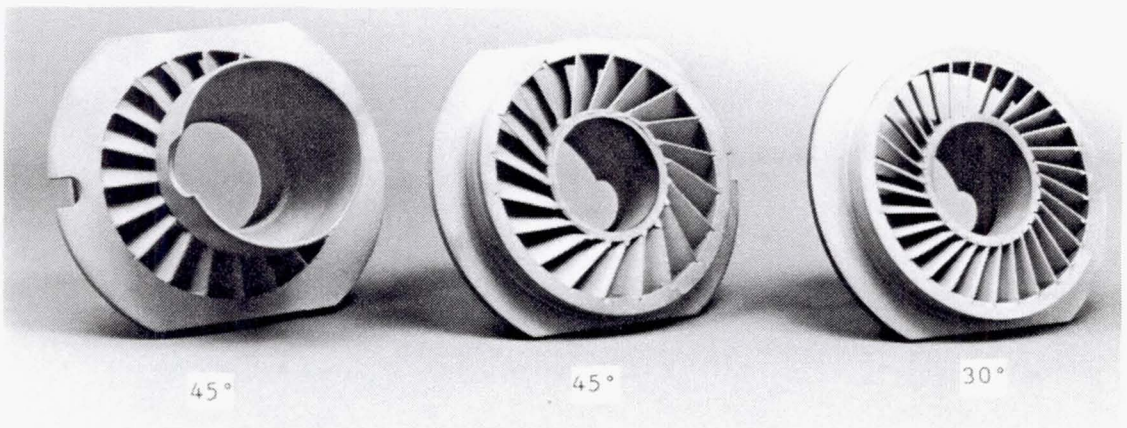

Figure 4-9 Swirlers for Variable Geometry Combustor.

Combustor Liner Airflow Schedule

Three different schedules of combustor airflow addition through the liner were used in the evaluation of the variable geometry combustor. Figure 4-10 shows these schedules with the nominal airflow distribution in the combustor when the valves were in the closed (low power level) position. The initial schedule, used for the evaluation of Configurations V-2, V-3 and V-4 which involved systematic changes in the fuel injectors had no primary or intermediate air addition through the liners but approximately 25 percent of the combustor airflow (down to about 16 percent when the valves were opened) entered as dilution air relatively far downstream through the fifth louver panels. As such, these configurations relied on the swirl strength of the swirler and fuel injector discharge flows to stabilize the combustion zone in the front end.

Following evaluation of the first three configurations, it was evident that the flow structure in the primary combustion zone had to be stabilized further in the low power level valve closed mode if the program goals for carbon monoxide and unburned hydrocarbons emissions were to be achieved. Consequently, in Configuration V-5 one half of the dilution air entering the rear of the combustor, in particular, that entering through the inner liner was admitted behind the primary combustion zone through holes in the third louver panels of the inner and outer liners. This change in liner air schedule was thought to have two beneficial effects: the jets would tend to reinforce the position of the recirculation zones behind each fuel injector

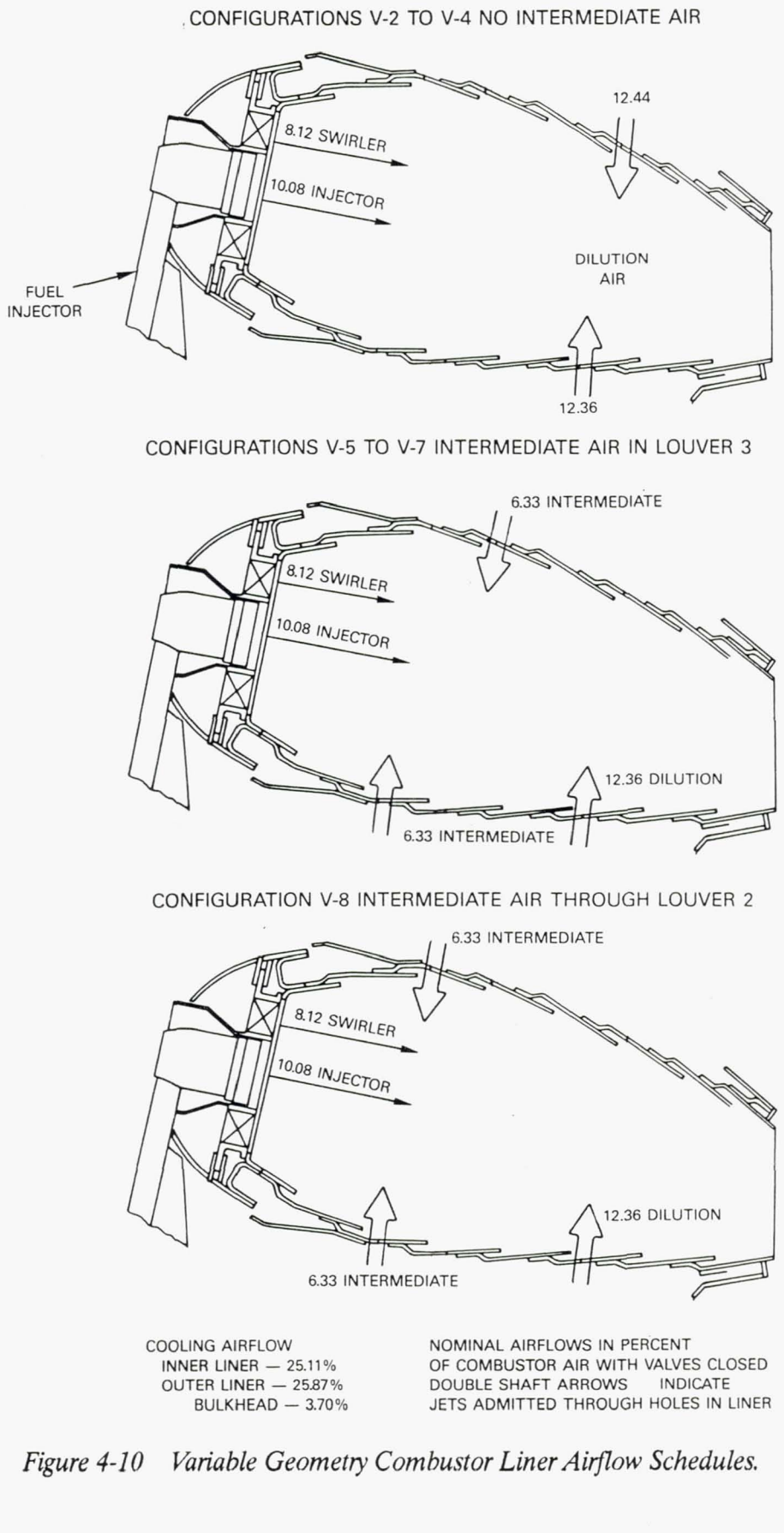

Figure 4-10 Variable Geometry Combustor Liner Airflow Schedules.

to provide a stronger and better defined combustion zone. They would also provide leaning of the intermediate zone of the combustor in the event that the high carbon monoxide and unburned hydrocarbons were caused by excessively rich mixtures with inadequate capability for oxidation of these species in the intermediate zone. While the use of the intermediate zone air jets did not produce any significant improvement in the low power performance of Configuration V-5 of the variable geometry combustor, the approach of improving performance by forcing the primary combustion region to position downstream of each fuel injector appeared sound. In Configuration V-8, the jet stabilization process was strengthened by moving the holes upstream to the second louver panel as shown on Figure 4-10. While the use of the 45 degree vane angle swirler could also increase the strength of the recirculating flow in the primary zone of Configuration V-8, the 30 degree vane angle swirler was used in this configuration to avoid overly stratifying the primary zone flow at high power levels when the valves are open.

Swirler Deflectors

As the evaluation of the variable geometry combustor progressed, it became evident that the basic design concept of introducing variable airflow through a large swirler concentric with a fuel injector was limiting the capability of achieving the full potential of this concept. While bulk equivalence ratios in the primary combustion zone were moderate at high power levels with the valves open, it was evident the swirler and fuel injector discharge flows were stratified and not well mixed. At low power levels, when the valves were closed, the purge airflow through the swirler was still relatively large - comparable to that through the fuel injectors - and had adverse effects on low power flame stabilization and emissions.

To demonstrate that the performance characteristics of the basic variable geometry combustor concept could be enhanced toward its full potential with appropriate redefinition of the air management system, Configurations VG-6 and VG-7 incorporated conical deflectors on the swirlers to alter the mixing between the swirler and fuel injector discharge flows for specific purposes.

Figure 4-11 shows cross-sections of the combustor with the swirler deflectors while Figure 4-12 shows photographs of these components. Configuration V-6 incorporated a convergent deflector attached to the trailing edge of the swirler vanes near the outer diameter shroud and converged inward at a 45 degree angle so as to deflect the swirler flow into the stream emanating from the fuel injector. This approach was intended primarily to benefit operation at high power levels because it would promote strong intermixing of these streams which would lead to a more uniform, leaner mixture in the primary combustion zone that would be expected to be conducive to reduced smoke output and lower heat load at high power levels. Figure 4-13 shows an interior view of the combustor with the convergent deflectors installed.

The opposite approach of deflecting the swirler airflow was investigated in Configuration VG-7. In this configuration, divergent conical extensions were attached to the inner shroud of the swirlers, immediately adjacent to the fuel injector in an attempt to deflect the airflow that passed through the swirler radially outward to eliminate premature mixing with the injector airflow at low power. In this manner, it was anticipated that undesirable mixing of the swirler and the injector airflows could be delayed to produce improvements in the idle emissions. By studying the composite performance of both of these configurations at their optimum power level, the potential of a refined version of the variable geometry combustor could be assessed.

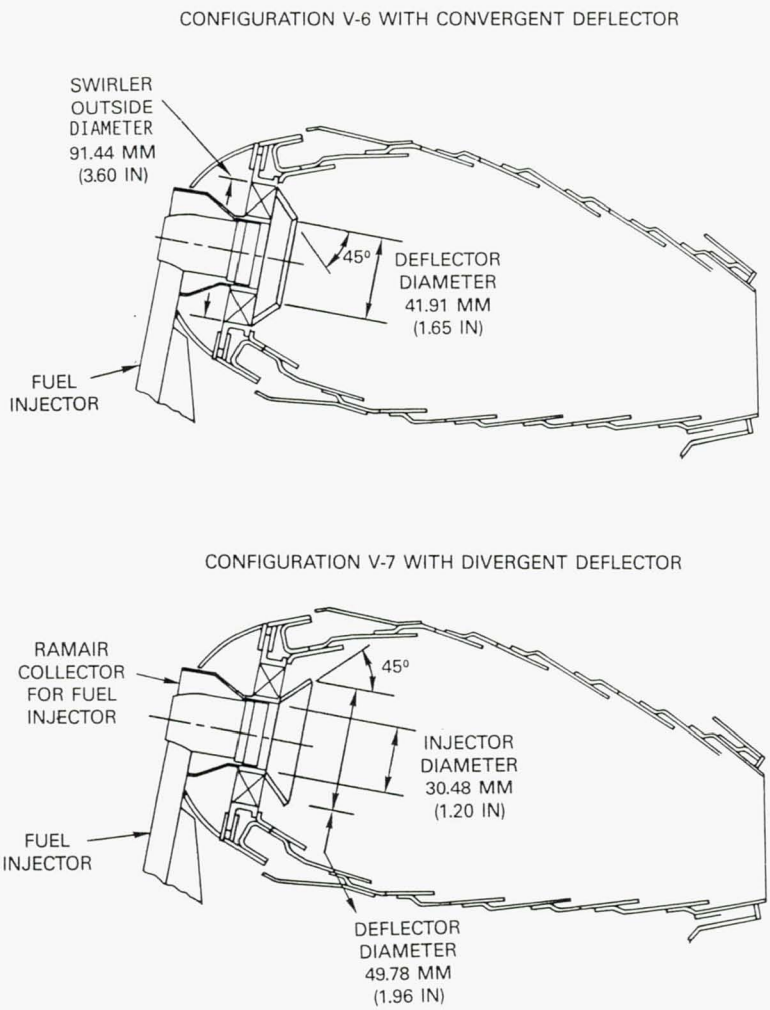

Figure 4-11 Variable Geometry Combustor With Conical Deflectors on Swirlers.

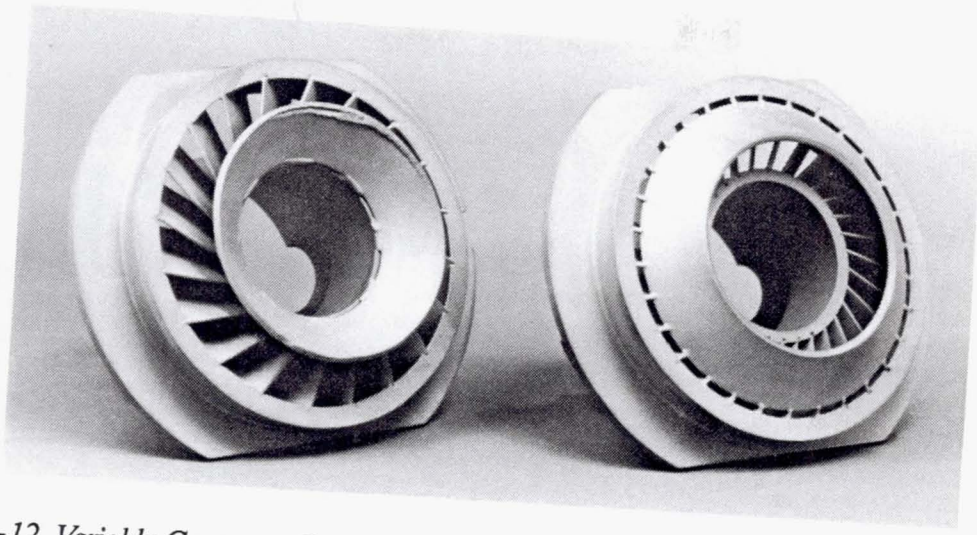

Figure 4–12 Variable Geometry Combustor Swirlers with Divergent and Convergent Deflectors.

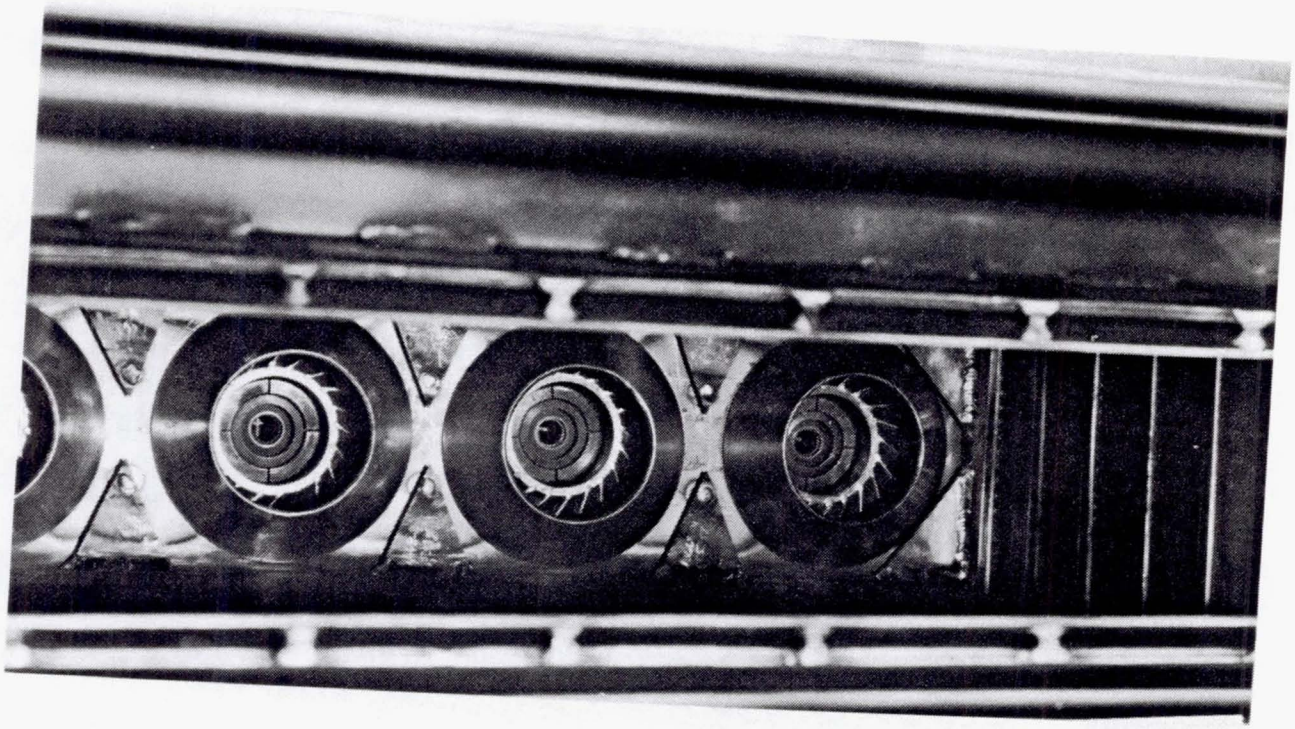

Figure 4-13 Interior of Variable Geometry Combustor with Convergent Deflectors on Swirlers.

4.3 MARK IV SWIRL COMBUSTOR

A staged Vorbix combustor was evaluated as a candidate advanced technology combustor concept in the Phase I program. The principal feature of staged combustors is the use of two distinct combustion zones, each serviced by an independent fuel injection system. By operating the combustor on only one zone at low power levels and both zones at high power, the combustor may be optimized at two operating conditions, rather than a single condition. Use of a rich mixture strength in the low power stage produces low carbon monoxide and unburned hydrocarbon emissions at idle. When the two stages are used in combination, a low equivalence ratio can be maintained at high power to minimize NOx and smoke output. This type of stoichiometry control appears useful in circumventing some of the problems associated with broadened properties fuel.

However, the staged combustor has a significant disadvantage that can be particularly detrimental when the combustor is operated on broadened properties fuels with their potentially poorer thermal stability. The staged fuel system arrangement requires low fuel flows and complete shutdown of the high power stage fuel system at certain engine operating conditions - a situation that can lead to rapid coke deposition in the fuel injectors. Conversely, both the reference PW2037 combustor and the variable geometry combustor employ "single pipe" aerating fuel injectors which are an improvement over prior technology in this regard because they are capable of operating over the entire engine fuel flow turndown without shutting down parts of the system.

Pratt and Whitney has been investigating a new advanced combustor concept, designated the Mark IV, that is an outgrowth of the Vorbix combustor evolved under the NASA/PWA Experimental Clean Combustor and Energy Efficient Engine programs. This combustor retains the characteristics of a staged two zone burner but is more compact and has the potential of operating with only a common "single pipe" fuel system. It also incorporates features that can enhance hot section durability and reduce combustor section pressure loss to improve specific fuel consumption. Since the Mark IV was a logical outgrowth of the Vorbix combustor evaluated in Phase I, and offered unique features consistent with minimizing sensitivity to fuel composition, it was incorporated as the second advanced technology combustor concept in the Phase II program.

4.3.1 MARK IV COMBUSTOR CONCEPT

Figure 4-14 shows the conceptual definition of the Mark IV combustor in terms of a schematic front view of the annular combustor and cross-sections at two representative planes. The dominant feature of the Mark IV combustor is a series of air admission modules protruding through the front bulkhead of the combustor. The air admission modules are spaced about one bulkhead height apart in the circumferential direction. Conceptual design studies indicate that a Mark IV combustor for the PW2037 engine would incorporate 24 such modules, i.e., the same number as fuel injectors in the current production combustor. The Mark IV combustor is unique in that, with the exception of liner cooling air, all of the combustor air is admitted through the front end

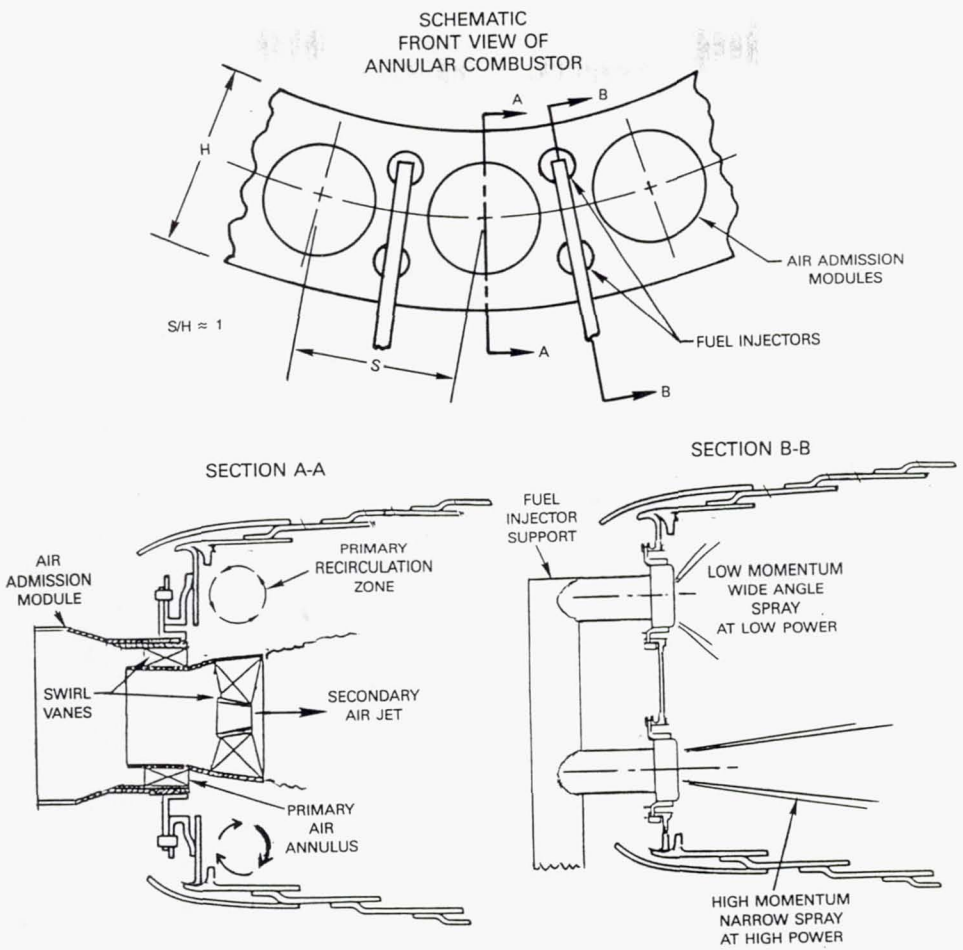

Figure 4-14 Conceptual Definition of Mark IV Combustor.

of the burner. This air, comprising about 75 percent of the combustor airflow, enters the burner through concentric annular passages in the air admission modules. The majority of the air, about 60 percent of the burner airflow, passes through swirl vanes in the center of the module and discharges in the combustion zone where it will function as both secondary combustion air and dilution air. The remaining 15 percent of combustor airflow entering the air admission module is removed from the outer radii of the entering stream and passes through an annular passage to become the primary or pilot stage airflow. This flow is also swirled and upon discharge from the module is diverted radially outward by centrifugal forces to form torroidal recirculation zones that are radially disposed around the centerline of the module and become the flame stabilization mechanism for the pilot combustion zone.

As shown on Figure 4-14, fuel is introduced into the combustor through small single pipe airblast type fuel injectors that protrude through the bulkhead between the air admission modules. At low power levels, such as idle, these injectors produce a wide angle low momentum fuel spray that is confined to the torroidal recirculating flow in the pilot combustion zone near the bulkhead and produces stable efficient combustion in this region.

The overall flow structure in the combustor is one of a swirling jet of combustion inlet air eminating from the center of the inlet module and surrounded by the hot combustion products in the pilot combustion zone. Because of the low density of the combustion gases relative to the central jet the angular momentum of the swirling flow field decreases with increasing radius from the module centerline. This leads to instability of the interface between the central jet and the pilot combustion products with subsequent rapid mixing. This mixing situation is identical to that attempted in the vicinity of the multiplicity of swirler tubes employed in the high power stage of the Vorbix combustor. (References 8, 9 and 10).

At high power levels, additional fuel is admitted to the burner, and the outer periphery of the central air jet is vitiated, with the pilot or primary stage acting as an ignition source. This fuel is introduced through the same airblast injectors used to fuel the pilot stage by tuning the spray angle - fuel flow characteristics to provide a spray with higher axial momentum at the higher fuel flows so that the majority of the fuel is sprayed into the interface region shown on Figure 4-14 and only the lower momentum elements of the spray are entrained in the pilot stage recirculation zone. Note that this would be the inverse of the spray angle - flow characteristics of fuel injector types A and B for the variable geometry combustor described in Section 4.2.3. The fuel arriving in the interface region is rapidly vaporized by the pilot combustion products in the same manner as that introduced into the pilot discharge of the Vorbix combustor and is burned rapidly at the interface with the central jet in a manner conducive to low NOx and smoke production.

At the completion of combustion, the combustion products are concentrated around the periphery of the combustion zone surrounding the nonvitated central core of the center air jet. The centrifugal instability of the interface between these gases persists and the core of the central jet continues to mix, in the same rapid mode, with the combustion products to produce a uniform temperature distribution conducive to a low pattern factor at the combustor discharge. The rapid progress of both the initial combustion and the final dilution of the combustion products leads to short combustor liner length requirements. This, in turn, minimizes liner cooling air and leaves more airflow available for use in optimizing stoichiometry.

The basic Mark IV combustor concept is one of a compact combustor with radial air staging to produce a two stage type of low pollutant formation combustion process similar in character to that occurring in the Vorbix burner. The two stage characteristic is accomplished with a "single pipe" type of fuel system, thereby eliminating one of the major concerns associated with previous staged combustor concepts, and one that can be particularly acute with the use of broadened properties fuels.

The combustor described above could be installed in the annular combustor section of the PW2037 and operate with the air admission modules and the airblast fuel injectors accepting ram induced air from the dump of the prediffuser. However, because the Mark IV burner operates with nearly all of the air entering through the modules, unique diffuser-combustor integration approaches can be incorporated to reduce the burner section total pressure loss by reducing the most critical losses in the diffuser system. Reducing burner section pressure loss reduces fuel consumption, and the trade factors for subsonic turbofan engines provide incentive to pursue such approaches.

The diffuser-combustor integration concept used with the Mark IV combustor is based on the fact that the critical pressure drop required in the combustor section is that between the burner shrouds and the interior of the combustor volume to generate flow through the liner cooling system and the turbine inlet vane leading edge. Since the quantity of air that must flow through these cooling systems is small, of the order of 30 percent of the compressor discharge airflow, it follows that minimum section pressure losses may be achieved by extracting this air from the most advantageous source and independently diffusing it in the most efficient manner.

Figure 4-15 shows the diffuser-combustor integration concept used to accomplish this objective with the Mark IV combustor. The engine prediffuser is used to achieve an initial level of pressure recovery from the total compressor discharge flow. Between air admission modules, the airflow that will eventually be fed to the burner shrouds for liner and turbine cooling is captured from the center of the gaspath where the total pressure is highest. This flow is then turned outward and diffused further in individual conical diffusers. The remainder of the prediffuser discharge flow, including strut wakes, endwall boundary layers and other low total pressure parts of the flow are collected in an end cap on the prediffuser and piped directly into the air admission modules on the burner. Since this air is dumped into the combustor liner and does not have to pass through the liner pressure drop, a lower level of total pressure can be tolerated in this stream without increasing the overall pressure loss of the system.

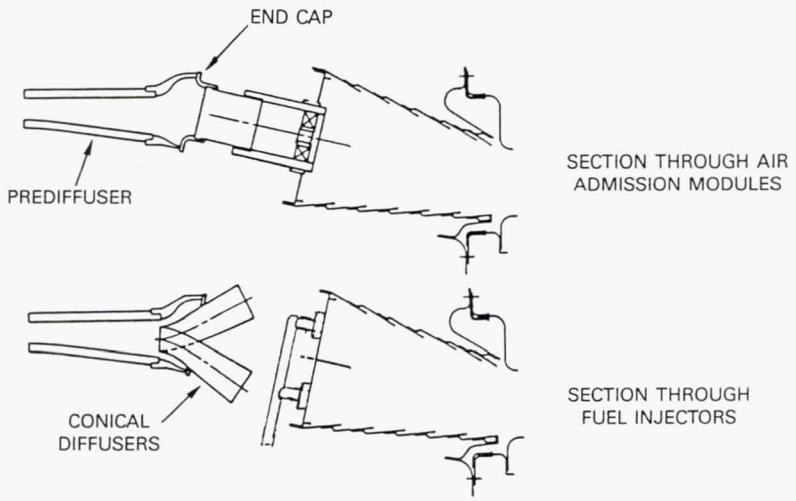

Figure 4-15 Mark IV Combustor Diffuser System.

4.3.2 MARK IV TEST COMBUSTOR CONFIGURATION

Figure 4-16 shows several cross-section views of Mark IV test combustor sector and Figures 4-17 through 4-22 show details of the components. The test sector is a rectangular combustor incorporating three air admission modules and two sets of radially adjacent fuel injectors spaced between them. Figure 4-17 shows the liner assembly for the combustor sector. The combustor was designed to be installed in the same rectangular section test rig used to evaluate the reference PW2037 and the variable geometry combustors. As such, the details of the liner at the last louver and the rear mount and retention features are identical to the previously discussed test combustors.

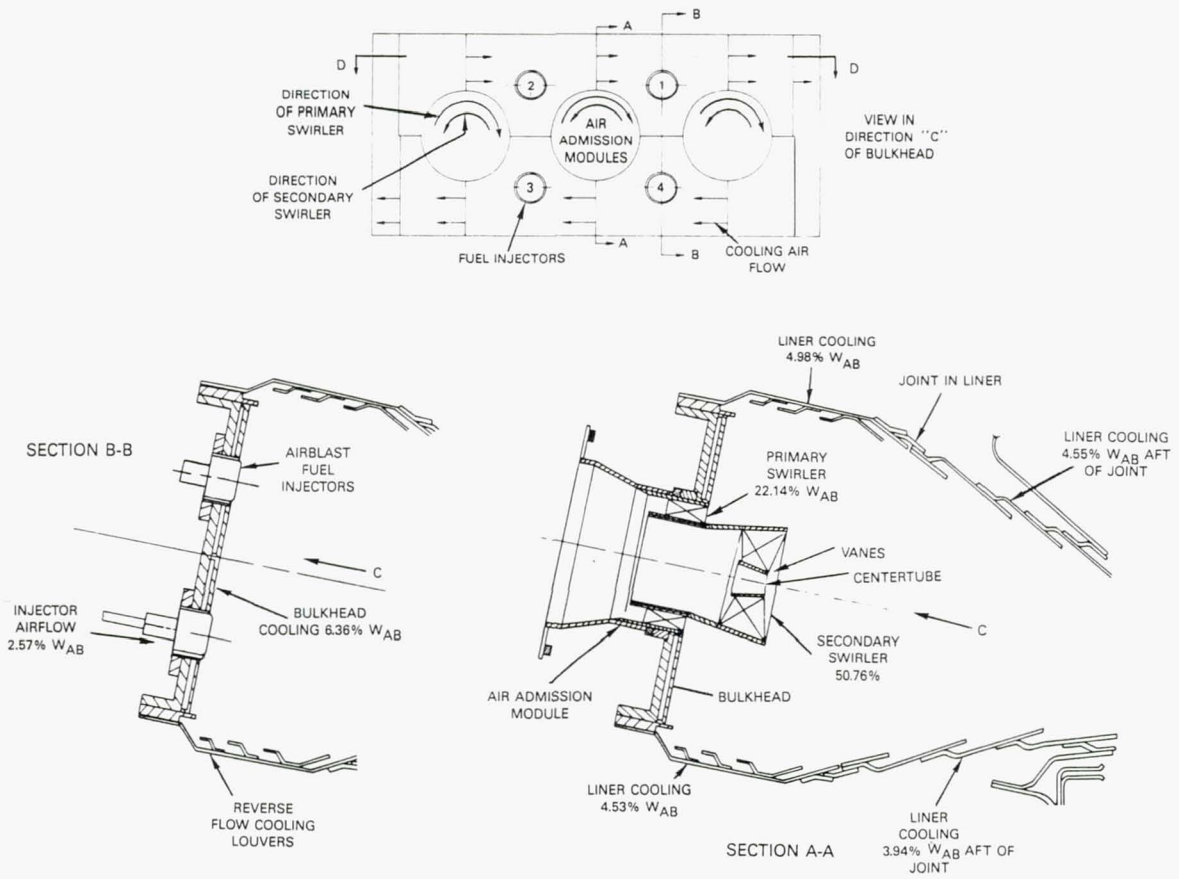

Figure 4-16 Details of the Mark IV Combustor Test Sector.

Figure 4-17 Mark IV Combustor Sector Liner Assembly.

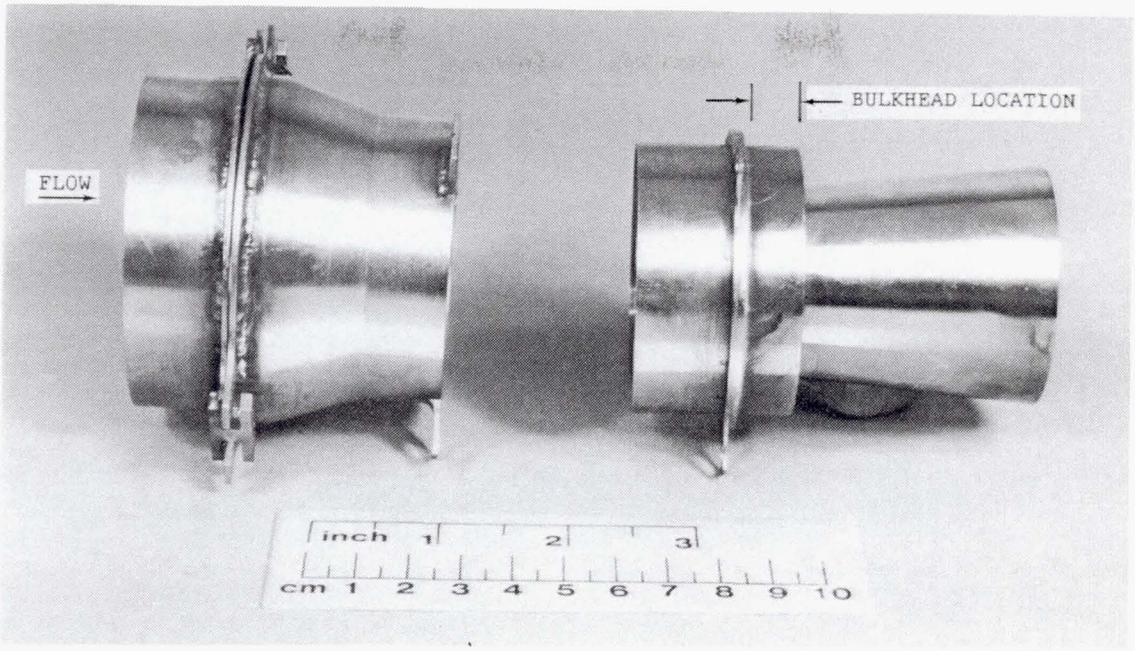

Figure 4-18 Mark IV Combustor Air Admission Module.

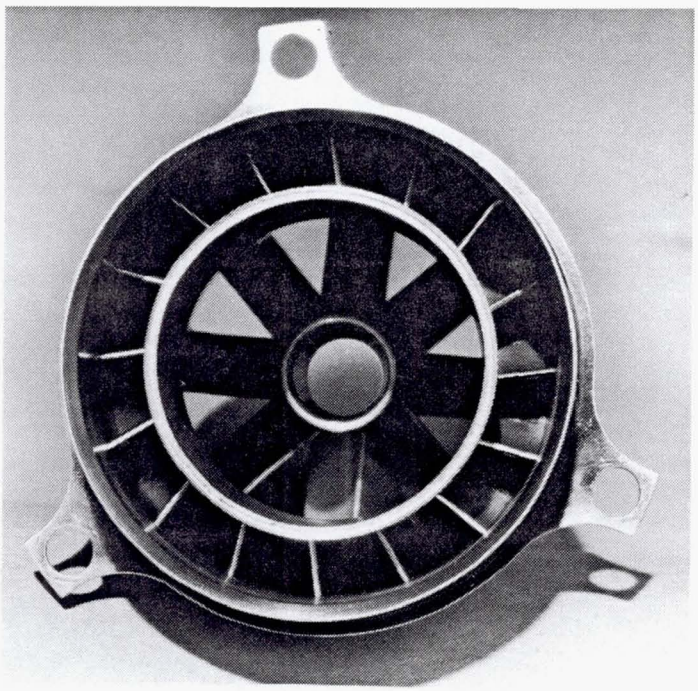

Figure 4-19 Swirler Assembly for Mark IV Air Admission Module.

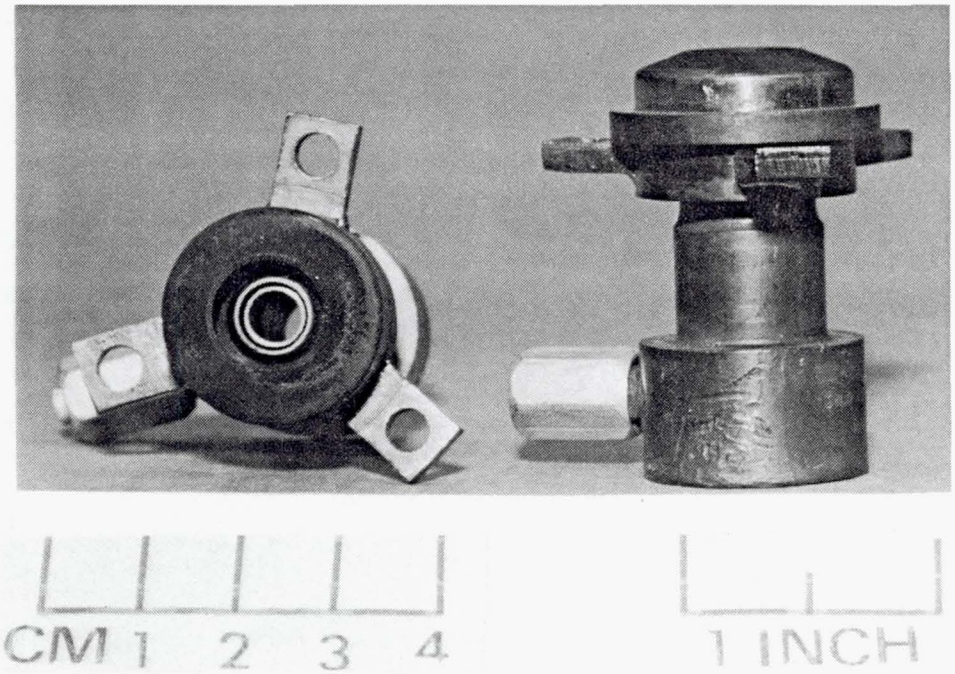

Figure 4-20 Fuel Injector for Mark IV Combustor.

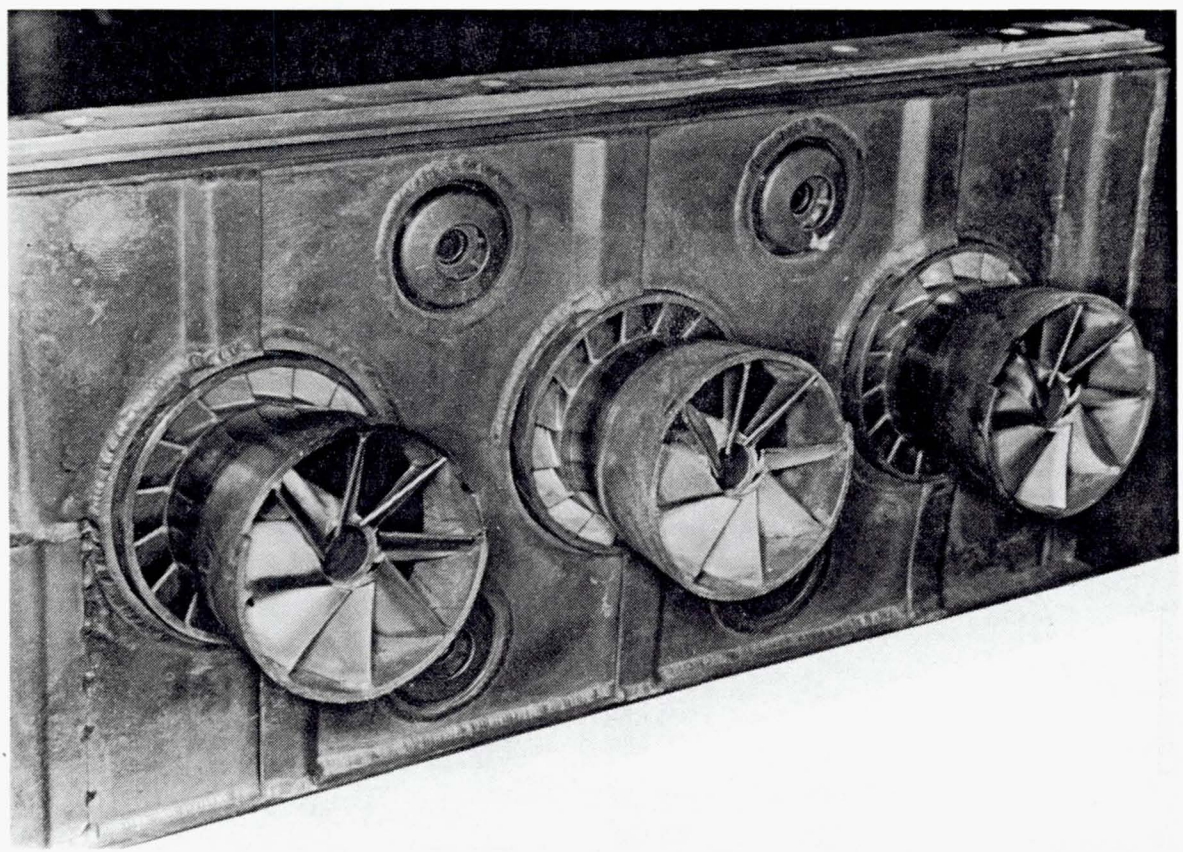

Figure 4-21 Mark IV Combustor Bulkhead with Air Admission Modules and Fuel Injectors Installed.

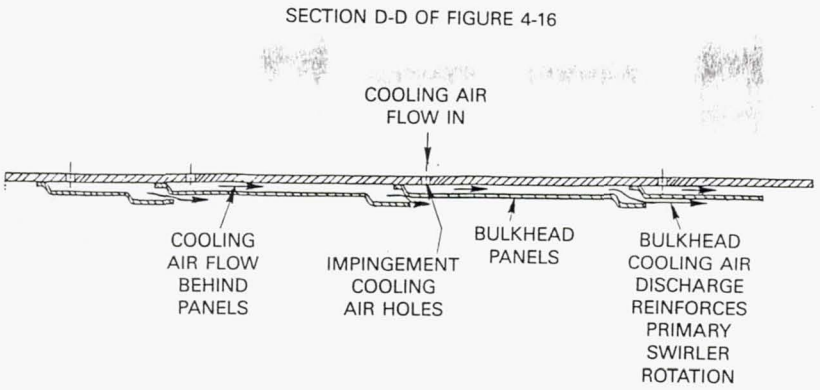

Figure 4-22 Mark IV Combustor Bulkhead Cooling System.

It was indicated in Section 4.1 that the reference PW2037 combustor test sector and that used for the variable geometry combustor sector were designed before the engine airflow size had been finalized and as a result, the radial dimensions of the combustors were about 10 percent smaller than the production engine combustor. When the Mark IV test combustor sector was designed, it was recognized that geometric proportions of the burner may be critical to performance - in particular, those of the front end region could have a strong influence on flame stabilization in the pilot combustion zone. Consequently, the Mark IV combustor sector was designed to the radial height consistent with current PW2037 engine airflow size and, as will be shown in Section 5.2.1, the adjustment to the reduced gaspath size of the test rig cases was made in the prediffuser. Consideration of this height and air/admission module to burner height spacing criteria established the transverse module spacing on the Mark IV combustor sector. Sector width limitations, dictated by the width of the rig cases, required that this sector be built with only three air admission modules as opposed to the four fuel injectors incorporated in the smaller airflow sized reference PW2037 and variable geometry combustor sectors.

Anticipating that most configuration changes of the Mark IV combustor would involve revisions to the air admission modules and the fuel injectors, a modular construction approach was used to facilitate access to these components. The three air admission modules mounted on the combustor bulkhead from the upstream side. The fuel injectors, rather than being installed on case mounted support struts as in Figure 4-14, were also attached directly to the bulkhead. Figure 4-18 shows a side view of one of the air admission modules and the bulkhead pass through region. Figure 4-19 shows a view of the downstream part of the air admission module looking downstream into the combustor. The outer annulus is the primary or pilot air passage with swirler vanes, while the secondary air swirler vanes and centertube are visible in the central passage. The three mount lugs fit over studs protruding axially upstream from the front bulkhead to provide retention.

Figure 4-20 shows one of the four fuel injectors which are representative of those used in most of the configurations evaluated. The view at the left is looking upstream from inside the combustor. The injector is a miniature version of the airblast type fuel injectors used in the reference PW2037 and variable geometry combustor with the aerating air entering through the front of the injector, i.e., upward in the right side view of Figure 4-20 and through the larger diameter aircap to impinge on the fuel film radially from

both sides. The maximum diameter of the injector, at the outer aircap, is 23.8 mm (0.938 inches). As in the case of the air admission modules, the three mount lugs are used to attach the injector to the front face of the bulkhead. Fuel feed to the injector is through individual steel tubes connecting to the capped fitting on the side of the injector body.

Figure 4-21 shows the assembled bulkhead with air admission modules and fuel injectors installed. This assembly fits directly into the rectangular front end of the sector liner assembly of Figure 4-17.

Prior experience with a predecessor Mark IV combustor sector under a company sponsored concept development program indicated that the stabilization of the torroidal recirculation zones in the pilot was critical to the operation of the combustor. For this reason, the louvers on the forward part of the combustor liner were reversed so as to discharge their effluent upstream toward the bulkhead to reinforce the recirculating flow in the primary zone by augmenting the rotary motion imparted by the primary swirler. Figure 4-22 shows a cross-section through the bulkhead revealing its double walled construction with cooling air flowing transversely between the walls before discharging as a film at the end of a panel. As shown on Figure 4-16, the direction of the cooling air flow is reversed on the opposite side of the bulkhead and reinforces the local rotation induced by the primary swirler vanes when they are all clockwise oriented.

The combustor airflow distribution shown on Figure 4-16 is representative of that in most configurations evaluated and is that experimentally observed in Configuration M-1, the first configuration evaluated under this program. Relative to the reference PW2037 production combustor and the variable geometry burner, the length of the Mark IV combustor at 178 mm (7.0 inches) is considerably more aggressive. The nominal penetration of the secondary swirler tube in the combustor is 51 mm (2.0 inches), but this distance was also varied during configuration changes.

Early test experience with this combustor under a company funded program revealed that the bulkhead cooling system did not contribute significantly to the stabilization of the pilot recirculation zone, and that the preferred arrangement for the primary zone air swirlers was alternating direction of rotation in adjacent modules as shown on Figure 4-23, rather than all clockwise as originally defined in Figure 4-16. This led to the definition of different combinations of operational fuel injectors in the combustor identified as operating Modes A, B and C.

In mode A, all four injectors were fueled while only injectors 2 and 4, (identified in Figures 4-16 and 4-23) were operational in Mode B. Mode C consisted of operation on Injectors 1 and 3. Relating the injector positions to the direction of rotation of the primary swirlers on the air admission modules in Figure 4-23 indicates that the vortical flows induced by the primary swirler flow tend to move the fuel from Injectors 2 and 4 (Mode B) in the transverse direction, while these flows tend to spread the fuel from Injectors 1 and 3 (Mode C) in the radial direction between the modules. These injection modes were found to have a significant effect on combustor performance and were a test variable in many of the configurations evaluated.

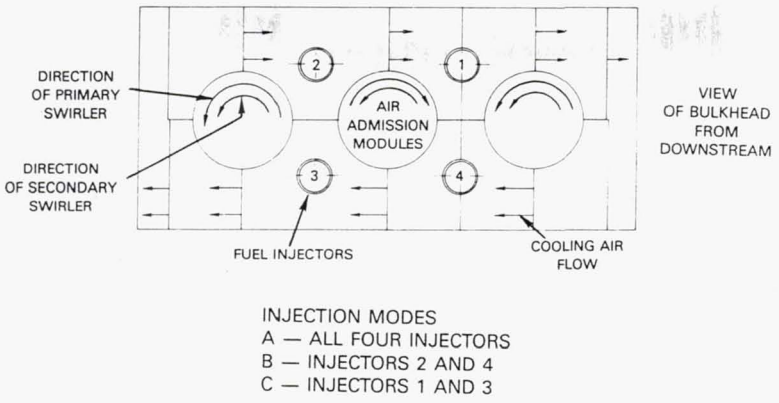

Figure 4-23 Fuel Injector Operating Modes Used During Evaluation of Mark IV Combustor.

The sequence of direction of rotation of the primary and secondary swirler vanes was not changed from that of Figure 4-23 in any of the combustor perturbations evaluated under this program. The nominal vane turning angle of the secondary swirlers was also maintained unchanged at 40° off axial in all configurations.

4.3.3 MARK IV COMBUSTOR MODIFICATIONS

A total of thirteen perturbations of the Mark IV combustor concept were evaluated during the Phase II program. The modifications evaluated are listed on Table 4-3 and are categorized in groups consisting of:

1. Use of different types of bulkhead mounted fuel injectors,
2. Geometric variations to influence primary zone flow structure,
3. Secondary swirler immersion,
4. Secondary swirler centertube airflow,
5. Secondary swirler vane angle distribution,
6. The use of an advanced technology liner cooling approach, and
7. The use of a duplex or staged fuel distribution system.

The basic test program was conducted in two elements. The first element consisted of the evaluation of Configurations M-1 through M-6 and culminated in the test of Configuration M-7, which was a demonstration of the aggregate of the best features established through that point in the program. Examination of Table 4-3 indicates that the initial element of the program involved screening of a number of combustor design parameters. Several of these parameters, including the primary swirler vane angle, secondary swirler immersion and centertube airflow were found to have distinct optimums and were maintained at that level while perturbations to other parameters were assessed. The second element of the programm, involving the evaluation of Configurations M-8 through M-13 was characterized more by evaluation of individual potential improvements, rather than systematic optimization, and the assessment of the long term potential of the Mark IV concept.

TABLE 4-3
MARK IV COMBUSTOR TEST CONFIGURATIONS

Combustion	Bulkhead Fuel Injectors: Airblast Type	Bulkhead Fuel Injectors: Modes Evaluated	Primary Swirler Angle	Secondary Swirler: Immersion mm (in.)	Secondary Swirler: Angle Distribution	Secondary Swirler: Centertube Flow Area	Pilot Zone Liner Construction	Other Features
M-1	Low Airflow	A, B, C	60°	51 (2.0)	Free Vortex	100%	Louver	Bulkhead Cooling Air about 6% Wab
M-2	High Airflow	A, C	60°	37.6 (1.5)*	Free Vortex	100%	Louver	
M-3	High Airflow	A, B, C	60°	37.6 (1.5)*	Free Vortex	0%	Louver	Bulkhead Cooling Air Reduced to about 3% Wab*
M-4	High Airflow	A, B, C	60°	37.6 (1.5)*	Free Vortex	35%*	Louver	
M-5	High Airflow	A, B, C	75°*	37.6 (1.5)*	Free Vortex	35%	Louver	
M-6	High Airflow	A	75°*	37.6 (1.5)*	Linear	35%	Louver	
M-7	High Airflow	A	75°*	37.6 (1.5)*	Free Vortex	35%	Segmented*	
M-8	Flat Spray	C	75°*	37.6 (1.5)*	Free Vortex	35%	Segmented*	
M-9	High Airflow	A	75°*	37.6 (1.5)*	Linear	35%	Segmented*	Trip Rings on Secondary Swirler Tubes
M-10	See Other Features	A	75°*	37.6 (1.5)*	Linear	35%	Segmented*	High Airflow Injectors at Locations 1 & 3, Reduced Spray Angle at 2 & 4
		Configurations with Fuel Injectors in Secondary Swirler						
M-11	High Airflow	C	75°	37.6 (1.5)	Linear	0%	Segmented	Spray Angle of Secondary Fuel Injectors = 90°
M-12	High Airflow	C	75°	37.6 (1.5)	Linear	0%	Segmented	Spray Angle of Secondary Fuel Injectors = 65°
M-13	High Airflow	C	75°	37.6 (1.5)	Free Vortex	0%	Segmented	Spray Angle of Secondary Fuel Injectors = 90°

* No subsequent change to this variable unless indicated otherwise.

The remainder of this section includes a description of the variations of the Mark IV combustor evaluated and the rationale for their selection.

Bulkhead Fuel Injector Variations

As indicated in Section 4.3.2, the four bulkhead mounted fuel injectors, one of which is shown in Figure 4-20, were essentially miniature versions of the single pipe airblast type injector used in the reference PW2037 production combustor with the fuel being atomized by concentric swirling air streams impinging radially on the annular fuel film in the injector. The initial version of these injectors, designated "Low Airflow" on Table 5-3 and used in Configuration M-1, flowed 2.59 percent of combustor airflow through all four injectors. This provided injector air loading ratios (injection airflow/fuel flow) only slightly above unity at takeoff conditions, as opposed to an air loading ratio, in excess of 3 in the reference PW2037 combustor at takeoff; and raised concerns over the ability to atomize the fuel with these injectors. These concerns were substantiated in the testing of Configuration M-1 which demonstrated poor idle performance and could not be operated at power levels above approach because of high liner temperatures caused by injector streaking.

An alternate configuration of this injector was produced which increased the airflow capacity by 60 percent and is designated the "High Airflow" injector on Table 4-3. The increased airflow capacity was achieved by compromising slightly on the swirl angle of the atomizing air, increasing the exit diameter of the outer air cap and the use of thinner swirl vanes in the injectors. While not subjected to the extensive spray characterization of the fuel injectors for the variable geometry combustor, limited spray evaluation indicated that the increase in airflow resulted in only a slight reduction in spray angle - from 80° with the Low Airflow injector to 75° with the High Airflow at a representative idle operating condition - and an improvement in the visual quality of the spray.

The High Airflow airblast bulkhead injectors were introduced in Configuration M-2 and, in conjunction with a reduction in secondary swirler tube immersion, were found to produce improved performance and the capability of operating the combustor to high power levels without overtemperaturing the liner. These injectors were incorporated in subsequent Configurations M-3 through M-7 and M-9, all of which addressed the optimization of other combustor geometric parameters.

A further perturbation of the basic airblast bulkhead fuel injectors was pursued in Configuration M-10. As indicated in Section 4.3.1, the desired fuel injection mode was one which produced a divergent low momentum spray that would be entrained in the pilot combustion zone at low power, but that would also transist to a higher momentum narrower cone angle spray at high power to provide fuel to the secondary combustion zone. The evaluation of prior configurations had indicated that the "High Airflow" injectors were achieving this performance at low power fuel flows but were not capable of producing the transition to a downstream directed spray at high flow rates.

By removing the swirl vanes from the inner passage of "High Airflow" injectors, the airflow capacity of the injector was increased 24 percent and the spray angle reduced to 50° to 55°. In Configuration M-10, two of the four "High Airflow" bulkhead injectors were replaced with these "Reduced Spray Angle" injectors. With reference to Figure 4-23, the High Airflow injectors were installed in locations 1 and 3 because the vortical motion induced by the primary air swirlers would draw the fuel from these injectors between the secondary air swirler tubes, promoting its retention in the pilot combustion zone. The "Reduced Spray Angle" injectors were installed in locations 2 and 4 where the higher momentum spray could be more effectively directed downstream. The combustor was operated only in the A injection mode of Figure 4-23, i.e., all four injectors receiving an equal fuel flow with no attempts to bias the fuel flow from one type of injector to the other as combustor fuel air ratio was changed.

Configuration M-8 incorporated a different airblast fuel injector concept. As shown on Figure 4-24 this approach involved use of two flat spray fuel injectors that protruded through the bulkhead into the pilot combustion zone. Further details of the configuration of the injectors are shown in the photograph of Figure 4-25. The injector body has a rectangular cross-section airflow path with fuel being filmed on the inner radius side of the deflector plate from which it is atomized by the airflow on either side of the plate at the discharge to form a fan shaped spray approximately parallel to the combustor bulkhead. The injectors are installed in locations 1 and 3 so as to direct the fuel spray radially between the secondary swirler tubes in the same direction as the induced rotation caused by the air entering through the primary swirlers in the air admission modules. As the combustor power level is increased from idle to cruise and takeoff, the momentum of the air passing through the injector increases more rapidly than that of the fuel film, atomization is improved and the fuel laden air jet discharging from the injector follows a trajectory that is directed further downstream, as shown on Figure 4-24. This variation in bulk trajectory with power level is consistent with the intent of the Mark IV single stage-dual combustion zone concept.

Pilot Zone Aerodynamic Variations

During evaluation of the Mark IV combustor, several modifications were made to enhance the strength of the recirculating flow in the pilot zone with the objective of improving the stability and efficiency of the combustion process in this zone.

As indicated in Section 4.3.2, the cooling system in the front bulkhead of the combustor had been designed to augment the rotary flow induced by the primary air swirler in the air admission module of the later produced clockwise rotation. However, prior experience in company sponsored tests had indicated superior performance with the alternating direction primary swirler arrangement of Figure 4-23 and all configurations evaluated in this program incorporated the alternating primary swirler sequencing. It was also evident that the directed bulkhead cooling air introduction was not effective in augmenting the pilot zone flow and no attempt was made to reconfigure the cooling system for compatibility with the preferred alternating primary

swirler sequencing. However, to minimize any inhibiting effect, efforts were made to reduce this airflow to a minimum. The initial bulkhead cooling system flowed about 6.3 percent of combustor airflow and when thermal paint applied during the evaluation of Configuration M-2 indicated the bulkhead was running cool, the airflow was reduced in half to slightly over 3.0 percent by plugging half the cooling air inlet holes. This modified bulkhead was first tested in Configuration M-3 and was retained for the remainder of the program without exhibiting any thermal distress.

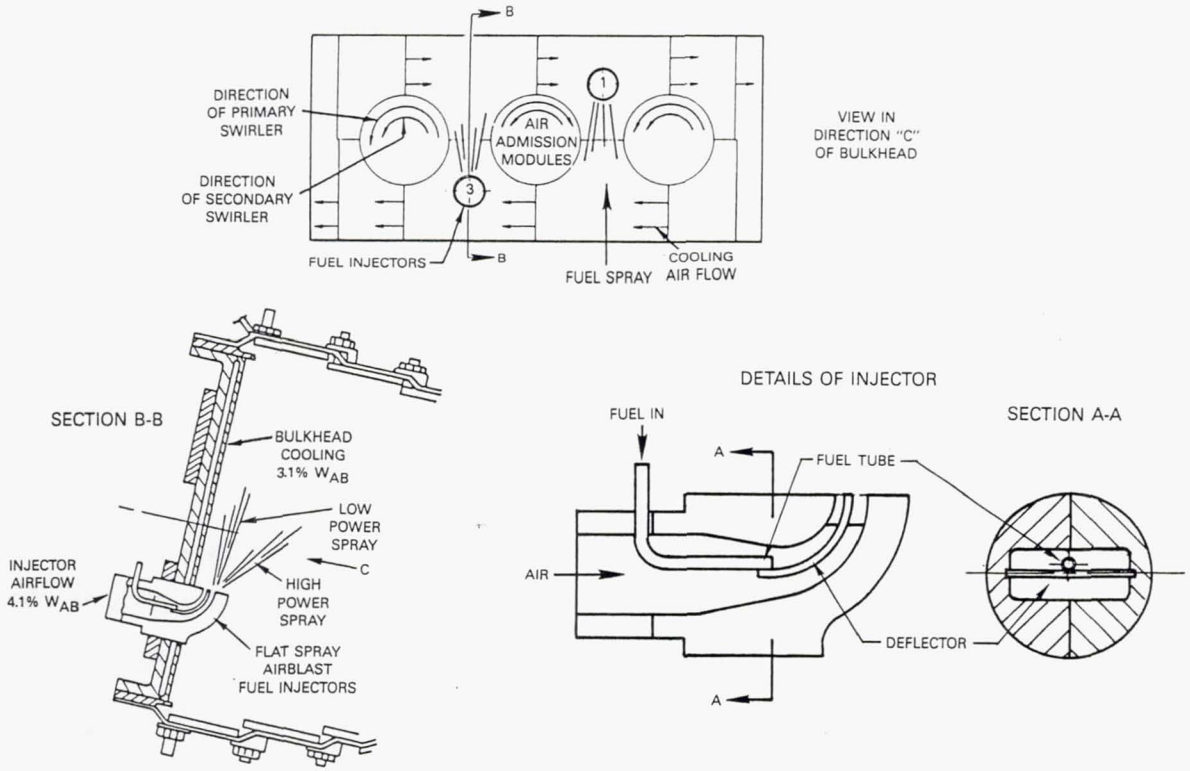

Figure 4-24 Detaills of Configuration M-8 of the Mark IV Combustor with Flat Spray Fuel Injectors.

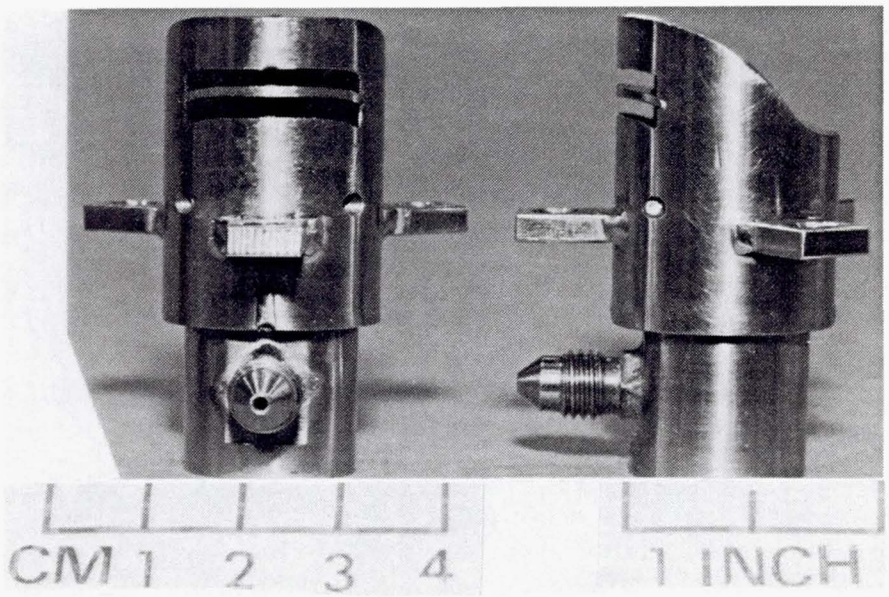

Figure 4-25 Flat Spray Fuel Injector for Mark IV Combustor Configuration M-8.

The effect of primary swirler vane turning angle was investigated in Configuration M-5. Prior configurations had incorporated primary swirler assemblies with vane exit angles of 60° off axial. In Configuration M-5, swirler assemblies with vane exit angles of 75° off axial were installed. The increased air turning reduced the nominal airflow through this component from about 22 to 17 percent of the combustor airflow with the difference being diverted into the secondary swirler. Since this revision led to significant improvement in the lean stability characteristics of the combustor, it was included in all subsequent test configurations.

An additional variation in the pilot zone geometry was made by installing deflectors or trip rings on the outside diameter of the secondary swirler tubes in the air admission modules as shown on Figure 4-26. The rings were installed to interrupt any ejector action caused by the secondary swirler discharge jet that might entrain and prematurely quench products of incomplete combustion from the pilot combustion zone and to deflect the entering flow from the primary swirler into that zone. The trip rings were 6.4 mm (0.25 inches) in radial height and were installed 24.7 mm (0.90 inches) upstream of the end of the secondary swirler tube. The rings were evaluated in Configuration M-9 of the combustor and when they were found to have no significant effect on performance were not used on any subsequent configuration.

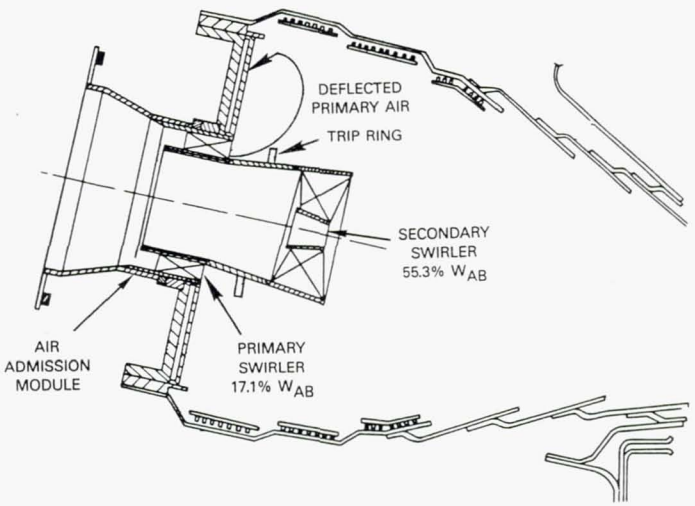

Figure 4-26 Configuration M-9 of Mark IV Combustor with Trip Rings on Secondary Swirler Tube.

Secondary Swirler Tube Immersion

The immersion of the secondary swirler tube into the combustor is an important variable because it dictates, to some extent, the volume of the pilot combustion zone adjacent to the bulkhead, the flow structure in that zone and the length available for the secondary combustion and dilution zone. The initial Configuration M-1 had a swirler immersion of 37.6 mm (2.0 inches) from the bulkhead to the swirler discharge plane into the 178 mm (7.0 inch) long combustor. In Configuration M-2 the immersion was reduced to 37.6 mm (1.5 inches). The shorter swirler tubes had the same inlet and exit radii as

the 37.6 mm (2.0 inch) long tubes, but a more divergent cone angle. The results of the test of Configuration M-2 indicated a significant improvement in performance and the shorter immersion depth secondary swirler tubes were incorporated in all subsequent configurations of the combustor.

Secondary Swirler Centertube Airflow

The secondary swirler tubes on the Mark IV combustor incorporate a small centertube to create a central axial flow at the core of the otherwise swirling jet. The centertube flow was typically 7 percent of combustor airflow out of a total secondary swirler flow of 50 to 55 percent combustor airflow. The axial flow in the center of the jet had been employed to fill the core of the jet as it expanded, and may have helped to prevent vortex breakdown and instability of the swirling jet. A test was conducted in Configuration M-3 in which the centertube was blocked to eliminate the central jet to see if the more rapidly expanding jet might enhance performance. The results of the test indicated that, relative to Configuration M-2 with open secondary swirler centertubes, the low power emissions and lean stability deteriorated and the flame was visibly more erratic at all power levels.

While complete blockage of the secondary swirler centertube appeared to be undesirable, another variation was explored in Configuration M-4. As shown on Figure 4-27, the centertube was partially but uniformly blocked by welding a screen over the centertube inlet. Flow calibration indicated the centertube flow was 35 percent of that in the unblocked tube. The results of testing Configuration M-4 indicated significant improvements in performance relative to the configuration with fully open and fully blocked centertubes, suggesting that an optimum blockage existed. This optimum was not pursued further, but subsequent configurations of the combustor incorporated that 35 percent flow area swirler centertube.

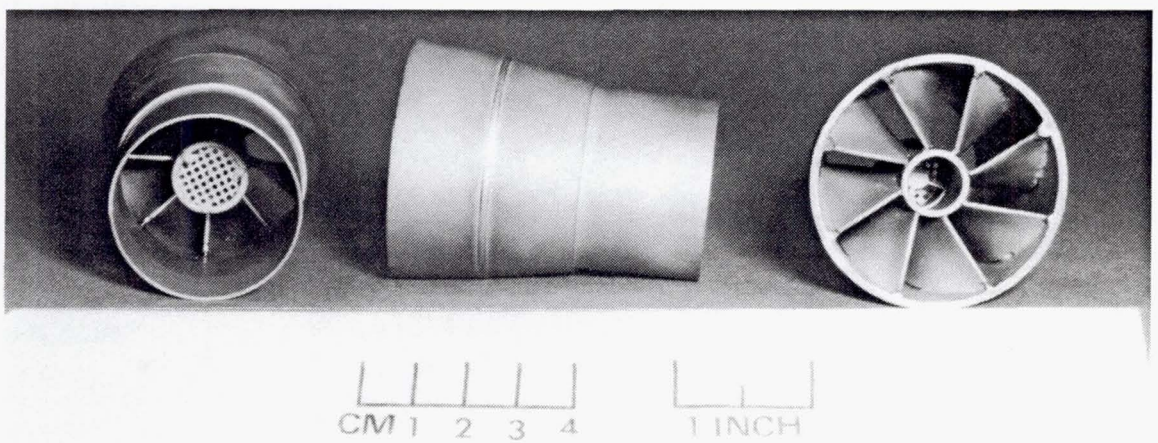

Figure 4-27 Secondary Swirler Tube with Blockage Screen on Center Tube Inlet.

Secondary Swirler Vane Angle Distribution

While all of the secondary swirlers used in the test combustor produced counterclockwise rotation of the flow and had nominal vane discharge angles of 40° off axial at the area mean average radius, two types of swirlers having different radial distribution of turning angle were evaluated.

The majority of the combustor configurations incorporated swirlers with a free vortex tangential velocity distribution (Tangential velocity x radius = constant). The vanes in this type swirler had a larger turning angle at the root than at the tip. A second set of swirlers were designed to produce a linear increase of vane exit angle with increasing radius. Table 4-4 shows the radial variation of vane exit turning angle and indicates that the linear angle distribution swirler produces a much higher swirl at the outer radii of the jet and very little angular momentum near the core, whereas, the reverse situation occurs in the free vortex swirler. Use of the linear angle distribution swirler would be expected to produce a higher degree of centrifugal instability mixing of the secondary jet with the pilot zone combustion gases, but that there would be much less intense centrifugal mixing further downstream in the combustor where the process was driven by the low angular momentum core of the secondary jet. The converse would occur with the free vortex swirler in that the initial mixing would be more moderate, but the uniform angular momentum distribution across the jet would enhance centrifugal mixing further downstream.

TABLE 4-4
SECONDARY SWIRLER EXIT ANGLE DISTRIBUTION

Vane Exit Angle From Axial	Free Vortex	Linear
Root	67°	14°
Mean	40°	40°
Tip	31°	55°

All of the earlier test configurations, through Configuration M-5, incorporated the free vortex secondary swirlers in the air admission modules. Linear angle distribution swirlers were evaluated in Configuration M-6 but were found to have an adverse effect on low power emissions, suggesting that the more intense initial mixing between the pilot combustion products and the secondary swirler airflow was not desirable. Consequently, the free vortex swirlers were reinstalled in Configurations M-7 and M-8. For continuity of reference, the free vortex swirlers would have been retained through the remainder of the program, but these parts were damaged in a hot shutdown at the conclusion of testing Configuration M-8. For expediency, the linear vane angle swirlers were used in several subsequent configurations as shown on Table 4-3 until replacement free vortex swirlers could be fabricated.

Liner Cooling Technology

Configurations M-1 through M-6 of the Mark IV combustor incorporated a film cooled liner with the louvers being directed upstream on the walls, enclosing the pilot combustion zone as shown on Figure 4-16. The cooling air flow to these reverse flow louvers, nominally totaling only about 10 percent of the combustion air for all louvers upstream of the joints in the inner and outer liner, was set at this low level to simulate the use of an advanced technology more effective liner cooling concept intended to be incorporated in later configurations of this combustor. This approach was acceptable in this program because these early test configurations were evaluated in a facility that was limited to operating pressures of 1.52 MPa (220 psia) or about half that encountered in the PW2037 engine at takeoff. Consequently, the pilot zone liners never experienced the peak heat load and could survive the relatively short duration exposure in this facility with the lower cooling effectiveness of the reversed louvers.

However, Configurations M-7 through M-13 were tested in a different facility that was capable of operating at pressure levels up to more than 85 percent of the PW2037 engine combustor inlet total pressure at takeoff, and liner survival dictated that the advanced technology liner concept be incorporated in this zone for these tests.

Figure 4-28 shows the basic features of this liner construction which consists of axial rows of cast segments mechanically attached to a sheet metal liner shell. In a full annular combustor, the segments would subtend arcs of 10 to 30 degrees depending on the diameter of the liner and would be installed in a staggered sequence as shown. Retention to the shell is by nuts on threaded studs that are cast integral with the segments. The segments can be cast from more brittle high temperature turbine airfoil alloys because they do not have to sustain high circumferential and buckling stresses requiring the use of more ductile metals in more conventional liner constructions.

The segmented liner is cooled by admitting air through a circumferential row of holes in the support shell to impinge on the rear surface of the segment, and flow axially upstream and downstream behind the segment. The segment is cast with pin fin extended surfaces on the rear to augment convective heat transfer to the cooling air. When the cooling air discharges from under the segment it becomes part of a cooling air film on the gas side surface of a segment. Depending on the radial stepping of the axially adjacent segments, this air either discharges over the surface of an adjacent segment or is entrained by the effluent from an adjacent segment to become part of the film on its gas side surface. The net effect is a strong convective cooling mode on the rear surface of the segment combined with film cooling of the gas side surfaces that leads to significantly higher overall cooling effectiveness than the conventional film cooled liner.

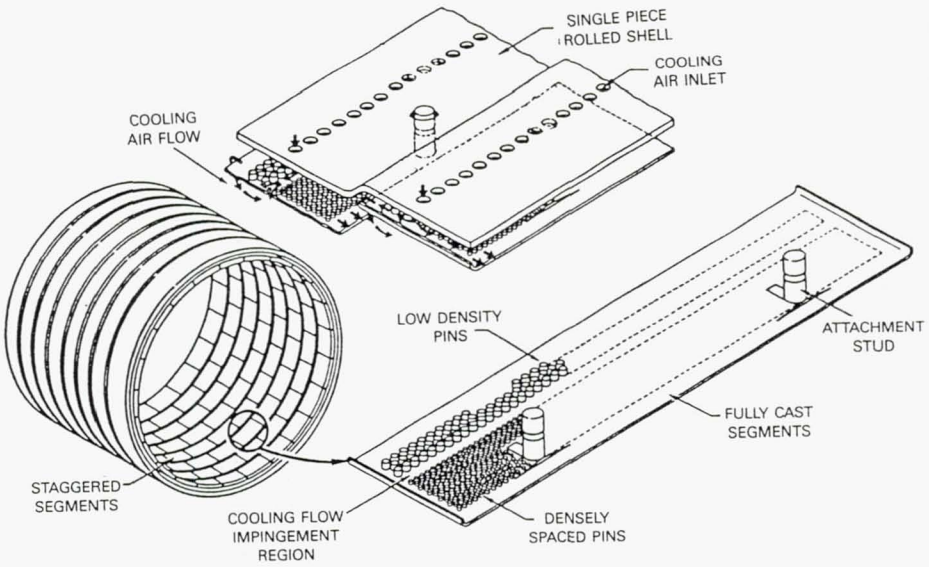

Figure 4-28 Segmented Liner Construction.

Figure 4-29 shows a cross-section of the upstream part of the outer liner of the Mark IV combustor showing the details of the installation and cooling air flow behind the segments while Figure 4-30 shows the segments installed in the test combustor shell. This photograph also shows the details of the pin-fin array on the rear surface of one of the flat segments used at the first two positions. The segment has a transverse strip devoid of pins on which the cooling air passing through the holes in the shell impinges. Downstream of the coolant inlet is a short region of low density pins while the longer upstream part of the segment has higher density smaller diameter pins. The lower flow resistance of the short low pin density downstream section promotes most of the coolant flow to discharge in that direction. In the two segments nearest the bulkhead, this cooling air is deflected by the radial step in the shell and the upstream end of the downstream segment into the forward direction to form the desired upstream flow of cooling air on the gas side faces of these segments.

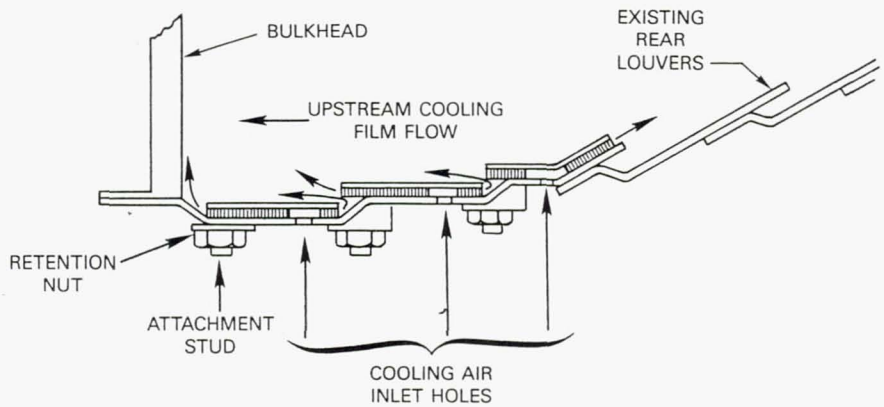

Figure 4-29 Details of Segmented Liner in Pilot Zone of Mark IV Combustor.

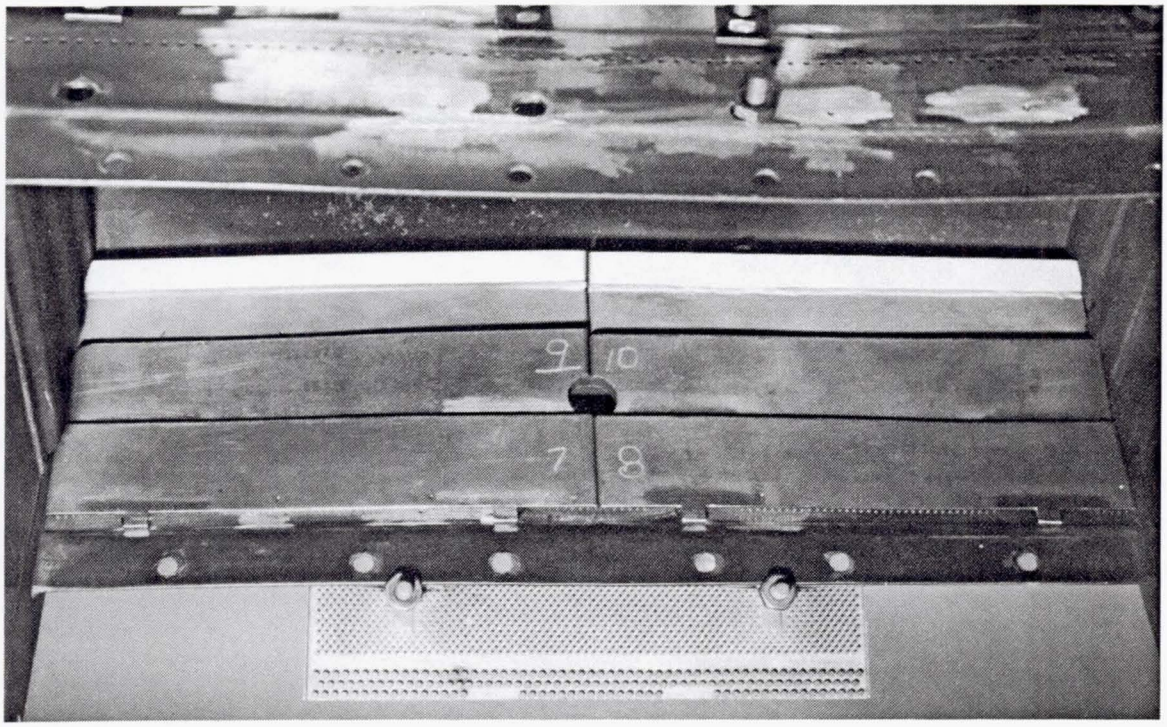

Figure 4-30 Segmented Liner in Mark IV Combustor Sector Rig.

The third segment provides the transition between upstream and downstream directed liner cooling air and also accommodates the bend in the liner contour. It was fabricated by welding parts of two segments to produce the bend. The cooling air impingement region is at the bend and the upstream and downstream portions of the segment have high pin density so as to produce an equal airflow split in both directions. This segment is cooled entirely by the rear surface convection and has no surface film cooling.

Duplex Fuel Systems

Following the evaluation of Configurations M-1 through M-10, it was evident that while the Mark IV combustor concept was achieving some of the program goals, its performance was not consistent with the expectations outlined in Section 4.3.1. It was also apparent that one of the most significant departures was the inability of the fuel injection system to function in a varying mode with fuel flow rate as described in that section. None of the conventional airblast type injectors used in the combustor produced the desired fuel spray - flow rate characteristics. While the flat spray injectors of Configuration M-8 apparently did produce some variation in spray direction with flow rate, their use also led to serious overtemperaturing problems. It was evident that the production of injectors with the desired spray variation characteristics would in itself require an extensive development effort beyond the scope and schedule of this program. Consequently, the last few configurations evaluated in the program were directed at demonstrating the potential of the Mark IV combustor. Specifically, since the fuel systems evaluated were incapable of supplying fuel to both the pilot and secondary combustion zone from a single source, a duplex or staged system would be employed to provide this distribution artificially.

The approach selected is shown on Figure 4-31 and consisted of installing a small hollow spray cone pressure atomizing fuel injector in the centertube of each of the three secondary swirler tubes in the test combustor. Operating the combustor on two "High Airflow" airblast injectors in the bulkhead provided fuel to the pilot combustion zone while the injection in the secondary swirler tube was used at higher power levels to spray fuel into or radially across the swirling secondary air jet into the pilot discharge - secondary air juncture where the second stage of combustion was to be sustained at high power. In effect, the approach was a fallback to the staged type of fuel system that is considered an undesirable design approach for combustors operating on broadened properties fuels. However, these configurations were not considered candidates for concept evolution but rather artifacts for simulating the potential of the Mark IV concept.

A total of three configurations were evaluated with this duplex or staged type fuel system. The spray angle of the secondary fuel injectors was varied between 90° and 65° in Configurations M-11 and M-12 while free vortex rather than linear secondary swirler vane angle distribution was evaluated in Configuration M-13. Figure 4-32 shows air admission modules with the secondary fuel injectors mounted in the swirler centertubes.

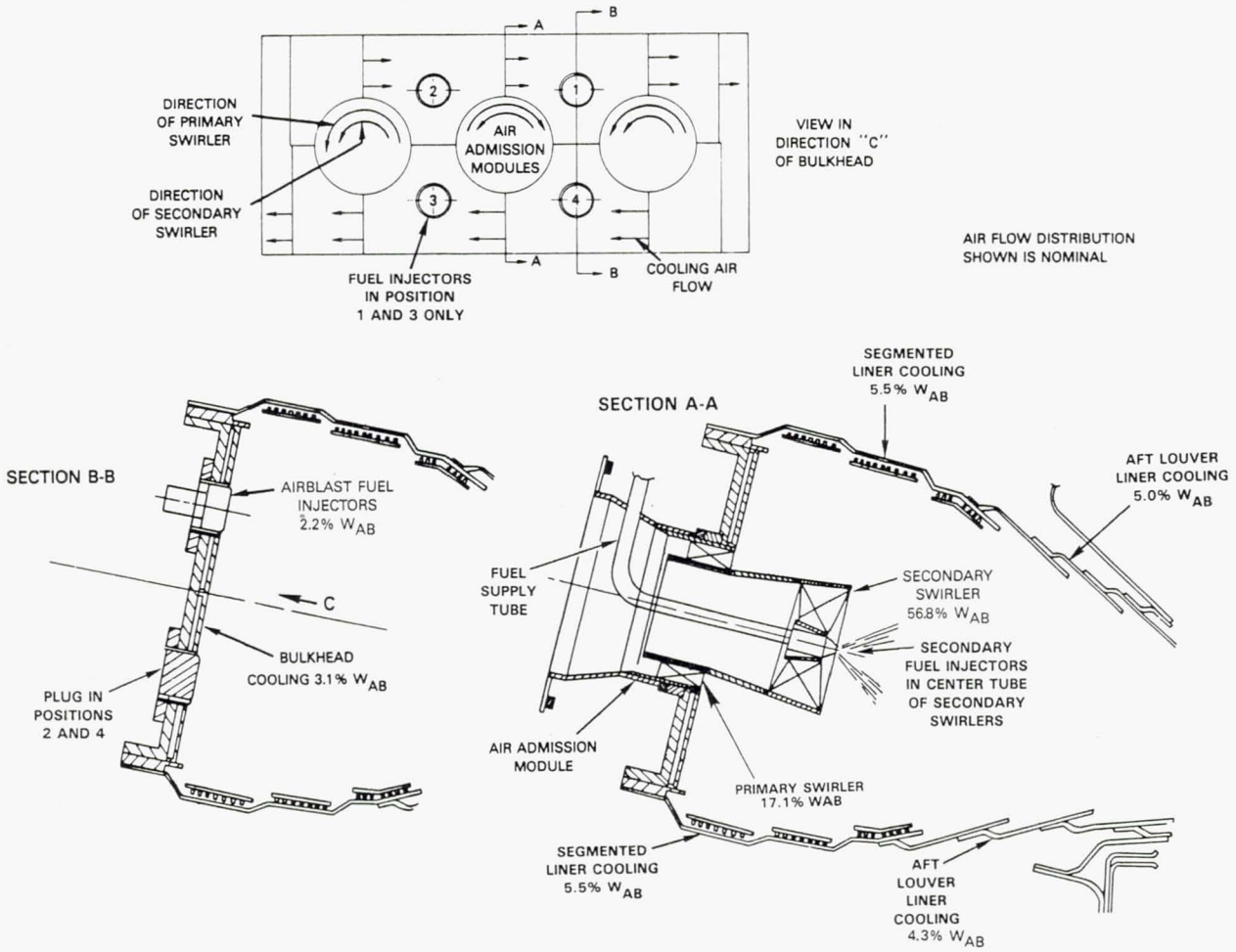

Figure 4-31 Details of Configuration M-11 Through M-13 of the Advanced Mark IV Combustor.

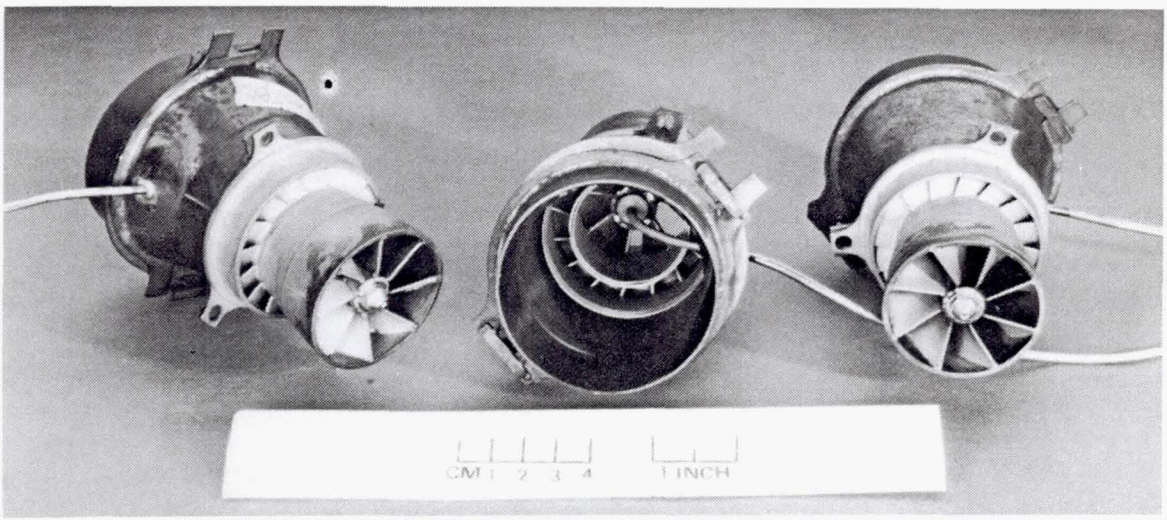

Figure 4-32 Mark IV Combustor Air Admission Modules with Fuel Injector in Secondary Swirlers Center Tube.

SECTION 5.0

EXPERIMENTAL APPARATUS

This section contains the results of analysis of the physical and chemical properties of the test fuels used during the evaluation of the combustor concepts. Also included are descriptions of the test rigs, instrumentation, and the test facilities employed in the program.

5.1 TEST FUELS

Four different test fuels were used during the program. The principal test fuel was Experimental Referee Broad Specification (ERBS) fuel, which was used in the evaluation of every combustor configuration. The majority of the configurations was also evaluated with commercial Jet A fuel at selected operating conditions. Two additional fuels were used in limited quantities to extend the range of fuel composition during the more critical tests of the initial and final configurations of each combustor. One of these was produced by adding a blending stock to the ERBS fuel to reduce its hydrogen content from a nominal level of 12.9 percent to 11.8 percent. The fourth test fuel was a No. 2 commodity fuel similar to that used for domestic heating in the New Engine area and having a hydrogen content of 12.25 percent.

The ERBS and the 11.8 percent hydrogen content blended fuel was procured by NASA from Suntech, Inc. of Marcus Hook, PA. These fuels were surplus from the Phase I Broad Specification Fuel Combustion Technology Program as a result of test procedure economies accomplished during that program. The ERBS and 11.8 percent hydrogen fuels were blended to final proportions at the refinery and delivered to the Pratt and Whitney test facility in Middletown, CT, in single lots. Both of these fuels were stored in dedicated tanks in the tank farm near the test facility over the duration of the Phase I and Phase II programs. These tanks were drained and steam cleaned before the test fuel was delivered.

The fourth test fuel used during Phase I of the Broad Specification Fuel Combustion Technology Program was a second mixture of ERBS and blending stock in which the proportions were selected to produce a fuel hydrogen content of 12.3 percent. In planning the Phase II test program, this fuel was replaced by the No. 2 Commodity fuel. The primary reason for this change was to investigate the effect of a low hydrogen content fuel that was also less volatile and substantially more viscous than the Jet A or ERBS fuel. Operation with this fuel could produce more pronounced effects on the low power emissions output, ignition and stability than the 11.8 percent hydrogen blend. It also provided the opportunity to evaluate a more representative refinery product relative to the blended fuels of comparable hydrogen content. The No. 2 Commodity fuel was purchased from a local distributor. While the desired property ranges for this fuel had been established, vendors could not assure retention of a particular lot or avoid co-mingling while samples were analyzed extensively. Consequently, the available sources were screened on the basis of specific gravity, and when one source was found to be in the appropriate range, i.e, 86. to .87, a sample was obtained for analysis of its hydrogen content, viscosity and volatility upon which the decision to procure was made. This fuel was stored in a rented tanker

trailer which had been drained and steam cleaned prior to loading with the test fuel. The trailer was parked next to the X-902 high pressure test stand at the Middletown, CT, facility from which it could be connected directly to a hydrant entering the test stand fuel system.

The Jet A fuel was supplied from the standard source at each test facility. The Jet Burner Test Stand at United Technologies Research Center had its own dedicated tank for Jet A fuel that only had to be refilled once during the course of the testing. The high pressure X-902 test stand at Middletown, however, drew Jet A fuel from a large tank farm supplying the entire facility. Since the properties of fuel drawn from the farm could vary over the duration of the test activity, samples were obtained periodically to monitor their variation.

All of the samples of the test fuels were analyzed in the Materials Engineering Research Laboratory at the Pratt and Whitney Middletown test facility. Extensive analyses were conducted to determine the physical properties and chemical composition of the four test fuels and additional analyses of a more limited scope were conducted on samples of the Jet A fuel used in the various test facilities over the duration of the test program. The results of these analyses are presented in this section.

5.1.1 Test Fuel Properties

Table 5-1 shows the results of the analyses of the composition and properties of the test fuels that were used in all of the combustor tests. The analysis of the Jet A is of the fuel that was being used in the high pressure X-902 test facility at the time the variable geometry combustor Configuration V-8 was evaluated. The table also lists the American Society for Testing and Materials (ASTM) Standard Procedure used to measure the indicated property. In general, the procedure is that stipulated in the ASTM D1655 specification for Jet A fuel. However, in the case of a few parameters, alternate analytical methods were preferred and are indicated in this table. The distillation temperature distribution of the test fuels is plotted on Figure 5-1.

The ERBS and 11.8 percent hydrogen blended fuels were stored for nearly three years since their delivery for use in the Phase I program, and their storage stability was reviewed before being used in Phase II. A sample of both fuels was drawn and found to be visibly clear. The existent gum content had increased from less than 1.0 mg/100 ml when procured to 11.6 and 33.5 mg/10 ml for the ERBS and 11.8 percent hydrogen, respectively. While the ASTM D1655 specification for Jet A fuel stipulates a maximum gum content of 7mg/100 ml, these levels are not excessively high and certainly would not compromise the operation of the test facility fuel system components or the rig fuel injectors. Measurements were also made of the most important compositional and physical properties of the ERBS fuel for comparison with similar data obtained when the fuel was first delivered. This comparison is shown on Table 5-2 and indicates that any changes in compositional or physical properties were within the experimental uncertainty in the measurement.

Table 5-1

Properties of Test Fuels

Composition	Jet A*1	ERBS *2	No. 2 Commodity	11.8% Hydrogen *2	ASTM Procedure
Aromatic content, % vol.	20.0	30.4	39.8	52.2	D1319
Napthalene content, % vol.	1.57	11.9	15.3	15.4	D1840*3
Olefin content, % vol.	0.3	0.2+	0.7	0.2	D1319
Sulfur content, % vol.	0.05	0.04+	0.18	0.18	D3120
Hydrogen content, % wt.	13.68	12.88	12.25	11.80	*4
Hydrogen/Carbon Ratio	1.89:1	1.76:1	1.66:1	1.59:1	*4
Physical Properties					
Viscosity, cs. @ 249°K (-10°F)	6.54	8.57+	*5	6.48	D445
@ 299°K (80°F)	1.89	2.16	3.29	1.82	
@ 338°K (150°F)	1.07	1.19+	1.62	1.06	
Surface Tension, dynes/cm @ 298°K (77°F)	29.9	30.3+	32.6	30.8	D971
Gravity, °API, 289°K (60°F)	41.5	36.9	31.4	32.6	D1298
Specific Gravity, 289/289°K (60/60°F)	0.8181	0.8403	0.868	0.8623	D1298
Heat of Combustion, MJ/kg, Net	43.03	42.61	42.21	41.97	D2382
Gross	-----	45.37	44.81	44.47	
(Btu/lb) Net	(18,520)	(18,330)	(18,170)	(18,060)	
Gross	-----	(19,540)	(19,280)	(19,140)	
Flash Point, °K (°F) Open Cup	338 (148)	347 (165)+	360 (188)	336 (145)	D92
Closed Cup	323 (124)	318 (114)+	338 (150)	311 (100)	D93
Freezing Point, °K (°F)	223 (-57)	243 (-21.1)+	255 (0.0)	244 (-20.2)	D2386
Smoke Point, mm	20	14	11	9	D1322
Distillation					
Temperatures, °K (°F) Initial	418 (329)	428 (348)	450 (352)	420 (297)	D86
10%	460 (370)	472 (392)	483 (410)	447 (346)	
20%	468 (384)	480 (406)	497 (406)	459 (368)	
30%	476 (396)	487 (418)	510 (459)	471 (389)	
40%	481 (407)	494 (430)	522 (480)	485 (414)	
50%	487 (418)	500 (441)	533 (500)	498 (438)	
60%	493 (430)	509 (456)	545 (522)	511 (461)	
70%	495 (443)	518 (472)	555 (545)	524 (484)	
80%	510 (459)	532 (498)	573 (572)	539 (512)	
90%	523 (482)	556 (540)	594 (610)	561 (551)	
Final	555 (540)	599 (619)	623 (662)	603 (626)	
Recovery, % vol.	99.0	98.0	98.2	98.5	
Residue, % vol.	1.0	1.3	1.8	1.0	
Loss, % vol.	0.0	0.7	0.0	0.5	
Carbon Residue 10% Bottoms, % wt.	0.16	0.19+	0.39	0.24	D524

*1: Jet A analysis is for sample obtained at high pressure facility during test of Configuration V-8.

*2: Data on 11.8% Hydrogen and properties of ERBS marked with (*) from analysis conducted during Phase I program.

*3: Specification D-1840 modified for napthalene contents above 5% volume.

*4: Perkin-Elmer Model 240 Elemental Analyzer.

*5: 11.04 cs at 261°K (10°F).

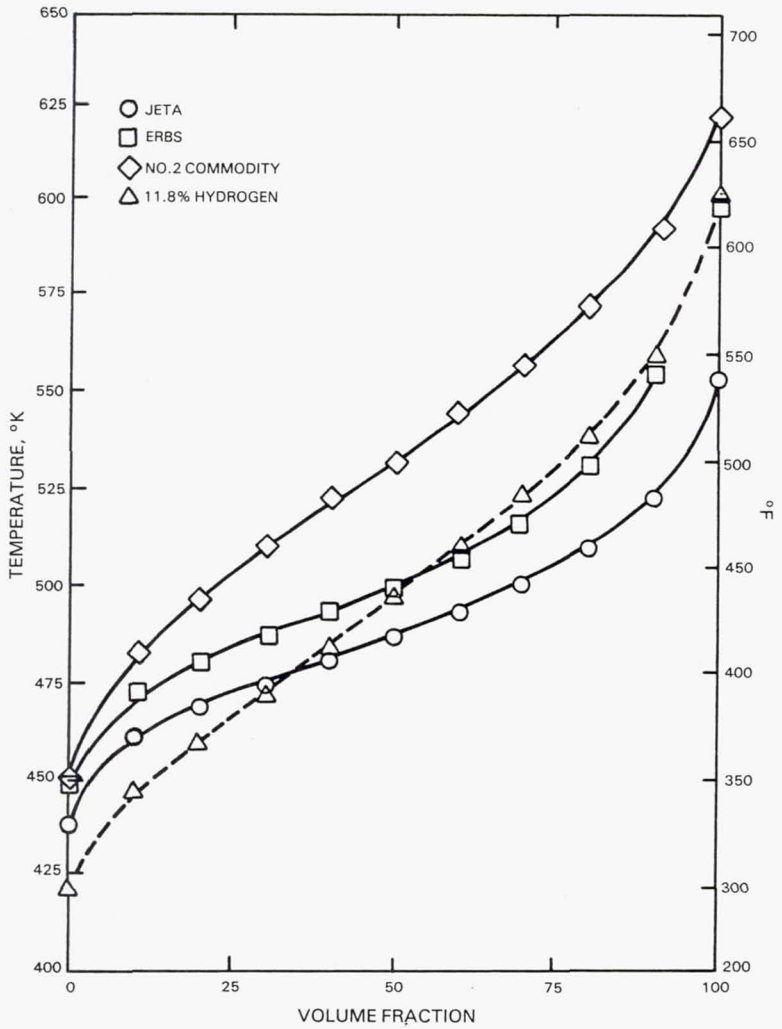

Figure 5-1 Distillation Characteistics of the Test Fuels.

Table 5-2

COMPARISON OF ORIGINAL AND CURRENT PROPERTIES OF THE ERBS TEST FUEL

	Phase I	Phase II	ASTM Procedure
Date of Analysis	Sept 1980	March 1983	
Composition			
Aromatic Content - % vol	31.5	30.4	D1319
Napthalene content - % vol	11.7	11.9	D1840 *1
Hydrogen content - % wt	12.93	12.88	*2
Hydrogen/Carbon Ratio	1.77:1	1.76:1	*2
Physical Properties			
Viscosity, cs. @ 299°K (80°F	2.16	2.16	D445
Gravity, API, 289°K (60°F)	36.9	36.9	D1298
Specific Gravity, 289/289°K (60/60°F)	0.8403	0.8403	D1298
Heat of Combustion - MJ/kg, Net	42.59	42.61	D2382
Gross	45.33	45.37	
- (Btu/lb) Net	(18.330)	(18.350)	
Gross	(19,510)	(19,521)	
Smoke Point - mm	12	14	D1322
Distillation			
Temperatures - °K(°F) Initial	422 (336)	428 (348)	D86
10%	471 (389)	472 (392)	
20%	479 (403)	480 (406)	
30%	485 (414)	487 (418)	
40%	490 (423)	494 (430)	
50%	498 (438)	500 (441)	
60%	506 (451)	509 (456)	
70%	514 (466)	518 (472)	
80%	528 (492)	532 (498)	
90%	550 (531)	556 (540)	
Final	594 (611)	599 (619)	
Recovery - % vol	98.5	98.0	
Residue - % vol	1.4	1.3	
Loss - % vol	C.1	0.7	
Stability			
Existant Gums mg/100ml	0.4	11.6	D381

*1 - Specification D-1840 modified for napthalene contents above 5% volume
*2 - Perkin-Elmer Model 240 Elemental Analyzer.

The only exception appears to be a consistent increase in the distillation temperature of 1 to 5°K (3 to 9°F) over the entire boiling range. Because of this lack of significant shifting in the properties of the ERBS fuel, no re-analysis of the 11.8 percent hydrogen fuel was conducted. The properties of this fuel listed on Table 5-1 are those measured during the Phase I program.

The data of Table 5-1 show the particular Jet A fuel analyzed is well within the current ASTM D1655 specification but that the aromatic content at 20 percent by volume and the smoke point at 20 mm are both at the limit of the normal specification. Since 1976, footnotes to the specification have permitted use of Jet A fuels with aromatic contents up to 25 percent volume and smoke points to 18 mm on a reportable basis.

The ERBS fuel was prepared by Suntech, Inc. to approach the limits on critical parameters of the specification established by NASA and consisted of a blend of kerosene and catalytic gas oil. The principal composition controlling parameter in the ERBS specification is the hydrogen content and it was maintained in the desired range of 12.8 ± 0.2 percent. Relative to the Jet A sample, this was accomplished by an increase of the order of ten percent by volume in both the total aromatics and the napthalenes. This implies that the concentration of single ring aromatics in the ERBS is comparable to that in the Jet A, and that the higher level of total aromatics in the ERBS is due primarily to high concentrations of multi-ring aromatics. These shifts in chemical composition was expected to alter the combustion characteristics of the fuel, and this alteration was evident on comparison of the smoke points of the Jet A and ERBS fuel.

Comparison of the distillation temperature characteristics of ERBS and Jet A in Table 5-1 or Figure 5-1 indicates that the boiling temperature of ERBS is about 20 to 28°K (40 to 50°F) higher than that of Jet A at the upper end of the distillation range. However, at low distillation fractions the temperature differential is much smaller, implying comparable volatility. Relative to the specification limit of Table 2-1, the viscosity of the ERBS test fuel was also very moderate and even complied with the specification for Jet A shown on this table. The combination of comparable volatility, and only a moderately higher viscosity of ERBS relative to Jet A, implies that the use of this fuel should not have a profound effect on such atomization and evaporation dependent processes as ignition and combustion stability.

The 11.8 percent hydrogen content test fuel was produced by addition of a blending stock to the basis ERBS fuel. The blending stock consisted of catalytic gas oil and xylene tower bottoms and had an aromatic content in excess of 80 percent. The blend proportions had been selected to produce fuel with nominally one percent lower hydrogen content than the ERBS. As shown in Table 5-1, this required increases of the order of 20 percent volume in the total aromatic content of the fuel. Table 5-1 and Figure 5-1 show that while the addition of the blending stock to the ERBS produced some increases in the distillation temperature of the higher fractions, the dominant effect was a reduction of the distillation temperatures for the early fractions. This resulted in an increase in volatility as evidenced by the lower flash point of the 11.8 percent hydrogen test fuel relative to ERBS. The blending stock also had a relatively low viscosity which produced a lower viscosity of this

fuel relative to ERBS. The combination of volatility and viscosity relates to the ignition and stability characteristics of the combustor, and the trend of both these properties in the ERBS and the blended fuel is toward enhanced ignition/stability with decreasing hydrogen content. This characteristic is counter to expectations in that a shift was expected toward higher distillation temperatures and increased viscosity with the higher aromatic concentrations that produced the reduction in hydrogen content. This phenomena is apparently due to the production of the low hydrogen content fuels by the blending of narrow and unique cuts rather than with a broader distillation of a complete crude.This was the principal reason for the introduction of the No. 2 Commodity fuel oil as the fourth test fuel during the Phase II program. This fuel, shown on Table 5-1, has low end distillation temperatures higher than ERBS, considerably higher flash points and higher viscosity and is considered more representative of a production fuel of this hydrogen or aromatic content.

As indicated previously, the Jet Burner Test Stand (JBTS) at United Technologies Research Center had a dedicated Jet A fuel supply. This supply was replenished only once during evaluation of twelve combustor configurations under this program. Analysis of fuel samples before and after replenishment provided precise definition of the properties of the Jet A fuel used in the testing of each configuration. Conversely, the Jet A fuel used at X-902 high pressure test stand was drawn from a tank farm, affording no opportunity to control the Jet A fuel that was used over the duration of the program. However, the composition and properties of the Jet A fuel were monitored by analyzing samples collected at various times during the course of the test sequence. Table 5-3 presents the results of the analyses of all the Jet A fuel samples. Sample C was obtained during the test of Configuration V-8 in X-902 stand and is the Jet A fuel of Table 5-1. The combustor configurations associated with samples C and D of Table 5-3 were those being evaluated or evaluated immediately before and after the sample was drawn. All of the measured properties are within the ASTM D1655 specification for Jet A fuel and with the exception the aromatic contents of Sample C are reasonably consistent.

5.2 TEST RIG AND INSTRUMENTATION

This section contains a description of the test rig and the instrumentation used in the evaluation of the reference PW2037 combustor and the advanced technology variable geometry and Mark IV combustor concepts.

5.2.1 Test Rig

All of the combustor tests in Phase II of the Broad Specification Fuel Combustion Technology Program were conducted in a PW2037 rectangular sector rig. Figure 5-2 shows a cross section of this rig with the reference PW2037 combustor sector (Configuration V-1) installed while Figure 5-3 shows an overall side view of the rig. The rig consists of six axially stacked cases: the transition duct, inlet flow development duct, prediffuser, fuel injector mount case, combustor case and the exit instrumentation mount case. The nominal transverse width of the gaspath in the rig is 34.7 cm (13.67 inches) but the fuel injector mount and the combustor cases are wider to accommodate combustor endwall clearance and cooling. The inlet transition duct converts

TABLE 5-3
PROPERTIES OF JET A FUEL USED DURING COMBUSTOR RIG TESTS

Sample	A	B	C	D
Test Facility	JBTS	JBTS	X-902	X-902
Configurations Test	V-2 thru V-7 M-1 thru M-3	M-4, M-5 M-6	V-8	M11, M12
Aromatic Content - % vol	18.4	18.5	20.0	17.7
Napthalene Content - % vol	1.46	2.09	1.57	0.4
Hydrogen Content - % wt	13.88	13.63	13.68	13.73
Smoke Point - mm	21.0	21.0	20.0	20.0
Heat of Combustion, Net MJ/kg (BTU/lb)	43.12 (18,560)	43.10 (18,550)	43.03 (18,520)	43.03 (18,520)
Specific Gravity @ 289/289°K (60/60°F)	.8022	.8114	.8181	.8170
Viscosity, CS @ 299°K (80°F)	1.53	1.66	1.89	1.85

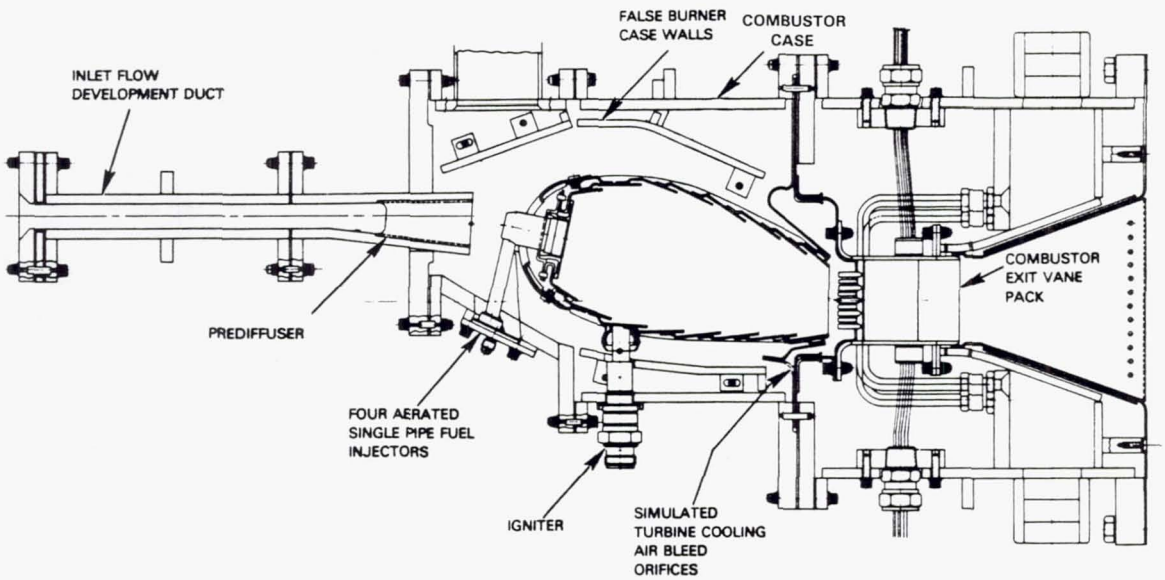

Figure 5-2 PW2037 Segment Combustor Rig with Reference Combustor.

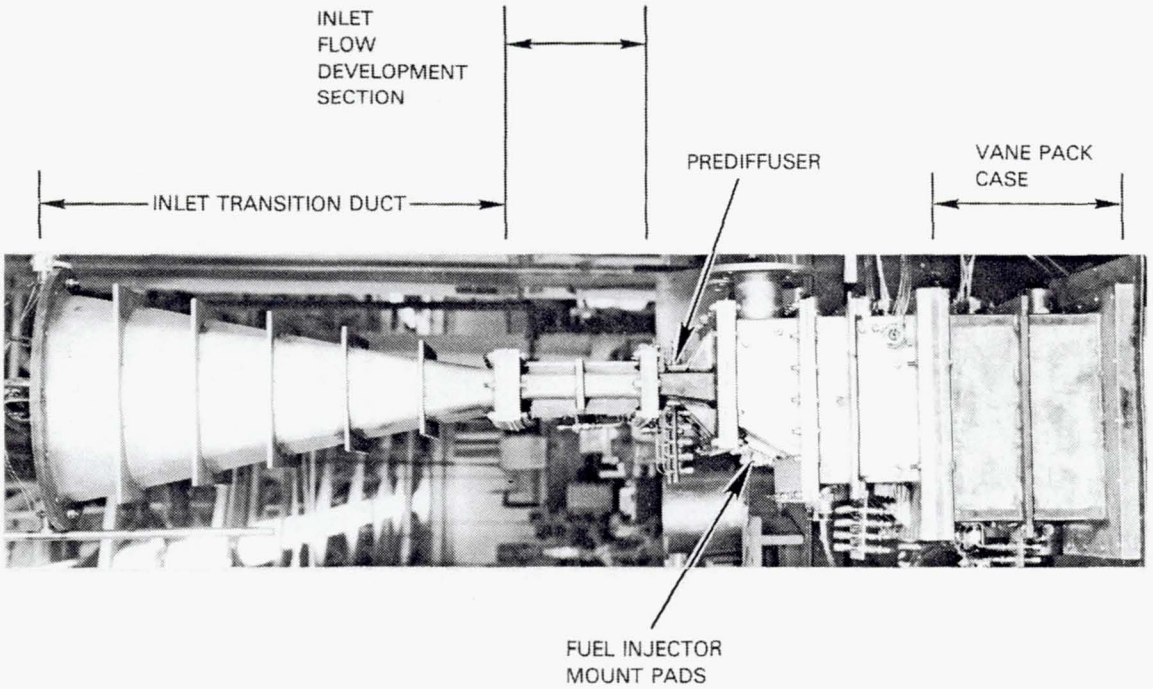

Figure 5-3 Assembled Combustor Rig.

the airflow path from the 30.4 cm (12-inch) diameter of the inlet duct on X-902 Stand to a rectangular gaspath consistent with the prediffuser inlet radial height. The flow development duct serves as a settling section after the inlet transition and provides for velocity profile development before the flow enters the prediffuser. If desired, screens could be trapped between the upstream flanges of this duct to induce distortions in combustor inlet flow. Three different prediffuser sections were used in the rig depending on the type of combustor being evaluated. When the reference PW2037 combustor, Configuration V-1, was being tested, a cascade prediffuser section with three struts spaced transversely between the four fuel injectors was employed. The diffuser geometry, i.e., area ratio and length to height ratio were consistent with the PW2037 engine configuration scaled to the 90 percent of gaspath radial height. When the variable geometry combustor concept, Configurations VG-2 through VG-8, was being evaluated, another prediffuser was incorporated. This diffuser section did not have any struts to preclude the possibility of strut wakes interfering with the flow of air into the variable geometry air valves on the combustor hood. To compensate for the lack of strut blockage, the diffuser wall included angle and exit height were decreased to produce the same exit Mach number as the cascade diffuser used with Configuration V-1. The third prediffuser section had been designed for use exclusively with the Mark IV combustor sector. As indicated in Section 4.3, when the Mark IV combustor was designed, it was considered important that the geometric parameters defining the front end of that combustor duplicated those of the PW2037 engine as closely as possible. Scaling up to the full radial height of the combustor required a ten percent increase in the airflow per unit width in the combustor to maintain the correct reference velocity. To accommodate this increase in airflow while maintaining the same diffuser exit Mach number, this prediffuser had a proportionately higher area ratio. It was also a cascade type diffuser and incorporated two struts for compatibility with the three air admission modules on the Mark IV combustor sector.

The fuel injector mount section enclosed the dump volume upstream of the combustor. When the reference PW2037 and variable geometry combustor configurations were being evaluated, the four fuel injectors were mounted on the outer wall of this case. When the Mark IV combustor was installed in the rig this section enclosed the prediffuser end cap with the integral shroud air diffuser and the ducts to the three air admission modules on the combustor bulkhead. The combustor case enclosed the combustor liner proper and was also common to all of the combustor configurations evaluated. Both the combustor case and the fuel injector mount case incorporated false walls to simulate the contours of the diffuser and burner cases of the PW2037 engine.

The final module in the rig assembly was the exit instrumentation case which contained an array of twelve air cooled transversely spaced vanes. Gas temperature thermocouples and gas sampling - total pressure sensing probes were mounted on eight of these vanes.

The combustor liner assembly was positioned in the combustor case by trapping a flange on the downstream end of the liner between the combustor case and the exit instrumentation case of the rig as shown on Figure 5-2. Holes drilled through the flange on the combustor liner permitted the bypassing of air into the exit instrumentation case to simulate turbine cooling air extraction from the combustor shroud passages. The mount flanges and turbine bleed holes can be seen on the photographs of the combustor lines assemblies in Figures 4-1 and 4-17. The reference PW2037 combustor sector and the variable geometry combustor sector fit in the combustor case with nominal gaps of about 2.0 cm (0.8 inches) between the endwalls of the liner sector and the case walls. The endwalls of all of the combustor sectors were cooled by louvers with lips protruding into the gaspath and the cooling air fed from the gap between the sector and case endwalls. A flexible metal seal strip was welded to the endwalls of the reference PW2037 and the variable geometry combustor. This strip pressed against the rig case to inhibit crossflow between the inner and outer shroud passages of the combustor. Details of the endwall construction are shown on several of the photographs of Section 4.0. Figures 4-1, 4-5 and 4-6 show the endwall cooling air inlet holes and the sealing strips, while the lips of the louvers on the inside of the endwalls are visible in Figures 4-13 and 4-17. When the Mark IV combustor was scaled up to the full gaspath size of the PW2037 engine, including only three air admission modules, the combustor sector became narrower than the reference PW2037 and variable geometry combustor and the gaps between the combustor sector and case endwalls increased to about 4.3 cm (1.7 inches). To seal these endwall gaps and preserve the split of airflow between the inner and outer burner shrouds and the apparent combustion gaspath, transverse extensions were attached to the combustor endwall. These extensions approximately replicated the contour of the combustor hood and liner and pressed against the case endwalls to compartment the flow into three passages. The downstream end of the central passage, that adjacent to the combustor proper, was blocked with a perforated plate which was sized to duplicate the pressure drop across the combustor so as to maintain uniform airflow rate across the transverse width of the rig. These transverse endwall extensions, the endwall louver cooling air inlet holes and the perforated blockage plates at the downstream end of the endwalls of the Mark IV combustor sector can be seen in Figure 4-17 of Section 4.3.

The modular construction of the rectangular sector rig was used to protect the integrity of the instrumentation leads during reconfiguration of the test combustor. During teardowns, the rig exit instrumentation case was left mounted on the rear bulkhead of the test chamber with the instrumentation leadouts from the exit vane pack undisturbed, while the remainder of the rig was moved forward to allow the combustor liner assembly to slide out of the combustor case. In addition, both the variable geometry and the Mark IV combustor sector were designed so that the front end of the combustor including the bulkhead could be removed from the front after removal of the prediffuser and fuel injector mount modules to provide access. This permitted making revisions to the front end of the combustor without having to remove the liner proper from the combustor case. The liners were extensively instrumented with thermocouples and this feature eliminated the need for handling the leads from this instrumentation during combustor conversions, thereby promoting its longevity.

5.2.2 Instrumentation

Figure 5-4 shows the instrumentation on the combustor rig which was essentially common for all concepts evaluated. Two five head total pressure rakes and the two shielded Chromel-Alumel thermocouple total temperature probes were installed in the prediffuser section of the rig at the diffuser inlet plane. Details of the total pressure rake and total temperature probes are seen on Figure 5-5. Four static pressure taps were also located at the diffuser inlet plane for further definition of combustor inlet condition. Additional pressure taps on the prediffuser wall were used to monitor performance of this component. Static pressure taps were also installed on the false walls in the fuel injector mount case and the combustor case. In conjunction with pressure measurements from instrumentation on the combustor liners, these data permitted computation of the airflow distribution in the combustor and simulated turbine cooling air bleed system. A hydrocarbon sniffer was installed in a port in the side of the outer burner case to detect fuel in the burner shroud in the event of fuel system malfunction, damage or aspiration from the combustor.

Since the effect of fuel composition on liner temperature and durability was a major concern in the program, the combustor liners were extensively instrumentated with metal temperature thermocouples. Typically, 21 to 26 Chromel-Alumel thermocouples were installed on each liner sector. Figures 5-6, 5-7 and 5-8 show the location of these thermocouples on the reference PW2037 and the variable geometry combustor sectors. The thermocouple junctions were embedded in the liner by welding the junction into small tranvesely oriented slots in the metal. Figure 5-9 shows a photograph of the inner liner side of the variable geometry combustor prior to installing the air scoop over the first louver panel and the combustor hood assembly and shows the details of the instrumentation installation and lead routing which is representative of that on all of the sectors. The thermocouples were installed with the junctions positioned immediately upstream of the weld between a film cooled panel and the riser of the following louver. Since the temperature gradient between this region and the cooler louver knuckle is critical to cyclic fatigue, the measurements were relevant to liner life. The transverse distribution of thermocouples generally favored positions downstream of the two center fuel injectors and midway between these injectors.

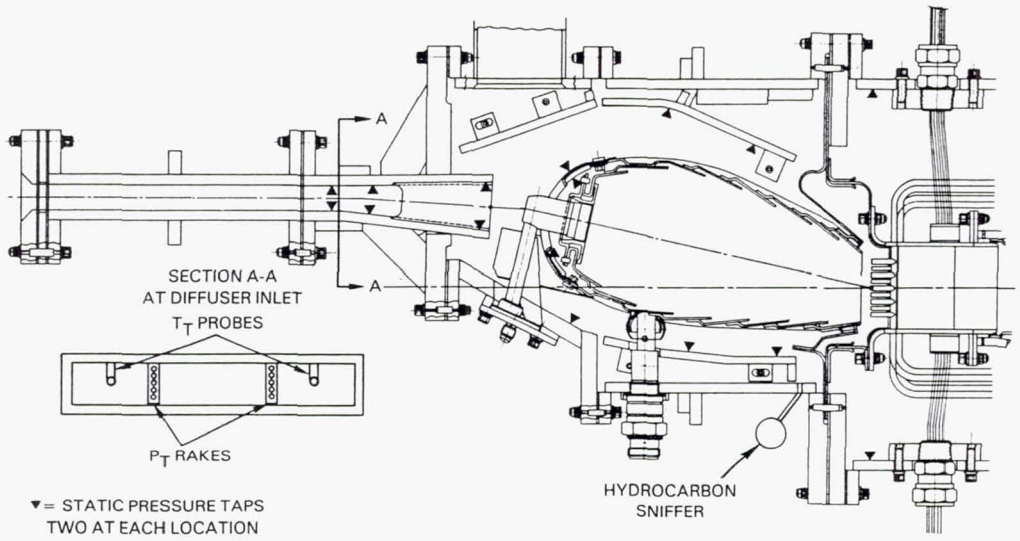

Figure 5-4 Typical Rig Instrumentation.

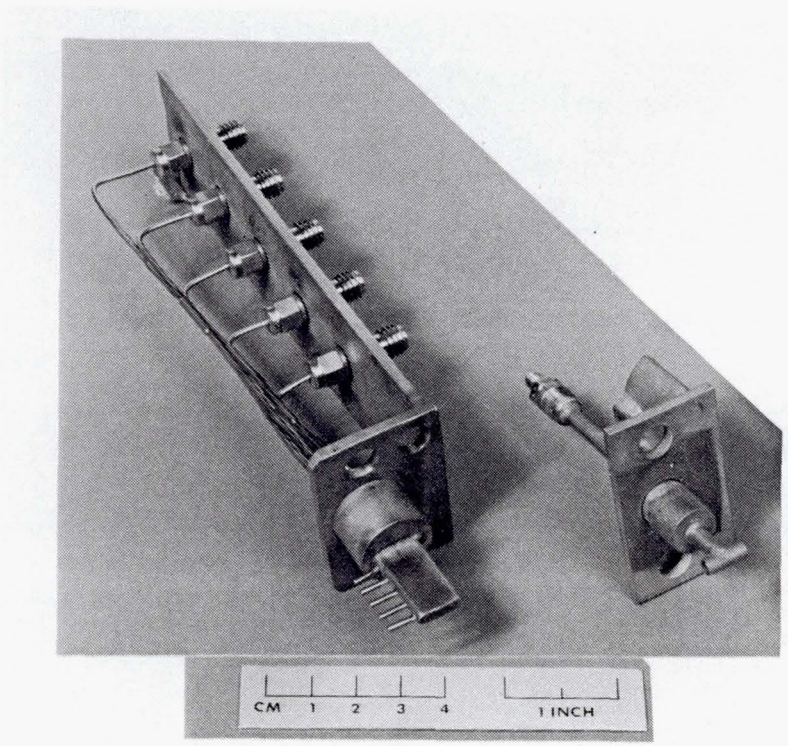

Figure 5-5 Combustor Rig Inlet Total Pressure Rake and Total Temperature Probe.

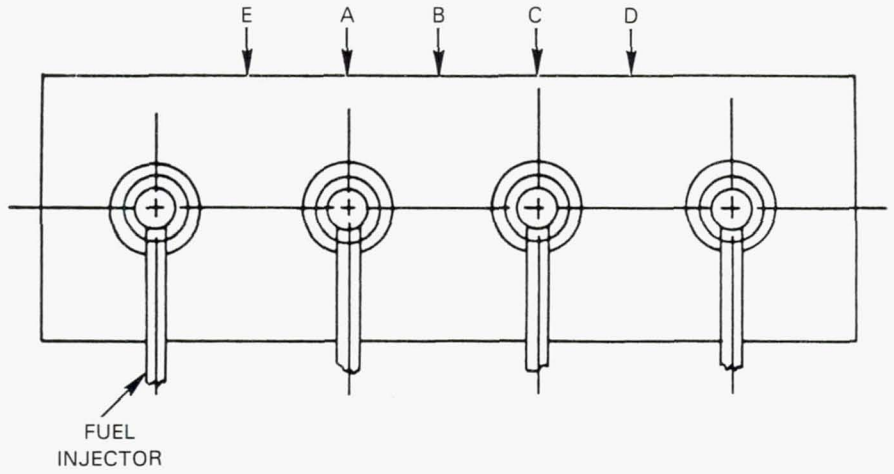

SCHEMATIC FRONT VIEW

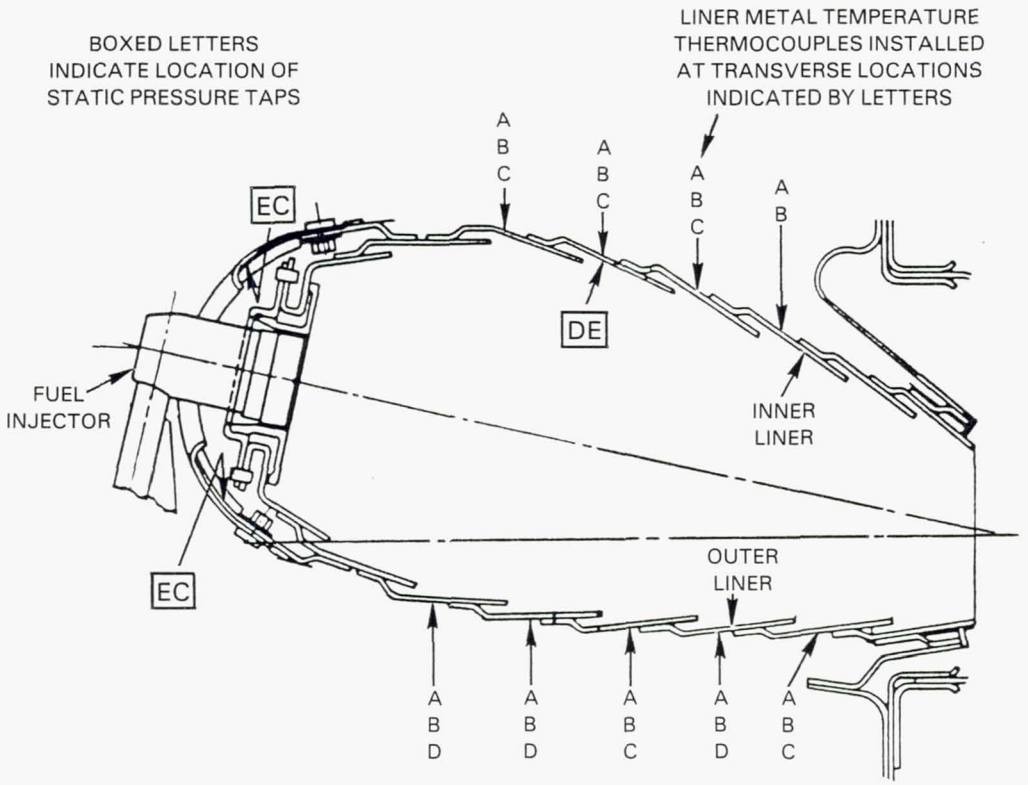

Figure 5-6 Location of Thermocouples and Pressure Taps on the Reference PW2037 Combustor Liner (Configuration V-1).

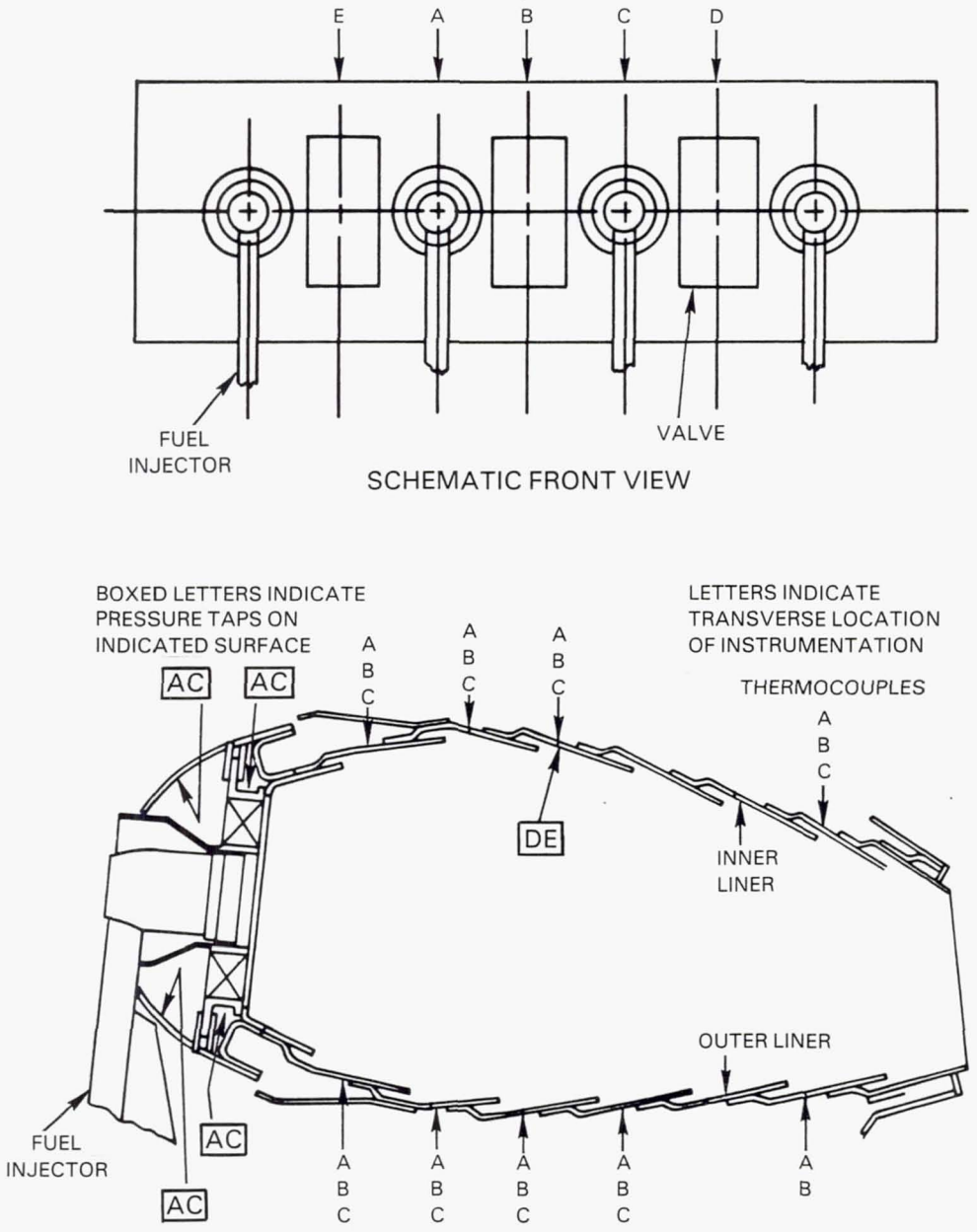

Figure 5-7 Location of Thermocouples and Pressure Taps on Variable Geometry Combustor Liner (Configurations V-2 to V-7).

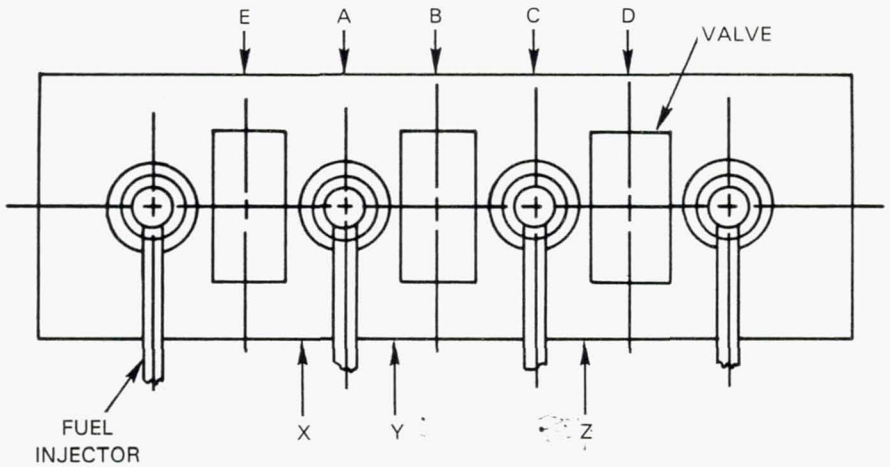

SCHEMATIC FRONT VIEW

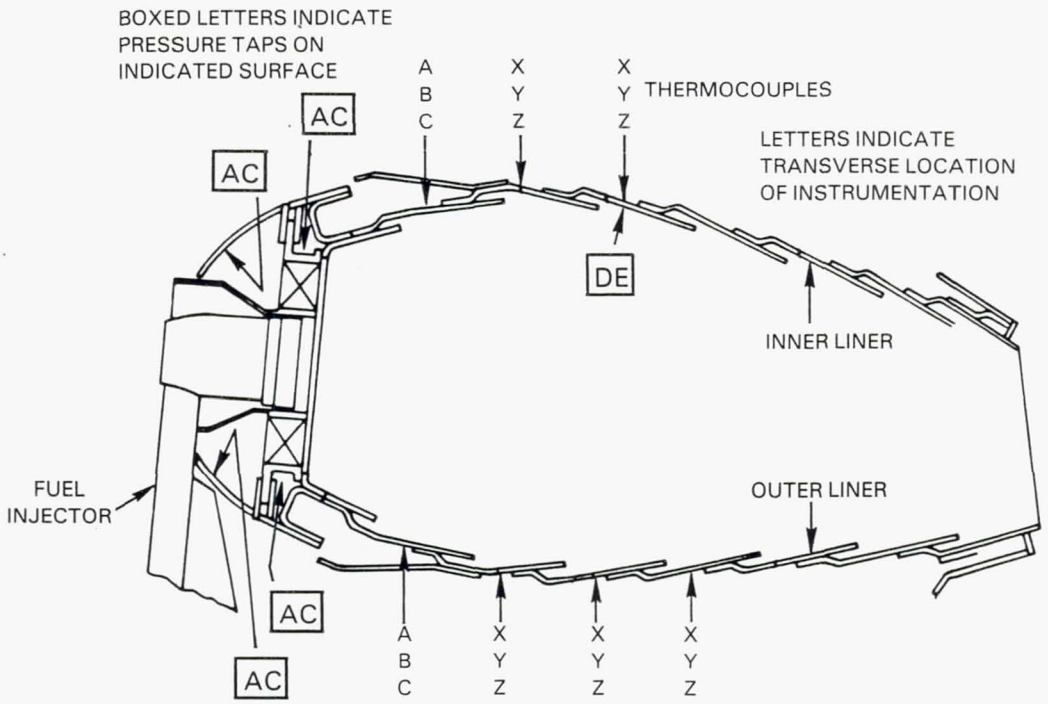

Figure 5-8 Locaation of Thermocouples and Pressure Taps on Final Configuration of Variable Geometry Combustor Liner (Configuration V-8).

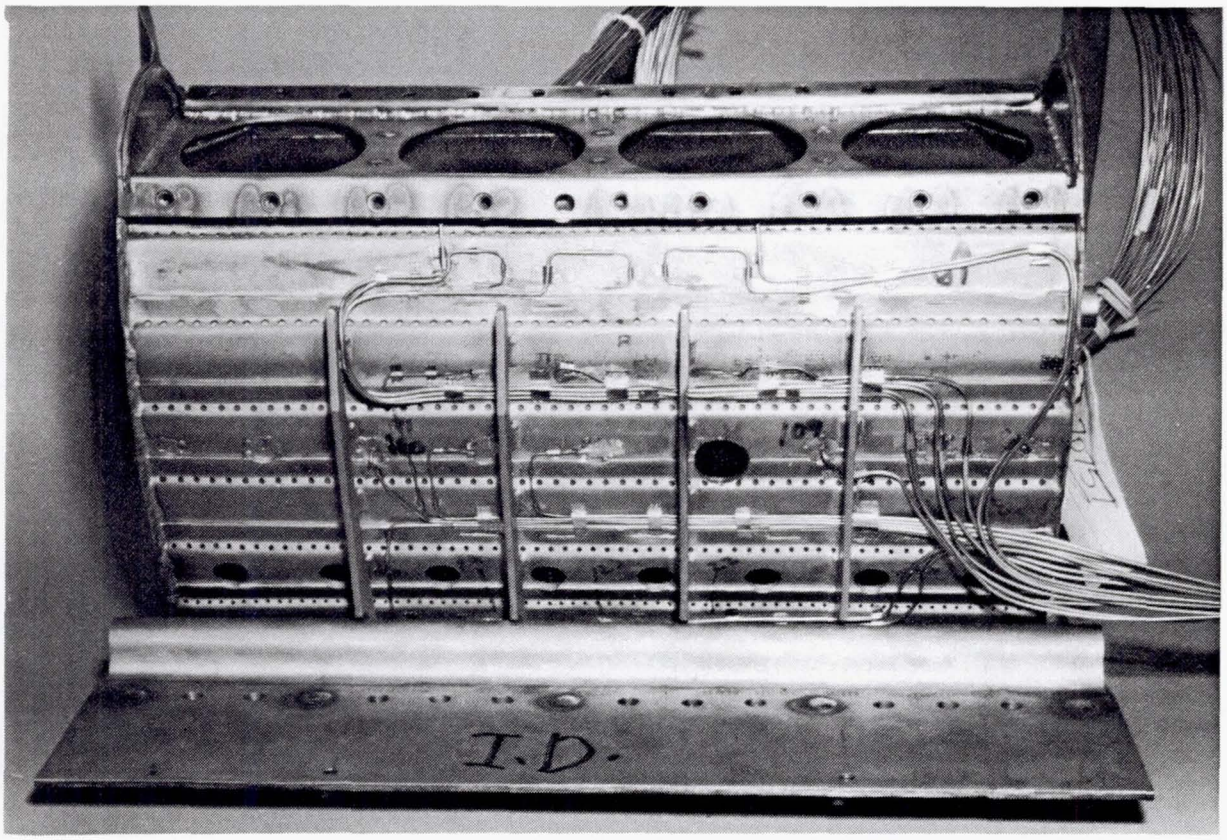

Figure 5-9 Thermocouple and Pressure Tap Instrumentaion on Inner Liner Side of Variable Geometry Combustor.

Static pressure taps installed on the liners and under the hood of the reference PW2037 and the variable geometry combustor were used in conjunction with those on the false walls in the rig cases to compute the pressure drops across and airflow distributions in the combustors. Additional pressure taps were installed in the cavity between the bulkheads of the variable geometry combustor to monitor the performance of the bulkhead cooling air feed system.

The instrumentation on the Mark IV combustor sector closely paralleled that described above and is shown on Figures 5-10 and 5-11. The earlier configurations (M-1 through M-6) were evaluated in a lower pressure test facility, and as indicated in Section 4.3.3, incorporated a simple internal louver construction to produce the desired upstream directed cooling flow in the front end of the combustor. As shown on Figure 5-10 the thermocouples on this section of the liner were installed on the outer skin adjacent to the louver standoff. Thermocouples on the conventional downstream facing louvers on the rear of the combustor liner were embedded in the liner in the same manner as those on the reference PW2037 and the variable geometry combustor.

Configurations M-7 through M-13 of the Mark IV combustor incorporated the advanced technology pin-fin segments in the liners enclosing the primary combustion zone and required more elaborate thermocouple installations. A small transverse saw cut extending about 2.5 cm (1.0 inches) was made in the hot side of the panel and terminated at a hole drilled through the segment. A 0.8 mm (0.032 inch) diameter sheathed Chromel- Alumel thermocouple wire was threaded through the hole and welded in the slot with the junction at the

extreme end. When the segment was installed in the combustor shell, the lead wire was directed radially out through a small hole in the shell and strapped to the shell as it was routed to the lead bundling location. A small washer was welded to the thermocouple sheath to inhibit leakage of cooling air flow around the wire. The thermocouples were positioned axially near the forward edge of the liner segments, because with the upstream flow of cooling air behind the segments, this was expected to be the hottest region. The transverse position of the thermocouple was established downstream of the air admission modules and the bulkhead mounted fuel injectors.

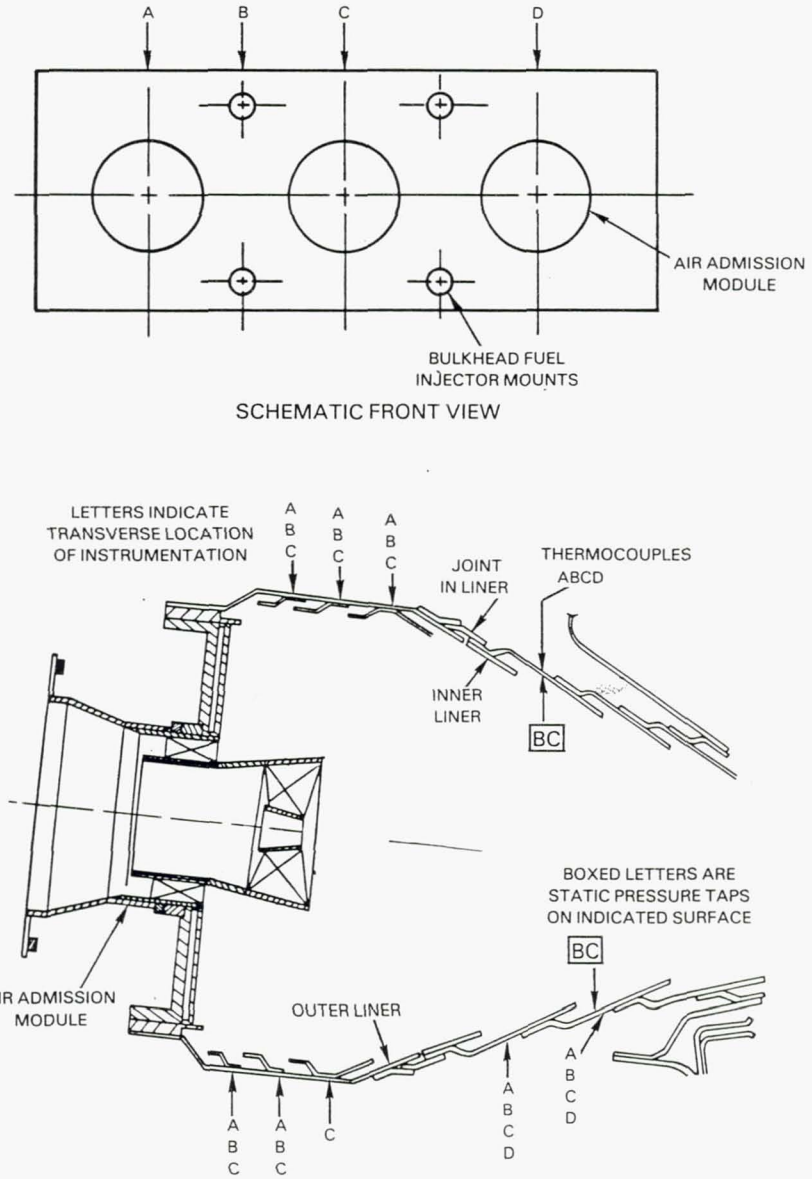

Figure 5-10 Location of Thermocouples and Pressure Taps on Mark IV Combustor Liner (Configurations M-1 to M-6).

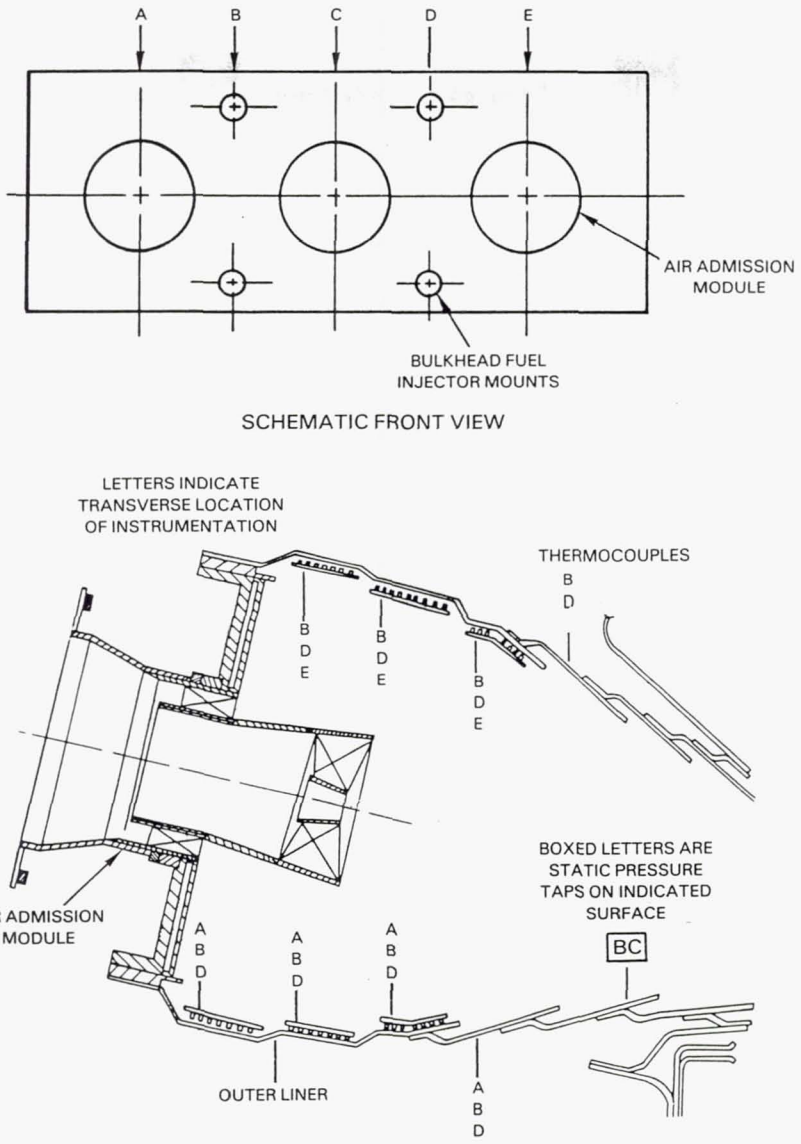

Figure 5-11 Location of Thermocouples and Pressure Taps on Mark IV Combustor Liner (Configurations M-17to M-13).

During evaluation of the reference PW2037 combustor (Configuration V-1) and the final configuration of the variable geometry combustor (Configuration V-8), instrumentation was also used to measure the heat flux incident on and through the combustor liner. Two different types of sensors were used to measure the radiant heat flux to the combustor liner. Figure 5-12 shows a cross-section view of the porous plug radiometer which was used previously in the testing of selected combustor configurations under Phase I of this program. The probe is an evolution of a concept conceived by Moffat, et al, (Ref. 20) and consists of a transpiration cooled device designed to measure incident total hemispherical radiation in the presence of strong convective conditions. These radiometers use a controlled flow of transpiration cooling through the sensor to blow the free stream thermal boundary layer from the front surface of the probe. This technique allows a direct measurement of the radiant heat flux without complication from convective or reactive effects.

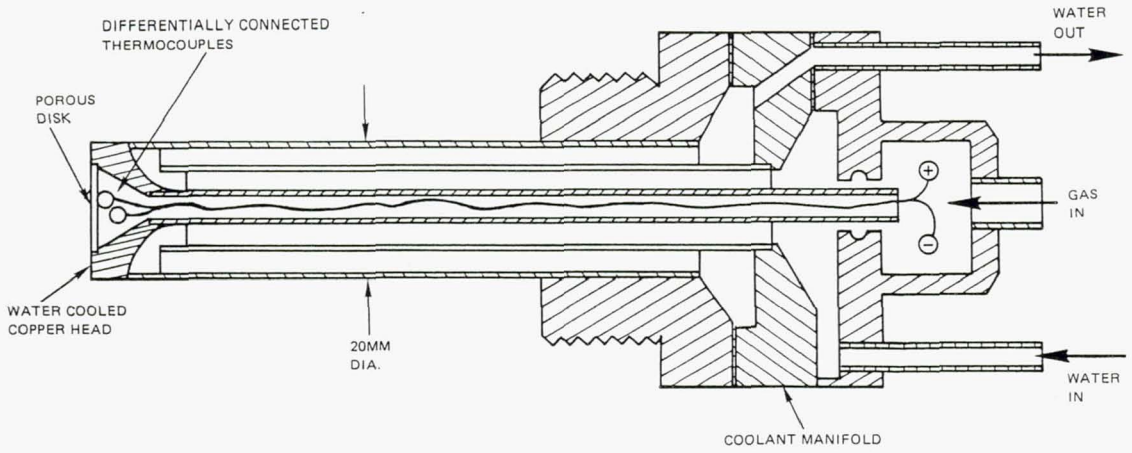

Figure 5-12 Cross Section of Porous Plug Radiometer.

The sensing element consists of the thin porous plate through which a precisely metered quantity of transpiration gas, either filtered shop air or bottled nitrogen, is passed. A differential Chromel-constantan thermocouple measures the temperature difference between the gas and the plate, which is related to the heat flux into the porous plug. The probe was calibrated prior to use to establish the relation between incident heat flux, gas flow rate and gas temperature rise. During test, the output from the differential thermocouples in the sensor was processed on a digital millivoltmeter that is incorporated in a portable Hewlett Packard computer. Pre-programmed calibration data on the radiometer was used to provide real time readout of the heat flux and sensor surface temperature.

The second type of radiometer was a commercially manufactured unit made under the brandname Medtherm. Figure 5-13 shows this probe which was also mounted in a boss on the rig case with the tip protruding through a hole in the combustor liner. The tip of the probe consists of a sapphire window to isolate the internal sensor from convective heat load and a gas purge is employed to keep the window clean during operation. A calibration curve provided by the manufacturer for the radiometer was confirmed in a calibration apparatus in the Instrumentation Laboratory at Pratt & Whitney prior to its use.

At the time Phase II of the Broad Specification Fuels Combustor Technology Program was being conducted, Pratt & Whitney was also working on the development of small heat flux sensors that could be mounted in combustor liners under Contract NAS3-22133 with NASA Lewis Research Center. Under that contract, prototypes of these sensors were fabricated and installed in the liner of Configurations V-1 and V-8. Subsequent exposure to a high temperature and pressure environment during testing of these combustor configurations demonstrated the durability of the sensors.

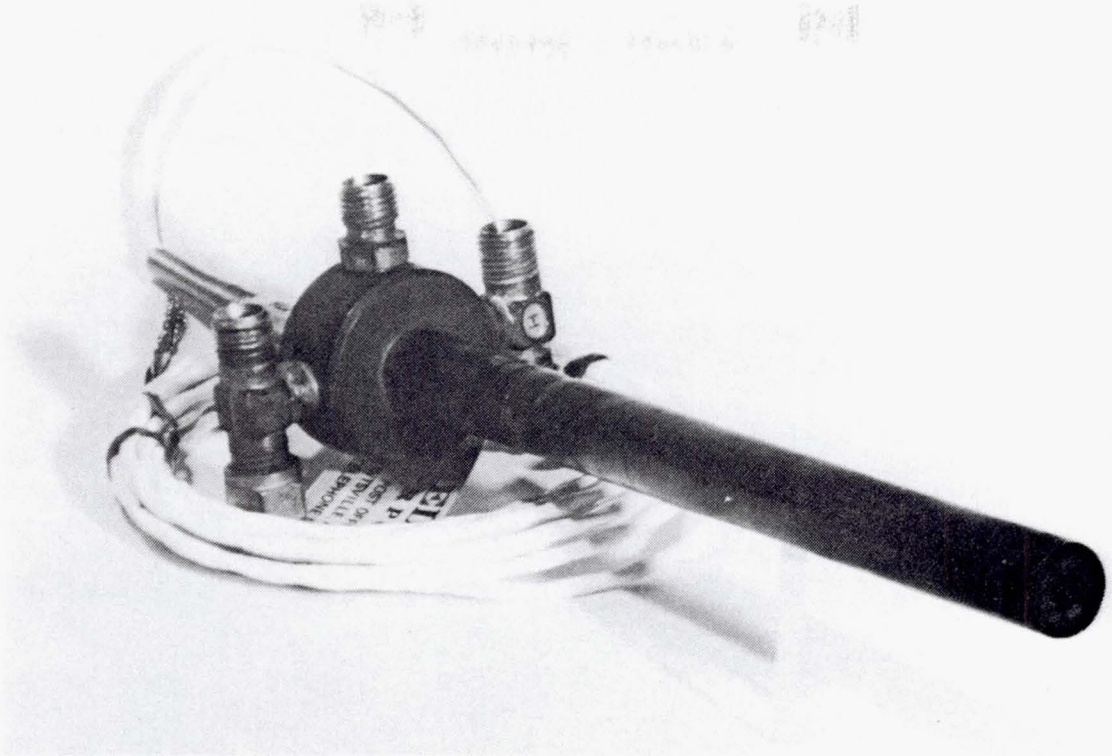

Figure 5-13 Medtherm Radiometer Probe.

Details of the design, fabrication and operation of the liner heat flux sensors are provided in Reference 21 and are described briefly herein. The sensors consist of a metallic disk, 0.8 cm (0.315 inches) in diameter by 0.11 cm (0.043 inches) thick, that are pressed or cemented into pre-drilled holes in the sheet metal combustor liner. Three different sensor concepts were employed: an embedded thermocouple sensor, a laminated sensor and a Gardon Gauge sensor. The embedded sensor consisted of a disc of Hastelloy X material used for the liner walls with Chromel and Alumel leadwires embedded in the disc to form junctions at the hot and cold sides. The sensor was calibrated prior to test by correlating the differential output from the hot and cold surface junctions against a known heat flux. The laminated sensor consists of a layer of Alumel diffusion bonded between two layers of Hastelloy-X. A ceramic filled groove electrically insulates the Alumel and the cold side Hastelloy-X layers in the sensor from the surrounding liner. The sensor output is obtained from sheathed Hastelloy-X wires attached to the hot side Hastelloy-X layer and to the insulated cold side Hastelloy-X layer. The output is representative of the temperature difference across the Alumel layer and can be calibrated to measure the heat flow through the combustor wall. The third type of heat flux sensor, the Gardon Gauge, consisted of a disc of the Hastelloy X liner material with a small central cavity, the floor of which became a thin "foil" of metal at the hot side. A sheathed bundle of two Alumel and one Chromel wires are led into the cavity where the Chromel lead attaches to the center of the foil and the two Alumel wires to the walls of the cavity. The cavity is then filled with ceramic cement. The output

represents a combination of the temperature difference between the center and the edge of the "foil" and part of the temperature drop across the bulk sensor thickness and is calibrated to measure the heat flow through the combustor wall. Figure 5-14 shows typical installations of two of these sensors on the liner of the variable geometry combustor.

Figures 5-15 and 5-16 show the location of the radiometer probes and the liner heat flux sensors on the reference PW2037 (Configuration V-1) and the variable geometry combustor (Configuration V-8), respectively. In both configurations, the radiometer probes were installed in directly opposite positions through the inner and outer liner so as to view the same region of the combustor downstream of a fuel injector from opposite sides. However, it should be noted that the porous plug radiometer had an essentially hemispherical field of view while the construction of the Medtherm radiometer restricted its view to a cone of 50° included angle.

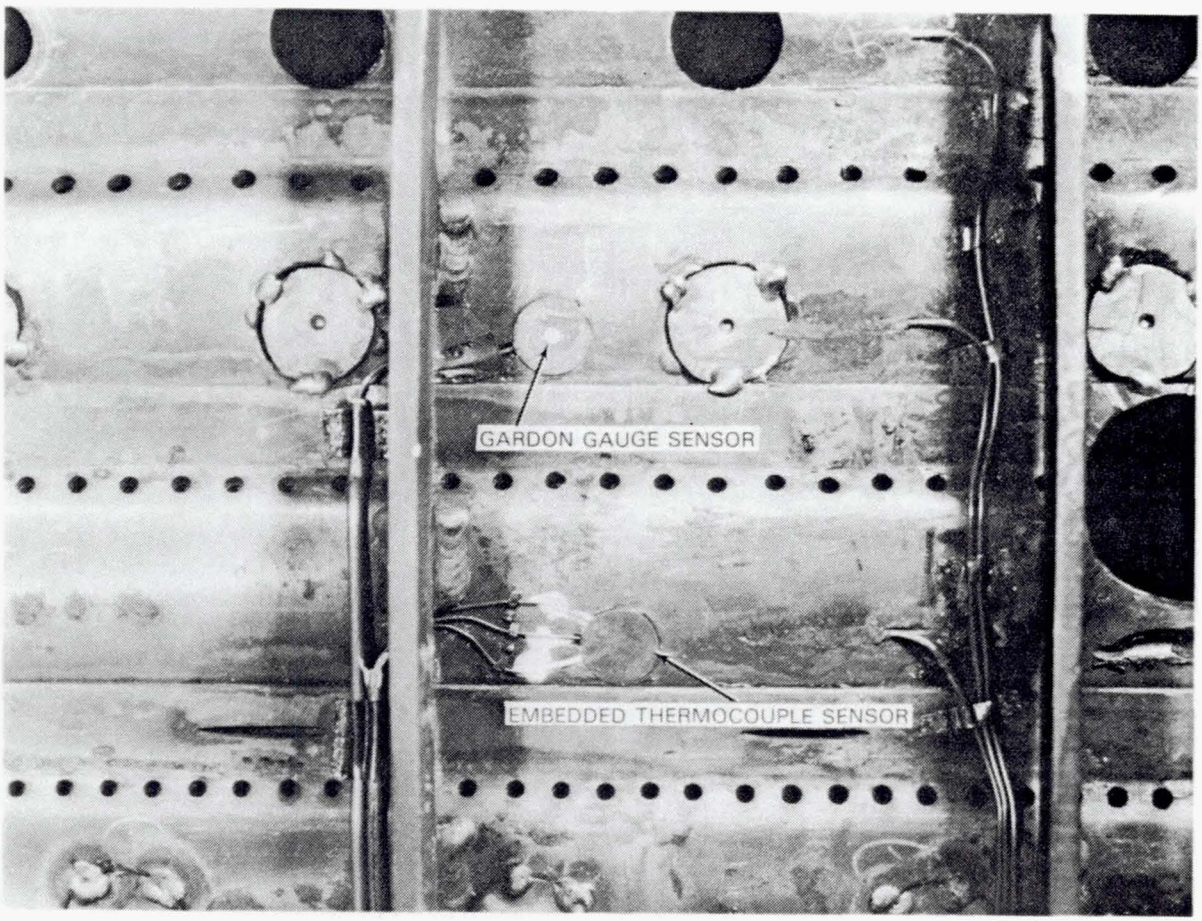

Figure 5-14 Cold Side Embedded Thermocouple Sensor and Gardon Gauge Installations.

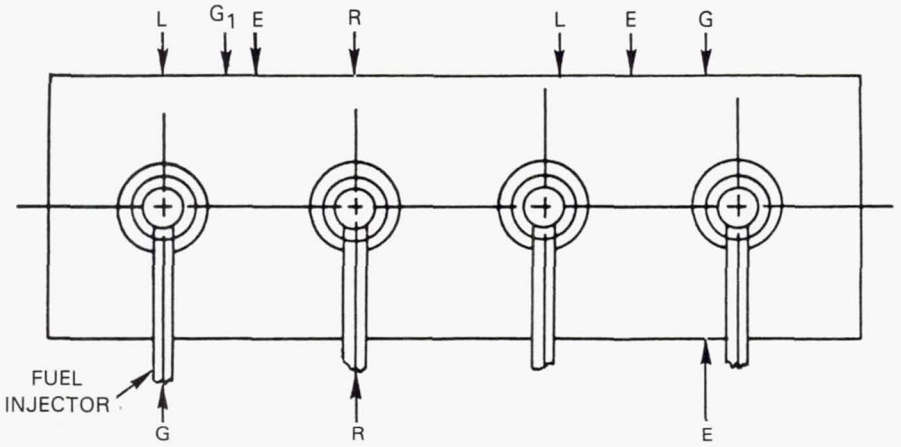

SCHEMATIC FRONT VIEW

WALL HEAT FLUX SENSOR TYPES
E — EMBEDDED
G — GARDON
L — LAMINATED

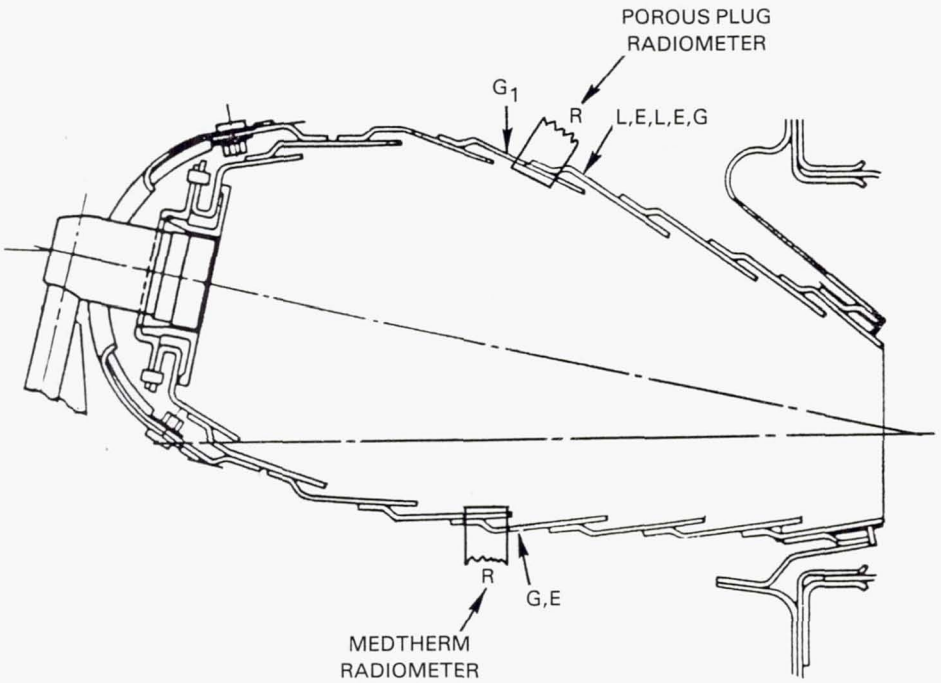

Figure 5-15 Location of Heat Flux Sensors on Reference PW2037 Combustor (Configuration V-1).

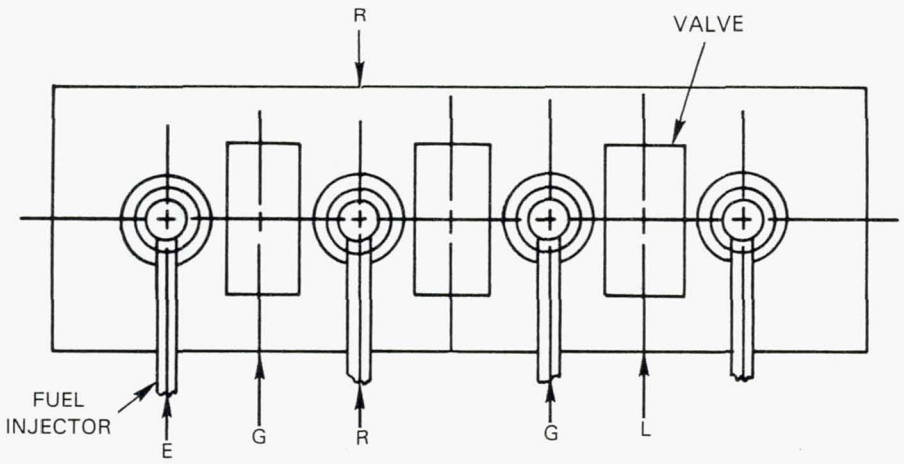

SCHEMATIC FRONT VIEW

WALL HEAT FLUX SENSOR TYPES
E – EMBEDDED
G – GARDON
L – LAMINATED

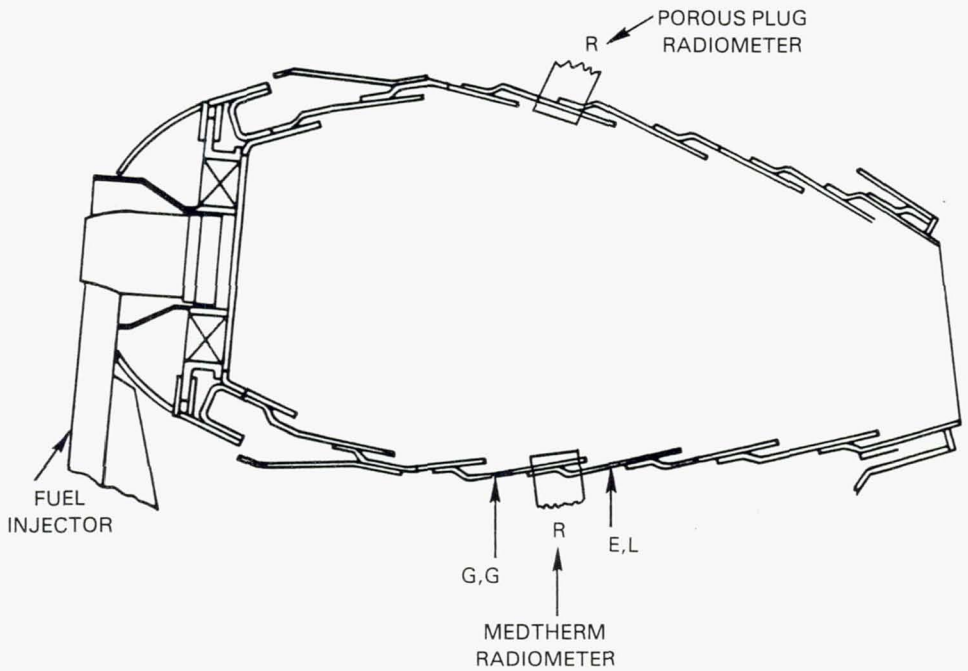

Figure 5-16 Location of Heat Flux Sensors on Reference PW2037 Combustor (Configuration V-8).

The combustor exit conditions were measured with a fixed array of instrumentation mounted on a vane pack in the rig case immediately behind the combustor. Figure 5-17 shows an overall front view of the vane pack assembly while Figure 5-18 is a closeup of the details of individual vanes. The pack consists of twelve air cooled vanes with the center eight carrying instrumentation. The vane cooling air is extracted from the rig air supply upstream of the facility heater and flow measurement equipment and provides a combination of film and transpiration cooling of the vane surfaces. The instrumentation on each vane consists of four gas sampling/total pressure probes and five shielded gas temperature thermocouples spaced across the "radial" extent of the combustor exit. Relative to the downstream end of the inner liner, the thermocouples were located at 18, 35, 53, 70 and 87 percent of the span while the gas sampling/total pressure probes were positioned at 26, 44, 62 and 78 percent span.

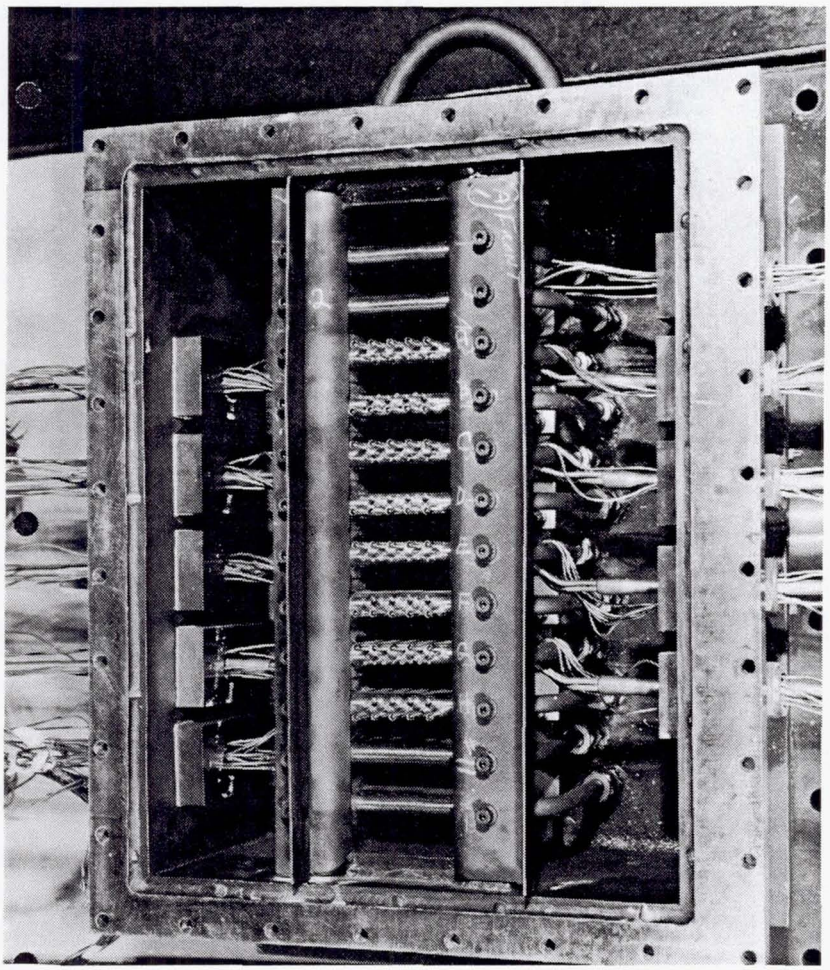

Figure 5-17 Front View of Combustor Exit Vane Pack.

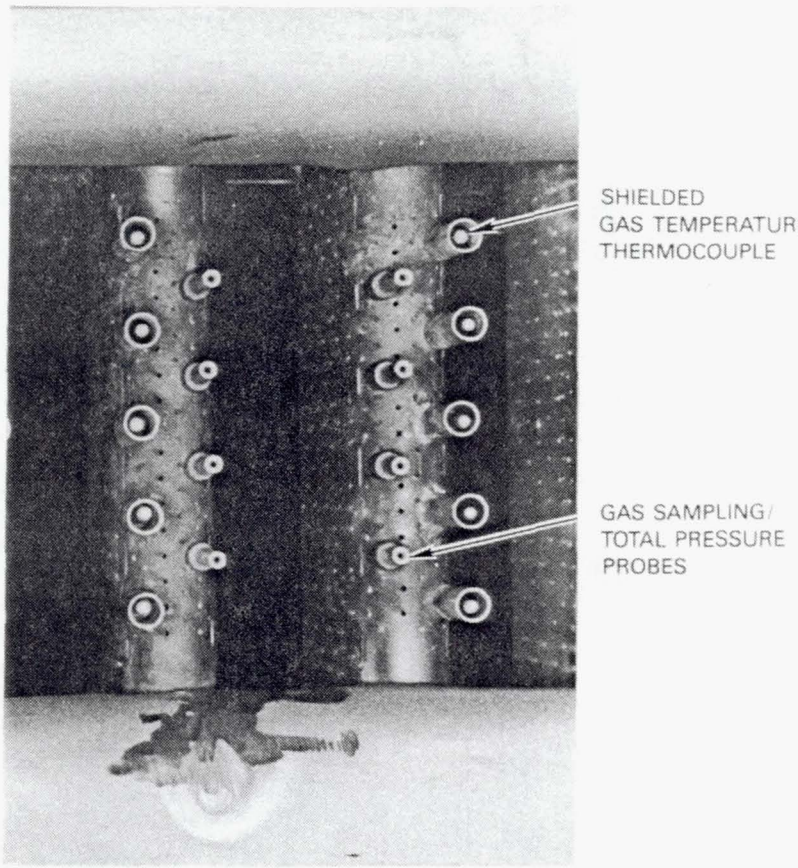

Figure 5-18 Closeup of Instrumented Combustion Exit Vanes.

The gas temperature thermocouples in the vane pack employ a grounded immersion type of junction with ISA Type B thermocouple wire (6% Platinum, Rhodium vs Platinum, 30% Rhodium). The calibration of this wire is accurate to 1975°K (3100°F). The gas sampling heads were made from platinum - 20% rhodium alloy while the remainder of the lines were made from stainless steel tubing. When emissions or smoke is measured, the samples from all four heads on each vane are mixed together. The samples from each vane are then routed through selected valves to a second mixing manifold before being fed to the analysis equipment. In this way a single mixed average sample or a combination of sample mixtures from various transverse positions could be selected for analysis. Temperature measurements in the vane pack indicated that the gas samples were quenched to 425 to 475°K (300 to 400°F) by the cooling air in the vane pack and the sample lines between the rig and the analysis equipment were heated to maintain the sample temperature at about 425°K (300°F). When these sensors are used to measure total pressure, the sample lines are dead-ended by closing the selector valves, and the pressure is recorded on a transducer in the automatic data recording system.

5.3 TEST FACILITIES

The combustor rig tests were conducted in two different test facilities. X-902 stand at the Pratt & Whitney Middletown, Connecticut facility was used for the evaluation of combustor configurations that were critical to the concept definition and selection process and for the final series of perturbations to the Mark IV combustor because it had the capability of precisely reproducing nearly all of the PW 2037 engine operating conditions. The Jet Burner Test Stand located at United Technologies Research Center in East Hartford offered greater economy of operation allowing more combustor configurations to be evaluated during the initial concept screening part of the program. However, this facility was limited in its capability of achieving the high power operating conditions of the PW2037 engine and required more significant departures from those conditions. These two facilities, their capabilities and supporting equipment are described in this section.

5.3.1 X-902 Test Stand

X-902 is one of four high pressure combustor development stands located in the test complex at the Pratt & Whitney Middletown, Connecticut plant. Figure 5-19 shows a schematic diagram of the air supply system in this facility. Airflows up to 11.4 kg/sec (25 lb/sec) at pressure levels up to 4.3 MPa (625 psia) are provided by two steam driven, two stage Elliot turbocompressors operating in parallel into a six stage steam driven boost compressor. After a small part of this air is bled off for rig tank pressurization and rig exit vane pack cooling, the air going to the test rig is preheated in an indirect fired heat exchanger to temperatures as high as 923°K (1200°F). The combustor test rig is mounted within a cylindrical pressure tank. Tank pressurization is automatically controlled to 0.04 MPa (6 psi) above rig pressure. In this manner, the pressure load is supported by the facility pressure vessel, permitting experimental hardware to be of relatively light construction. The pressure level in the rig is regulated by a water cooled back pressure valve and the exhaust gases are collected in a water-cooled exhaust chamber and ducted underground to an expansion and liquid separation pit at the base of the main exhaust stack.

With the above cited airflow and rig inlet total pressure and total temperature capabilities, X-902 stand had sufficient capacity to duplicate the combustor inlet conditions of the PW2037 engine at all power levels of Table 3-1, up to and including the climb condition in the sector combustor rig. However, after upstream extraction of tank pressurization and vane pack cooling air, the rig inlet airflow was insufficient to achieve inlet Mach Number similarity at the takeoff condition of Table 3-1. This necessitated restricting operation of the rig to about 85 percent of the design inlet total pressure at the takeoff condition to maintain the correct inlet Mach Number.

The control room immediately adjacent to the test cell contains all of the facilities and emissions equipment necessary to operate the rig. The data acquisition system incorporates, in addition to the standard pressure and temperature instrumentation, analytical instruments for emission measurements consistent with those specified in the latest EPA requirements. Steam-traced emission sampling lines are routed to the emission console located in the control room, where they can be manifolded as desired.

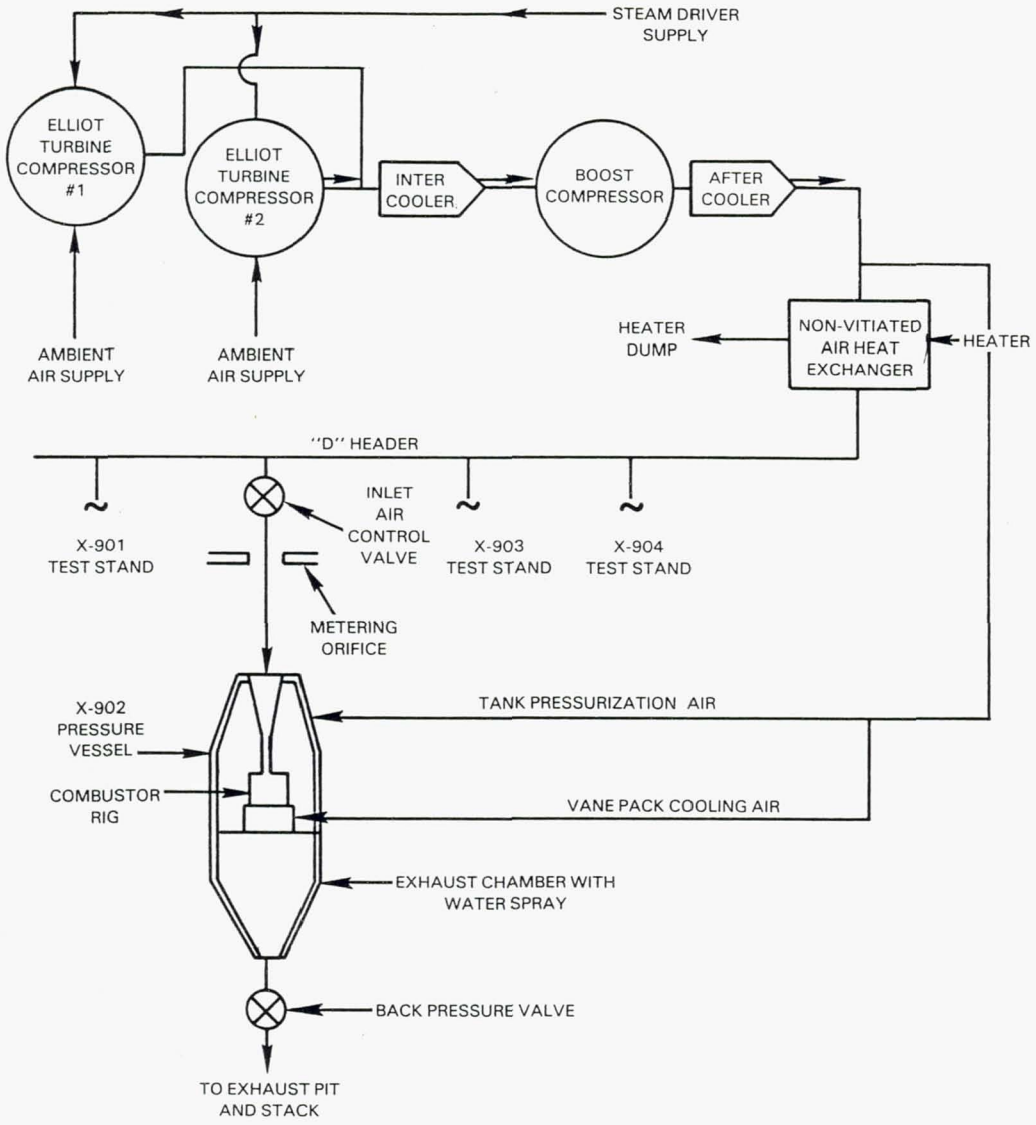

Figure 5-19 Schematic Diagram of Air Supply System at X-902 Stand.

The fixed-station emission measurement system is designed to measure exhaust constituents from the high-pressure burner facility. The instrumentation and sample-handling system were designed to conform to specifications in SAE ARP-1256, subsequently adopted, with some exceptions by the Environmental Protection Agency (Reference 22). The laboratory is self-contained and incorporates gas analysis instruments to measure the following:

- Carbon dioxide and carbon monoxide are measured with Beckman Model 865 Non-Dispersive Infrared (NDIR) instruments.
- Nitrogen dioxide is measured with a Beckman Model 255A Non-Dispersive Ultraviolet (NDUV) analyzer.
- Nitric oxides, the total oxides of nitrogen, are measured with a TECO Model 14D Chemiluminescence analyzer.
- Oxygen is measured with a Scott Model 250 Paramagnetic 02 analyzer.

The combustor rig exhaust gas sample is distributed to the various instruments, with each instrument having its own flow metering system. The sample handling is shown schematically in Figure 5-20.

Emissions analysis systems are regularly calibrated against a complete set of standard gases. Where possible, these gases are traceable to the National Bureau of Standards through a set of Standard Reference Materials including:

SRM 1673-1675 Carbon Dioxide in Nitrogen

SRM 1677-1681 Carbon Monoxide in Nitrogen

SRM 1665-1669 Propane in Air

Burner exhaust smoke measurements were obtained through use of a smoke measuring system that conforms to specifications of the Society of Automotive Engineers Aerospace Recommended Practice, ARP-1179. Figure 5-21 shows the smoke measuring system, or smoke meter, which is a semi-automatic electromechanical device. It incorporates a number of features to permit the recording of smoke data with precision and relative ease of operation. The unit is designed to minimize variability resulting from operator-to-operator differences. One of these features is a time-controlled solenoid-activated main sampling valve (Valve A of Figure 5-21) having "closed," "sample" and "bypass" positions. This configuration permits close control of the sample size over relatively short sample times. In addition, this timing system operates a bypass system around a positive displacement volume measurement meter to ensure that the meter is in the circuit only when a sample is being collected or during the leak check mode. Other design features include automatic temperature control for the sample line and filter holder and silicon rubber filter holders with support screens for ease of filter handling. The filter holder has been constructed with a 2.54 cm (1.0 in) diameter spot size, a diffusion angle of 7.25° and a converging angle of 27.5°.

A photovolt Model 670 reflection meter with a type Y search unit conforming to ASA Ph 2.17-1958 "Standard for Diffuser Reflection Density" was used to determine the reflectance of the clean and stained filters. A set of Hunter Laboratory reflectance plaques, traceable to the National Bureau of Standards, was used to calibrate the reflection meter.

The burner test stand complex in the Middletown Test Facility is equipped with a computer controlled automatic data acquisition system. All data with the exception of those related to the radiometer heat flux sensor and smoke measurements are processed through an on-line Univac computer that provides near real time data analysis. The data reduction program processes all data into engineering units and computes combustor operating parameters such as diffuser inlet Mach number, fuel/air ratio, ideal temperature rise and emission indices.Preselected critical parameters including those derived from emissions analysis are presented on a scope in the control room for screening to establish data validity before proceeding to the next point in the test program. Hard copy printout of the entire data reduction program output is available at a printer terminal in the Engineering Building in East Hartford within minutes after the data is acquired.

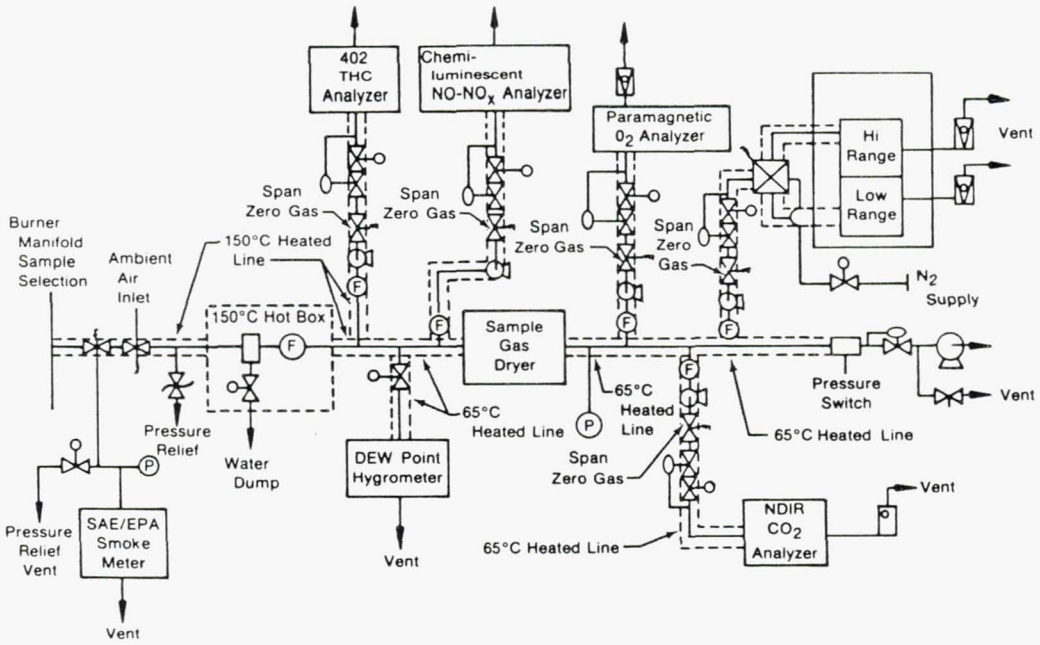

Figure 5-20 Gas Emissions Analysis Systems.

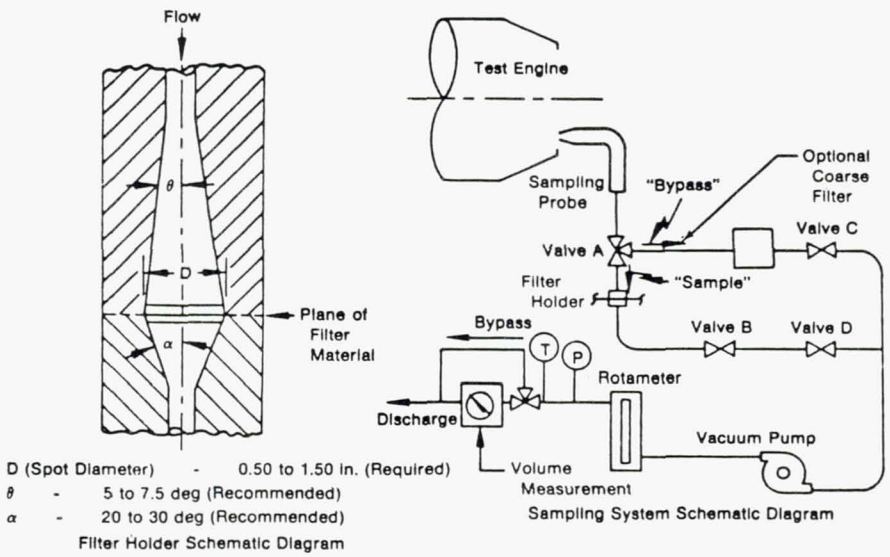

Figure 5-21 Smoke Meter.

The Jet A fuel for X-902 Stand was drawn directly from the tank farm at the Middletown test facility. The Experimental Referee Broad Specification Fuel (ERBS) was drawn from a 20,000 gallon storage tank near the test facility. The 11.8 percent hydrogen content test fuel was stored in another permanent storage tank of 6000 gallon capacity near the test stand while the Number 2 Commodity fuel was stored in a leased tank trailer at a transfer station near the test complex. Figure 5-22 shows a simplified schematic diagram of the fuel supply system. Transfer and high pressure pumps are located in the line from each fuel source and the desired fuel was selected by operating the appropriate pumps and opening the selector valve in that line. A single pipe delivers the fuel from the selector valve to the rig. Switching of fuels

during testing was accomplished by activating the pumps in the line from the second source and bringing the fuel pressure up to the level in the system after which the selector valves were actuated. The selector valves are on-off type valves and the control system is set up so that only one of the four selector valves can be open at a time. The entire pump and selector valve operation sequence is actuated from the control room of the test stand and was accomplished with the rig operating. Check valves in the lines upstream of the selector valves prevent backflow through the lines which could contaminate the fuel in storage tanks. A timed delay bypass valve downstream of the high pressure pump diverts fuel to a dump tank for several minutes to avoid long system purge times after a change in test fuel.

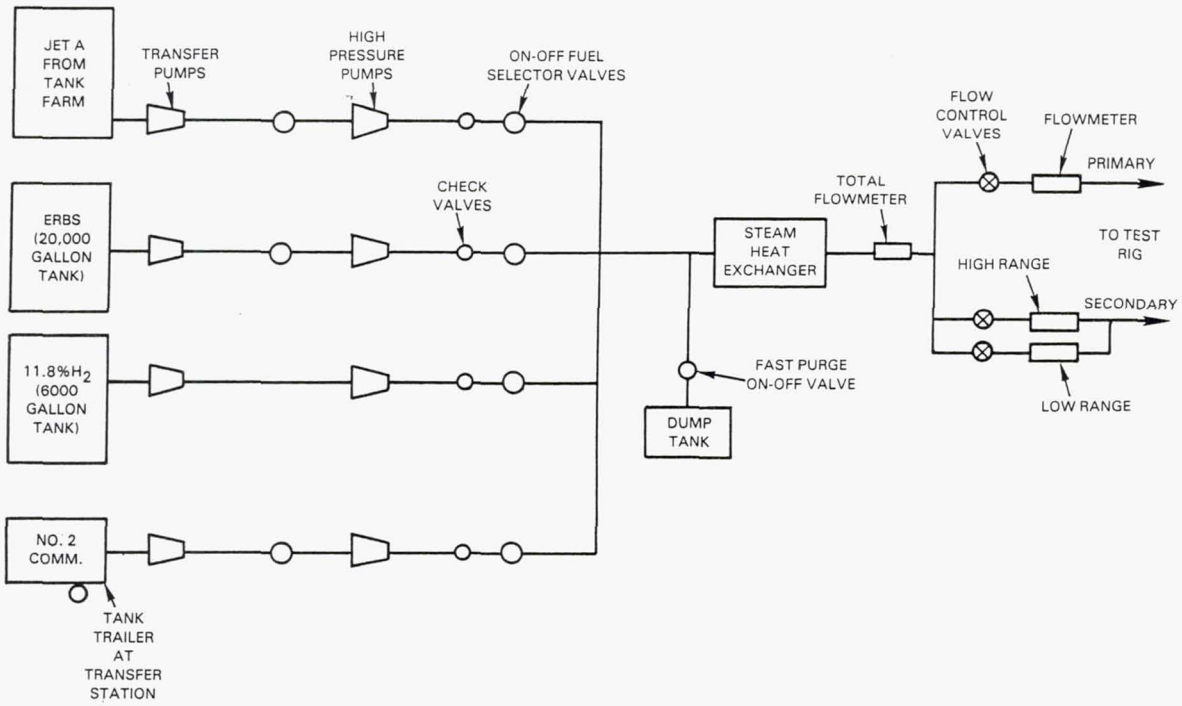

Figure 5-22 Simplified Schematic Diagram of Fuel Supply System in X-902 Test Stand.

The fuel passed through a steam heat exchanger capable of producing fuel temperatures of 450°K (350°F) before being metered and distributed to the rig. The fuel flow was measured with turbine type meters. The reference PW2037 combustor, all configurations of the variable geometry combustor and some configurations of the Mark IV combustor incorporated single pipe fuel injection systems. When these configurations were tested, the primary fuel system shown on Figure 5-22 was inactive and all fuel passed through either of the two parallel paths in the secondary system. These paths differed in the flow capacity of the control valves and flowmeters. The dual range system was required to obtain accurate fuel flow rate measurements over a wide range when the combustor was operated with single pipe fuel injectors. The primary fuel system of Figure 5-22 was used in the evaluation of some configurations of the Mark IV combustor which had either split feed to the four bulkhead mounted fuel injectors in pairs or, in the case of configurations M-12 and M-13, a duplex primary - secondary fuel system with two discrete injector locations. A fourth fuel flow meter was employed to provide a redundant measurement of the total fuel flow to the rig. Each meter was calibrated over

the anticipated range of fuel flows prior to the initiation of testing. Appropriate correction factors for the differences in specific gravity and viscosity of the test fuels, derived from the laboratory analysis of these fuels, were incorporated in the data reduction programs. Fuel supply temperatures were measured with immersion type thermocouples in the fuel system and the fuel supply pressures were measured in the manifolds immediately upstream of the injectors.

5.3.2 Jet Burner Test Stand

The Jet Burner Test Stand is located at the United Technologies Research Center (UTRC) adjacent to Pratt & Whitney in East Hartford, Connecticut. The Jet Burner Test Stand is a self-contained combustion facility, having seven test cells, three control rooms, an engine room, a work area, and a fuel pump room. Four of the seven test cells are specifically designed for hot-flow or combustion type testing. Figure 5-23 shows a schematic diagram of the airflow system in the facility. Compressed air is supplied to any one of the test cells by two multistage reciprocating compressors. The air system provides continuous airflows of up to 4.5 kg/sec (10 lb/sec) at pressures up to 2.52 MPa (365 psia) for unlimited periods of time. Larger airflows are also available by operating the facility in a blowdown mode in which the compressors are used to pressurize an accumulator tank prior to blowdown. The airflow may be preheated in an indirect fired (nonvitiated) heat exchanger to temperatures of 505°K (450°F). Higher inlet air temperatures are achieved by operating an in line heater burner on hydrogen fuel. The effect of pre-vitiation of the combustor inlet air is reduced by replenishment of the consumed oxygen prior to entering the test combustor. The combustor rig proper was mounted in a pressure vessel similar to that in the X-902 facility. Rather than having the inlet air supplied to the combustor through the circular to rectangular transition duct shown in Figure 5-3, the rig was cantilever mounted from the rear bulkhead of the pressure vessel which functioned as a plenum chamber. Smooth airflow into the flow development duct of the rig was assured by a small bellmouth section mounted on the upstream flange. The combustor discharge gases were quenched by a water spray downstream of the exit vane pack and a water cooled back pressure valve maintained the desired pressure level in the combustor.

The limited range of operation of the Jet Burner Test Stand relative to X-902 placed restrictions on the combustor inlet conditions that could be achieved in this facility. These are summarized on Table 5-4 and compared against the design combustor inlet conditions for the PW 2037 combustor. As shown by the table, when the PW2037 sector rig used in this program was tested in this facility, it could be operated in the steady state condition with the indirect fired inlet preheater at the idle condition. Consequently, realistic data on the idle emissions, combustion efficiency and lean stability (blowout) boundaries could be obtained in this facility. Achieving higher inlet temperatures at approach and higher power levels required use of the hydrogen vitiating heater burner and oxygen replenishment. The approach operating condition also required an airflow that is just slightly over the compressor limit of 4.5 kg/sec (10 lb/sec) for steady airflow operation of the Jet Burner Test Stand, and all operating conditions above this airflow were run in the blowdown mode. In that mode, the facility was limited to a practical maximum combustor inlet pressure of about 1.52 MPa (220 psia) which required that the climb and takeoff condition be simulated at below design

pressure levels. With these pressure constraints, the total rig airflow was in the range of 5.9 to 6.36 kg/sec (13 to 14 lb/sec) and the accumulator system was capable of providing intervals of steady flow of about 30 minutes duration. Because equilibration time was short, this was sufficient time to acquire two test points. The pump-up time of the accumulator between runs at these flow rates was also about 30 minutes.

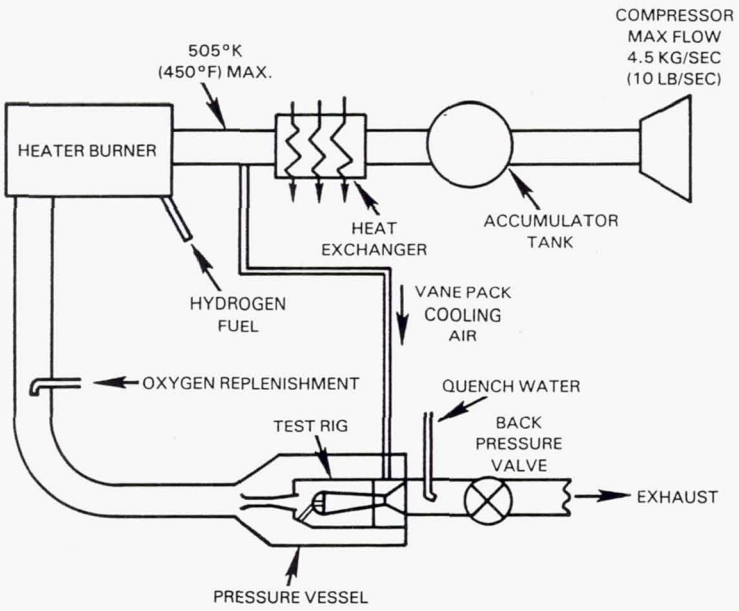

Figure 5-23 Jet Burner Test Stand Airflow System.

Table 5-4

JET BURNER TEST STAND CAPABILITIES

	DESIRED COMBUSTOR RIG INLET						ACHIEVABLE JBTS COMBUSTOR INLET		
PW2037 ENGINE CONDITION	Temperature °K	(°F)	Pressure MPa	(psia)	Airflow* Kg/sec	(lb/sec)	Pressure MPa (psia)	Temperature Achieved by	Airflow Mode
IDLE	474	(395)	0.43	(62)	2.4	(5.2)	0.43 (62)	Nonvitiated	Steady Flow
APPROACH	607	(633)	1.08	(156)	4.8	(10.5)	1.08 (156)	Vitiated	Blowdown 30 Minutes Duration
CRUISE	744	(880)	1.41	(205)	5.9	(13.0)	1.41 (205)		
CLIMB	758	(905)	2.37	(344)	9.8	(21.6)	1.52 (220) max		
TAKEOFF	790	(963)	2.72	(395)	10.8	(24.0)	1.52 (220) max		

*For Rectangular PW2037 Combustor Rig at Design Inlet Mach Number

While the use of vitiation and oxygen replenishment can cause concern over the accuracy of some combustor performance and emission data, prior experience with operating this facility in this mode has been favorable. Strong quantitative consistency of smoke and liner temperature measurements has been observed between combustors tested in the Jet Burner Test Stand and in subsequent evaluations in an engine. Analytical studies and surveys (Reference 23) also indicate that efficient pre-vitiation with oxygen replenishment should not produce strong influences on smoke formation, heat transfer and emissions of carbon monoxide and unburned hydrocarbons. The formation process of oxides of nitrogen in the heater burner-test combustor combination is considerably more complex and, at best, it could be anticipated that comparative effects of different combustors and fuels might be discernible if all other operating conditions were maintained the same.

All the controls and instrumentation required to operate a test rig in the Jet Burner Test Stand and monitor its performance are contained in a separate control room adjacent to the cell. Automatic controls regulate air and fuel flows and temperature. The facility includes a common gas sampling and analysis system and a smoke sampling and analysis system. Conventional performance related measurements are processed through an automatic data acquisition system consisting of one low speed (25 channel) and one high speed (20 channel) analog-to-digital converting system. The two systems are designed to accept output from 48 port pressure scanivalves, 26 junction temperature scanners, single pressure transducers, load cells and turbine flow meters. The total time required for a complete data scan with the high speed system is less than 5 seconds and less than 35 seconds with the low speed system. The digitized binary equivalent of the analog inputs is stored on Univac 1100/81A compatible magnetic tape. The high speed system uses a direct link to the Univac 1100/81A for online processing of the data.

The emissions analysis system at the Jet Burner Test Stand defines the gaseous emissions of oxides of nitrogen, carbon monoxide, oxygen, carbon dioxide and total hydrocarbons. All emissions measurements are carried out using procedures conforming to SAE ARP 1256 (Ref. 22). The accuracy of the emissions data is assured through the use of standard and special gas mixtures for calibration, zero and span reference. The gas sample is transferred from the probe to the analytical instruments through 0.63 cm (1/4 in.) inner diameter stainless steel teflon coated lines maintained at an average temperature of 205°C (400°F). The sample line length is approximately 15 M (50 ft), and the sample temperature is monitored at several axial locations.

The emissions sampling and analysis system is shown schematically in Figure 5-24. The signal output and attenuator position are automatically transferred to the data acquisition system for on-line recording of emission concentrations. The following gas analyzers are housed in an instrumentation console at the UTRC Jet Burner Test Stand:

- A Beckman Model 315B nondispersive infrared analyzer (NDIR) for measurements of carbon dioxide (CO_2) concentrations.
- A Beckman Model 315B nondispersive infrared analyzer (NDIR) for measurements of carbon monoxide (CO) concentrations.

- A Beckman Model 402 total hydrocarbon analyzer which is equipped with a heated flame ionization detector (FID) for measurements of concentrations of unburned hydrocarbons (HC).
- A TECO model 10A chemiluminescence detector for measurements of concentrations of oxides of nitrogen (NOx). This unit is equipped with a switchable converter so that total concentration of NO plus NO_2 may be measured.
- A Scott Model 150 paramagnetic analyzer for measurements of oxygen (O_2) concentrations.

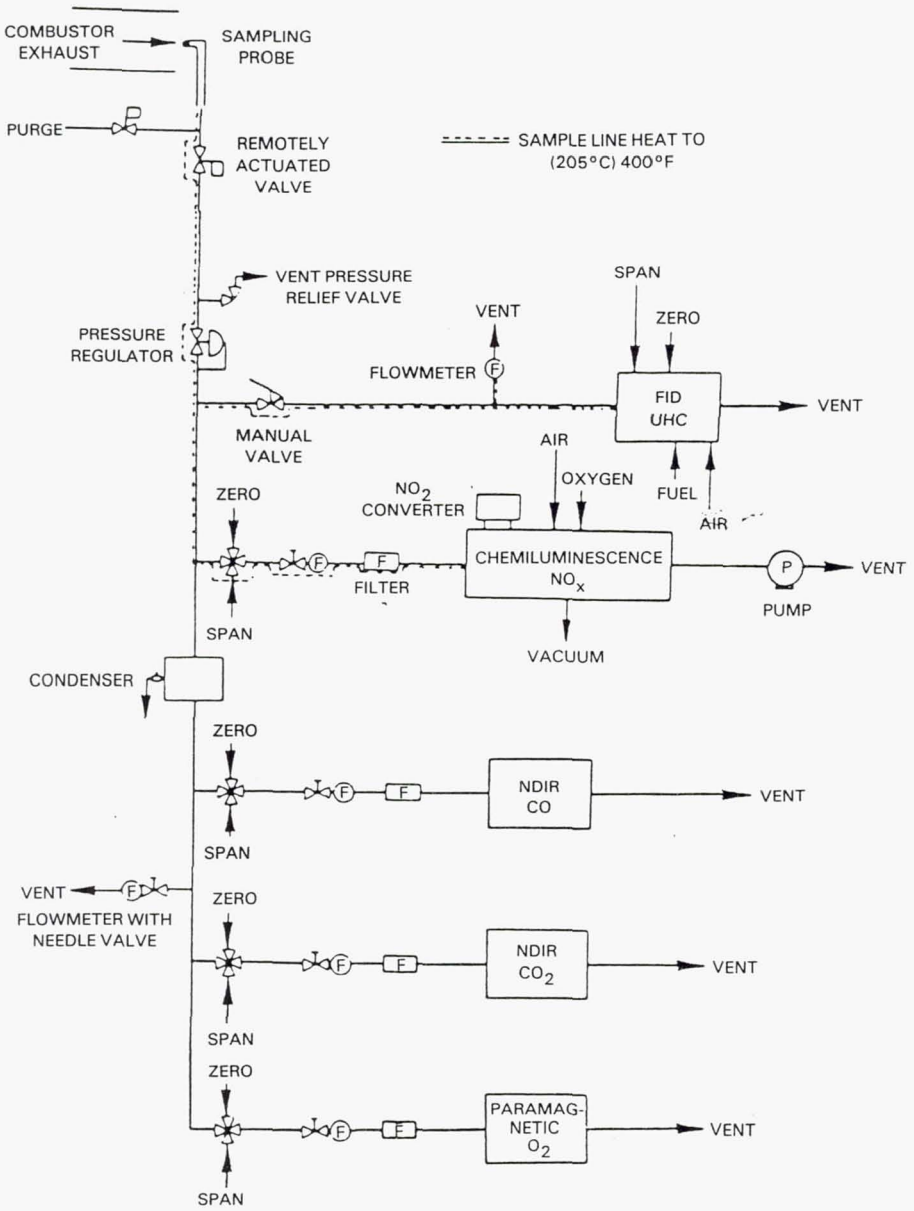

Figure 5-24 Emission Sampling and Analysis System in the Jet Burner Test Stand.

A smoke measurement system, designed and fabricated to sample smoke according to the specification in SAE ARP 1179 is also installed in the Jet Burner Test Stand. This system is essentially identical to that employed in X-902 Test Stand as described in Section 5.3.1 and shown in Figure 5-21.

The tests conducted at the Jet Burner Test Stand involved the use of only two fuels, Jet A and Experimental Reference Broad Specification Fuel (ERBS). The Jet A fuel was drawn from the central storage tank at the facility while the ERBS fuel was stored in a smaller dedicated tank at the test stand. ERBS fuel was trucked from the large storage tank at the Pratt & Whitney Middletown facility to United Technologies Research Center as required to maintain an adequate supply for testing. The fuel delivery system in the test stand was essentially identical to that in X-902 Stand as shown in Figure 5-24 except that it included only two rather than four fuel sources, i.e. Jet A and ERBS, and did not have a heat exchanger for preheating the fuel.

SECTION 6.0

EXPERIMENTAL PROCEDURES

This section defines the parameters used in assessing the performance and emissions characteristics of the combustors and describes the test procedures. The various combustor performance and emissions parameters that are discussed as program results are listed in Table 6-1. Symbols are defined in the Nomenclature List.

TABLE 6-1
SUMMARY OF COMBUSTOR PERFORMANCE PARAMETERS

Parameter	Symbol	Units	Measured	Calculated
Total Airflow	W_{at}	Kg/sec (lb/sec)	X	
Burner Airflow	W_{ab}	Kg/sec (lb/sec)	X	X
Inlet Total Pressure	P_{Tin}	MPa (psia)	X	
Inlet Total Temperature	T_{Tin}	°K (°F)	X	
Reference Velocity	V_{Ref}	M/sec (ft/sec)		X
Total Fuel Flow	W_F	Kg/sec (lb/sec)	X	
Fuel Flow Split	% of W_F	%	X	
Fuel Air Ratio	F/A	--		X
Burner Total Pressure Loss	$\Delta P/P_{Tin}$	% of P_{Tin}	X	
Metal Temperature	Tm	°K (°F)	X	
Fuel Temperature	T_{fuel}	°K (°F)	X	
Pattern Factor	PF	--		X
Carbon Balance Fuel/Air Ratio	FA_{CB}	--		X
Emissions Index	EI	g/kg		X
Combustion Efficiency	nc	%		X
EPA Parameter	EPAP	g/kN		X

6.1 COMBUSTOR EXIT CONDITION DEFINITION

Figure 6-1 shows schematic rear views of the combustor segments and the transverse position of the eight instrumented vanes in the rig exit vane pack relative to the fuel injectors and other principal features of the combustor. In the case of the reference PW2037 combustor and the variable geometry combustor configurations, the instrumentated vanes spanned 57 percent of the total width of the combustor segment, including the regions downstream of the two center fuel injectors. This central sector was considered free of end effects such as those produced by endwall cooling or corner flameholding so that averages determined from data acquired from all eight vanes would be representative of the average combustor exit conditions. Consequently, average combustor exit total temperature was computed as the numerical average of the readings from 40 gas temperature thermocouple probes on these eight vanes after excluding any that were not operational. Likewise, the average combustor exit total pressure was obtained by averaging the pressure at each of the 32 total pressure probes on the vane pack while average combustor exit emissions concentrations were those determined from analysis of a single sample produced by extracting combustor products through all 32 of these probes simultaneously and drawing them into a common mixing chamber.

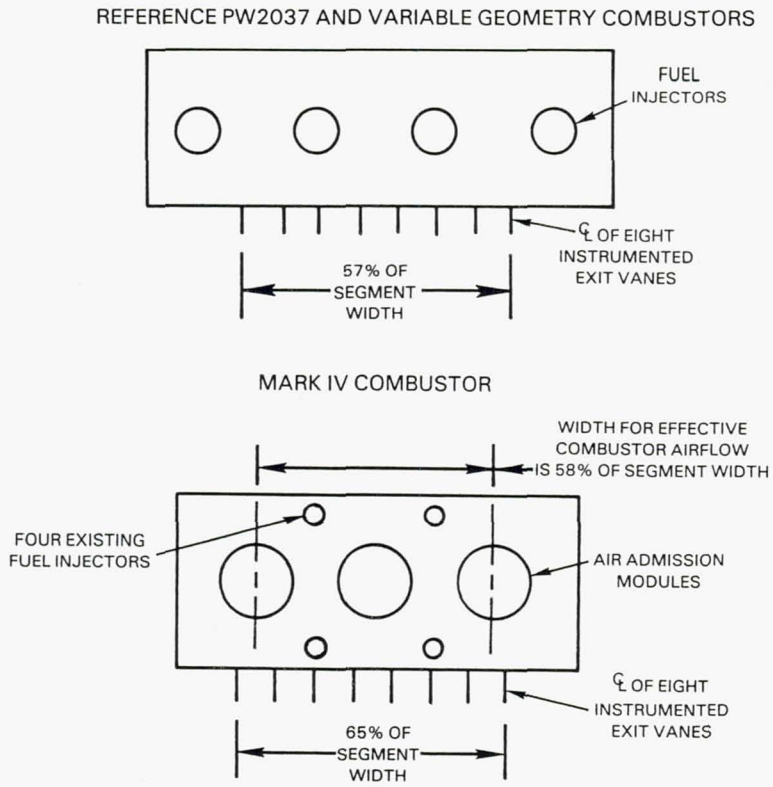

Figure 6-1 Schematic Rear Views of Combustors and Exit Instrumentation Vanes.

Additional considerations were required in evaluating data from the Mark IV combustor. Early testing experience with this configuration indicated that the combination of three air admission modules and only the two pairs of fuel injectors between them was insufficient to produce transverse uniformity of the fuel-air mixture. In effect the combustor was missing two additional pairs of "half fuel injectors" near the endwalls of the rig. To compensate for this, examination of the exit conditions was restricted to the center region of the combustion and bulk fuel air ratios were computed on the basis of all of the fuel mixing with the air entering through the center air admission module and half of that through each of the modules to either side. As shown on Figure 6-1, this made the effective width of the segment 58 percent of the endwall to endwall width and placed the two outermost of the eight instrumented exit vanes outside this region. Consequently, when computing average exit total temperatures or total pressures for the Mark IV combustor, only the measurements obtained from sensors on the six center vanes of the vane pack were used in determining the average. However, even with this restriction, the fuel air ratios computed from a carbon balance on a mixed gas sample extracted from the probes on these six vanes were found to be much lower than anticipated from the measured rig air and fuel flow. Restricting the gas sampling to the four centermost vanes during the evaluation of Configuration M-3 produced better agreement between metered and carbon balance fuel air ratios. Emissions sampling was restricted to extracting mixed samples from the probes on these four vanes for computing average emissions values for the remaining configurations of the Mark IV combustor.

6.2 PERFORMANCE PARAMETER DEFINITIONS

Combustor performance was determined from the following computed parameters:

Combustor Airflow

The combustor airflow Wab is calculated by subtracting the measured simulated inner and outer turbine cooling air bleed flows, the estimated combustor endwall cooling airflow and, in the case of the Mark IV combustor, the flow which bypassed the burner between the rig case and combustor endwalls from the measured total rig airflow. For purposes of computing an effective fuel air ratio of the Mark IV combustor, an effective combustor airflow equivalent to two thirds of that described above, as defined in Section 6.1, was used.

Reference Velocity

The reference velocity is defined as that flow velocity that would result if the total combustor airflow at the combustor inlet temperature and static pressure were passed through the combustor liner at the maximum cross sectional area. This area is 369 cm^2 (57.2 in^2) for the reference PW2037 combustor and the variable geometry combustor concept and 382 cm^2 (59.4 in^2) for the Mark IV combustor sector.

Total Pressure Loss

The total pressure loss across the burner section includes losses in the diffuser as well as those across the burner proper and is referenced to the average burner section inlet total pressure as:

$$\frac{\Delta P_T}{P_{Tin}} = \frac{P_{Tin} - P_{Texit}}{P_{Tin}} \qquad \text{(Eq. 1)}$$

Pattern Factor

The combustor exit temperature nonuniformity is characterized by the pattern factor which is defined as:

$$P.F. = \frac{T_{Texit\ max} - T_{Texit}}{T_{exit} - T_{Tin}} \qquad \text{(Eq. 2)}$$

where: $T_{Texit\ max}$ = maximum temperature measured at exit
T_{Texit} = average exit temperature
T_{Tin} = average inlet temperature

Metered Fuel/Air Ratio

The metered fuel/air ratio is the ratio of the total combustor fuel flow, as defined by turbine meters in the fuel supply system, to Wab, the combustor airflow or, in the case of the Mark IV combustor, the effective combustor airflow.

6.3 EMISSIONS ANALYSIS PARAMETERS

Carbon Balance Fuel Air Ratio

The carbon balance fuel/air ratio was computed using the equation:

$$F/A_{CB} = \frac{M_C + \alpha M_H}{M_{AIR}} \quad \frac{N_{CO} + N_{CO2}}{100 - \frac{1}{2} + \frac{\alpha}{4} N_{CO} - \frac{\alpha N}{4} CO2} \qquad \text{(Eq. 3)}$$

Where: M_x is the molecular weight of the x^{th} specie
N^x is the mole fraction of the x^{th} specie
α^x is the hydrogen to carbon ratio of the fuel

Emissions Indices

Concentrations of emissions constituents were reduced to emission indices in the form of grams of constituent per kilogram of fuel using the carbon balance fuel/air ratio of the sample to make the conversion from concentrations. Corrections were applied to the emissions indices to account for deviation of the test condition from standard conditions. These included correction of NOx emissions for inlet humidity and of all constituents for deviations of the inlet total pressure relative to the PW2037 engine cycle and had the form:

$$\text{Corrected } EI_{THC} = \text{Measured } EI_{THC} \times \frac{P_{Tmeas}}{P_{Tcorr}} \qquad \text{(Eq. 4)}$$

$$\text{Corrected } EI_{CO} = \text{Measured } EI_{CO} \times \frac{P_{Tmeas}}{P_{Tcorr}} \qquad \text{(Eq. 5)}$$

$$\text{Corrected } EI_{NOx} = \text{Measured } EI_{NO} \times \frac{PTcorr}{P_{Tmeas}} \exp\left(0.0188 \left(H_{meas} - H_{corr}\right)\right) \qquad \text{(Eq. 6)}$$

where: H = Inlet specific humidity

For operation at the idle, approach or cruise condition, the pressure corrections were small and consisted only of corrections for experimental inaccuracy in setting test conditions. At the climb and takeoff power levels, the pressure correction factors were more significant and reflected the inability of the test facilities to achieve the full engine combustor inlet pressure as described in Section 5.3. However, at these conditions the carbon monoxide and unburned hydrocarbon emissions were very low and the pressure correction is only of significance for the oxides of nitrogen.

The humidity correction on the emissions oxides of nitrogen is referenced to a standard of 6.34 gm/kg, and during operation at X-902 Test Stand was based on a measured specific humidity at the combustor rig inlet. No attempt was made to apply this correction factor to the test combustor inlet humidity when operating in the Jet Burner Test Stand at United Technologies Research Center with the hydrogen fired heater burner, since the resulting humidity levels were substantially above the extremes of atmospheric humidity that had been used in generating this correction factor. Since the oxides of nitrogen emissions determined in this facility at power levels above idle, where use of heater burner was required, were already compromised by uncertainties in the NOx generated in the heater burner and during the subsequent oxygen replenishment, this data could not be adjusted to reflect that generated only in the test combustor. Consequently, the reported levels reflect uncorrected total NOx output from both combustors in series.

Combustion Efficiency

Combustion efficiency is calculated from gaseous emissions data on a deficit basis using the average carbon monoxide and total unburned hydrocarbon emissions. The calculation is based on an assumption that the total concentration of unburned hydrocarbons can be assigned the heating value of methane (CH4) and the equilibrium concentration of carbon monoxide is negligible. The equation is:

$$\eta_c = 1 - \frac{10\ EI_{CO} + 50.2\ EI_{THC}}{1000\ HV} \qquad \text{(Eq. 7)}$$

where: HV = heating value of the fuel (MJ/kg)

EPA Weighted Emissions Parameter

The average emissions at the idle, approach, climb and takeoff conditions are used to compute the EPA parameter for a landing and takeoff cycle in the form:

$$EPAP = \frac{\sum_j EIj\ Wfj\ tj}{Fn} \qquad \text{(Eq. 8)}$$

where: EI = Emission Index (gm/kg of fuel)
Wf = Fuel flow (kg/hr)
t = Time in mode (hrs)
j = Mode, i.e., idle, approach, climb and takeoff
Fn = Rated engine thrust (kilonewtons)

This equation reduces to the form

$$EPAP = \sum_j Aj\ EIj \qquad \text{(Eq. 9)}$$

where Aj is a coefficient unique to the particular engine cycle. Table 6-2 lists the values of the coefficients for the PW 2037 engine cycle.

TABLE 6-2
VALUE OF EPAP COEFFICIENTS FOR PW2037 ENGINE CYCLE

Mode	Time In Mode	Coefficient A
Idle	26.0	1.315
Approach	4.0	0.572
Climb	2.2	0.999
Takeoff	0.7	0.386

6.4 TEST PROCEDURES

The test combustors were evaluated over matrices structured around the combustor operatiing conditions in the PW2037 engine as listed in Table 3-1. The rig operating conditions were maintained as close as possible to those of the engine within the constraints of facility limitations described in Section 5.3. Because of the program objective of evolving the combustor concepts toward operation on broadened properties fuels, the majority of the test points involved operation with ERBS fuel. The basic matrix included operation with ERBS at the combustor design condition at each of the four power levels in the Environmental Protection Agency landing and takeoff cycle and at the cruise aerodynamic design point of the engine. Comparative data were also obtained with Jet A fuel, and parametric variations were conducted at the idle and takeoff conditions. A second and more extensive test matrix was used for evaluation of the performance of selected combustor configurations. This test matrix paralleled the structure of the basic matrix with the principal feature being the inclusion of test points with the two additional test fuels, i.e., the No. 2 Commodity fuel and the 11.8 percent hydrogen content blended fuel. The matrix involved operation of the combustors on both Jet A and ERBS at the five major operating conditions, i.e., the four conditions in the EPA landing and takeoff cycle and cruise condition. Operating with No. 2 Commodity and 11.8 percent hydrogen content test fuels was limited to the idle, cruise and takeoff operating conditions. The tests matrices also included parametric variations of combustor operating conditions including fuel air ratio, various combinations of bulkhead mounted fuel injectors on the Mark IV combustor and operation of the variable geometry combustor with the air valves either open or closed. While these valves were linked together for simultaneous actuation from outside the rig case by rotating a drive rod, the installations in the test stands did not include a remote controlled drive mechanism inside the pressure vessels. Consequently, the test programs for the variable geometry combustor evaluations were formulated in two phases. After all of the desired test data was acquired with the valves in one position, the facility was shut down and the valve actuating drive rod turned manually to the other position by removing a cover plate of the pressure vessel.

The steam heat exchanger in the fuel system in X-902 Stand was used to heat the fuel during the evaluation of selected configurations. The lean stability and the idle emission characteristics of the reference PW2037 combustor (Configuration V-1) AND Configutations M-12 and M-13 of the Mark IV combustor concept were investigated over a range of fuel temperature from ambient to about 425°K (305°F).

In conducting the combustor tests, efforts were made to conserve the ERBS and other special test fuels. The combustors were operated on Jet A fuel during transitions between test conditions as well as during the initial startup. The remote test fuel selection system was used to switch operation to ERBS or one of the other special test fuels only after inlet condition stabilization had been achieved at the desired test conditions.

The data of Section 5.1 indicate that the heating value of the test fuels decreases with decreasing hydrogen content. In operating an engine on lower However, the difference in the heating value of Jet A and ERBS was less than one percent and increments in the fuel/air ratio of this magnitude would be less than the accuracy to which rig operating conditions could be maintained.

SECTION 7.0

EXPERIMENTAL RESULTS

During the experimental investigation, a total of twenty one combustor configurations were evaluated. Twelve of these were evaluated in the moderate pressure Jet Burner Test Stand at United Technologies Research Center while the remaining nine were tested in the Pratt and Whitney high pressure combustor test facility. All configurations were evaluated with Jet A and Experimental Referee Broad Specification (ERBS) fuels and four of the configurations evaluated in the high pressure facility were subjected to more extensive testing with a No. 2 Commodity fuel and a lower hydrogen content fuel produced by blending a selected feedstock with ERBS. Data from these tests are tabulated in Appendix C and the results are discussed in this section.

Section 7.1 presents the results of the evaluation of the reference PW2037 type combustor and is significant because it establishes a baseline for fuel sensitivity of a current technology combustor against which the advanced technology concepts could be compared. Section 7.2 includes a discussion of the results of the evaluation of the final configuration of the variable geometry combustor concept while Section 7.3 presents the results of the evaluation of intermediate configurations of the variable geometry combustor. Sections 7.4 and 7.5 provide a parallel discussion of the status of the Mark IV advanced technology combustor with the former presenting a detailed assessment of the performance of a selected configuration while the latter describes the evolution of the concept through various configuration changes.

7.1 FUEL SENSITIVITY OF THE REFERENCE PW2037 COMBUSTOR

The fuel sensitivity of the reference PW2037 combustor was established by extensive testing of Configuration V-1 in the Pratt and Whitney high pressure test facility using all four of the above cited test fuels. As indicated in Section 4.1, the Configuration V-1 test combustor was an early developmental version of the production PW2037 combustor and, while there were some minor differences in construction details and local stoichiometry, it was considered representative of the production combustor for the purpose of establishing a fuel sensitivity baseline.

7.1.1 Liner Heat Load

Typically, fuels with lower hydrogen content have been found to form higher concentrations of carbonaceous particulates in the initial combustion zone. These particles become luminous when heated to near stoichiometric temperatures by the combustion gases. This radiant heat flux to the liner becomes a significant part of the net heat load. In this test program, radiant heat flux to the combustor liner was measured using two radiometers which protruded through holes in the third louver of the inner and outer liner respectively. These radiometers were positioned downstream of the same fuel injector so that the same volume of combustion products were viewed from opposite sides.

One radiometer was of the porous plug type, while the other was a Medtherm commercial unit. The latter tended to produce erratic readings, attributed to soot accumulation on its window, and are not reported. The porous plug radiometer provided more consistent results both in terms of heat flux level at the operating conditions of interest and the variation of radiant heat flux with fuel composition. Figure 7-1 shows that the trend in measured radiant heat flux is qualitatively consistent with accepted empirical models of the combined gas/luminous particle radiation process (Reference 24). These data show a general trend of increasing heat flux with decreasing hydrogen content. The change from Jet A (13.7 percent hydrogen) to ERBS (12.9 percent hydrogen) produced an increase in heat flux of up to 17.5 percent at the cruise operating conditions. At lower hydrogen contents and at the higher power takeoff and climb operating conditions the heat flux is higher in magnitude but less sensitive to fuel hydrogen content variations. This leveling could be caused by saturation of the number density of luminous particles at which, according to current empirical models such as that of Reference 24, the "effective emissivity" of the combustion products exponentially approaches that of a blackbody radiator and there is no further increase in heat transfer.

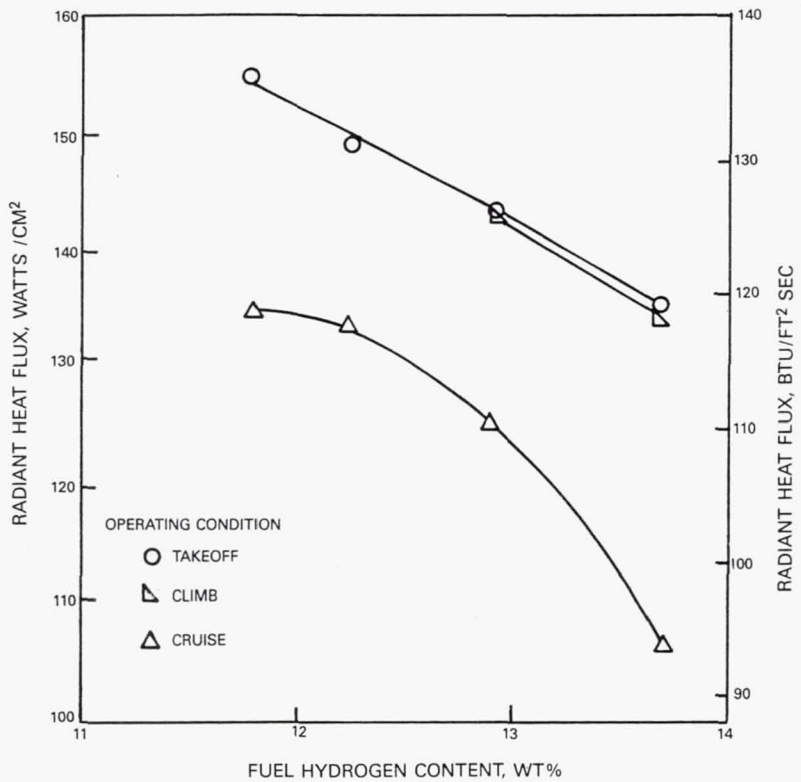

Figure 7-1 Radiant Heat Flux to Liner in Primary Zone of Reference PW2037 Combustor (Configuration V-1).

While it would be expected in normal engine operation that the heat flux at the climb (85% thrust) condition would be less than at takeoff (100% thrust), the data of Figure 7-1 shows it to be essentially identical. This is because facility airflow limitations dictated that both the takeoff and climb conditions be run at the same inlet total pressure, and the only difference in rig operating conditions was a 32°K (57°F) difference in combustor inlet total temperature.

Relative to the JT9D combustors tested in Phase I of this program (Reference 5), the measured heat fluxes in the PW2037 combustor are 60 to 100 percent higher. This can be attributed to several factors, the most significant of which is the higher pressure ratio of the PW2037 engine cycle. Other contributing factors include richer primary zone stoichiometry and axial placement of the radiometer relative to the regions of most intense combustion.

7.1.2 Liner Metal Temperatures

Use of lower hydrogen content fuels increases radiant heat flux which increases local metal temperatures in the combustor liner, reducing structural life. As indicated in Section 5.2.2, thermocouples were installed in the combustor liner sectors to measure these temperature increments. The thermocouple junctions were positioned near the weld between a film cooled panel and the riser of the following louver. Since the temperature gradient between this region and the cooler louver knuckle is critical to cyclic fatigue in both conventional sheet metal louvered liner of Configuration V-1 and the rolled ring liner construction of the PW2037 engine combustor, the measurements were relevant to liner life in either combustor. Figures 7-2 and 7-3 show the measured temperature distribution in the liner of the reference PW2037 (Configuration V-1) combustor for cruise and takeoff respectively. Local metal temperatures observed during operation on Jet A fuel and the incremental increases in metal temperature encountered with ERBS fuel and the 11.8 percent hydrogen content fuel relative to Jet A are presented. The data demonstrate a progressive increase in local metal temperatures with decreasing hydrogen content. The increments in liner temperature are generally more pronounced in the primary zone than in the dilution zone.

Within the primary zone, which is defined as that enclosed by the first three louver panels, the increases in liner temperature associated with the use of ERBS relative to Jet A fuel are in the range of 17°K to 43°K (31°F to 77°F) and 11°K to 34°K (20°F to 61°F) at cruise and takeoff, respectively. Comparable data for the shift from Jet A to the 11.8 percent hydrogen content fuel show liner temperature increases of 23°K to 50°K (41°F to 90°F) and 19°K to 43°K (34°F to 77°F) in the louvers enclosing the primary zone at cruise and takeoff, respectively. Relative to the measured liner temperature increments in the JT9D bulkhead type combustor tested under the Phase I program (Reference 5), the range of the increments aassociated with changes in fuel composition in the reference PW2037 combustor are comparable but there are greater distributions of temperature within these ranges. The relative uniformity of the liner temperature increments in the JT9D combustors led to the conclusion that the combustion process was global and the radiant source was diffuse. In the case of the PW2037, the higher temperature levels and the temperature increments associated with changes in fuel hydrogen content generally occurs in regions downstream of fuel injectors, suggesting combustion is more concentrated in these regions than in the JT9D combustor.

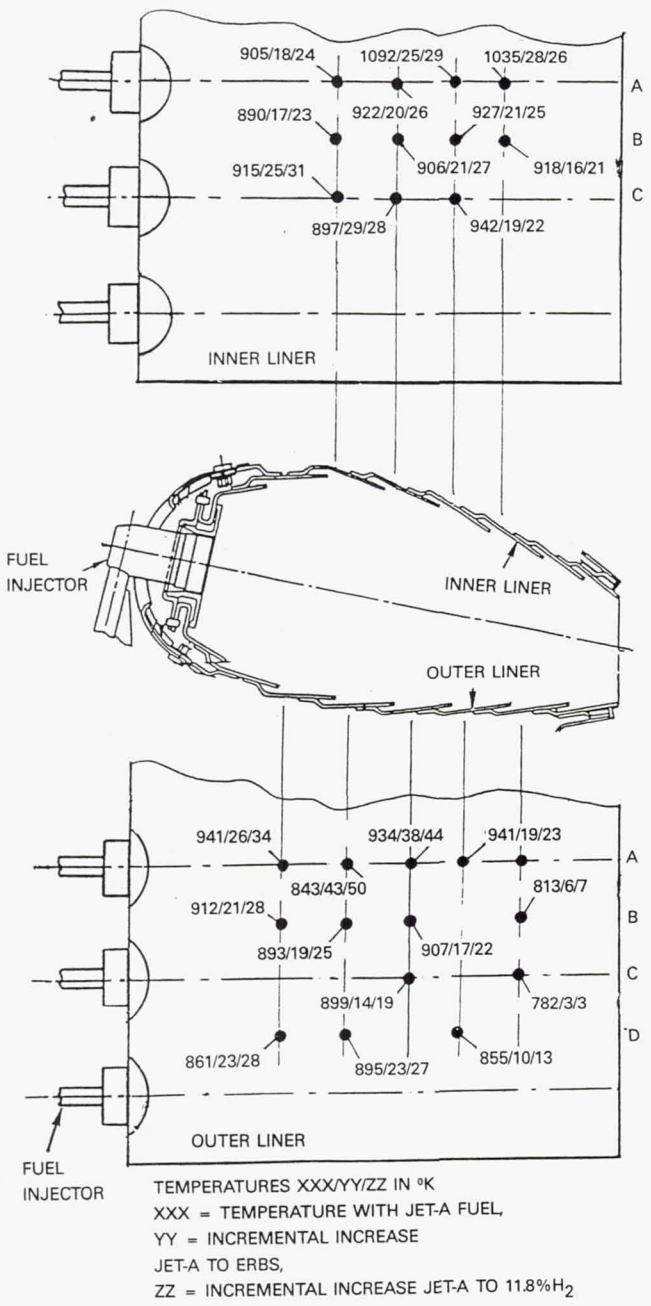

Figure 7-2 Liner Temperature Distribution of Baseline Reference PW2037 Combustor (Configuration V-1) at Cruise.

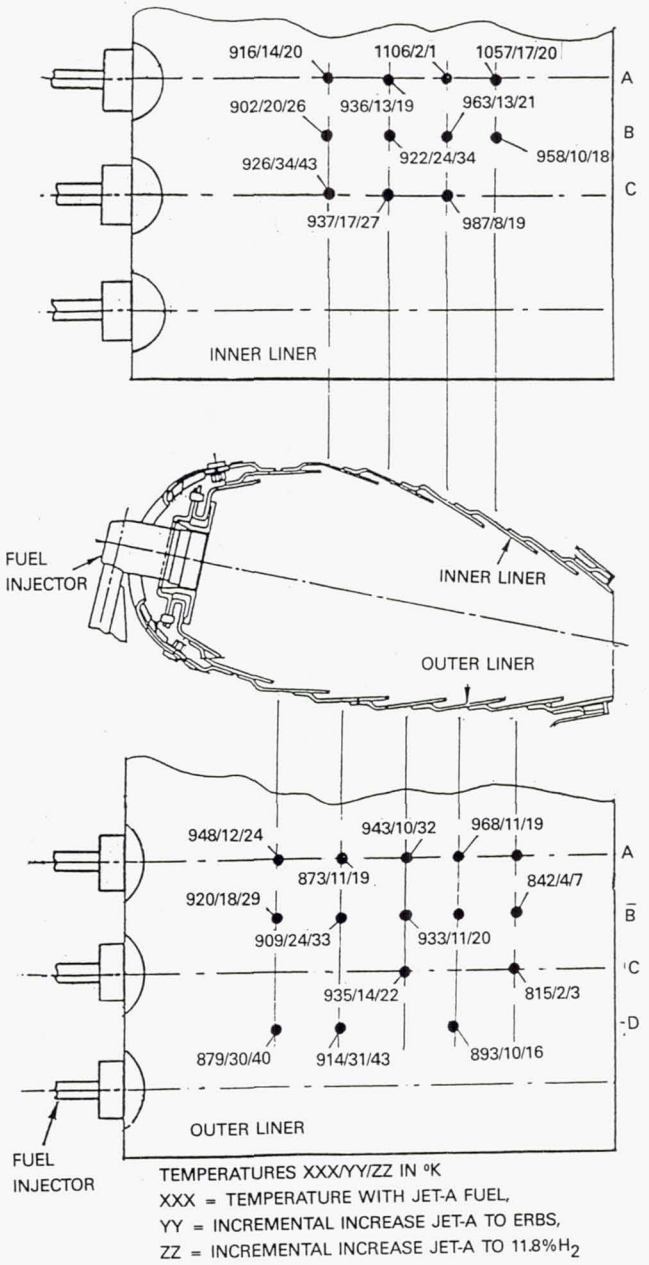

Figure 7-3 Liner Temperature Distribution of Baseline Reference PW2037 Combustor (Configuration V-1) at Cruise.

Figure 7-4 provides an overview of the impact of fuel composition on the liner temperatures of the reference PW2037 combustor. The metal temperatures presented are averages of all combustor liner thermocouples enclosing the primary and dilution zones, respectively. Positioning the thermocouples near the weld region of the louver makes the measurements a representative indicator of temperatures in the life limiting regions and not an average metal temperature for the entire liner surface. The average liner temperatures are higher in the dilution zone of the combustor, despite the lower nominal combustion gas temperatures in this zone, because the cooling air flows to the louvers in this part of the combustor are less than those in the primary zone.

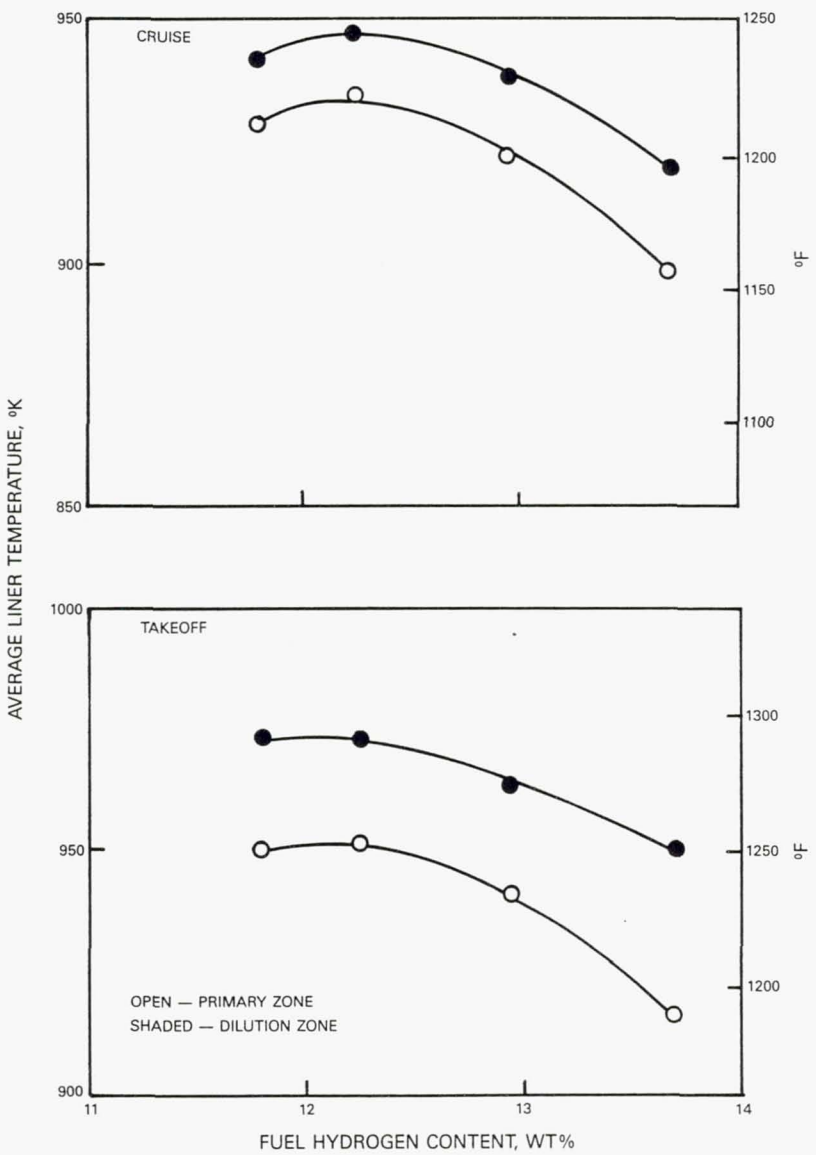

Figure 7-4 Effect of Fuel Composition on Average Liner Temperatures of Reference PW2037 Combustor (Configuration V-1).

The data of Figure 7-4 are generally consistent with the anticipated trend of increasing liner temperature with decreasing fuel hydrogen content at both cruise and takeoff conditions. The singular exception is the reversal in temperature rise between the Commodity fuel (12.25% hydrogen) and the 11.8% hydrogen blend fuel at the cruise condition, and this may be an artifact of the numerical averaging process. The use of ERBS (12.9% hydrogen) as opposed to Jet A fuel (13.7% hydrogen) produced increases in average primary zone liner temperature of 23°K (42°F) and 21°K (38°F) respectively at the cruise and takeoff condition. These increments are about double those observed in the JT9D bulkhead type combustor evaluated in the Phase I Broad Specification Fuels Combustion Technology Program (Reference 5) and may be attributable to the richer stoichiometry of the primary combustion zone of the reference PW2037 combustor. Comparison of the sensitivity of the liner temperature in the dilution zone to fuel composition reveals even greater differences between the JT9D and PW2037 combustors. Figure 7-4 indicates that the sensitivity of the metal temperatures in the dilution zone of the reference PW2037 to fuel composition is comparable to that in the primary zone. Conversely, the JT9D combustors evaluated in Phase I revealed essentially no sensitivity of dilution zone liner temperatures to fuel hydrogen content. These differences in sensitivity must be attributed to the differences in combustor length. In the JT9D bulkhead combustor, with a burning length of 368mm (14.9 inches), the primary and dilution zones are separated spatially and the liner enclosing the dilution zone has a relatively low view factor from the luminous combustion products in the primary zone. However, in the PW2037 combustor, with a burning length of 60 percent of that in the JT9D, the primary and dilution zones are more closely coupled spatially, the primary combustion zone is operating at richer stoichiometry and the burnout of luminous combustion particles extends well into the dilution zone. All of these factors can contribute to the high sensitivity of liner temperature to fuel hydrogen content throughout the length of the PW2037 combustor.

Liner life can be related to the incremental changes in metal temperature associated with the changes in fuel composition. Stress analyses of louvered liners, of both the conventional spun sheet metal and the rolled ring constructions, in combination with empirical data on the fatigue strength of Hastelloy X liner material provide correlations between the temperature gradient across the louver knuckle at takeoff and the cyclic fatigue life of this region. Measured temperature increases in the weld region of louvers in the combustors at takeoff have been used to calculate the reduction in liner life for several situations. These data are summarized in Table 7-1.

The projections indicate that, when based on the average measured temperatures in the critical weld juncture region, the increase in liner temperature and hence, reduction in life of a sheet metal hoop liner, is greater in the reference PW2037 combustor than the JT9D bulkhead combustor evaluated in Phase I when the fuel is changed from Jet A to ERBS. However, the PW2037 engine combustor incorporates the advanced technology rolled ring liner and when the same increments in liner temperature are incorporated in the cyclic fatigue analysis of that liner construction, the equivalent loss in life is only about 70 percent of that projected for the JT9D, despite the higher increments in liner temperature associated with the Jet A to ERBS transition.

Table 7-1

Projected Effect of Use of ERBS Fuel vs.
Jet A on Life of Combustor Liners

Combustor Liner Type	JT9D* Sheet Metal	PW2037 Sheet Metal	PW2037 Rolled Ring
Based on Average Liner Temperature Increase °K (°F)	12.3 (22)	18.4 (33)	18.4 (33)
Reduction in Life - %	11	16	8
Based on Maximum Liner Temperature Increase °K (°F)	40 (72)	34 (61)	34 (61)
Reduction in Life - %	36	30	15

* Configuration VG-1 of Phase I (Reference 5)

A similar trend is evident in the projections made on the basis of the maximum measured liner temperature where first failure would occur. While the largest temperature increment produced by the fuel change occurred in the JT9D combustor, the projected advantage of the rolled ring liner construction in the PW2037 production combustor is still evident. The projected loss of liner life increased by a factor of two or more when based on the maximum as opposed to the average temperature implying that sensitivity to fuel composition may be reduced by reducing the severity of the heat load at these isolated locations.

7.1.3 Emissions

Figure 7-5 shows the measured carbon monoxide and unburned hydrocarbon emissions from the reference PW2037 combustor at the idle combustor inlet conditions. Data are presented for a range of fuel/air ratios centered about the design proportions. The data indicate the low power emissions characteristics of this combustor to be extremely good with the goal levels of these constituents being achieved over the entire range of fuel/air ratios investigated and with all four test fuels. These goal levels are consistent with the program goal of compliance with the previously proposed EPA Class T-2 standards for engines certified after January 1, 1984 and with the assumption of reasonably low emissions of these constituents at higher power levels.

The unburned hydrocarbon emissions reveal a distinct minimum in output at a fuel air ratio of about 0.012 on all four test fuels. This mixture strength is about 25 percent higher than the design idle fuel air ratio of 0.0096 and is probably indicative of stoichiometric proportions in the actual mixture involved in the primary combustion process. While not as pronounced, a similar trend of minimum carbon monoxide emissions output is also evident at about the same fuel air ratio.

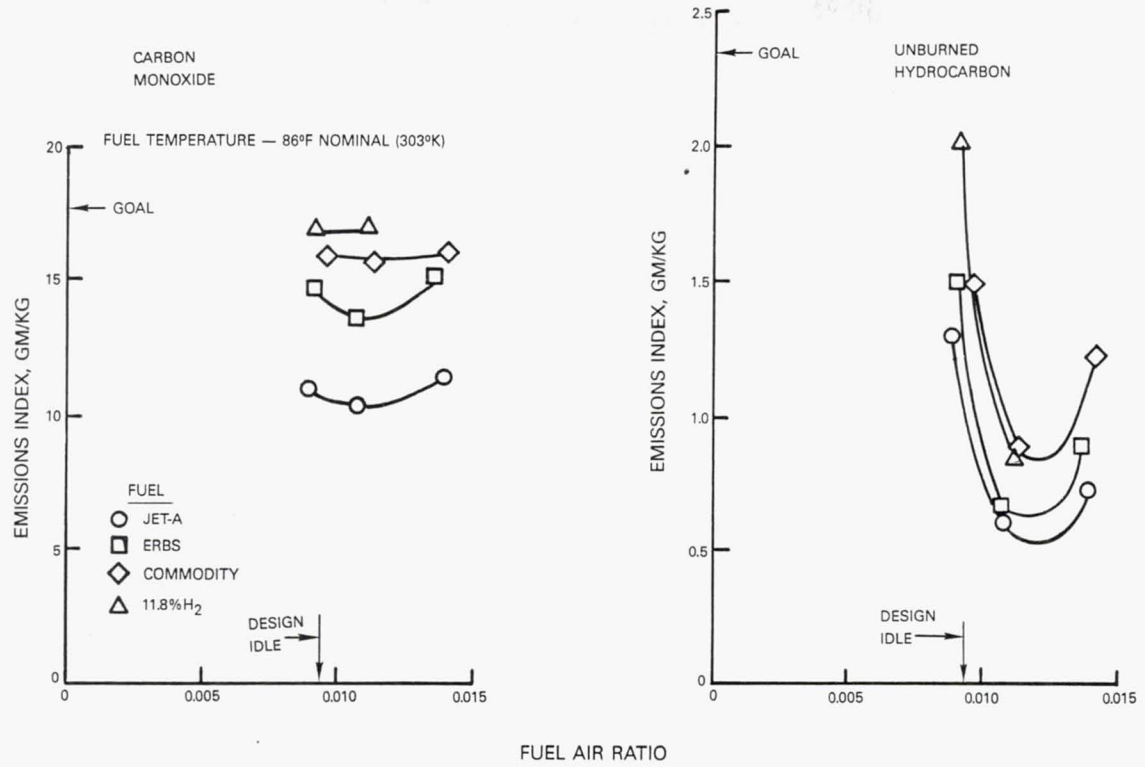

Figure 7-5 Idle Emissions Characteristics of Reference PW2037 Combustor (Configuration V–1).

A distinct sensitivity of the emissions output to fuel composition is also evident with the carbon monoxide emissions increasing with decreasing hydrogen content of the fuel. The unburned hydrocarbon emissions also exhibit a trend of increasing emissions output with decreasing fuel hydrogen content. However, the trend is not as distinct and may also be influenced by other factors such as fuel viscosity and volatility.

While the data of Figure 7-5 were obtained at essentially ambient fuel supply temperature, additional tests were conducted at the engine idle conditions with the fuel preheated in a steam heat exchanger to 372°K (208°F). Emissions measurements in the form of Figure 7-5 were interpolated to define the emissions indices at the design idle fuel air ratio of 0.0096 and the results are presented in Figure 7-6. The unburned hydrocarbon emissions, while already very low relative to the program goal at ambient fuel temperature, are reduced further by preheating the fuel and reach a common concentration of 0.8 gm/kg. It is suspected that the sensitivity of unburned hydrocarbon emissions to fuel changes is dominated by the influence of viscosity on the atomization process. At ambient temperatures, the viscosities of the test fuels were shown in Section 5.1.1 to vary between 1.8 and 3.2 centistokes, whereas at 372°K (208°F), they would all be in the narrow range of 0.75 to 1.10 centistokes. This would explain the lowering and converging of the unburned hydrocarbon emissions with the four different test fuels when the fuel was preheated.

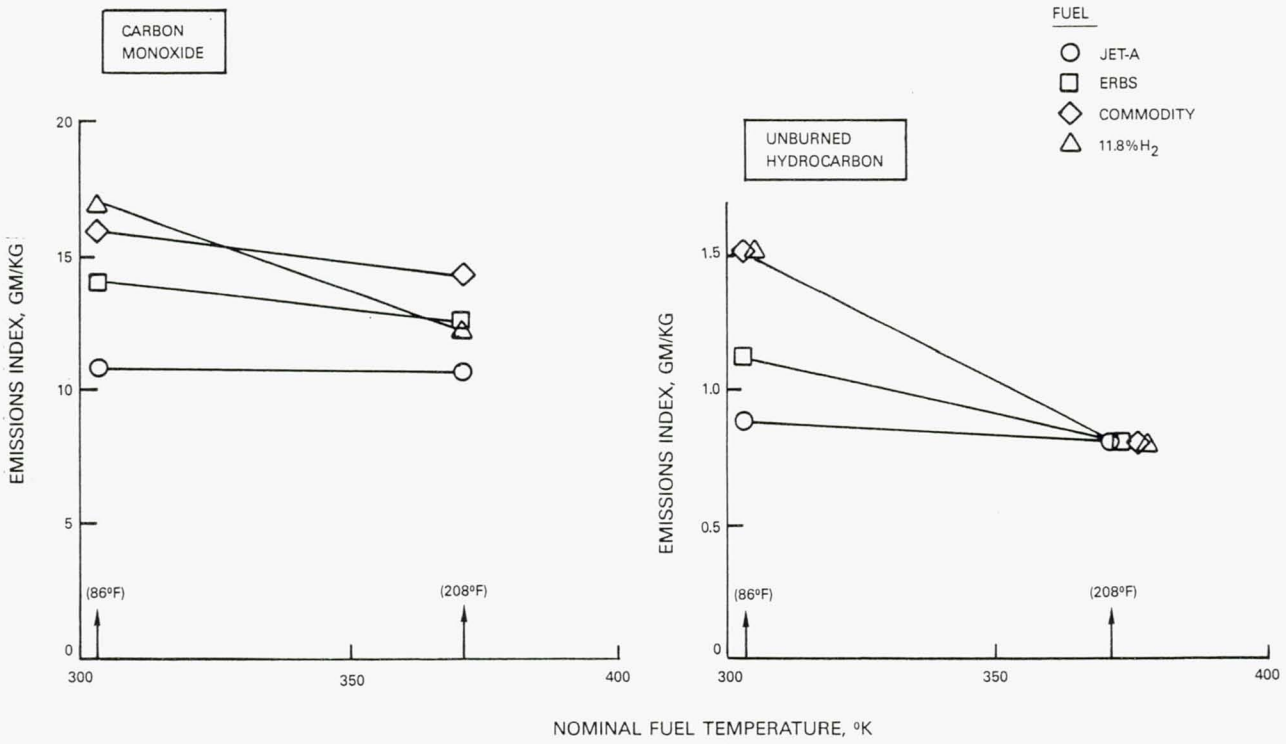

Figure 7-6 Effects of Fuel Temperature on Emissions Characteristics of Reference PW2037 Combustor at Design Idle (Configuration V-1).

Conversely, the carbon monoxide emissions output appears to be generally insensitive to fuel temperature - a result which supports the hypothesis that the fuel sensitivity of carbon monoxide emissions from a highly efficient rich primary zone combustor such as the reference PW2037 is dominated by fuel composition as opposed to physical properties such as viscosity and volatility. Curiously, the test fuel that exhibits the strongest response of carbon monoxide emissions to fuel temperature is the 11.8 percent hydrogen content blend that has disproportionately favorable viscosity and volatility for its composition.

Similar measurements of the carbon monoxide and unburned hydrocarbon emissions characteristics of the reference PW2037 combustor were obtained at approach (30% takeoff thrust) and higher power levels. These measurements were consistent with development experience in that the emissions were low and the combustion efficiency equaled or exceeded 99.97 percent with all combinations of test fuel and power level (above approach) investigated.

Figure 7-7 shows the variation of the emissions of oxides of nitrogen from the reference PW2037 combustor with fuel hydrogen content. Data are presented at the nominal cruise and takeoff operating conditions, the latter being corrected to the full combustor inlet total pressure of the PW2037 engine cycle according to the procedures of Section 6.0. The data at the cruise condition was obtained at essentially the design fuel air ratio but that at takeoff had to be acquired at a lower fuel air ratio than design (0.020 vs. 0.0241) to avoid overtemperaturing the rig exit instrumentation.

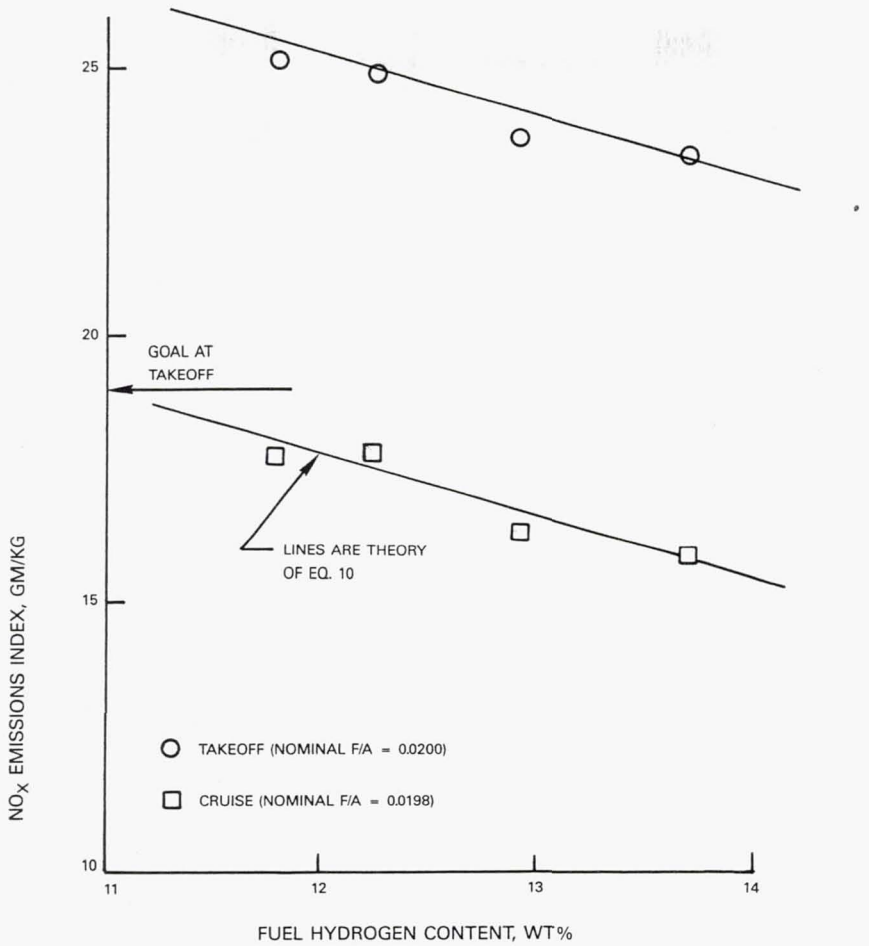

Figure 7-7 Emissions Characteristics of Reference PW2037 Combustor (Configuration V-1).

The data indicate a progressive increase in NOx emissions with decreasing hydrogen content. This has generally been attributed to the increase in adiabatic flame temperature caused by the reduced hydrogen content of the fuel. In Reference 4 an interpretation was advanced in which kinetic analysis of the NOx formation in a combustor led to the following relation between NOx emissions and flame temperature:

$$\frac{EINOx}{EINOx\ ref} = \left(\frac{Tf}{Tf_{ref}}\right)^{-0.53} \exp\left(\frac{67,400}{Tf_{ref}} - \frac{67,400}{Tf}\right) \qquad \text{(Eq. 10)}$$

In current technology combustors, with their swirl stabilized combustion zone, diffusion is the dominant mode of combustion and the majority of reactions occur at or near stoichiometric proportions. The theoretical variation of NOx emissions with hydrogen content was determined from Equation 10 using computed flame temperatures at an equivalence ratio of unity and combustion of Jet A fuel as the reference condition. The solid lines on Figure 7-7 show the theoretical variation for each flight condition and are in good agreement with the experimental measurements.

There are currently no constraints on the emissions of oxides of nitrogen from engines like the PW2037. However, goals for the advanced technology combustors being evolved under this program have been established consistent with the previously proposed Environmental Protection Agency Class T-2 requirements for engines certified after January 1, 1984. Assuming a reasonable relative distribution of emissions levels over the four points of the landing and takeoff cycle, an emissions index of 19gm NOx/kg must be achieved at takeoff if this overall goal is to be met. As shown on Figure 7-7, the reference PW2037 combustor did not achieve this goal and substantial reductions in NOx emissions will be required to do so.

7.1.4 Smoke

Unless they are oxidized in the remainder of the combustor, the carbon particulates formed in the primary zone are emitted with the other combustion products in the form of visible smoke. The smoke output of the reference PW2037 combustors was measured at selected high power operating conditions. Figure 7-8 shows the variation in measured SAE Smoke Number with fuel hydrogen content at combustor inlet conditions consistent with takeoff operation of the PW2037 engine but at reduced fuel/air ratios imposed by the exit instrumentation temperature limitations. The data indicate that smoke output varied considerably with fuel composition. The trend defined by the measurements with the 11.8 percent hydrogen blended fuel, the No. 2 Commodity fuel and ERBS is consistent with the hydrogen content variation of these fuels but the corresponding data obtained with Jet A deviates widely. Development experience with the PW2037 production engine combustor operating on Jet A fuel would indicate the Jet A data point on Figure 7-8 is high because of erroneous measurement. Assuming this is the case, the trend established by the other three fuels indicates that the reference PW2037 combustor would just achieve the program goal of an SAE Smoke Number less than 21 when operating on ERBS fuel.

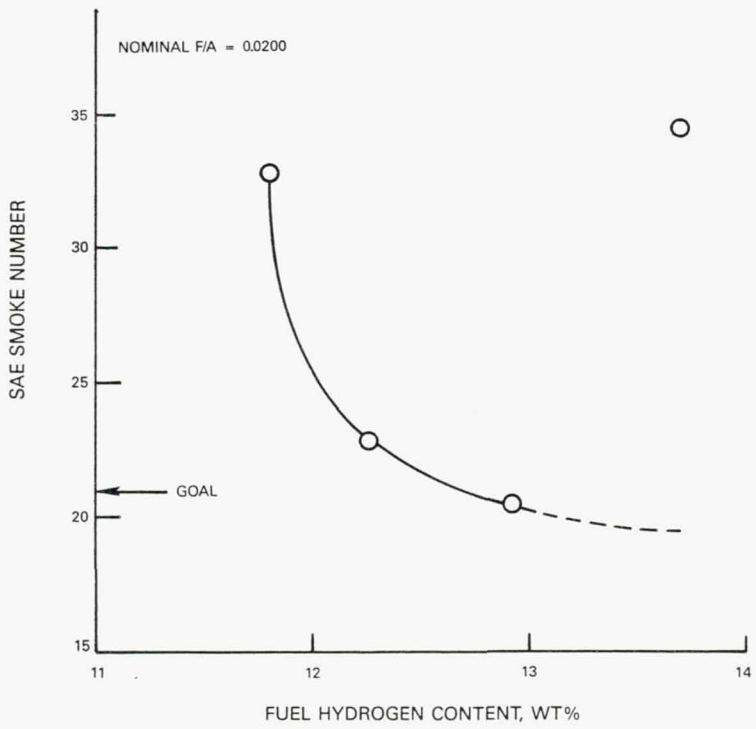

Figure 7-8 Smoke Characteristics of Reference PW2037 Combustor (Configuration V-1) at Takeoff.

7.1.5 Combustor Exit Temperature Distribution

While refining the combustor exit temperature distribution to achieve the program goals for pattern factor and radial profile was not a major objective of the technical effort, the sensitivity of these parameters to variations in fuel composition was investigated. Figure 7-9 shows a representative comparison of combustor exit temperature distribution with Jet A and ERBS fuel. This data was obtained with the combustor operating at takeoff conditions with the fuel/air ratio reduced to 0.020 because of exit instrumentation temperature limitations.

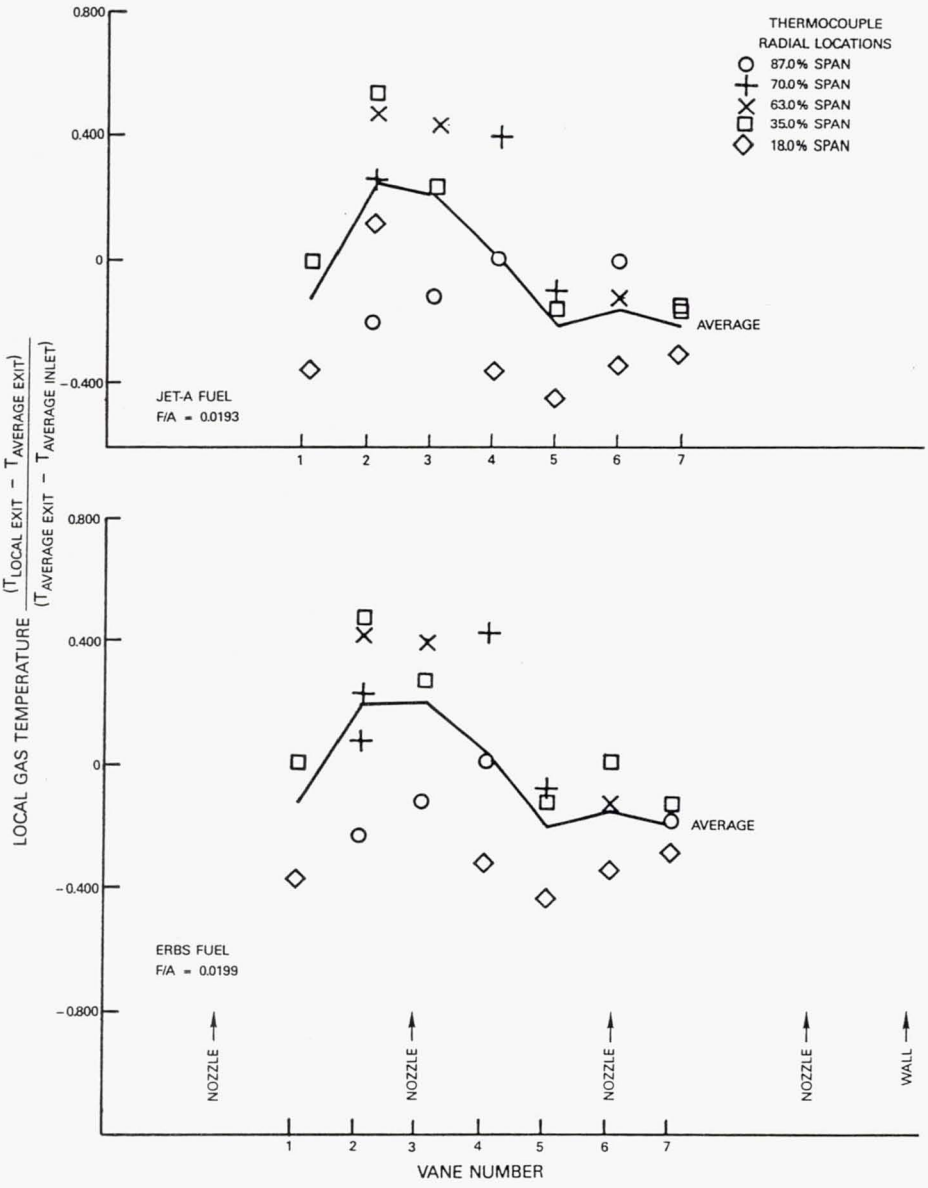

Figure 7-9 Exit Temperature Distribution of Baseline PW2037 Combustor (Configuration V-1) at Takeoff.

The data of Figure 7-9 indicate that the use of ERBS fuel rather than Jet A did not have a significant impact on the overall combustor exit temperature distribution. The temperature distribution is dominated by a hot region at Vane positions 2, 3 and 4 and the circumferential distribution of the local radially averaged temperature on the figure is essentially identical for both fuels. Operation on Jet A fuel produced a temperature pattern factor of 0.55 while this factor decreased to 0.48 when the combustor was operated on ERBS fuel. Operation on the other two test fuels produced similar results with pattern factors between the two values cited above.

To achieve the required turbine blade life in the PW2037 engine, the circumferentially averaged radial temperature profile at the combustor exit must comply with the target profile defined in Figure 3-4. Figure 7-10 shows the radial temperature profiles obtained from the exit temperature distribution for the four test fuels evaluated. The data indicate that the radial temperature distribution at the exit of the combustor is essentially insensitive to fuel composition except for a slight spreading at the 53 percent span position where the ERBS and Jet A fuels tended to produce a slightly more peaked profile. The nominal experimentally observed temperature profile deviates from the target in that it is more peaked and hotter at the outer (high span percentage) side and below target temperatures at the inner side. Moderate additional refinement to the dilution air scheduling would be required to achieve the target profile.

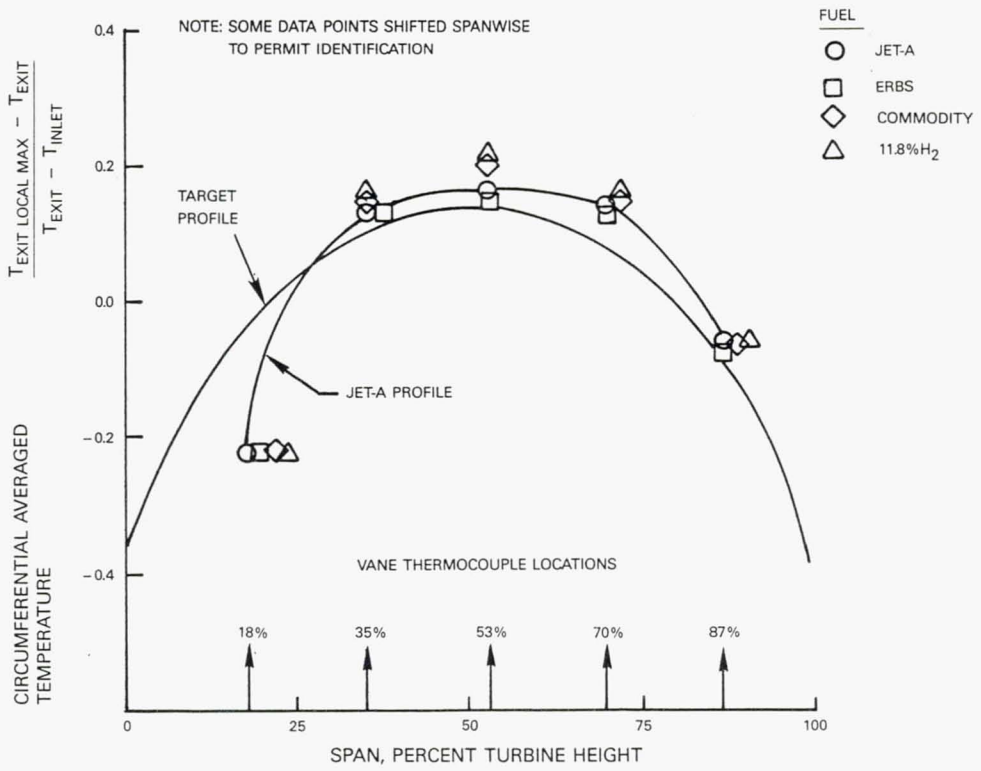

Figure 7-10 Radial Exit Temperature Profile of PW2037 Combustor (Configuration V-1) at Takeoff.

7.1.6 Combustion Stability

The lean blowout fuel/air ratios of the reference PW2037 combustor were measured at the idle inlet condition. This parameter indicates the risk of blowout during engine deceleration and provides a qualitative or relative measure of the altitude stability and ignition characteristics of the combustor. Data was obtained for all four test fuels at both ambient and preheated fuel supply temperatures. The results are presented in Figure 7-11 and reveal some unusual trends. First, the lean blowout fuel air ratio reduces, i.e., lean stability improves, with increasing nominal viscosity. Furthermore, preheating the fuel to 372°K (208°F) which reduced the fuel viscosity and had a favorable effect on unburned hydrocarbon emissions at idle had an adverse effect on lean stability. It has generally been considered advantageous to reduce fuel viscosity because it enhances fuel atomization producing finer droplets that vaporize more rapidly and sustain marginal combustion near blowout. The data of Figure 7-11 imply that the opposite is required in the reference PW2037, i.e., that poor atomization near the lean stability limits is advantageous. This can be interpreted as indicating that local regions of rich mixture strengths are sustaining combustion near the extinction limit. While a fine uniform fuel spray may be desirable for fuel vaporization at these conditions, the more critical factor in the PW2037 is apparently the sustaining of the richer flame zones which serves as a continuing ignition source. Maintaining rich mixtures in these zones requires that the injector also provide a continuing supply of larger fuel droplets characteristic of those produced by poor atomization of a higher viscosity fuel.

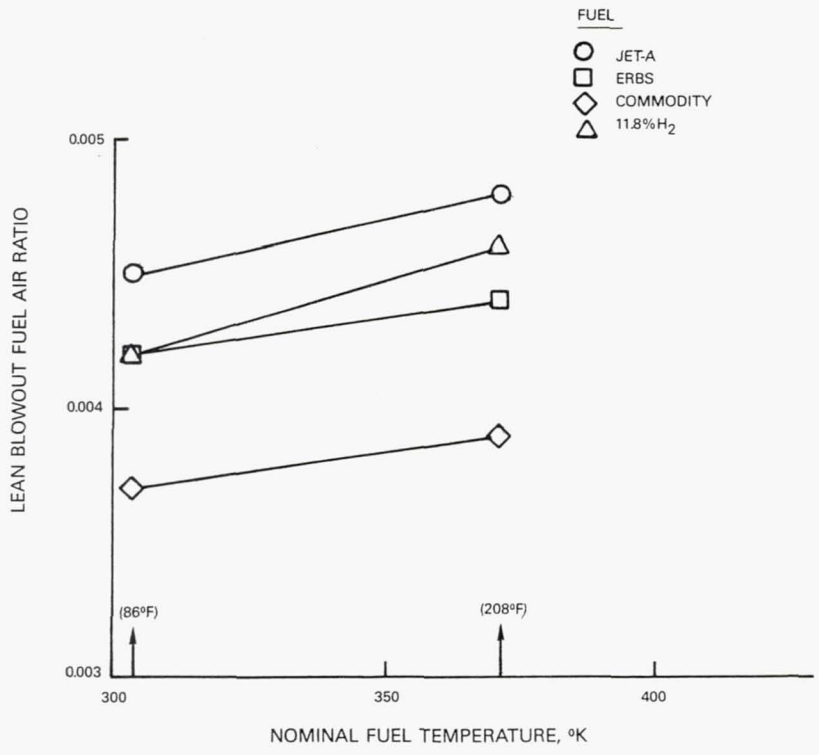

Figure 7-11 Lean Blowout Fuel Air Ratio of Reference PW2037 Combustor (Configuration V-1) at Idle.

The PW2037 engine has not encountered any difficulties associated with lean stability during operation on Jet A fuel. Since the data of Figure 7-11 indicates that this situation should improve with the use of ERBS and more viscous fuels, no operability problems of this nature would be anticipated in a Jet A to ERBS transition. However, cold starting and altitude relight capability have not been addressed in this evaluation and may lead to further limitations.

7.1.7 Status of the Reference PW2037 Combustor

The results presented in this section summarize the capabilities of a state-of-the-art combustor to accommodate the use of broadened properties fuels. The combustor has been shown to meet the program low power emissions goals for unburned hydrocarbons and carbon monoxide by wide margins with ERBS fuel. The combustor was not designed to meet the program goals for emissions of oxides of nitrogen and, in addition, a modest increase of the order of three to five percent must be anticipated in these emissions if ERBS were substituted for Jet A fuel. The combustor was also demonstrated to marginally meet the program goal for smoke output when operating on ERBS fuel. While the combustor exit temperature distribution of the tested configuration would need additional refinement to meet the program goals, the temperature distribution was shown to be essentially independent of fuel composition. The reference PW2037 combustor was also found to have unusual lean stability characteristics which would be enhanced by a change from Jet A to ERBS. However, other operability aspects such as cold starting and altitude relight were not investigated and could be compromised by the use of ERBS fuel.

The test results indicate that increased liner temperatures, caused by increased radiant heat load, are a major obstacle in accommodating broadened properties fuels. Reductions in liner life of up to 15 percent are projected with ERBS fuel despite the production version of this combustor employing an advanced technology liner construction. The reference PW2037 combustor has the decided advantage of incorporating a single pipe fuel system. By avoiding duplex and staged fuel systems, the risk of forming deposits in low flowing or inactive system components is precluded. This is particularly advantageous when operating on broadened properties fuel that are likely to have poorer thermal stability characteristics.

7.2 FUEL SENSITIVITY OF THE VARIABLE GEOMETRY COMBUSTOR

The experience derived during the Phase I program, in which the performance characteristics of variable geometry combustors was synthesized by the evaluation of pairs or sequences of fixed geometry combustors, indicated that the enhanced control of stoichiometry could be used to advantage in accommodating broadened properties fuels. Consequently, the variable geometry combustor concept was selected for further assessment during the Phase I program. As shown in Section 4.2 the variable geometry test combustor consisted of a PW2037 combustor sector, identical to the reference combustor of Section 7.1, that had been modified to provide variable airflow into the primary combustion zone. A total of seven configurations, designated V-2 through V-8, of this concept were evaluated. While it did not produce the best performance and emissions characteristics of the configurations tested, Configuration V-8 was selected to identify the basic performance and fuel sensitivity of the variable geometry combustor concept because it was the

only configuration evaluated in the Pratt & Whitney high pressure combustor test facility where it could be operated at simulated high power levels at higher pressure and with nonvitiated inlet air while using all four of the available test fuels. The remaining configurations of the variable geometry combustor, Configurations V-2 through V-7, were evaluated under more limited operating conditions in the Jet Burner Test Stand at United Technologies Research Center. The evaluation of those configurations addressed performance improvements and long term potential of the variable geometry combustor and are discussed in Section 7.3.

7.2.1 Combustor Airflow Distribution

One of the first aspects of the variable geometry combustor concept to be investigated was the ability to shift the airflow distribution in the combustor through actuation of the hood mounted air valves. Figure 7-12 shows the local pressures and airflow distribution in Configuration V-8 with the hood valves opened and closed. The data indicate that the objective of substantial airflow shifts has been achieved. With the valves closed the controlled leakage around the valve plates and fuel injector airscoops allowed 6.1 percent of the combustor airflow to enter through the swirlers so as to cool the exposed surfaces of the vanes and prevent aspiration into the hood cavity. In combination with the aerated nozzle and dome cooling airflow, this flow produced a total primary zone airloading of about 20 percent of combustor air. This produced a bulk primary zone equivalence ratio of about 0.7 at the idle fuel air ratio. With the valves closed the pressure drop across the overall combustor and in particular across the liners are nearly identical to those of the reference PW2037 combustor sector of Section 4.1. The liner cooling airflow, at a total of about fifty percent of combustor airflow is also essentially identical to that of the reference combustor, thus assuring adequate liner cooling even at high power levels.

When the valves were in the opened position, the flow through the swirler was increased to 39.8 percent of the combustor airflow with the increase in this flow being drawn from the liner cooling and the intermediate and dilution jet air. Opening the valves resulted in significant drops in the liner pressure drop as well as the overall total pressure loss across the combustor section. While the liner pressure drop is low relative to state-of-the-art combustors, it appears adequate for cooling air distribution and the low combustor section pressure loss offers potential for improved specific fuel consumption. The combination of the high swirler airflow and the aerating fuel injector and dome cooling airflows leads to a primary zone airloading of over 50 percent of the combustor airflow when the valves are open. This loading is also equivalent to a bulk equivalence ratio of about 0.6 in the primary zone at the takeoff fuel air ratio and would be expected to be conducive to low smoke and oxides of nitrogen emissions at this flight condition.

Opening the hood valves depleted the liner cooling flow from the approximately 50 percent of combustor airflow; that had been found to be adequate in the evaluation of the reference PW2037 combustor of Section 7.1; to less than 35 percent of the combustor airflow. Achieving adequate long term durability at this reduced cooling air level would require significant reduction in the heat load on the liner and must be obtained as a consequence of the lean combustion in the primary zone.

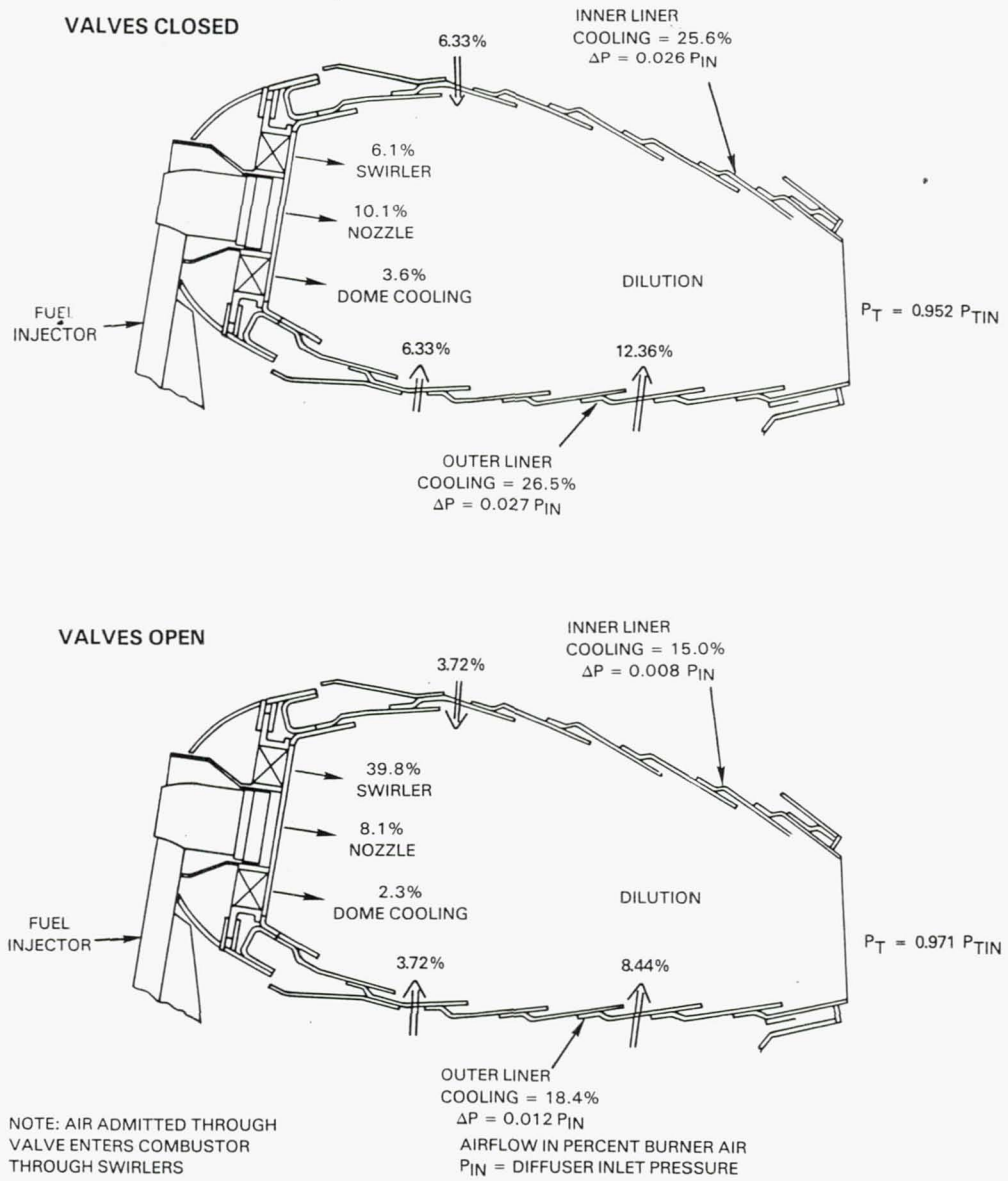

Figure 7-12 Pressure and Airflow Distribution in Variable Geometry Combustor Configuration V-8.

It is evident that the design objective of shifting airflow into and out of the primary combustion zone of the variable geometry combustor was achieved. Actuation of the hood valves diverted more than 30 percent of the combustor airflow between the primary zone swirlers and the aperatures in the liner. However, as the test results discussed in the remainder of Section 7.2 indicate, the basic variable geometry combustor was deficient in that the mixing of the diverted air was not controlled and the combustion processes did not occur at the intended bulk equivalence ratios. When the valves were open admitting large quantities of air through the swirler this air did not mix effectively with the fuel laden air from the injector and led to stratification with locally rich combustion occurring in the center of the combustor. Conversely, when the valves were closed and the combustor was

operating at simulated low power the purge and cooling air entering through the swirlers was an uncontrolled but relatively large fraction of the primary zone airloading. These functional difficulties with the variable geometry combustor were recognized in the evaluation of the initial configuration of this concept and, as will be discussed in Section 7.3, were the subject of most of the modifications made to the combustor during the program.

7.2.2 Liner Heat Load

Like the reference PW2037 combustor sector of Section 7.1, Configuration V-8 of the variable geometry combustor was instrumented with radiometers to measure the radiant heat flux incident on the liner. The installation was identical to the reference combustor (Configuration V-1) with the sensors protruded through holes in the third louver of the inner and outer liner respectively. The radiometers were positioned downstream of the same fuel injector so that the same volume of combustion products were viewed from opposite sides. The radiometers were the same sensors used in the reference PW2037 combustor, i.e., a porous plug radiometer on the inner liner and a Medtherm commercial unit on the outer liner side. The latter experienced the same erratic readings encountered during its use in the evaluation of Configuration V-1 because of soot accumulation on its window. The data from this sensor is not reported. Figure 7-13 shows the heat flux incident on the porous plug radiometer as a function of fuel hydrogen content for the variable geometry combustor with the primary zone air admission valves open at the cruise and 85 percent thrust climb condition. (No data is shown for the takeoff condition because the probe calibration started to deteriorate at this point in the test.) For reference the figure includes the corresponding data from the evaluation of the reference PW2037 combustor from Section 7.1.1.

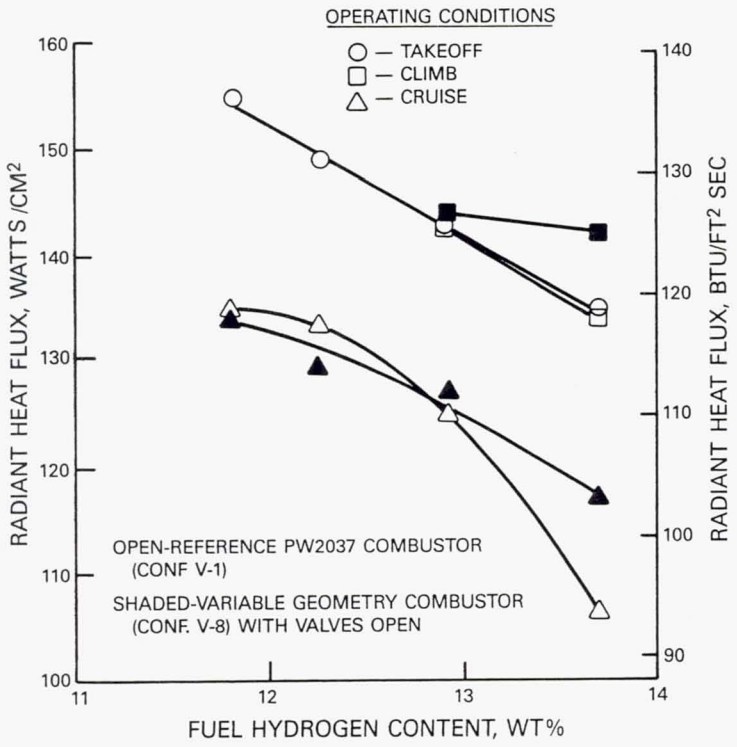

Figure 7-13 Radiant Heat Flux to Liner of Variable Geometry Combustor.

The data show that with the exception of the results obtained when operating on Jet A fuel the heat flux measured in the variable geometry combustor was nearly identical to that observed in the reference combustor. As indicated in Section 7.1.1 this variation of heat flux with fuel hydrogen content is consistent with accepted models of the combined gas/luminous particle radiation process. The increase in incident radiation with Jet A fuel in the variable geometry combustor relative to the baseline combustor leads to an apparent reduction in the sensitivity of heat flux to fuel hydrogen content in that combustor. The transition from Jet A (13.7 percent hydrogen content) to ERBS (12.9 percent hydrogen) produces only an 8.8 percent increase in heat flux in the variable geometry combustor as opposed to a 17.5 percent increase in the reference PW2037 combustor. At the higher power climb condition the sensitivity of the variable geometry combustor to the Jet A-ERBS hydrogen content change is significantly less, being only about two percent.

While the parallels in the response of the heat flux to fuel hydrogen content in the two types of combustor was to be expected the identity in the level of heat flux was not. At the high power cruise to takeoff fuel air ratio conditions the bulk equivalence ratio in the primary combustion zone of the reference PW2037 combustor is of the order of 1.5. This would be expected to be conducive to high smoke and particulate concentrations in the primary combustion zone that would produce high luminous particle thermal radiation. Conversely, at these same power levels the airflow distribution data on the variable geometry combustor with the valves open in Section 7.2.1 indicate a bulk equivalence ratio of only 0.7 or less in the primary combustion zone. If combustion were occurring at these bulk equivalence ratio levels a much lower smoke and particulate concentration with an accompanying lower radiant heat flux would be anticipated. While the radiant heat flux was measured at only one location in each combustor and the unexpected similarity in intensity may have been only a coincidence, it can also be an indication of the presence of the fuel injector-swirler air stratification mentioned in Section 7.2.1.

7.2.3 Liner Metal Temperature

Use of lower hydrogen content fuels increases radiant heat flux which increases local metal temperatures in the combustor liner, reducing structural life. As indicated in Section 5.2.2, thermocouples were installed in the combustor liner sectors to measure these temperature increments. The thermocouple junctions were positioned near the weld between a film cooled panel and the riser of the following louver. Since the temperature gradient between this region and the cooler louver knuckle is critical to cyclic fatigue in the conventional sheet metal louvered liner of both the variable geometry test combustor and the PW2037 engine combustor sector these measurements were relevant to liner life in either combustor.

Figure 7-14 provides an overview of the impact of fuel composition on the liner temperatures in the variable geometry combustor (Configuration V-8) relative to that in the reference PW2037 test combustor (Configuration V-1). The metal temperatures presented are the average of all of the combustor liner thermocouples on liners enclosing the primary combustion zone which is defined as the first three louver panels of the liner. The average temperatures are based on comparable number of measurements - all 12 of the thermocouples on the primary zone liner panels of the referenced PW2037 and 10 operational thermocouples on these panels in the variable geometry

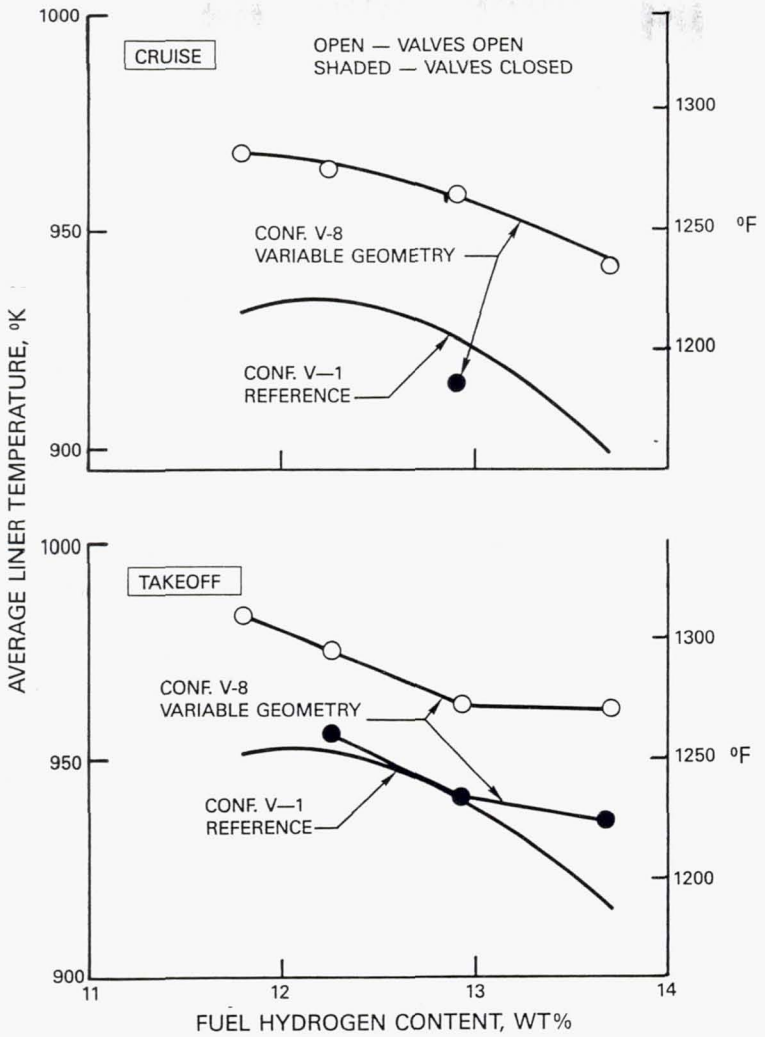

Figure 7-14 Effect of Fuel Composition on Variable Geometry Combustor Primary Zone Liner Temperature.

combustor. It is also noted that the positioning of the thermocouples near the weld region of the louver makes the measurements a representative indicator of temperatures in the life limiting regions and not an average metal temperature for the entire liner surface.

At the cruise and takeoff flight conditions of Figure 7-14 the data are generally consistent with the anticipated trend of increasing metal temperatures with decreasing fuel hydrogen content. The variable geometry combustor would normally operate with primary air valves open and at the cruise condition the liner temperature-hydrogen content characteristic closely parallels that obtained from the referenced PW2037 combustor. The change in average primary zone liner temperature associated with the transition from Jet A (13.7 percent hydrogen) to ERBS (12.9 percent hydrogen) is 13°K (24°F) in the variable geometry combustor compared to 23°K (42°F) in the reference PW2037 combustor at the cruise condition.

At the takeoff condition the parallels between the average liner temperature-fuel hydrogen content characteristics of the variable geometry combustor with the valves open and the reference PW2037 combustor remain but become more qualitative. While the latter exhibited more sensitivity to fuel hydrogen content in the high hydrogen content range than at the lower levels the variable geometry combustor produced the opposite trend to the extent that there was essentially no change in primary zone liner temperature in the transition between ERBS and Jet A fuel. This low level of sensitivity of the primary zone liner temperature is consistent with the observation of Section 7.2.2 in which the variation in radiant heat flux to the liner of the variable geometry combustor operating on the higher hydrogen content fuels at the climb condition was found to be much less than expected based on experience with the reference PW2037 combustor.

The variable geometry combustor (Configuration V-8) was also operated at some high power conditions with the primary zone air valves in the closed position to assess the effect on liner temperatures. As shown on Figure 7-14 closing the valves while operating on ERBS fuel at cruise led to a 44°K (80°F) reduction in average primary zone liner temperature. Likewise, reductions in liner temperature of 19 to 28°K (35 to 50°F) were observed when the valves were closed with different fuels at takeoff. The liner temperature reductions are obviously due in the most part to the increase in liner cooling air when the valves were closed. As indicated in Section 7.2.1 closing the valves was found to increase the total liner cooling flow for the variable geometry combustor from a nominal 35 to 50 percent of the combustor airflow - an increase that would readily produce liner temperature reductions of these magnitudes. The average primary zone liner temperature levels produced when the valves were closed are also shown to be close to those observed in the reference PW2037 engine when operating at the same simulated power levels and on the same fuels. This is consistent with the construction of the test combustors and the aerodynamic characteristics of the variable geometry combustor discussed in Section 7.2.1. Except for details in the airflow feed to the first liner panel the construction of the liners are identical in both combustors. When the primary zone valves are closed the pressure drops across the liners and the fuel injectors are essentially identical to those in the reference PW2037 combustor. Hence, as shown by comparison of the airflow distributions in Figure 4-2 and 7-12 the liner cooling airflow and the primary zone airloading are nearly identical so similar thermal performance is to be expected.

In the discussion of the evaluation of the reference PW2037 combustor in Section 7.1.2, the changes in liner life associated with the incremental changes in liner temperature produced by changes in fuel composition were estimated. These projections were based on stress analyses of louvered liners which, in combination with empirical data on the fatigue strength of the liner material, relate the temperature gradient across the louver knuckle at takeoff to cyclic fatigue life of this region. These procedures could be applied to the variable geometry combustor with the valves open and the very small increment of liner temperature of 1°K (2°F) that occurs in a Jet A-ERBS transition at takeoff would lead to an unconsequential loss in estimated liner life. The more significant factor in establishing liner life in the variable geometry combustor is the level of liner cooling air. The variable geometry configuration evaluated in this program allowed very low liner

pressure drops at high power levels and without compensating for the reduced cooling flow has allowed liner temperature levels to increase significantly. The corresponding decrease in liner life would more than exceed those projected for a Jet A to ERBS transition in more conventional combustors such as those in Table 7-1.

7.2.4 Emissions

Figure 7-15 shows the measured carbon monoxide and unburned hydrocarbon emissions from Configuration V-8 of the variable geometry combustor with the primary zone valves closed at the PW2037 engine idle combustor inlet conditions. Data are presented for a range of fuel air ratios distributed near the design proportions. Also shown are the goals for these emissions constituents which were defined in Section 7.1.3 as the levels required for compliance with the previously proposed EPA Class T-2 standards for engines certified after January 1, 1984 with the assumption of reasonably low emissions of these constituents at higher power levels. Relative to these goals and the performance of the reference PW2037 combustor the idle emissions characteristics of the variable geometry combustor are extremely poor. Even with Jet A fuel the unburned hydrocarbon emissions index exceeds 150 gm/kg and that for carbon monoxide is nearly 70 gm/kg at the design idle. In combination these imply a combustion efficiency of only 80 percent. While Configuration V-8 did produce particularly poor idle emissions characteristics, other perturbations of the variable geometry combustor concept did not produce profoundly better characteristics. The lowest idle emissions levels observed in these configurations, which will be discussed in Section 7.3, still exceeded the above cited program goals for both carbon monoxide and unburned hydrocarbons by factors of two.

Comparison of the idle emissions characteristics of the Configuration V-8 variable geometry combustor, and in particular the unburned hydrocarbon emissions with those of the reference PW2037 combustor of Section 7.1.3 indicates that the variable geometry combustor was apparently operating at very lean mixture strengths in the actual primary combustion zone. The steep negative slopes of both the unburned hydrocarbon and carbon monoxide emissions characteristics with fuel air ratio imply Configuration V-8 was operating dangerously close to the lean blowout stability limit at the design idle fuel air ratio. This configuration had the intermediate combustor air holes in the liner moved further forward than in any other configuration of the variable geometry combustor concept. These holes were located in the second louver panel of the liner whereas other configurations had them located further downstream in the third panel or had no intermediate combustion air addition. The intermediate holes had been located upstream in the second liner panel in Configuration V-8 in an attempt to enhance aerodynamic stabilization of the primary recirculating flow region and had apparently contributed excessively to the air loading of the primary zone as well. Data from other variable geometry combustor configurations cited above which had no intermediate air addition through the liner did indicate a tendency for the carbon monoxide and unburned hydrocarbon emissions to level off with increasing fuel air ratio near design idle proportions. While this observation may provide validation for the exceptionally poor low power emissions characteristics of Configuration V-8, it offers no interpretation for the generally inadequate low power performance of the remaining variable

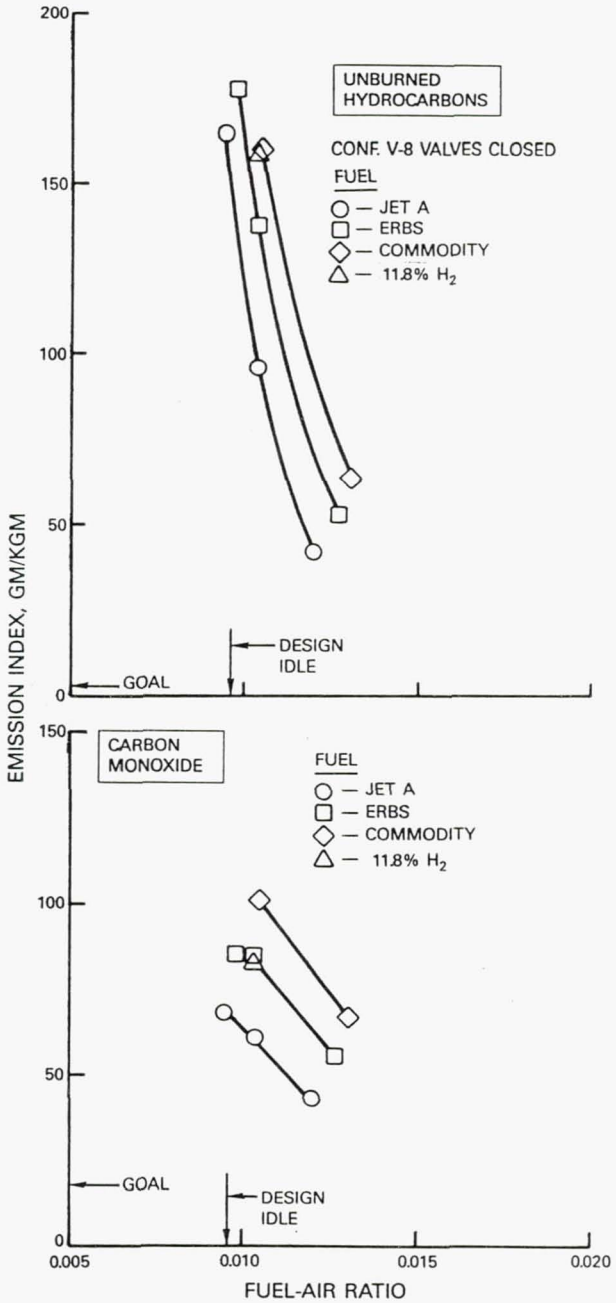

Figure 7-15 Idle Emissions Characteristics of Variable Geometry Combustor.

geometry combustor configurations as well. The remaining performance deficiencies at low power appear to be caused by the lack of aerodynamic control of the hood purge and swirler cooling air when the primary zone air valves are closed. As indicated in Section 7.2.1 this airflow through the hood-swirler area is necessary during valve closed operation to prevent aspiration of combustion gases upstream of the bulkhead by transverse pressure gradients. While the quantity of purge air is small, being only about six percent of combustor airflow, it is large relative to the primary zone airloading, which should be about 14 percent combustor airflow to produce stoichiometric mixture proportions in that zone at the design idle fuel air ratio. Entering in an uncontrolled distribution because of the small pressure drop across the large flow area swirlers, this purge air leads to large excursions in local mixture strengths in the primary zone at low power and the resultant erratic performance.

While the idle emissions characteristics of Configuration V-8 of the variable geometry combustor were high, significant trends with fuel composition and physical properties were evident in the data of Figure 7-15. Consideration of the emissions levels produced by the Jet A, ERBS and the Commodity fuels indicate a systematic increase in output of both carbon monoxide and unburned hydrocarbon with reducing fuel hydrogen content. The single measurement obtained with the 11.8 percent hydrogen content blended fuel indicates lower output of both constituents than would be anticipated based on the trend with the hydrogen contents of the other three test fuels. As indicated in a similar discussion of the low power emissions characteristics of the reference PW2037 combustor in Section 7.1.3, this effect appears to be due to the unusually low viscosity and volatility of this fuel blend relative to the other test fuels and indicates these properties also have significant effects.

Similar measurements of the carbon monoxide and unburned hydrocarbon emissions characteristics of the Configuration V-8 variable geometry combustor were obtained at approach (30% takeoff thrust) and higher power levels of the PW2037 engine. The results obtained with ERBS fuel are presented in summary form on Figure 7-16 and include the corresponding data from the idle point as well. When operated at high power, i.e., cruise, climb (85% takeoff thrust) and takeoff with the primary zone valves open the emissions of these constituents were low and the combustion efficiency equaled or exceeded 99.95 percent with all combinations of test fuel and power level investigated. Measurements were obtained at approach with the valves in both the open and closed positions because this power level would probably be close to the point of transition between these two modes of combustor operation. The results of these measurements and their impacts are summarized on Table 7-2.

TABLE 7-2

EMISSIONS CHARACTERISTICS OF VARIABLE GEOMETRY COMBUSTOR CONFIGURATION V-8 AT APPROACH WITH ERBS FUEL

	Valve Position	
	Open	Closed
Emission Index - gm/kg		
Carbon Monoxide	12.06	3.49
Unburned Hydrocarbons	3.12	0.70
Combustion Efficiency - %	99.35	99.78
Approach Contribution to EPAP		
Carbon Monoxide	6.7	2.0
Unburned Hydrocarbons	1.8	0.4
EPAP Goal		
Carbon Monoxide	25	25
Unburned Hydrocarbons	3.3	3.3

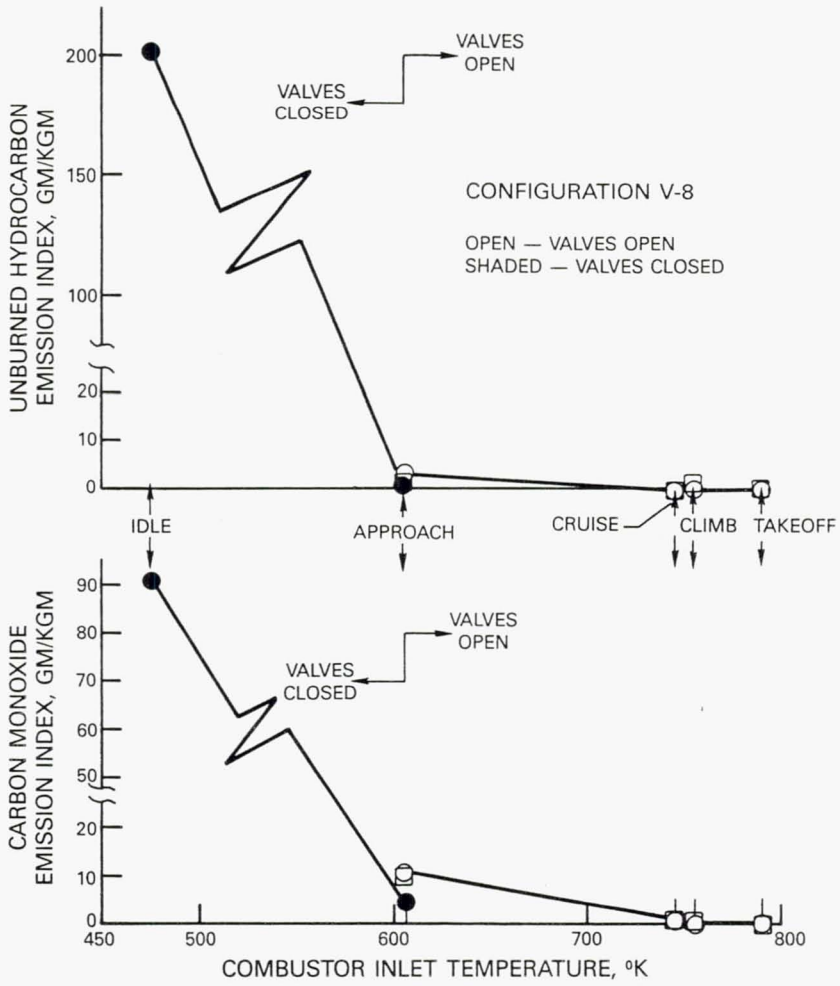

Figure 7-16 Emissions Characteristics of Variable Geometry Combustor with ERBS Fuel.

The tabulated results indicate that operating with the primary zone air valves open at approach leads to increases of both the carbon monoxide and unburned hydrocarbons by factors of the order of four. However, the nominal levels are low and with combustion efficiency well in excess of 99 percent in both modes it would appear that the combustor could be operated in either mode at approach without a performance or operability deficiency. Consideration of the effect on compliance with the previously proposed Environmental Protection Agency Class T-2 requirements established as a program goal indicates these differences in emissions are significant. Table 7-2 indicates the contribution of the approach emissions to the Environmental Protection Agency Parameter (EPAP) of the PW2037 engine and indicates that the difference in the approach contribution to the total EPAP with the valves open versus closed is nearly 20 percent of the total EPAP goal level. The corresponding difference in the approach contribution to the unburned hydrocarbon EPAP is more than 40 percent of the goal total EPAP for this constituent. On this basis consideration of operating in the valves open or closed mode is a significant factor in emissions compliance and leads to an incentive to schedule the valve closed to open transition point at power levels above approach. While this consideration is relevant to the acceptability of a variable geometry combustor the data of Figure 7-16 and the foregoing discussion indicate that from the point of view of low power emissions the dominant problem remains achieving substantial reductions in these constituents at idle.

Figure 7-17 shows the variation of the emissions of oxides of nitrogen from the Configuration V-8 variable geometry combustor with fuel hydrogen content. Data are presented at the nominal cruise and takeoff operating condition, the latter being corrected to the full combustor inlet total pressure of the PW2037 engine cycle according to the procedures of Section 6.0. The data at the cruise condition was obtained at essentially the design fuel air ratio but that at takeoff had to be acquired at a slightly lower fuel air ratio than design (0.022 vs. 0.0241) to avoid overtemperaturing the rig exit instrumentation. While the normal mode of operation would be to have the valves open on the combustor at these power levels a limited amount of data was obtained at the valve closed position for comparative purposes.

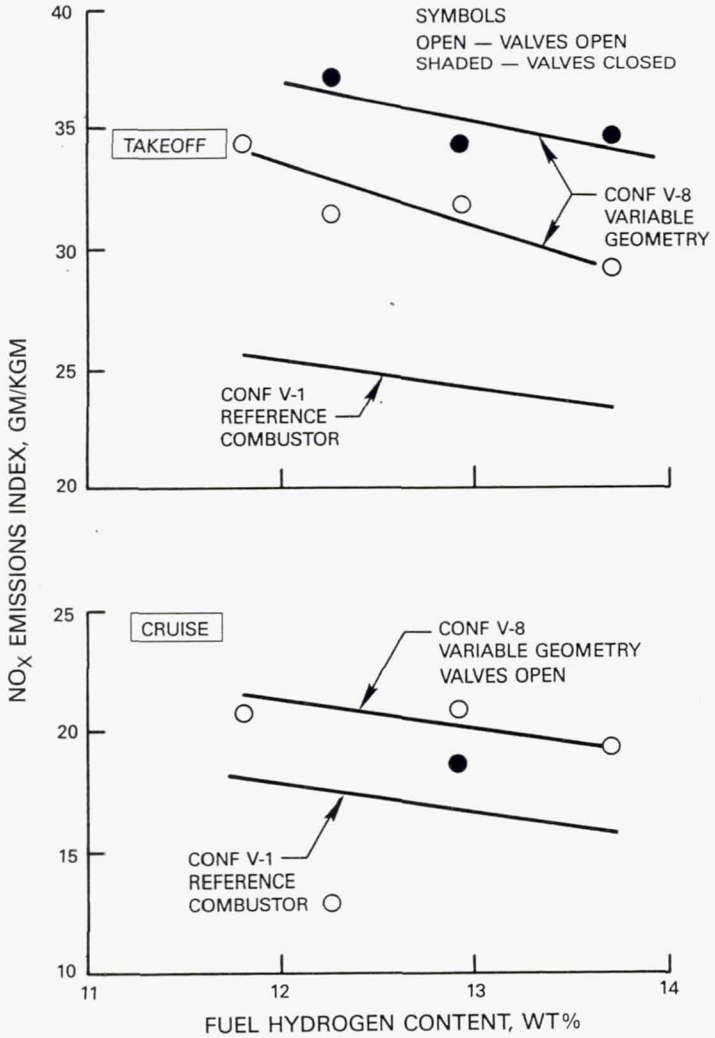

Figure 7-17 NOx Emissions Characteristics of Variable Geometry Combustor.

With the exception of one apparently erroneous measurement at cruise with the Commodity fuel the data indicate progressive increases in NOx emissions with decreasing fuel hydrogen content. As indicated in Section 7.1.3 this has generally been attributed to the increase in adiabatic flame temperature caused by the reduced hydrogen content of the fuel and Equation 10 of that section was shown to predict consistent slopes for the oxides of nitrogen emissions variation with fuel hydrogen content in the reference PW2037 combustor. These emissions characteristics of the latter (Configuration V-1) are reproduced on Figure 7-17 and are qualitatively parallel to those of the variable geometry combustor.

The data from Configuration V-8 indicate that opening the valves to lean the bulk equivalence ratio in the primary combustion zone reduces the level of oxides of nitrogen output somewhat at takeoff but to a much lower extent at the cruise operating condition. Furthermore, the levels of output of oxides of nitrogen, regardless of valve position, are substantially higher than those produced by the reference PW2037 combustor. While these unusual discrepancies cannot be resolved on the basis of available data there are several factors which could be contributing to the high NOx output of the variable geometry combustor relative to the reference burner. These include:

- The suspicion advanced in Section 7.2.1 that while the air admitted through the swirler in the valve open mode is sufficient to produce a bulk equivalence ratio of about 0.7 at takeoff the flow is actually stratified with the bulk of the combustor occurring in a fuel rich core at higher equivalence ratio.

- The residence time - temperature history of the combustion products may be significantly different in the variable geometry combustor in the valve open mode leading to higher formation rates of oxides of nitrogen because the liner air admission schedule is different and the low liner pressure drop inhibits penetration and dispersion of intermediate and dilution air jets.

- The reference PW2037 combustor has a bulk primary zone equivalence ratio of about 1.5 at takeoff and, on the basis of the investigation of Section 7.1, appears to have a well mixed primary combustion zone. NOx formation processes in fuel rich combustion zones are known to be more complex and slower than the usual lean burning Zeldovich mechanism. If the primary zone of the reference PW2037 combustor were operating in such a combustion mode, it could explain the lower NOx output observed from that combustor.

It was indicated previously in Section 7.1.3 that to achieve the goals for advanced technology combustors being evolved under this program the emissions of oxides of nitrogen would have to comply with the previously proposed Environmental Protection Agency Class T-2 requirements for engine certified after January 1, 1984. Assuming a reasonable relative distribution of emissions levels over the four points of the landing and takeoff cycle, an emissions index of 19 gm NOx/kg must be achieved at takeoff if this overall goal is to be met. Based on the data of Figure 7-17 a 40 percent reduction in the oxides of nitrogen output would be required for the variable geometry combustor to achieve this goal when operating on ERBS fuel with the primary zone air valves open.

7.2.5 Smoke

Unless they are oxidized in the remainder of the combustor, the carbon particulates formed in the primary zone are emitted with the other combustion products in the form of visible smoke. The smoke output of the Configuration V-8 variable geometry combustor was measured at selected high power operating conditions with the valves open. Figure 7-18 shows the variation in measured SAE Smoke Number with fuel hydrogen content at combustor inlet conditions simulating cruise and takeoff operation of the PW2037 engine. The data indicate that smoke output increases slightly with decreasing fuel hydrogen content at both flight conditions but that the trend is within the scatter of the measurements. As in the case of oxide of nitrogen emissions the anomolity with the smoke output of the variable geometry combustor is with the high level relative to the reference PW2037 combustor. The latter was found to marginally meet the program goal of an SAE Smoke Number of 21 when operating at takeoff on ERBS fuel whereas Configuration V-8 of the variable geometry combustor produced an SAE Smoke Number of 36 at the takeoff condition. The combination of simultaneous higher than anticipated smoke and oxides of nitrogen emission is unusual because the mechanism causing high NOx production, i.e., high residence time at elevated temperatures, enhances smoke consumption. While high smoke output can also be related to an excessively high initial production rate in the primary combustion zone post-test inspection of the combustor did not reveal any significant surface carbon disposition or sooting that could be interpreted as indicative of excess carbon formation in the front end of the combustor.

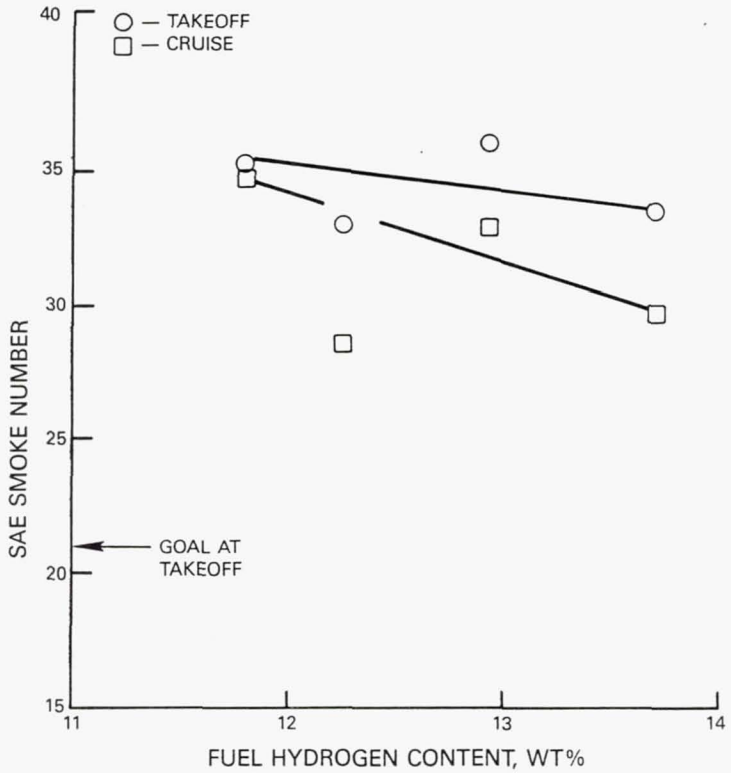

Figure 7-18 Smoke Characteristics of Variable Geometry Combustor Configuration V-8 with Valves Open.

7.2.6 Combustor Exit Temperature Distribution

While refining the combustor exit temperature distribution to achieve the program goals for pattern factor and radial profile was not a major objective of the technical effort, the sensitivity of these parameters to variations in fuel composition was investigated. There was additional interest in the exit temperature distribution produced when the variable geometry combustor was operated with the primary zone air valves in the open and closed positions because these altered dilution air jet quantities and liner pressure drop that could influence the exit temperature distribution. Figure 7-19 shows the exit temperature distribution from the Configuration V-8 variable geometry combustor while operating on ERBS fuel. The data was obtained with the primary zone air valves open and the combustor operating at takeoff with the fuel/air ratio reduced to 0.022 because of exit instrumentation temperature limitations. The distribution is representative of that observed with all the test fuels and is characterized by wide variations in temperature in the radial or spanwise direction with the maximum temperatures being dictated by hot spots immediately downstream of fuel injectors and centered in the 53 to 70 percent span locations. (Outer vane platform is 100 percent span.)

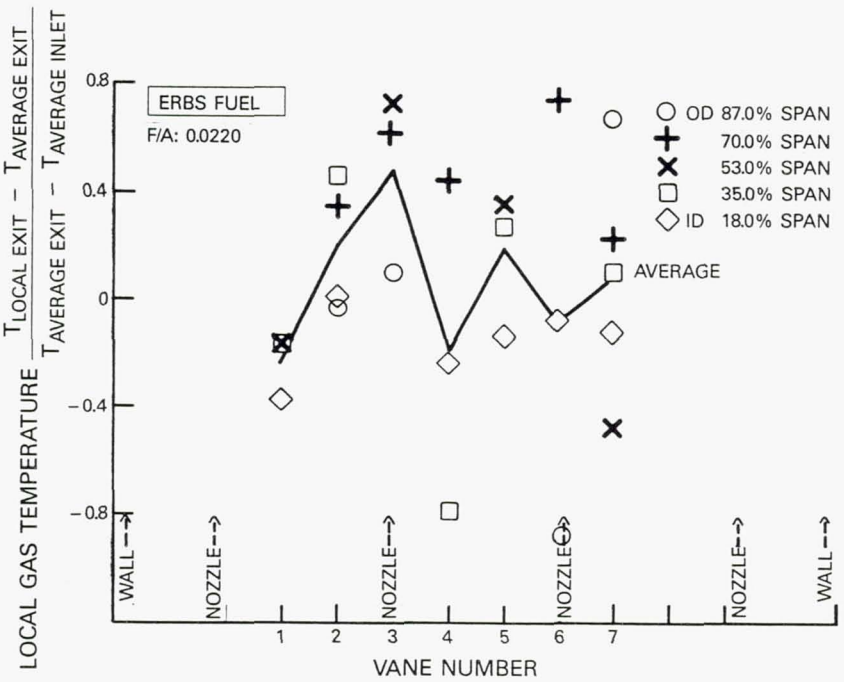

Figure 7-19 Exit Temperature Distribution of Variable Geometry Combustor Configuration V-8 at Takeoff with Valves Open.

Table 7-3 lists the exit temperature pattern factors for all of the takeoff power conditions investigated. Because the pattern factor is dictated by a single highest measured gas temperature the variation in this parameter with test fuel is not of strong significance. In contrast, when the primary zone air valves were closed the exit temperature distributions not only remained dominated by the hot spots downstream of fuel injectors but the pattern factors observed with two of the three test fuels were essentially identical to those observed when the valves were open and the combustor air scheduling and liner pressure drops were substantially different.

TABLE 7-3

VARIABLE GEOMETRY COMBUSTOR
EXIT TEMPERATURE
PATTERN FACTORS AT TAKEOFF

Fuel	Valves Open	Valves Closed
Jet A	0.706	0.701
ERBS	0.745	0.492
Commodity	0.573	0.574
11.8% Blend	0.657	---

The circumferentially averaged radial temperature profile at the combustor exit must comply with the target profile of Figure 3-4 to achieve the required turbine blade life in the PW2037 engine. This profile provides an additional characterization of the combustor exit temperature distribution that reduces distortion of the nominal features by random temperature perturbations. Figure 7-20 shows the radial temperature profiles obtained from the exit temperature distribution when the combustor was operated with the primary zone air valves open with each of the four test fuels. The temperature profiles are shown to be essentially independent of test fuel - a result that is consistent with those observed in the evaluation of the reference PW2037 combustor in Section 7.1.5 and the JT9D and Energy Efficient Engine based combustors of Phase I of this program. The profiles are shown to deviate considerably from the target temperature profile with a pronounced peak at the seventy percent span location. As will be shown in Section 7.3 earlier configurations of the variable geometry combustor did not have intermediate air into the second or third louver and the exit radial temperature profile was closer to the target profile. When the use of intermediate air was introduced in Configurations V-5 through V-8 it was accomplished by plugging dilution air holes in the outer liner and diverting that air to new upstream holes. The absence of dilution air jets from the outer liner precludes attenuating the hot temperature peak at seventy percent span. Redistribution of the current dilution air between the inner and the outer liner would probably result in suppression of the temperature peak and a shift of the overall profile closer to the target.

Figure 7-21 shows a comparison of the radial exit temperature profile of Configuration V-8 when it was operated with the primary zone air valves in the open and closed position. The profile with the valves open is the same as that shown on Figure 7-20 and is dominated by the high temperature peak at seventy percent span. Closing the primary zone air valves, which diverts more air to the liner cooling, intermediate and dilution air aperatures and increases the pressure drop across the liner is shown to produce a significant cooling of the midspan region of the radial temperature profile and elevation of the temperature levels at the inner span locations. Actuating the valves apparently has a significant effect on the dilution jet penetration with those emanating from the inner liner being weak when the valves are open and remaining near the inner liner to cool that region. Closing the valve increases the quantity of air and the momentum of the jet allowing it to penetrate to midspan and quench that region instead.

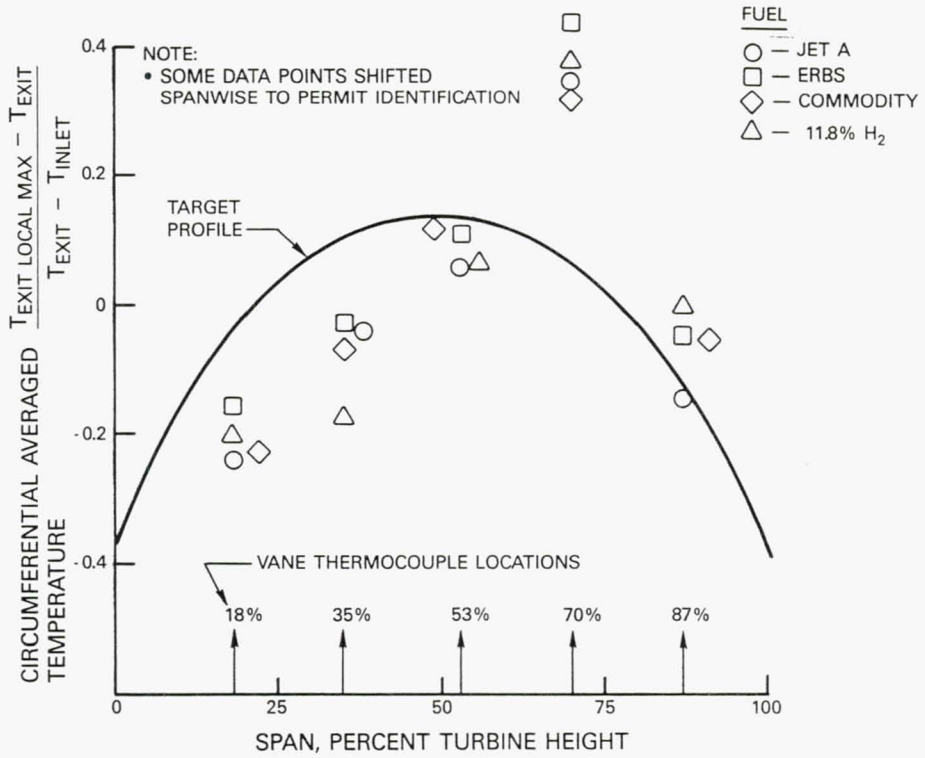

Figure 7-20 Effect of Fuel Composition on Radial Exit Temperature Profile of t Variable Geometry Combustor at Takeoff.

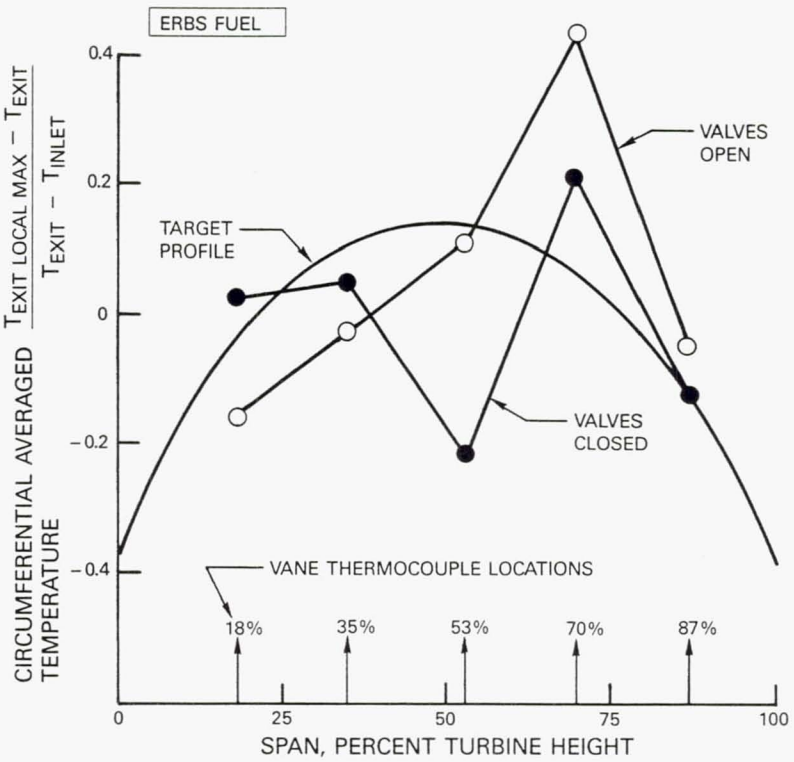

Figure 7-21 Effect of Valve Position on Radial Exit Temperature Profile of Variable Geometry Combustor at Takeoff.

7.2.7 Combustion Stability

The lean blowout fuel air ratio of Configuration V-8 of the variable geometry combustor was determined with each of the four test fuels. The tests were conducted at the PW2037 engine idle condition with ambient fuel supply temperature and the inlet air valves in the closed position. The results are listed on Table 7-4.

TABLE 7-4

LEAN BLOWOUT FUEL AIR RATIOS OF VARIABLE GEOMETRY COMBUSTOR AT IDLE INLET CONDITIONS

Fuel	Lean Blowout Fuel Air Ratio
Jet A	0.0083
ERBS	0.0084
Commodity	0.0098
11.8% Blend	0.0088

The trend of the results implies that lean blowout is dominated by fuel viscosity as opposed to volatility or hydrogen content. Relative to the reference PW2037 combustor (Configuration V-1), which produced lean blowout fuel air ratios in the range of 0.0037 to 0.0045 on these four fuels, the lean stability of the variable geometry combustor is poor. The stability margin relative to the design idle fuel air ratio of 0.0096 is definitely inadequate and when operating on the Commodity fuel the combustor was not capable of operation at the design idle fuel air ratio. These results are consistent with the observed high carbon monoxide and unburned hydrocarbon emissions at fuel air ratio near design idle and efforts to improve the low power emissions characteristics of this combustor concept would probably lead to significant improvements in the lean stability characteristics as well.

7.3 MODIFICATIONS TO THE VARIABLE GEOMETRY COMBUSTOR CONCEPT

The evaluation of Configuration V-8 described in Section 7.2 had been preceded by the testing of six perturbations of the variable geometry concept identified as Configurations V-2 through V-7. The details of the modifications incorporated in these configurations were described in Section 4.2.3. When the first of these configurations was evaluated some of the performance deficiencies observed in the evaluation of Configuration V-8 were encountered. These were associated with inadequate or uncontrolled fuel-air mixing in the primary combustion zone and the next three perturbations to the variable geometry combustor addressed means of improving these processes. When these were found to produce only small differences in the performance of the combustor the last two configurations, Configuration V-6 and V-7 incorporated features that were intended to separately enhance the high and lower power performance respectively. The results were combined to synthesize the performance of a hypothetical variable geometry combustor with improved primary zone fuel-air mixing features. Configurations V-2 through V-7 were tested in the Jet Burner Test Stand at United Technologies Research Center. As indicated in Section 5.3 this facility was limited relative to the X-902

Test Stand used for the evaluation of Configurations V-1 and V-8 in that operating pressures were limited to about 1.52 MPa (220 psia) precluding full pressure simulation at power levels above cruise of the PW2037 engine. The inlet airflow in the Jet Burner Test Stand was preheated by vitiation of hydrogen followed by oxygen replenishment at all power levels above idle. Consequently, realistic data on the idle emissions, combustion efficiency and lean stability could be obtained in this facility. At the higher power levels qualitatively accurate measurements for comparative evaluations of liner temperature, smoke output and combustion efficiency could be obtained. However, the previtration of the inlet air followed by oxygen replenishment precluded obtaining consistent measurements of oxides of nitrogen production in the test combustor.

7.3.1 Initial Variable Geometry Combustor Configuration

Since the performance of the initial variable geometry combustor configuration was considerably different from that of Configuration V-8 discussed in Section 7.2, the results of its evaluation are summarized to provide a perspective for the subsequent discussion of the results of evaluating the other perturbations to the variable geometry combustor. Configuration V-2 incorporated the same type B fuel injectors that were installed in Configuration V-8 and in the reference PW2037 test combustor. Configuration V-2 differed from Configuration V-8 in only two respects. The swirler through which the valved primary air entered the combustor around the fuel injector had vanes set at a 45° angle in Configuration V-2 whereas that in Configuration V-8 had the vanes set at 30° off axial to produce a less intense swirling motion in the entering air. The liner air schedule also differed between these configurations. Configuration V-8 had jets of intermediate air entering the combustor through holes in the second louver panels of the inner and outer liner while Configuration V-2 had no intermediate air addition and relied on the swirl strength of the airflow entering the primary combustion zone to achieve flame stabilization.

Table 7-5 summarizes the performance of this combustor when operating on Jet A and ERBS fuel. Relative to Configuration V-8 the carbon monoxide and unburned hydrocarbon emissions at idle are lower but remain above the program goals. The emissions of carbon monoxide are about three times the program goal of an emissions index of 17.8 gm/kg with both fuels. The unburned hydrocarbon emissions indices are substantially lower than those encountered with Configuration V-8 and approach the goal of an emission index of 2.34 gm/kg. Likewise, the lean blowout fuel air ratios at idle inlet conditions while still high relative to requirements are significantly lower than the 0.0083 to 0.0084 levels observed when Configuration V-8 was tested on these fuels.

The emissions of carbon monoxide at the approach condition with the primary air valves in the open position are essentially identical to those indicated in Table 7-2 for Configuration V-8 while the unburned hydrocarbon emissions are about one third those observed with Configuration V-8. This implies that the contribution of emissions to the total EPAPs for these constituents would be of concern with this configuration as well and there would be a preference to operate with the values closed at the approach flight condition.

TABLE 7-5
PERFORMANCE OF VARIABLE GEOMETRY COMBUSTOR CONFIGURATION V-2

Fuel	Jet A	ERBS
Idle - Valves Closed		
Emissions Index gm/kg		
Carbon Monoxide	52.5	58.2
Unburned Hydrocarbons	3.7	5.3
Lean Blowout Fuel Air Ratio	0.0063	0.0071
Approach - Valves Open		
Emissions Index gm/kg		
Carbon Monoxide	9.5	12.5
Unburned Hydrocarbons	0.9	1.1
Cruise - Valves Open		
Fuel/Air Ratio	0.024	0.023
Liner Temperature - °K (°F)		
Avg. Primary Zone	896 (1153)	899 (1159)
Maximum	963 (1274)	972 (1291)
SAE Smoke Number	19.8	21.0
Takeoff - Valves Open		
Fuel/Air Ratio	0.0242	0.0232
Liner Temperature - °K (°F)		
Avg. Primary Zone	956 (1262)*	970 (1288)
Maximum	1014 (1366)*	1032 (1399)
SAE Smoke Number	18.7	15.0
Pattern Factor	0.50	0.47

*Based on interpolation of data to fuel/air ratio of 0.0232

While the thermocouples on the liner enclosing the primary combustor zones of Configurations V-2 and V-8 were not in the same locations their density was comparable and the data should provide at least qualitatively comparable average primary zone liner temperatures. Comparison of the averages of Table 7-5 with those of Figure 7-14 indicates that the measured liner temperature levels are comparable at the takeoff condition but that the average primary zone liner temperatures were about 55°K (100°F) lower in Configuration V-2 at the cruise condition than they were in Configuration V-8. The direction of this difference in liner temperature is counter to expectations based on consideration that in the limited pressure capability facility that Configuration V-2 was tested the only appreciable difference between the combustor operating conditions at cruise and simulated takeoff was the 46°K (83°F) higher combustor inlet temperature at the latter.

Figure 7-22 shows the gas temperature distribution at the exit of Configuration V-2 as measured when operating at the takeoff condition on ERBS fuel. While skewing in the transverse direction the temperature distribution is much more uniform about the local transverse average temperature than that observed at the exit from Configuration V-8 - the latter being shown on Figure 7-19 of the preceding section. The reduced scatter of the temperature distribution with accompanying lower exit temperature pattern factors listed on Table 7-5 are apparently due to the larger quantity of dilution air utilized in Configuration V-2. Figure 7-23 shows a comparison of the exit transverse averaged radial temperature profiles from Configuration V-2 and V-8. The profile from Configuration V-2, while biased toward the inner span positions, is reasonably close to the target temperature profile dictated by turbine blade life in the PW2037 engine. The profile from Configuration V-8, which was discussed previously in Section 7.2.6, is shifted toward the outer span with a pronounced peak at the 70 percent span position. This occurred not only because dilution air flow was reduced to provide intermediate combustor air for admission further upstream to Configuration V-8 but it was removed by completely blocking the dilution air holes in the outer liner of the combustor.

The sensitivity of configuration V-2 of the variable geometry combustor to fuel composition in the Jet A to ERBS range is consistent with expectations based on the results of the Phase I program and that observed in the evaluation of Configuration V-8 of this program. The transition from Jet A to ERBS fuel led to increases in carbon monoxide and unburned hydrocarbon emissions at low power (idle and approach) and a reduction in lean combustion stability, i.e., higher lean blowout fuel air ratio at idle. At high power the use of ERBS rather than Jet a leads to increases in combustor liner temperatures.

Variations in smoke output with the two fuels at different high power test conditions are within experimental uncertainty and do not exhibit any consistent trend with fuel composition. While the smoke output of Configuration V-2 at high power meets the program goal of a maximum SAE Smoke Number of 21 and is substantially below that observed with Configuration V-8, shown in Figure 7-18, at the time the smoke output was considered to be very high for a combustor with the high primary zone air loading achieved in the valve open mode. This supported the hypothesis previously advanced that while the bulk primary zone equivalence ratio was low, the massive quantities of air entering through the swirler and the fuel laden air from the fuel injector remain stratified to produce a small fuel rich combustion zone in the central region. This situation was addressed in the evaluation of some of the subsequent configurations.

7.3.2 Alternative Fuel Injectors

As indicated in Section 4.2.3, when the reference PW2037 combustor sector upon which the variable geometry combustor is based, was fabricated, three different types of aerating fuel injectors were built. When the three injector configurations were tested in the combustor rig on Jet A fuel under the company sponsored PW2037 development program, significant differences in emissions and smoke output as well as the level and location of maximum liner metal temperatures were observed implying that the prototype fuel injectors had substantially different atomization and/or spray angle characteristics that might be exploited in optimizing the variable geometry combustor. To

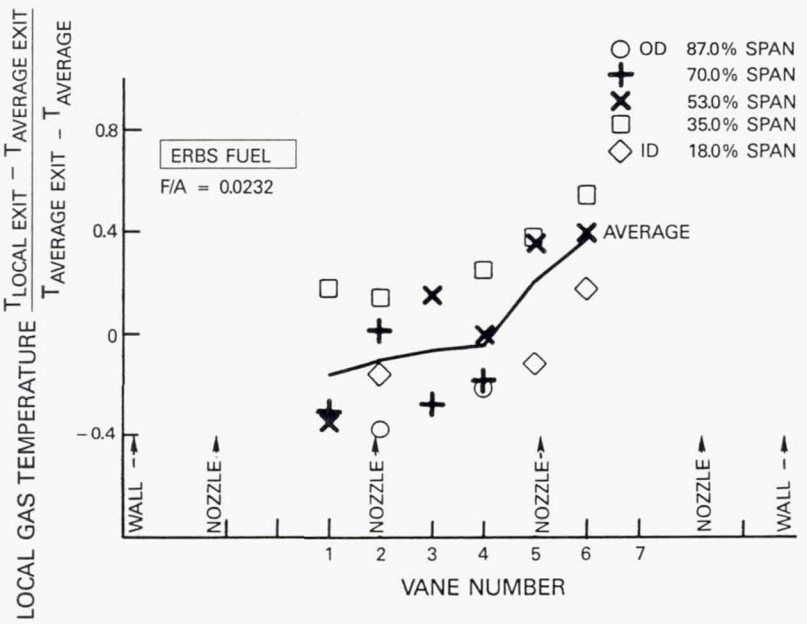

Figure 7-22 Exit Temperature Distribution of Variable Geometry Combustor Configuration X-2 at Takeoff with Valves Open.

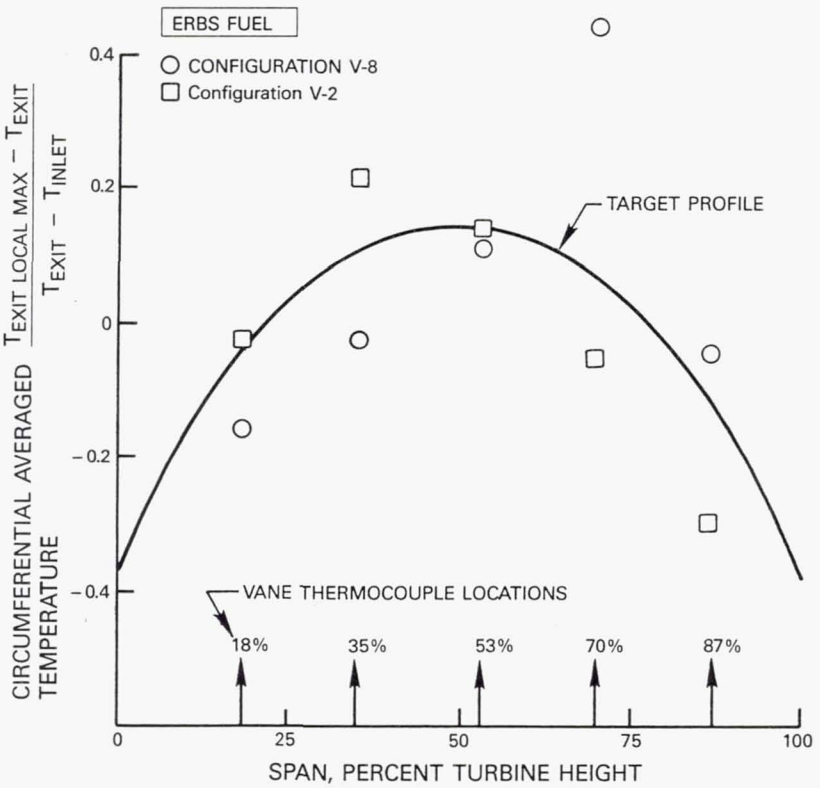

Figure 7-23 Radial Exit Temperature Profiles of Variable Geometry Combustors at Takeoff with Valves Open.

provide a more quantitative characterization of the three prototype injectors with regard to the accommodation of broadened properties fuels, bench spray tests were conducted under the present program to measure spray geometry and atomization at conditions simulating operation in the PW2037 engine using several different fuels. The results of these tests are reported in detail in Appendix B and a summary is presented in Section 4.2.3.

The results of these spray evaluations indicated the Injector B which had been used in Configuration V-2 produced a compact spray that was reasonably independent of fuel type with a total included angle of about 48° at start and idle but expanding to 82° at takeoff. This variation in spray angle appeared consistent with the changes in primary zone airflow distribution produced by the actuation of the air valves on the front end of the burner. At low power, when the valves are closed, the narrower spray would produce the desired rich central combustion zone and avoid overspray of fuel into the surrounding regions occupied by the purge and valve leakage air. At high power levels, where dispersion of the fuel throughout the large quantities of air admitted through the valves is required, the wide spray angle produced by this injector at these operating conditions would also be desirable.

When the evaluation of Configuration V-2 revealed that the combustor did not meet the idle emissions goals and the smoke output was higher than would be expected had the combustor actually been burning at the lean bulk primary zone equivalence ratios produced by the high primary zone air loading with the valves open, the use of the available alternate fuel injectors was considered. In particular injector A which produced a wider spray angle and a bias toward larger droplet sizes both of which would tend to enhance radial dispersion of fuel into the swirler air when the valves are open at high power. It had to be recognized that this injector also produced the wider spray angle spray at idle as well and this could cause undesirable spray dispersion at idle with possible adverse effects on low power emissions. This injector was incorporated in Configuration V-3.

Fuel Injector C differed from the other injector configuration in that it produced a narrow spray angle, in the range of 51° to 59° at all combinations of fuel and simulated engine operating conditions. As indicated above this narrow spray angle was considered desirable at low power levels at which the primary zone air valves are closed. This injector also produced substantially finer droplet sizes at all combinations of fuel and simulated engine operating conditions than did Injectors A or B. Injector C was incorporated in Configuration V-4 to evaluate the effect of a substantially finer atomized fuel spray on the performance of the variable geometry combustor. This configuration would also have the desired narrow spray angle at idle that would be expected to be consistent with low emissions at this condition but the combination of a narrow spray with fine rapidly evaporating droplets might inhibit the desired radial dispersion of fuel at high power levels.

Table 7-6 presents a comparison of the performance of Configurations V-2, V-3 and V-4. The only difference between these configurations is the fuel injector type and all data presented was obtained while operating on ERBS fuel. Relative to the initial Configuration V-2 the other two configurations produced significant improvement in low power combustion stability. When operating in the normal mode with the valves closed at idle, Configuration V-4

produced some improvement in the lean blowout fuel air ratio relative to Configuration V-2 but Configuration V-3 achieved a substantial further reduction to generally acceptable levels for operational combustors. Configurations V-3 and V-4 were also evaluated with the primary zone air valve open at idle and the lean blowout fuel air ratio was not found to differ substantially from that measured with the valves closed. In Configuration V-4 the lean blowout fuel air ratio was even lower when in the open valve mode. Despite wide variations in bulk primary zone equivalence ratio, there was evidently little intermixing of the flows through the swirler and the fuel injectors, with the result that the stability limits were being controlled by the mixture strengths in the immediate vicinity of the injector face.

TABLE 7-6
EFFECT OF FUEL INJECTOR TYPE ON
VARIABLE GEOMETRY COMBUSTOR PERFORMANCE

Configuration Fuel	V-2 ERBS	V-3 ERBS	V-4 ERBS
Fuel Injector	B	A	C
Lean Blowout F/A at Idle			
Valves Closed	.0071	0.0028	0.0053
Valves Open	---	0.0040	0.0041
Idle Emissions w/Valve Closed			
Carbon Monoxide - gm/kg	58.2	83	76
Unburned Hydrocarbons-gm/kg	5.3	31	21
Approach Emissions			
Valve Position	open	open/closed	open/closed
Carbon Monoxide - gm/kg	12.5	23.2/11.6	13.5/4.7
Unburned Hydrocarbons-gm/kg	1.1	1.5/2.2	3.9/0.3
Cruise-Valves Open			
Fuel/Air Ratio	0.023	0.0211	0.022
Liner Temperature - °K (°F)			
Avg. Primary Zone	899 (1159)	941 (1235)	941 (1234)
Maximum	972 (1291)	985 (1316)	1010 (1361)
SAE Smoke Number	21	37.1	14.9
Takeoff-Valves Open			
Fuel/Air Ratio	0.0232	0.0230	0.0228
Liner Temperature - °K (°F)			
Avg. Primary Zone	970 (1288)	964 (1280)	992 (1330)
Maximum	1032 (1399)	1020 (1377)	1074 (1475)
SAE Smoke Number	15.0	24.4	5 - 16
Pattern Factor	0.47	0.495	0.43
Location Max Liner Temp at Cruise/ Takeoff	Inner Liner Panel 2 Behind Fuel Injector	Inner Liner Panel 1 Between Fuel Injectors	

The emissions output measured with Configurations V-3 and V-4 at the idle condition were disappointingly high. Carbon monoxide output was more than 50 percent greater than in the initial Configuration V-2 and unburned hydrocarbon emissions were an order of magnitude higher. Some deficiencies were anticipated in the case of Configuration V-3 because the fuel spray from Injector A was wide over the entire operating range but the finely atomized narrow spray from Injector C in Configuration V-4 had been expected to be ideal for low idle emissions. At the approach operating condition, with the valves open, the emissions levels produced by Configurations V-3 and V-4 reduced toward those observed with the initial Configuration V-2. Closing the valves at this operating condition to produce a richer primary combustion zone also reduced carbon monoxide by 50 percent or more in both configurations and led to a significant reduction of unburned hydrocarbon emissions from Configuration V-4.

Use of the different fuel injectors in Configuration V-3 and V-4 produced some significant changes in the liner temperature levels and distributions. Relative to Configuration V-2 the location of the maximum liner temperature moved upstream and shifted transversely from immediately downstream of the fuel injector to midway between injectors. This shift occurred at all high power operating conditions with the valves open and with both alternative fuel injectors. With the exception of Configuration V-3 at takeoff, both of these fuel injector variations produced significantly higher primary zone average and maximum local liner temperatures than observed at the correspondingly condition in the initial Configuration V-2. The increments in liner temperature are large with the average primary zone temperature increasing by more than 42°K (75°F) at cruise. This is a significant increment that suggests different combustion mechanisms at high power levels. The only hypothesis consistent with the spray performance of the fuel injectors involved would be that the high momentum wide angle fuel spray of Injector A in Configuration V-3 was successful in shifting some of the combustion radially outward toward the liners so as to increase the heat load on these surfaces. However, this dispersion of the combustion would be expected to lead to a reduction in smoke formation rather than the increase noted in Table 7-6. Similarly, the increased primary zone liner temperatures associated with the use of Injector C in Configuration V-4 would have to be attributed to an even more concentrated central combustion core producing higher radial heat load on the liner. This hypothesis would have to be weighed against the observation that the finer atomization characteristics of Injector C led to fewer and/or smaller particulates in the primary combustion zone to be consistent with the lower Smoke Numbers observed with this combustor.

Observation of the combustor exit temperature distribution from Configurations V-3 and V-4 indicated they were comparable and similar to that produced by Configuration V-2 and shown on Figure 7-22. This is reflected in the consistency of the cited Pattern Factors on Table 7-6. Evidently, the relatively large quantity of dilution air introduced downstream in the combustor is dominating over any fuel dispersion effects in establishing the combustor exit temperature distribution.

7.3.3 Air Admission Schedule Revisions

At the conclusion of the evaluation of the alternate fuel injectors, it was evident that more significant changes had to be introduced to alter the flow structure in the primary combustion zone to achieve acceptable performance and emissions characteristics over the entire operating range of the variable geometry combustor. The controlling factors appeared to be enhancing the stability of the primary recirculation zone at low power level with the valves closed and enhancing intermixing between the swirler and the fuel laden air emanating from the aerating fuel injector during high power operation with the valves open. Configurations V-2, V-3 and V-4 had no primary or intermediate air addition through the liners but approximately 25 percent of the combustor airflow (16 percent when the valves were opened) entered as dilution air relatively far downstream through the fifth louver panels. As such these configurations relied on the swirl strength of the swirler and fuel injector discharge flows to stabilize the combustion zone in the front end. Since these mechanisms appeared to be inadequate, in Configuration V-5 one half of the dilution air entering the rear of the combustor, in particular that entering through the inner liner, was admitted behind the primary combustion zone through holes in the third louver panels of the inner and outer liners. This change in liner air schedule appears to offer several advantages:

- While not close enough to the injectors to lean the primary combustion zone at low power with the valves closed, the jets would produce aerodynamic blockage that would tend to reinforce the position of the recirculation zones behind each fuel injector to provide a stronger and better defined combustion zone.

- At low power levels with the air valves closed the jets provide leaning of the intermediate zone of the combustor in the event that the high carbon monoxide and unburned hydrocarbons were caused by excessively rich mixtures with inadequate capability for oxidation of these species in the intermediate zone.

- At high power levels where stratification of the concentric swirler and fuel injector airstreams was apparently causing rich burning the blockage produced by the intermediate air jets would create a stirring effect in the primary zone leading to more homogeneous, leaner fuel air mixtures.

Configuration V-5 incorporated the type B fuel injectors and with exception of the shift of airflow to provide intermediate airflow was identical to Configuration V-2. Additional tests were conducted on Configuration V-5 with the type B fuel injectors replaced by the type A injectors. This perturbation was identified as Configuration V-5A and when compared to the performance of Configuration V-3 provides additional data for isolating the influence of fuel injectors and intermediate air addition on the performance of the variable geometry combustor.

Table 7-7 presents a summary of the results of the evaluation of Configurations V-5 and V-5A with corresponding data from their counterpart configurations without the intermediate air. These data indicate the use of intermediate air did not have a pronounced effect on the performance of the combustor at idle with the valves closed. Comparison of Configuration V-5

with V-2 and V-5A with V-3 indicates the carbon monoxide is nearly invariant while the lean blowout fuel air ratios improve only slightly with the addition of intermediate air. In addition both unburned hydrocarbon emissions and SAE Smoke Number increase significantly when intermediate air is introduced in the configurations with the type B injectors while less substantial increases in these constituents occurred in the configurations with the type A injectors. Clearly, the introduction of intermediate air through the third liner panel did not have any substantial favorable effect on the emissions or stability of the combustor at idle and these performance aspects remain dominated by the fuel injector type.

TABLE 7-7

EFFECT OF INTERMEDIATE ZONE AIR ADDITION ON PERFORMANCE OF THE VARIABLE GEOMETRY COMBUSTOR

Intermediate Zone Air	None		12.66% Wab With Valves Closed	
Configuration	V-2	V-3	V-5	V-5A
Fuel Injector	B	A	B	A
Fuel	ERBS	ERBS	ERBS	ERBS
Idle With Valve Closed				
Carbon Monoxide - gm/kg	58.2	83	62.3	87.0
Unburned Hydrocarbons-gm/kg	5.3	31	29.9	38.7
SAE Smoke Number	0.8	28.8	7.0	38.0
Lean Blow Out F/A	0.0071	0.0028	0.0062	0.0023
Approach				
Valve Position	Open		Open/Closed	
Carbon Monoxide - gm/kg	12.5		9.7/5.3	
Unburned Hydrocarbons-gm/kg	1.1		1.1/0.24	
Cruise-Valves Open				
Fuel/Air Ratio	0.023		0.0182	
Liner Temperature - °K (°F)				
Avg Primary Zone	899 (1159)		937 (1230)	
Maximum	972 (1291)		989 (1321)	
SAE Smoke Number	21		18.3	
Takeoff-Valves Open				
Fuel/Air Ratio	0.0232		0.0190	
Liner Temperature - °K (°F)				
Avg. Primary Zone	970 (1288)		995 (1332)	
Maximum	1032 (1399)		1047 (1428)	
SAE Smoke Number	15.0		25.2	
Pattern Factor	0.47		0.84	
Location Max Liner Temperature at Cruise/Takeoff	Inner Liner Panel 2 Behind Fuel Nozzle		Inner Liner Panel 1 Between Fuel Nozzles	

At the approach operating conditions the emissions output of Configuration V-5 are slightly better than V-2 when the valves are open and reduce considerably on closing the valves at this power level.

As anticipated from the discussion of Sections 7.2.6 and 7.3.1, shifting air from the dilution zone of the combustor reduced the ability to control exit temperature distribution with the consequence that, because of the limitations imposed by the exit vane pack, the attainable fuel air ratios at cruise and takeoff were lower. However, even at these reduced fuel air ratios the average and the maximum liner temperatures in the primary combustion zone of Configuration V-5 were higher than those encountered in Configuration V-2. Smoke Number measurements at these simulated high power conditions were also contradictory, with the smoke output decreasing at cruise and increasing at takeoff when the intermediate air was introduced.

The lack of conclusive direction from the evaluation of Configuration V-5 complicated identification of subsequent configurations of the variable geometry combustor concept. Configurations V-6 and V-7 had been reserved to demonstrate aspects that might enhance the performance of the combustor significantly at either high or low power level but were not currently compatible with variable geometry within the context of the current test combustor or program scope. The last allocated test configuration of the variable geometry combustor concept was V-8 which was to be tested more extensively than its predecessors for which it was desirable for it to have a good baseline level of performance. While not demonstrating potential in Configuration V-5 the use of intermediate air still appeared the most effective means of enhancing the performance of the variable geometry combustor. Large quantities of intermediate air (18.6 percent combustor air) had been introduced through the third liner panel of the reference PW2037 combustor (Configuration V-1) and excellent low power emissions and performance was produced as documented in Section 7.1. Lacking the availability of more air without compromising exit temperature distribution control, Configuration V-8 was defined with the current intermediate air (12.66 percent combustor air with the valves closed) entering through holes in the second liner panel of the inner and outer liner. While this risked leaning the primary combustion zone excessively at idle moving the jets upstream could improve their effectiveness in stabilizing the primary combustion zone flow structure. To enhance performance at high power when the primary air valves were open the swirlers in the bulkhead were replaced with the set having vane angles of 30° off axial rather than the 45° used on prior configurations. This reduced the swirl strength of the entering air decreasing the tendency for it to be centrifuged away from the central fuel laden core. The results of the evaluation of this configuration were presented in Section 7.2.

7.3.4 Potential Improvement of the Variable Geometry Combustor Concept

With the performance and emissions characteristics of the current definition of the variable geometry combustor concept deficient relative to the program goals, Configurations V-6 and V-7 were directed at simulating more extensive modification to the variable geometry air admission and fuel delivery systems the incorporation of which were beyond the scope of the present program or not even defined at the time but which offer the potential of significantly improved performance in a future redesign of the combustor. Modifications

were readily identified which offered the potential of improving the performance of the combustor in one operating mode, i.e., either at high power with the valves open or low power with the valves closed; but would invariably be expected to produce even more adverse effects on performance in the other operating mode. By incorporating modifications that would enhance performance in one mode in one configuration and the other in a second the performance of an improved combustor could be synthesized by combining the test results. This process would define potential performance and criteria or objectives for their being achieved in the future redesign of the variable geometry combustor.

Proceeding on this approach it was evident that further improvement in the performance of the variable geometry combustor must be achieved by promoting or suppressing interaction of the flows entering the combustor through the concentric fuel injector and swirler. Promoting strong intermixing of these streams while operating in the high power valve open mode would lead to a more uniform leaner mixture in the primary combustion zone that would be expected to be conducive to reduced smoke output and lower heat load at high power levels. This was accomplished in Configuration V-6 in which convergent conical extensions were installed on the discharge of the swirlers. The extensions were welded to the trailing edge of the vanes in the swirler near the outer diameter shroud and converged inward at 45 degree angle so as to deflect the swirler flow into the stream emanating from the fuel injector. The swirlers with the vanes at 30° off axial rather than those with a 45°vane angle were also used in this configuration to enhance mixing with the fuel injector discharge flow by reducing the centrifugal forces on the swirler airflow to promote the desired radial inward flow.

Configuration V-7 incorporated features directed at resolving the emissions and stability deficiencies of the combustor when operating at low power with the valves closed. These deficiencies appear to be caused by the lack of aerodynamic control of the hood purge and swirler cooling air when the primary zone air valves are closed. This airflow through the hood-swirler area is necessary during valve closed operation to prevent aspiration of combustion gases upstream of the bulkhead by transverse pressure gradients. While the quantity of purge air is small, being only about six percent of combustor airflow, it is large relative to the primary zone airloading, which should be about 14 percent of combustor airflow to produce stoichiometric mixture proportions in that zone at the design idle fuel air ratio. Entering in an uncontrolled distribution because of the small pressure drop across the large flow area swirlers, the purge air leads to large excursions in local mixture strengths in the primary zone at low power and the resultant erratic performance. In Configuration V-7 divergent conical extensions were attached to the inner shroud of the swirlers immediately adjacent to the fuel injector in an attempt to deflect the airflow that passed through the swirler radially outward to eliminate erratic and premature mixing with the injector airflow at low power. The 45° vane angle swirlers were also incorporated in this configuration to enhance centrifuging of the purge air from the swirler to promote this stratification process in the primary zone. In all other respects Configurations V-6 and V-7 were identical to Configuration V-5 in that they incorporated intermediate air introduction through the third louver panels of the inner and outer liner and used the type B aerating fuel injector.

Table 7-8 shows the measured performance of Configurations V-6 and V-7 and includes for reference the corresponding data from Configuration V-5 without swirler deflector extensions. All data was obtained when operating on ERBS fuel. The data from Configuration V-6 indicates that the use of the convergent deflector had substantial beneficial effect on the performance at high power levels. The SAE Smoke Numbers at cruise and takeoff are substantially below those of Configuration V-5 and even after making allowance for the reduced pressure levels in the test facility relative to the PW2037 engine at takeoff this configuration appears to have sufficient margin to achieve the program goal of a Smoke Number of 21 at takeoff. Primary zone liner temperatures are also reduced substantially by the use of the deflector cone in Configuration V-6. The average primary zone liner temperatures are reduced more than 70°K (130°F) at cruise and 105°K (185°F) at takeoff relative to Configuration V-5. Comparison with average primary zone liner temperatures in the reference PW2037 combustor (Configuration V-1) of Figure 7-4 indicates that the temperatures in Configuration V-6 are more than 55°K (100°F) lower than those in the reference combustor at cruise and takeoff despite the liner being cooled by substantially less cooling air - nominally 35 as opposed to 50 percent of combustor airflow. Both the substantial reductions in smoke output and primary zone liner temperatures indicate that the convergent conical deflector and reduced vane angle on the swirler of Configuration V-6 was effective in promoting intermixing of the swirler and fuel injector airstreams to produce the intended lean combustion process at high power levels with the valves open.

However, as anticipated, the use of the convergent swirler extension was found to have an adverse effect on low power operation of the combustor. Combustion was unstable at the approach condition with the valves open and at the idle condition in the valve closed mode the lean blowout fuel air ratio was higher than the design idle fuel air ratio. Obviously the deflector was also effective in directing the swirler flow in the valve closed operating mode and produced an erratic or excessively lean mixture at the idle condition.

The results of Table 7-8 also indicate that the use of the divergent conical extension in Configuration V-7 was effective in inhibiting intermixing of the swirler and fuel injector airflows at low power levels in that the lean blowout fuel air ratio and emissions at idle were improved significantly. The lean blowout fuel air ratio at idle is below 0.003 and would be considered acceptable for engine operability requirements. While still deficient relative to the program goals of emissions indices of 17.8 and 2.34 gm/kg respectively for carbon monoxide and unburned hydrocarbon emissions at idle both constituents have been reduced substantially from those of Configuration V-5. The carbon monoxide emissions are the lowest observed in any configuration of the variable geometry combustor concept but the combustion efficiency at idle remains at 97.9 percent. Improvements are also observed in the emissions at approach with both the carbon monoxide and unburned hydrocarbon emissions being lower than observed with the same valve position in any of the previously tested configurations.

As anticipated the suppression, as opposed to enhancing, of mixing in the primary combustion zone had adverse effects on the performance of the combustor at high power. Relative to Configuration VG-6, in which the conical extension enhanced mixing, the average primary zone liner temperatures were increased back to the levels encountered in Configuration V-5 at both cruise

and takeoff power conditions. The smoke output at both of these flight conditions was also increased substantially to levels higher than those observed in Configuration V-5. Both of these effects are obviously due to the richer local combustion in the primary zone when the extension inhibited swirler-fuel injector airflow mixing. Inspection of the combustor after completion of the testing of Configuration V-7 indicated that the liner, bulkhead and fuel injector faces were devoid of any carbon deposition as they had been in all of the previously evaluated variable geometry combustor configurations. However, the tips of the conical extensions on the swirler were found to have been locally burned and melted over one tenth to one half of their periphery. The cones evidently acted as a flameholder at some high power operating conditions.

TABLE 7-8

EFFECT OF CONICAL DEFLECTORS ON SWIRLER ON VARIABLE GEOMETRY COMBUSTOR PERFORMANCE

Configuration	V-5	V-6	V-7
Deflector	None	Convergent From Outer Shroud	Divergent From Inner Shroud
Swirler Angle	45°	30°	45°
Fuel	ERBS	ERBS	ERBS
Idle With Valve Closed			
Carbon Monoxide gm/kg	62.3	Unstable at	36.4
Unburned Hydrocarbons gm/kg	27.9	Design Idle	11.8
Lean Blow Out F/A	0.0062	0.011	0.0028
Approach			
Valve Position	Open/Closed	Unstable When Open	Open/Closed
Carbon Monoxide - gm/kg	9.7/5.3	17.3 } Closed	5.3/3.4
Unburned Hydrocarbons-gm/kg	1.1/0.2	0.7 }	0.2/0.04
Cruise - Valves Open			
Fuel/Air Ratio	0.0182	0.0224	0.0228
Liner Temp. - °K (°F)			
Avg Primary Zone	937 (1230)	865 (1099)	971 (1290)
Maximum	989 (1321)	875 (1118)	1005 (1352)
SAE Smoke Number	18.3	4.4	46.0
Takeoff - Valves Open			
Fuel/Air Ratio	0.0190	0.0191	0.0194
Liner Temp. -°K (°F)			
Avg Primary Zone	995 (1332)	890 (1145)	1001 (1345)
Maximum	1047 (1428)	903 (1168)	1049 (1420)
SAE Smoke Number	25.2	4.1	31.7
Pattern Factor	0.84	0.62	0.43
Location Max Liner Temperature at Cruise/Takeoff	Inner Liner Between Fuel Injectors		
	Panel 1	Panel 1	Panel 2

In summary, consideration of the hypothetical variable geometry combustor that is a composite of the low power-valves closed performance characteristics of Configuration V-7 with the high power -valves open characteristics of Configuration V-6 reveals that significant advances in performance are projected relative to the other configurations evaluated in this program. The combustor is projected to have adequate lean stability margin to meet engine operability requirements when operating on ERBS fuel. While program goals for carbon monoxide and unburned hydrocarbon emissions at idle would still not be met the levels would be generally lower than those observed in previous configurations. The combustion efficiency would be substantially in excess of the program goal of 99 percent at all power levels above idle and smoke output goals would be met with wide margins. The lean combustion achieved in the primary combustion zone at high power with the valves open would lead to substantial reductions in liner metal temperatures relative to the reference PW2037 combustor. These reductions in liner temperature would more than offset the increments associated with a Jet to ERBS fuel transition and would be achieved with lower liner cooling flow rates and combustor section pressure drops than the reference combustor. While the limitations of the test facility in which Configurations V-6 and V-7 were evaluated precluded realistic determination of oxides of nitrogen production in the test combustor, the substantial reductions in smoke and liner temperature when the desired lean bulk combustion was achieved in Configuration V-6 imply that some reduction in oxides of nitrogen formation might also be achieved in this composite variable geometry combustor.

7.3.5 Status of the Variable Geometry Combustor Concept

The results presented in Sections 7.2 and 7.3 provide an indication of the viability of a variable geometry combustor for accommodating the use of broadened properties fuels. The concept assessed incorporated externally actuated valves on the hood of the combustor to vary the quantity of air admitted to the primary combustion zone of the burner. The functional capability of this system was demonstrated with the valves shifting more than 30 percent of the combustor air between the primary zone and cooling and intermediate/dilution air apertures in the liner. The combustor exhibited only moderate sensitivity to fuel composition and properties. Over the range of test fuels evaluated the emissions and smoke output and liner temperatures increased moderately with decreasing fuel hydrogen content while there was some evidence that fuel viscosity and volatility was influencing the lean stability characteristics. Fuel composition had no significant effect on the combustor exit temperature distribution. The variable geometry combustor concept incorporated the same single pipe aerating fuel injectors used in the reference PW2037 engine combustor. The single pipe supply system eliminates the risk of carbon deposition in inactive secondary fuel passages at low fuel flow conditions - a decided advantage when operating on broadened properties fuels with lower thermal stability.

The observed emissions and performance characteristics of the variable geometry combustor were generally deficient relative to the program goals but the concept had been subject to a very limited extent of development and its full potential could not be achieved in a program of this scope. However, the fundamental process causing many of these deficiencies was identified.

The variable airflow entered the primary combustion zone through swirlers concentric with the fuel injectors and the control of mixing between these airstreams was the controlling factor. Strong intermixing was required at high power levels while mixing had to be suppressed at low power. The evaluation of a pair of combustor configurations incorporating features that would induce an extreme of intermixing in each configuration indicated that significant refinement of the variable geometry combustor to accomplish this mixing control would offer significant improvements in performance and emissions relative to the program goals. While still somewhat deficient in emissions at idle, this long range variable geometry combustor was projected to meet program goals for combustion efficiency above idle, smoke, lean stability and potential for reduction of oxides of nitrogen while operating on ERBS fuel. Substantial reductions in liner metal temperatures were demonstrated relative to the reference PW2037 combustor. These reductions in liner temperature would more than offset the increments associated with a Jet A to ERBS fuel transition.

7.4 FUEL SENSITIVITY OF THE MARK IV COMBUSTOR

As indicated in Section 4.3, Pratt and Whitney has been investigating the Mark IV combustor concept which is an outgrowth of the staged Vorbix combustor evolved under the NASA/PWA Experimental Clean Combustor and Energy Efficient Engine programs. Since the results of Phase I of this program indicated that the stoichiometry control attainable with staged combustors could be used to advantage in circumventing some of the problems associated with broadened properties fuels, the Mark IV combustor was incorporated as the second advanced technology combustor concept in the Phase II program. A total of thirteen configurations of the Mark IV combustor were evaluated. These divided into two groups associated with the broad objective and the facility in which the configuration was evaluated. The first six configurations; Configurations M-1 through M-6; were directed primarily at optimization of the geometric and aerothermal features of the combustor. These configurations were evaluated in the Jet Burner Test Stand at United Technologies Research Center. As indicated in Section 5.3.2 this facility was capable of accurately reproducing the combustor inlet conditions of the PW2037 engine at idle and approach but was limited in attainable pressure and required vitiation of the inlet air with oxygen replenishment to simulate higher power levels. The remaining configurations of the Mark IV concept; Configurations M-7 through M-13; were directed principally at performance enhancement through fuel injector variations and demonstration of the long term potential of the Mark IV concept. These configurations were evaluated in the Pratt & Whitney high pressure combustor test facility where they could be operated at simulated high power levels at higher pressure and with non-vitiated inlet air. Configuration M-7 was selected to identify the basic performance and fuel sensitivity of the Mark IV combustor because it represented the accumulative evolution of the concept through the initial segment of testing and because it was evaluated with all four of the available test fuels. The results of the evaluation of the other configurations are discussed in Section 7.5.

7.4.1 Description of Configuration M-7

Figure 7-24 shows the geometry and experimentally observed airflow distribution in Configuration M-7 of the Mark IV combustor. The aerothermal configuration was based on the evaluation of the six configurations in the initial phase of the assessment of this concept in combination with experience derived from company sponsored activity on this combustor. These initial tests had led to optimization of several geometric parameters primarily on the basis of combustor stability and emissions at low power and fuel distribution over the entire operating range. These considerations led to establishing a secondary swirler tube immersion depth of 37.6mm (1.5 inches) from the bulkhead; secondary swirler vane turning angle distributions that produced a free vortex tangential velocity distribution as opposed to one which increased linearly with radius and partial blockage of the centertube of this swirler in Configuration M-7. It also established preference for the use of primary swirlers with a higher vane turning angle - 75° as opposed to 60° in earlier configurations - because it appeared to produce more intense stabilization of the flow and reduced the airloading on the pilot combustion zone. Configuration M-7 and all subsequent configurations of the Mark IV combustor incorporated the advanced technology segmented liner construction in the region enclosing the pilot combustion zone and the upstream portion of the main combustion zone. With the exception of the use of the segmented liner, Configuration M-7 was aerothermally identical to Configuration M-5 previously evaluated in the Jet Burner Test Stand facility. Configuration M-7 was operated over the entire simulated engine power range with the fuel system functioning in Mode A with fuel being admitted through all four bulkhead mounted injectors to be representative of the desired "single pipe" operating capability.

7.4.2 Liner Metal Temperatures

As described in Section 4.3.3 and shown in detail in Figure 4-29 the advanced technology segmented liner construction incorporated in Configuration M-7 consisted of axially spaced rows of segments mounted on a shell structure. The segments were convectively cooled by air admitted through a transverse row of holes in the shell to impinge on the rear of the segment and flow axially upstream or downstream behind the segment. Pin-fin extended surfaces cast on the rear of the segment augment convective cooling and establish the split between the upstream and downstream directed cooling air flow. Since the discharged cooling air was intended to reinforce the toroidal recirculatory flow in the pilot combustion zone the flow balance and radial stepping of the panels was established to produce upstream directed cooling air flow over the surfaces of the first and second segments. Thermocouples were imbedded near the upstream end of these segments because metal temperatures were expected to be the highest in these regions and would provide measurements consistent with life limiting mechanisms. The thermal environment of the third row of segments differed in that the pilot recirculation zone was expected to end at this axial position and this segment provided the demarcation between upstream and downstream directed cooling air flow. As shown on Figure 4-29 there was no cooling air film on the gas side surface of this segment and it was also subject to impingement by hot combustor products where the flow reversed direction in the pilot recirculation zone. The upstream end of the segments was expected to have the highest metal temperatures and thermocouples were imbedded in this region of the third row segments.

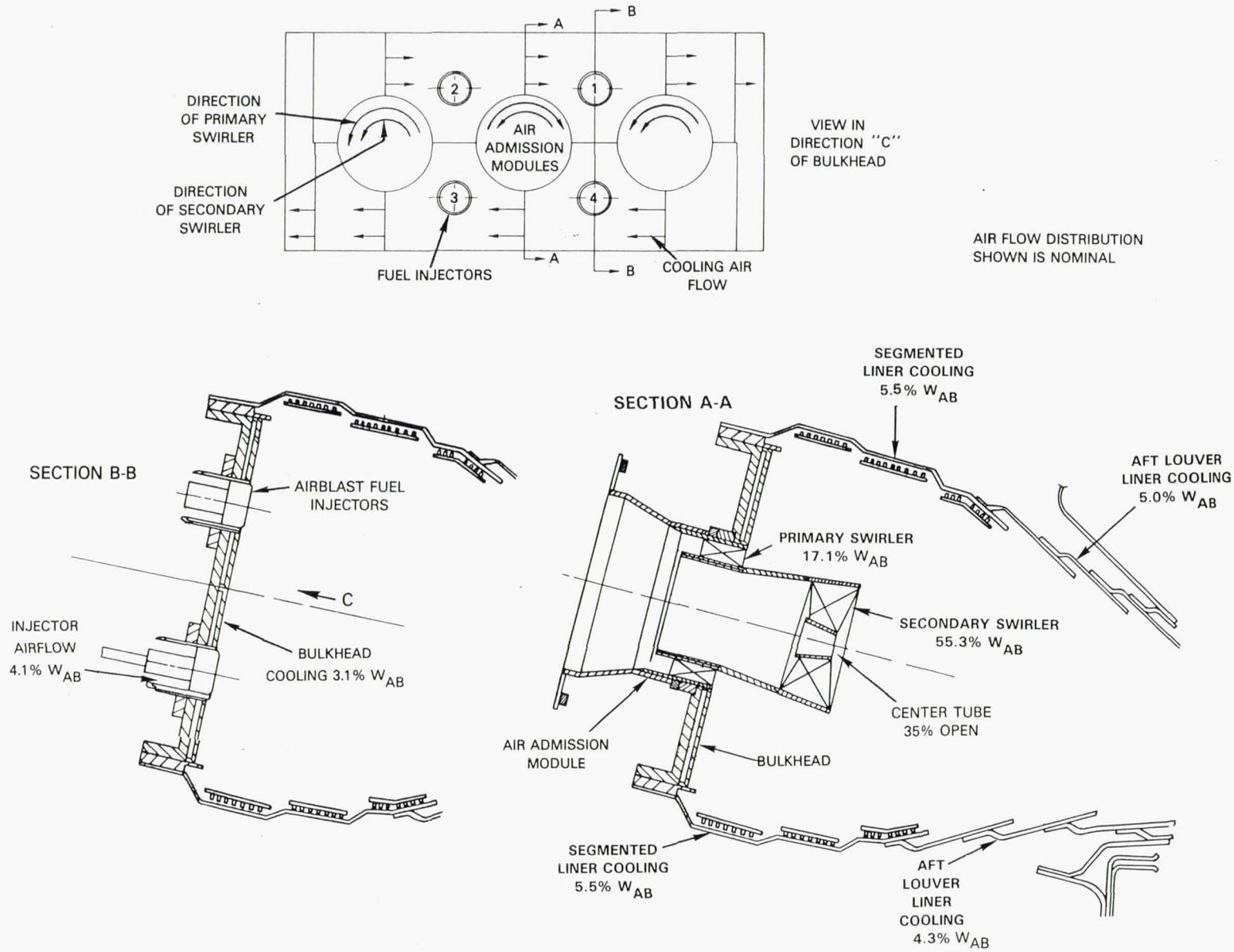

Figure 7-24 Details of Configuration M-7 of the Mark IV Combustor Concept.

Figure 7-25 shows the variation of the maximum and the average temperature on the three rows of segments enclosing the pilot combustion zone of the combustor with fuel hydrogen content. The average is that of ten operational thermocouples distributed over these segments while the maximum temperature always occurred at the same thermocouple - one installed on the third row segment on the outer liner axially downstream of a fuel injector. The measurements obtained at the takeoff operating condition indicate very little sensitivity of the liner temperatures to fuel hydrogen content. The average temperature scatters slightly about a nominal level of about 955°K (1260°F) while the single maximum temperature exhibits the typical progressive increase in level with decreasing fuel hydrogen content. The increase is very moderate with the Jet A to ERBS transition producing an increase of about 12°K (20°F).

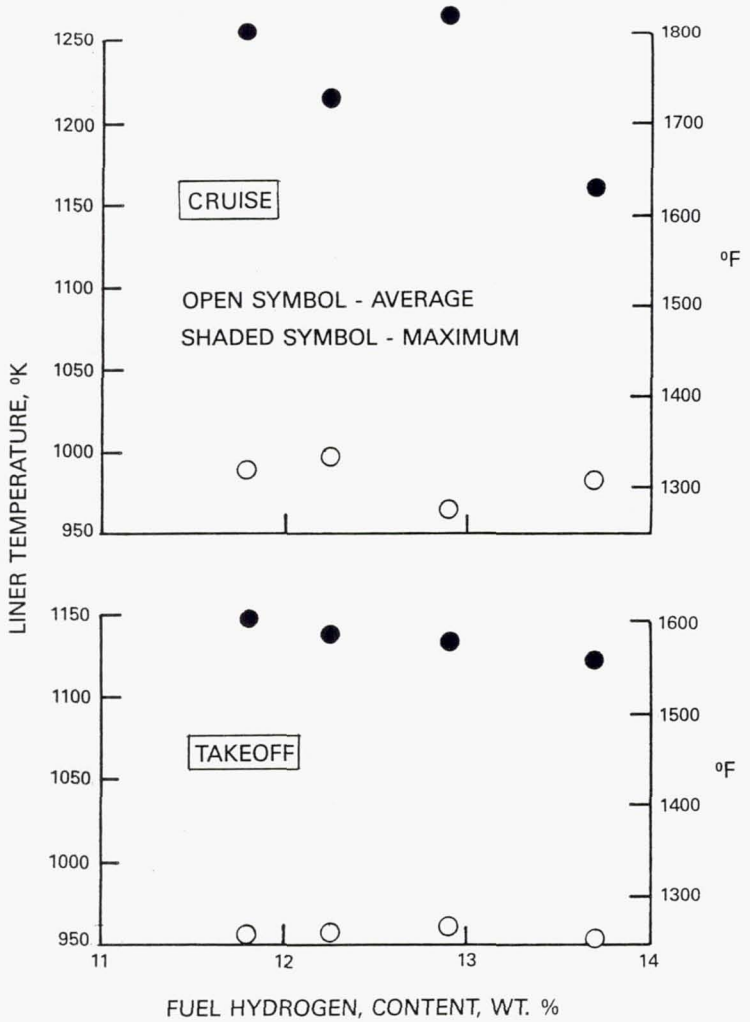

Figure 7-25 Effect of Fuel Composition on Liner Temperature in Configuratio M-7 of the Mark IV Combustor.

The liner temperatures measured at the cruise condition are higher than those observed at takeoff despite this operating condition having lower combustor inlet pressure, temperature and fuel air ratio. As at the takeoff condition, there is no consistent trend of variation of the average liner temperature with fuel hydrogen content with the scatter between test fuels exceeding any discernible slope. However, the maximum temperature location reveals considerable variation with a total range of nearly 111°K (200°F) with the different test fuels.

While the ERBS fuel produced a deviation, the other three test fuels reveal a consistent trend of increasing local temperature with decreasing fuel hydrogen content which would be indicative of sensitivity to radiation from progressively higher concentrations of luminous particles in the combustion gases. However, this thermocouple was located immediately downstream of one of the fuel injectors and at the axial location where the pilot recirculation zone was expected to end. These factors could also cause extreme sensitivity to convective heat transfer from the combustion products as well.

There are strong parallels between these results and the response of liner temperatures in the staged Vorbix combustor evaluated in Phase I of this program. That combustor also incorporated a segmented liner with internal convective cooling. At the cruise condition the incremental changes in liner temperature in both the pilot and main stage of the combustor during a Jet A to ERBS transition were very moderate and only a fraction of those observed in comparable conventional single stage combustors with louver liner constructions. At takeoff conditions the increments in liner temperature associated with reductions in fuel hydrogen content remained moderate in the pilot stage but became erratic in the main stage. Pronounced increases and decreases in temperature were observed with the Jet A to ERBS fuel change while only moderate increments (both positive and negative) were observed with further reduction in hydrogen content. With only two exceptions, temperatures on the outer liner increased and temperatures on the inner liner decreased as hydrogen content was reduced. This response implied that the liner temperature was responding to a strong change in convective heat load that was dependent on fuel composition. While a specific cause was not identified, the sensitivity of the fuel dispersion and atomization processes occurring in the carburetor tubes in the main stage of the Vorbix combustor might have produced this unusual response.

The temperature levels measured in the segmented liner of Configuration M-7 of the Mark IV combustor are moderate-reaching maximums of 1265°K (1820°F). At these temperatures the dominant segment distress mode would be cracking due to low cycle thermal fatigue. After significant exposure, cracks would be expected to develop at the upstream edge of a segment and gradually propagate into the segment. However, with the apparent minimal sensitivity of the metal temperature in this region to fuel composition life decrements to be associated with fuel changes cannot be defined. It appears that the more limiting factor influencing the life of a segmented liner in the Mark IV combustor will be localized heat loading such as that occurring on the third row segments of Configuration M-7.

7.4.3 Emissions

Figure 7-26 shows the measured carbon monoxide and unburned hydrocarbon emissions from Configuration M-7 of the Mark IV combustor at the PW2037 engine idle combustor inlet conditions. Data are presented for a range of fuel air ratios distributed near the design proportions. Also shown are the goals for these emissions constituents which were defined in Section 7.1.3 as the levels required for compliance with the previously proposed EPA Class T-2 standards for engines certified after January 1, 1984 with the assumption of reasonably low emissions of these constituents at higher power levels. Relative to these goals and the performance of the reference PW2037 combustor the idle emissions characteristics of the Mark IV combustor are deficient. While the combustor just achieves the goal of a carbon monoxide emissions index of 17.8 gm/kg with Jet A fuel, operation of the other fuels leads to higher concentrations of this constituent. Emissions of unburned hydrocarbons are three to four times the emissions index goal of 2.34 gm/kg at the design idle fuel air ratio with all test fuels. The negative slopes of both the unburned hydrocarbon and carbon monoxide emissions characteristics with fuel air ratio imply that the actual reaction zone was operating at leaner than stoichiometric proportions and might have been enhanced by enrichment. However, the departures from the goal levels are substantial and it appears that quenching of carbon monoxide consumption reactions and diversion of fuel from entrainment in the actual reaction zones are the dominant mechanisms causing the high emissions output.

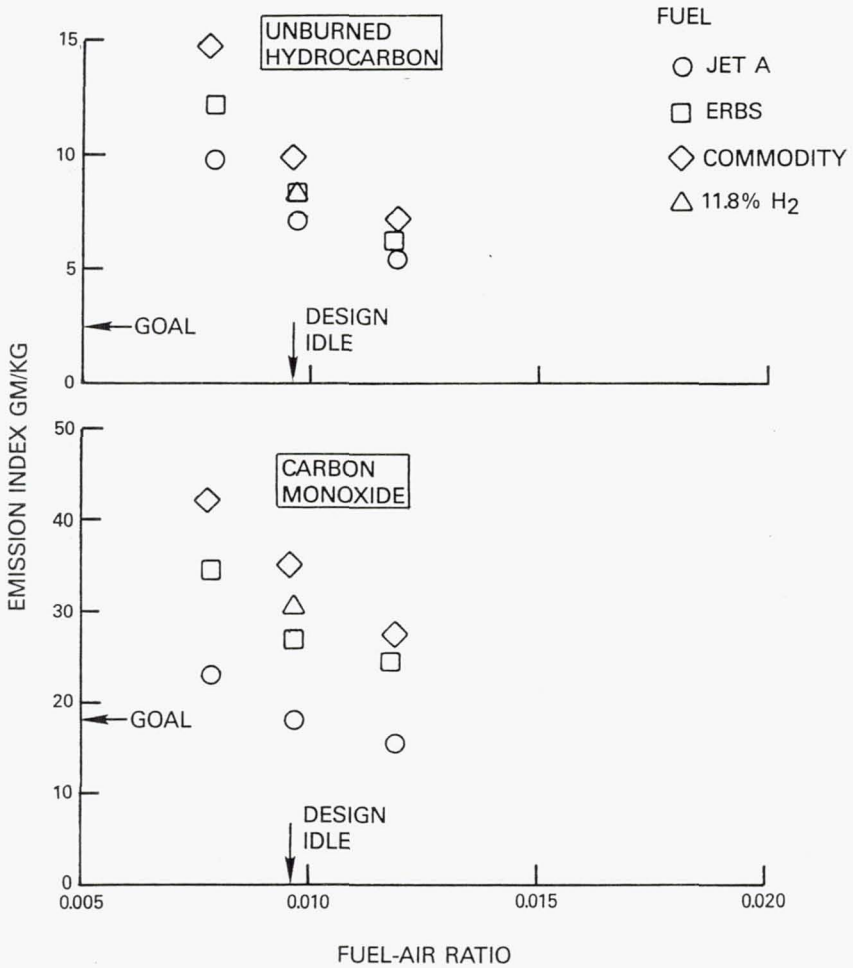

Figure 7-26 Idle Emissions Characteristics of Mark IV Combustor Configuration M-7.

It was indicated in Section 7.4.1 that Configuration M-7 was aerothermally identical to Configuration M-5 except for the use of the advanced technology segmented liner rather than the louver cooled liner in the front of the combustor. While the idle emissions characteristics of Configuration M-7 are deficient of the program goals and expectations for the Mark IV combustor concept, they are substantially improved relative to Configuration M-5. When operating on ERBS fuel the carbon monoxide emissions were reduced by a factor of three and the unburned hydrocarbons were less than half those observed in the evaluation of Configuration M-5. Evidently, the interaction of the pilot zone liner cooling air flow with the recirculating combustion products in that zone has a significant effect on the progress of combustion. The segmented liner employed essentially the same quantity of cooling air as the louver construction of Configuration M-5 and both discharged the coolant in the upstream direction to reinforce the recirculatory flow. However, the coolant discharged from segments is apparently more effectively directed along the liner surface, whereas that from the louvers of Configuration M-5 tended to be deflected into the recirculating zone by the raised lip of the upstream louver where it may have caused premature leaning, quenching of the mixture, or a destabilizing effect on the recirculation zone structure.

Significant trends of fuel composition and physical property effects are also evident in the data of Figure 7-26. Consideration of the emissions levels produced by the Jet A, ERBS and the Commodity fuels indicates systematic increase in output of both carbon monoxide and unburned hydrocarbons with reducing fuel hydrogen content. The single measurement obtained with the 11.8 percent hydrogen content blended fuel indicates lower output of both constituents and would be anticipated based on the trend with the hydrogen contents of the other three test fuels. As indicated in similar discussions of the low power emissions characteristics of the reference PW2037 and the variable geometry combustors, its effect appears to be due to the unusually low viscosity and volatility of this fuel blend relative to the other test fuels and indicates these properties also have significant effects.

Similar measurements of the carbon monoxide and unburned hydrocarbon emissions characteristics of the Configuration M-7 Mark IV combustor were obtained at approach (30% takeoff thrust) and higher power levels of the PW2037 engine. The results obtained indicated low emissions at all combinations of operating conditions and test fuels evaluated. Combustion efficiencies of 99.84 were observed at approach and levels in excess of 99.9 percent were achieved at the higher power operating conditions.

Figure 7-27 shows the variation of the emissions of oxides of nitrogen from the Configuration M-7 Mark IV combustor with fuel hydrogen content. Data are presented at the nominal cruise, climb and takeoff operating condition, the latter two being corrected to the full combustor inlet total pressure of the PW2037 engine cycle according to the procedures of Section 6.0. With the exception of some scatter in the data obtained at takeoff, these results indicate progressive increases in NOx emissions with decreasing fuel hydrogen content. As indicated in Section 7.1.3 this has generally been attributed to the increase in adiabatic flame temperature caused by the reduced hydrogen content of the fuel.

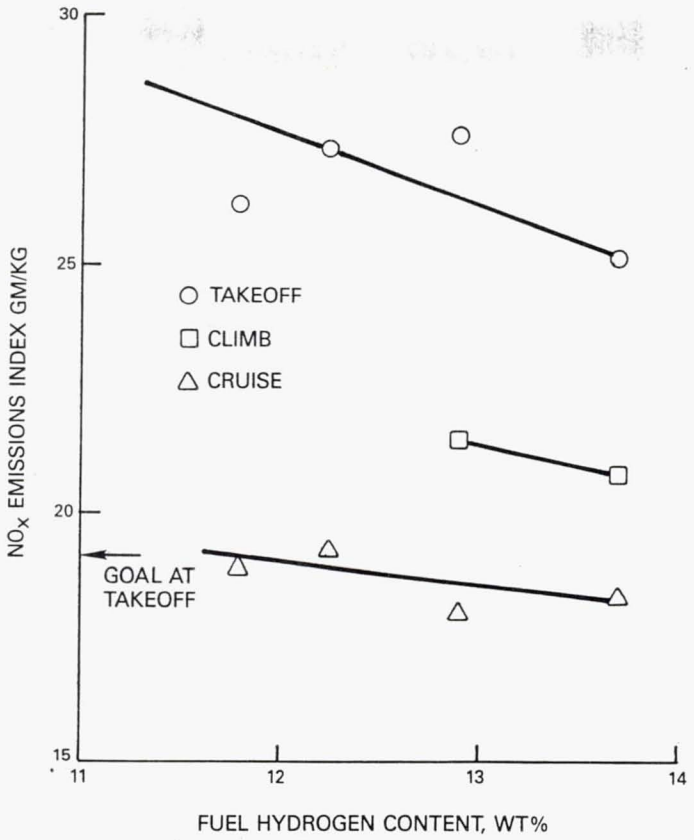

Figure 7-27 NOx Emissions Characteristics of Mark IV Combustor Configuration M-7.

To achieve the goals for advanced technology combustors being evolved under this program, the emissions of oxides of nitrogen would have to comply with the previously proposed Environmental Protection Agency Class T-2 requirements for engines certified after January 1, 1984. Assuming a reasonable relative distribution of emissions levels over the four points of the landing and takeoff cycle, an emissions index of 19 gm NOx/kg must be achieved at takeoff if this overall goal is to be met. Based on the data of Figure 7-27, a 30 percent reduction in the oxides of nitrogen output would be required for the Configuration M-7 combustor to achieve this goal when operating on ERBS fuel. Considering that the Mark IV combustor was intended to function as a staged burner with lean combustion in distinct pilot and main combustor zones, the demonstrated oxides of nitrogen emissions levels are high. Comparison with the corresponding data from the reference PW2037 combustor of Section 7.1.3 indicates the output is even higher than the levels produced by that current technology single stage combustor. It appears that the high rate of formation of oxides of nitrogen in Configuration M-7 of the Mark IV combustor was attributable to combustion occurring in a single rich combustion zone which was effectively an extension of the intended pilot zone rather than in two discrete lean zones. This conclusion will be further substantiated by assessment of the smoke output and exit temperature distribution from the combustor in the following parts of this Section. On the basis of the evidence it was apparent that the fuel injectors were not functioning as intended in the conceptual definition of this combustor in Section 4.3.1 and the majority of the effort on subsequent configurations of the Mark IV combustor were directed at refining the fuel system to achieve the intended dual zone mode of operation.

7.4.4 Smoke

The smoke output of Configuration M-7 of the Mark IV combustor was measured at selected high power operating conditions. Figure 7-28 shows the variation in measured SAE Smoke Number with fuel hydrogen content at combustor inlet conditions simulating cruise, climb and takeoff operation of the PW2037 engine. The data indicate the smoke output is very high with SAE Smoke Numbers ranging from 60 to more than 80 as opposed to a goal of a maximum of 21. While there is significant shifting of the measurements at the takeoff power level the data reveals a general trend of increasing smoke output with decreasing fuel hydrogen content.

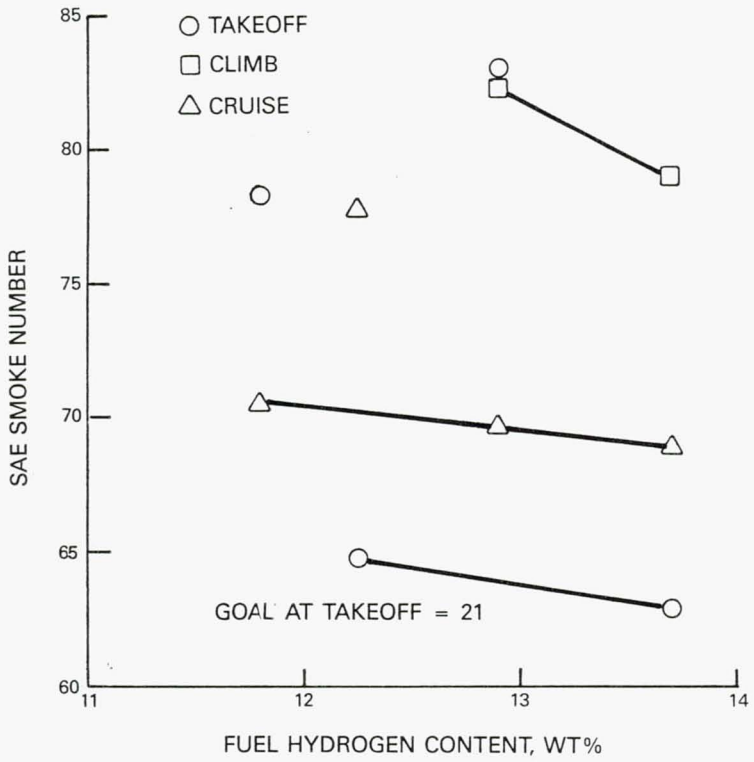

Figure 7-28 Smoke Characteristics of Mark IV Combustor Configuration M-7.

The combination of simultaneous higher than anticipated smoke and oxides of nitrogen emission is unusual because the mechanism causing high NOx production, i.e., high residence time at elevated temperatures, enhances smoke consumption. While high smoke output can also be related to an excessively high initial production rate in the combustion zone, post-test inspection of the combustor did not reveal any significant surface carbon disposition or sooting that could be interpreted as indicative of excess carbon formation on the bulkhead or liners of the combustor. Based on this evidence, it is hypothesized that the high smoke output must be attributable to very high smoke formation rates in a rich combustion zone adjacent to the liner but extending downstream of the intended pilot combustion zone and beyond the exit plane of the secondary swirler tube. Rather than being consumed in hot combustion products as they traversed the remaining length of the combustor, the particles leaving the rich combustion zone were probably entrained in the air entering through the secondary swirler. This would

quench the particles to compressor discharge temperature suppressing their consumption and leaving them as high residual smoke concentrations. If this hypothesis is valid, the revisions to the fuel injection system discussed in the context of reducing NOx emissions in Section 7.4.3 should also reduce the high power smoke output to more tolerable levels.

Configuration M-5 was aerothermally identical to Configuration M-7 except for the use of louvered rather than the advanced segmented liner construction in the front of the burner. When it was tested in the Jet Burner Test Stand the SAE Smoke Number was measured at 36 to 41 when operated on ERBS fuel at all power levels from idle to simulated takeoff. The increases in SAE Smoke Numbers to the 60 to 85 range of Figure 7-28 at high power levels is reasonable in view of Configuration M-7 being evaluated in the high pressure combustor test facility where the combustor could be operated at fuel air ratios and pressure levels closer to the actual PW2037 engine conditions rather than the limited levels of the Jet Burner Test Stand. However, at idle and approach conditions; which both facilities could accurately reproduce; the smoke output of Configuration M-7 was substantially lower.

Rather than the SAE Smoke Numbers of 37 and 36 observed at these conditions respectively in Configuration M-5 they were reduced to 12 and 8 respectively. The difference must be associated with the use of the advanced segmented liner in Configuration M-7. Apparently the same mechanisms producing the reduced idle emissions through more effective coolant introduction must also enhance the consumption of smoke particles when combustion levels are less intense and restricted to the forward or pilot zone regions of the combustor.

7.4.5 Combustor Exit Temperature Distribution

While refining the combustor exit temperature distribution to achieve the program goals for pattern factor and radial profile was not a major objective of the technical effort, the sensitivity of these parameters to variations in fuel composition was investigated. There was additional interest in the exit temperature distribution produced by the Mark IV combustor because of the unique approach to admitting the dilution air through the secondary swirlers in the front end of the combustor. Figure 7-29 shows the exit temperature distributions when Configuration M-7 was operated on Jet A and ERBS fuel at the takeoff condition. The temperature distributions are characterized by a wide spread in the radial direction but with distinct peaks in both the local maximum and average gas temperatures at instrumentation vanes immediately downstream of the bulkhead mounted fuel injectors. The exit temperature distributions observed with the other two test fuels were similar to those of Figure 7-29 and the exit temperature pattern factors observed at takeoff with all four fuels are summarized on Table 7-9. In all cases the pattern factor was dictated by a gas temperature peak at the 70 percent span location (Outer vane platform is 100 percent span) at instrumentation vane 3 downstream of a fuel injector pair. Because the pattern factor is dictated by a single highest measured gas temperature the variation in this parameter with test fuel is not of strong significance and is dictated by more random variations in the fuel dispersion.

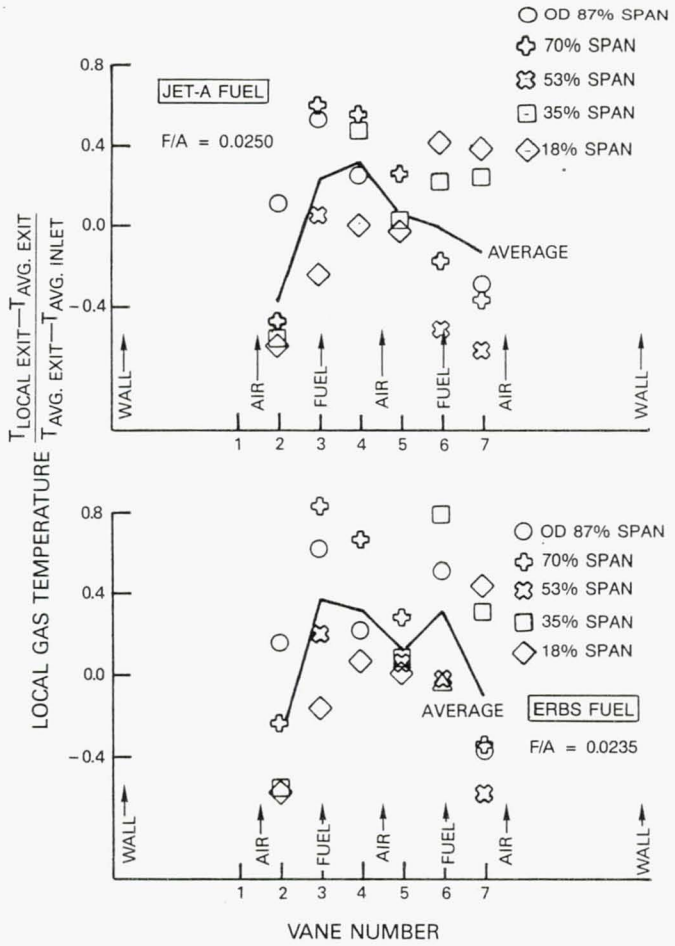

Figure 7-29 Exit Temperature Distribution of Mark IV Combustor Configuration M-7 at Takeoff.

TABLE 7-9

MARK IV COMBUSTOR
EXIT TEMPERATURE
PATTERN FACTORS AT TAKEOFF

Fuel	Pattern Factor
Jet A	0.60
ERBS	0.81
Commodity	0.62
11.8% Blend	0.74

The circumferentially averaged radial temperature profile at the combustor exit must comply with the target profile of Figure 3-4 to achieve the required turbine blade life in the PW2037 engine. This profile provides an additional characterization of the combustor exit temperature distribution that reduces distortion of the nominal features by random temperature perturbations. Figure 7-30 shows the radial temperature profiles obtained from the exit temperature distribution when the combustor was operated with each of the four test fuels. The temperature profiles are shown to deviate considerably from the target profile and are characterized by target level temperatures at the inner span, excessive temperatures at the outer span locations and a low temperature region at midspan. The unusual profile shape is obviously attributable to residual cold air from the secondary swirler jet that has not mixed with the hot combustion products at the periphery of the combustor. The profile shape is further evidence that the combustion process at high power was occurring in a single rich combustion zone extending downstream of the intended pilot combustion region rather than in a two-zone mode that would have involved more active combustion in the secondary swirler air with lower smoke and oxides of nitrogen emissions. It is reasonable to assume that fuel system refinement advocated to enhance the smoke and oxides of nitrogen emissions characteristics would also have a favorable effect on the exit radial temperature profile by eliminating the midspan low temperature region and shifting the profile closer to the target.

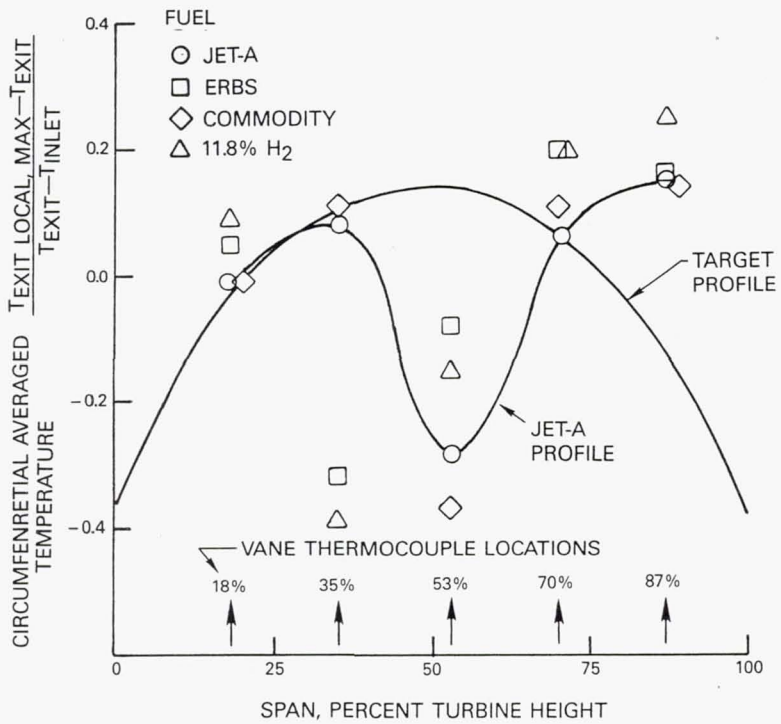

Figure 7-30 Effect of Fuel Composition on Radial Exit Temperature Profile from Mark IV Combustor Configuratio M-7 at Takeoff.

Figure 7-30 shows some variation in the radial temperature with the test fuels. While the temperature levels at the minimum of the low temperature mid span region are comparable with all four fuels the location of the minimum shifts inward from the 53 percent span location with Jet A and the Commodity fuel to 35 percent span with ERBS and the 11.8 percent hydrogen blended fuel. This is accompanied by an increase in gas temperature at the 70 percent span location. However, the variations are insignificant in comparison to the need to achieve major shifting of the exit temperature distribution to approach the target radial profile with any of the test fuels.

7.4.6 Combustion Stability

The lean blowout fuel air ratio of Configuration M-7 of the Mark IV combustor was determined with each of the four test fuels. The tests were conducted at the PW2037 engine idle condition with ambient fuel supply temperature. The results are listed in Table 7-10.

TABLE 7-10

LEAN BLOWOUT FUEL AIR RATIOS OF MARK IV COMBUSTOR AT IDLE INLET CONDITIONS

Fuel	Lean Blowout Fuel Air Ratio
Jet A	0.0046
ERBS	0.0043
Commodity	0.0052
11.8% Blend	0.0048

The trend of the results implies that lean blowout is not severely affected by fuel composition or physical properties. A slight bias toward higher blowout fuel air ratio with decreasing hydrogen content is evident and the reduced stability encountered with the Commodity fuel relative to the other fuels can be associated with its higher viscosity. The overall level of stability achieved with Configuration M-7 is reasonably good. In comparison the reference PW2037 combustor (Configuration V-1) of Section 7.1.6 achieved lean blowout fuel air ratios in the range of 0.0037 to 0.0045 on these four fuels. The refinements that must be made to the Mark IV combustor to achieve the program goals on carbon monoxide and unburned hydrocarbon emissions at idle are likely to enhance the stability further and provide greater margin.

7.5 MODIFICATIONS TO THE MARK IV COMBUSTOR

A total of thirteen perturbations of the Mark IV combustor concept were evaluated during the Phase II program. The basic test program was conducted in two elements - the first consisting of the evaluation of Configurations M-1 through M-6 and culminating in the test of Configuration M-7 which was a demonstration of the aggregate of the best features established through that point in the program. The results of that test have been discussed in Section 7.4. This initial element of the program involved screening of a number of combustor design parameters. Several of these parameters including the primary swirler vane angle, secondary swirler immersion and centertube

airflow were found to have distinct optimums and were maintained at that level while perturbations to other parameters were assessed. The second element of the program, involving the evaluation of Configurations M-8 through M-13, were characterized more by evaluation of individual potential improvements; rather than systematic optimization; and the assessment of the long term potential of the Mark IV concept. The results of both elements of this evolution of the combustor are discussed in this section. The details of the modifications incorporated were described in Section 4.3.3.

7.5.1 Initial Mark IV Combustor Configurations

Configuration M-1 was the first version of the Mark IV combustor concept to be evaluated in the PW2037 combustor rig. The aerothermal configuration was as described in Section 4.3.2 and the airflow distribution observed during the test is shown on Figure 4-16. While operation of Configuration M-1 was restricted to a maximum power level of approach by local overtemperaturing of a reverse flow louver in the primary zone, the investigation included extensive evaluation of the various fuel system operating modes at idle and approach power conditions with both Jet A and ERBS fuel. As indicated in Section 4.3.2; with particular reference to Figure 4-23; the four fuel injectors in the combustor could be operated in different modes identified as Modes A, B and C. In Mode A all four injectors were fueled while only Injectors 2 and 4, (identified in Figure 4-23) were operational in Mode B. Mode C consisted of operation on Injectors 1 and 3. Relating the injector positions to the direction of rotation of the primary swirlers on the air admission modules in Figure 4-23 indicates that the vortical flows induced by the primary swirler flow tends to move the fuel from Injectors 2 and 4 (Mode B) in the transverse direction, while these flows tend to spread the fuel from Injectors 1 and 3 (Mode C) in the radial direction between the modules.

Table 7-11 presents a summary of the evaluation of Configuration M-1 and includes carbon monoxide and THC emissions, combustion efficiency, smoke output and lean blowout fuel air ratio at the PW2037 idle condition for the three fuel system operating modes with both test fuels. The emissions and combustion efficiency data are interpolated to the design fuel air ratio of 0.0096. The results indicate that the combustion efficiency and emissions output of this configuration is deficient in all fuel system operating modes with efficiencies being limited to the 94 to 96 percent range. The failure of the emissions to respond significantly to local enrichment by operating on two injectors in Modes B and C implies that the combustion process is not concentration limited. However, local enrichment is shown to be effective in enhancing the combustion stability and Mode B, in particular, demonstrated lean blowout at fuel air ratios well below the goal level. Operation in this mode also produced the highest combustion efficiency levels because the carbon monoxide emissions were generally lower than in the other modes.

Operation of the combustor on ERBS rather than Jet A fuel generally led to an increase in the carbon monoxide and unburned hydrocarbon emissions with an accompanying decline in combustion efficiency, a result that has been typical throughout this program. The singular exception was the unburned hydrocarbon emissions when operating in fuel system Mode B. Another contradiction with general experience is the improvement in lean stability with all three fuel injector modes when the combustor was operated on ERBS rather than Jet A fuel.

TABLE 7-11
LOW POWER PERFORMANCE OF CONFIGURATION M-1
OF THE MARK IV COMBUSTOR

Fuel	Jet A	ERBS
Idle - Fuel Injection Mode A		
Fuel Injectors	1,2,3,4	1,2,3,4
Carbon Monoxide EI gm/kg	68.0	72.5
THC EI gm/kg	28.6	34.2
Combustion Efficiency (%)	95.2	94.6
Lean Blowout F/A	0.0050	0.0042
SAE Smoke Number	14.7	2.6
Idle - Fuel Injection Mode B		
Fuel Injectors	2,4	2,4
Carbon Monoxide EI gm/kg	49.5	53.5
THC EI gm/kg	26.7	23.6
Combustion Efficiency (%)	95.7	96.1
Lean Blowout F/A	0.0021	0.0015
SAE Smoke Number	1.0	26.3
Idle - Fuel Injection Mode C		
Fuel Injectors	1,3	1,3
Carbon Monoxide EI gm/kg	45.5	68.5
THC EI gm/kg	33.1	38.0
Combustion Efficiency (%)	95.1	94.1
Lean Blowout F/A	0.0033	0.0025
SAE Smoke Number	22.4	37.4
Approach		
Fuel Injectors (Mode A)	1,2,3,4	1,2,3,4
SAE Smoke Number	24.8	14.3
Fuel Injectors (Mode B)	2,4	2,4
SAE Smoke Number	42.4	28.2

When the combustor was operated at the PW2037 approach inlet condition, the combustor efficiency improved to between 99.8 to 99.9 percent with both fuels. The remaining inefficiencies were due primarily to the presence of small amounts of carbon monoxide in the combustion products. The smoke output from the combustor at both the idle and the approach conditions was extremely high which is suggestive of rich combustion. While the use of ERBS rather than Jet A fuel generally produced higher smoke output at the idle condition, the reverse was true at approach.

The testing of the Configuration M-1 was curtailed after obtaining the desired data at the approach conditions because a thermocouple on the liner enclosing the primary or pilot combustion zone indicated a temperature of nearly 1144°K (1600°F). Proceeding to the cruise operating condition would have necessitated increasing the combustor inlet temperature by nearly 139°C (250°F) and operating at higher fuel air ratios and would probably have increased the liner temperature to more than 1300°K (1900°F). This overtemperature was restricted to one location on the liner. Upon disassembly of the combustor after the test, the overtemperature was found to be caused by distortion of the reverse flow louver in this area - a situation

that was avoided in future configurations with minor modifications to the liners. Post test inspection also indicated accumulation of a dust-like carbon deposition on the face of the bulkhead and the liner in the primary or pilot zone region. Such a deposition could be anticipated in view of the high smoke output from this configuration.

Configuration M-2 of the Mark IV combustor incorporated several modifications beyond the modification to the combustor louvers to enhance their durability. The immersion depth of the secondary swirler tubes was reduced from 51 mm (2.0 inches) to 37.6 mm (1.5 inches) on the basis of the results of flow visualization tests which indicated this would lead to stronger recirculation of the flow in the primary or pilot combustion zone. Configuration M-2 also incorporated revised fuel injectors at all four positions in the bulkhead.

Concern over the low airflow loading ratios of the injectors used in Configuration M-1 had led to definition of an alternate configuration of this injector which increased the airflow capacity by 60 percent. Designated by "High Airflow" injector its increased airflow capacity was achieved by compromising slightly on the swirl angle of the atomizing air, increasing the exit diameter of the outer air cap and the use of thinner swirl vanes in the injectors. Limited spray evaluation indicated that the increase in airflow resulted in only a slight reduction in spray angle - from 80° with the Low Airflow injector to 75° with the High Airflow at a representative idle operating condition - and an improvement in the visual quality of the spray.

In operation in the rig, the local overtemperaturing of a louver that had limited the range of operation of Configuration M-1 has been resolved and Configuration M-2 was evaluated over the entire range of conditions up to the simulated takeoff condition. Table 7-12 summarizes the results of the evaluation of Configuration M-2 and includes, for comparison purposes, the corresponding available data from Configuration M-1. These data indicate that the revisions made to the combustor in Configuration M-2 did not lead to improvement in the idle performance. While the unburned hydrocarbon emissions output was comparable to that of Configuration M-1 when operating on ERBS fuel, the carbon monoxide emissions were generally higher. Comparative operation on Jet A and ERBS at idle produced the expected higher carbon monoxide emissions with ERBS fuel but, contrary to these expectations, the unburned hydrocarbon emissions were lower. This trend was evident in both fuel injection modes and led to higher combustion efficiency levels with ERBS fuel rather than Jet A. Nonetheless, the efficiency at idle remains substantially below the program goals and its improvement became a major objective of subsequent configurations. The modifications to the combustor to produce Configuration M-2 do not appear to have had any significant effect on the lean blowout characteristics of the combustor.

At the high power levels, operation in fuel injection Mode C led to high temperature streaks on the liners downstream of the operational fuel injectors that precluded operation of the combustor at or near the design fuel air ratios. Consequently, data is reported on Table 7-12 only for operation in injector Mode A. The tabulated results indicate that the use of the higher aromatic content ERBS fuel led to higher combustor liner temperatures at the high power operating conditions. Both the maximum metal temperature and the average of eleven measured metal temperatures on the

liner enclosing the primary zone increased with the change from Jet A to ERBS fuel. The magnitude of the increases is greater at cruise than at takeoff which is consistent with observations in more conventional combustors. The location of the maximum metal temperature did not shift with the change in fuel.

With the exception of the simulated takeoff condition, the smoke output increased substantially when the combustor was operated on ERBS rather than on Jet A fuel. The overall smoke levels are high and, at least with ERBS fuel at the approach condition, are higher than encountered in Configuration M-1.

TABLE 7-12
PERFORMANCE OF MARK IV COMBUSTOR CONFIGURATION M-2

	CONFIGURATION M-2		CONFIGURATION M-1
Fuel	Jet A	ERBS	ERBS
Idle - Fuel Injection Mode A			
Carbon Monoxide EI gm/kg	80.3	115.0	72.5
THC EI gm/kg	64.6	32.5	34.2
Combustion Efficiency (%)	90.5	93.0	94.6
Lean Blowout F/A	0.004	0.004	0.0042
SAE Smoke Number	9.5	37.6	2.6
Idle - Fuel Injection Mode C			
Carbon Monoxide EI gm/kg	77.4	86.7	68.5
THC EI gm/kg	37.4	25.6	38.0
Combustion Efficiency (%)	93.7	94.9	94.1
Lean Blowout F/A	0.001	0.002	0.0025
SAE Smoke Number	17.5	20.2	37.4
Approach - Fuel Injection Mode A			
Combustion Efficiency (%)	98.6	98.7	99.8
SAE Smoke Number	13.6	38.3	14.3
Cruise - Fuel Injection Mode A			
Fuel/Air Ratio	0.0020	0.0199	
Liner Temp. °K (°F)			
Avg. Primary Zone	868 (1104)	879 (1124)	
Maximum	982 (1309)	1005 (1351)	
SAE Smoke Number	16.4	44.4	
Takeoff - Fuel Injection Mode A			
Fuel/Air Ratio	0.0217	0.0217	
Liner Temp. °K (°F)			
Avg. Primary Zone	923 (1202)	927 (1209)	
Maximum	1039 (1412)	1034 (1403)	
SAE Smoke Number	38.3	33.7	
Location Max Liner Temp. at Cruise/Takeoff	Inner Liner Panel 2 Behind Fuel Injector 1		

7.5.2 Swirler Centertube Airflow Variations

Flow visualization tests have shown that the presence of a column of axial airflow on the centerline of the swirling jet eminating from the secondary swirlers has a strong effect on the rate of spreading or divergence of that jet. In particular, a high centerline axial velocity retards spreading while the absence of the central flow leads to rapid divergence or "bursting" of the jet. Recognizing that this spreading of the secondary air jet could have a strong effect on the strength of the recirculation and its structure in the primary of pilot zone of the combustor Configurations M-3 and M-4 were investigated particularly as a means of enhancing the low power emissions and combustion stability. In Configuration M-3 the centertubes of the secondary swirlers, which nominally flow about 7 percent of the combustor airflow, were blocked completely to eliminate the central jet. The tests indicated that this led to more erratic combustion and generally poorer performance of the combustor which appeared to indicate the need for some central airflow in the secondary swirler jet to maintain a stable flow pattern. Consequently in Configuration M-4 the centertubes were only partially blocked with finely perforated sheet metal restrictors so as to admit about 35 percent of the nominal centertube airflow or about 2.5 percent of the combustor airflow. These configurations also differed from Configuration M-2 in that the quantity of the cooling air on the front bulkhead of the combustor was reduced to 35 percent of the initial level because thermal paint indicated these surfaces were overcooled. However, the results of a company sponsored test on the combustor indicated that this change did not have a significant effect on the combustor performance. Consequently the results of the evaluation of Configuration M-2, M-3 and M-4 are examined in the context of a progressive variation of the secondary swirler centertube airflow.

Table 7-13 presents a summary of the results of testing Configurations M-2, M-3 and M-4. All of the reported data were obtained while operating on ERBS fuel in the fuel injection Mode A with the four injectors operational. The results indicate, as mentioned above, that completely blocking the centertube of the secondary swirler in Configuration M-3 had a substantial adverse effect on the performance of the combustor. Relative to Configuration M-2 with this passage completely open, the combustion stability and combustion efficiency deteriorated considerably. The latter was due to a nearly three-fold increase in unburned hydrocarbon emissions. Likewise the combustion efficiency was reduced at the approach condition. Visual examination of the flame structure in the combustor, with a television camera viewing upstream through a window in the exhaust duct, indicated the combustion to be less stable than seen in previous configurations and suggests that the central axial core of the secondary swirler jet is essential to stabilizing the flow in the combustor. Attempting to operate Configuration M-3 at simulated high power levels indicated that the metal temperature levels in the liner enclosing the pilot or primary zone were substantially higher than they had been in prior configurations. As shown in Table 7-13 at the simulated takeoff inlet conditions both the maximum and average metal temperatures in the liners enclosing the primary zone were higher at a fuel air ratio of 0.0129 than they had been at a fuel air ratio 0.0217 in Configuration M-2.

TABLE 7-13
EFFECT OF SECONDARY SWIRLER CENTERTUBE FLOW
ON THE PERFORMANCE OF THE ADVANCED CONCEPT MARK IV COMBUSTOR

Configuration	M-2	M-4	M-3
CENTERTUBE AIRFLOW percent of maximum	100	35	0
Idle			
Carbon Monoxide EI gm/kg	115.0	68.4	107.4
THC EI gm/kg	32.5	16.5	87.7
Combustion Efficiency (%)	93.0	96.5	87.2
Lean Blowout F/A	0.004	0.0057	0.0062
SAE Smoke Number	37.6	18	
Approach			
Combustion Efficiecy	98.7	99.8	96.1
SAE Smoke Number	38.3	16.0	9.0
Cruise			
Fuel/Air Ratio	0.0199	0.0149	
Liner Temperature °K (°F)			
Avg. Primary Zone	879 (1124)	858 (1085)	
Maximum	1005 (1351)	932 (1219)	
SAE Smoke Number	44.4	42.0	
Takeoff			
Fuel/Air Ratio	0.0217	0.0150	0.0129
Liner Temperature °K (°F)	927 (1209)	909 (1178)	938 (1230)
Maximum	1045 (1423)	973 (1292)	1062 (1453)
SAE Smoke Number	33.7	35.0	9.0
Location Max Liner Temp. at Cruise/Takeoff	Inner Liner Panel 2 Behind Fuel Injector 1	Inner Liner Panel 2 Behind Air Module	Inner Liner Panel 2 Behind Fuel Injector 1

*All data obtained in fuel injection mode A with ERBS fuel

The data of Table 7-13 indicate that Configuration M-4, in which the centertube was only partially blocked, produced performance characteristics that were generally superior to either Configuration M-2 or M-3 suggesting that an optimum centertube restriction exists. The combustion efficiency at idle was superior to either of the two previous configurations because of reductions in both the carbon monoxide and unburned hydrocarbon emissions. WHile the combustion efficiency at idle remained below the program goal of 99 percent, it is the only configuration of the three to achieve this goal at approach. Because of operational limits imposed on testing after the high liner temperatures were encountered with Configuration M-3 the data at the simulated cruise and takeoff conditions were acquired at lower fuel air ratios than necessary to protect the liner. However, it would appear that the measured liner temperature levels are much more consistent with those observed with Configuration M-2 when the differences in fuel air ratio are considered. At low power, the smoke output from Configuration M-4 was only about half that produced by Configuration M-2 but this advantage appears to vanish at the higher power levels.

Table 7-14 presents further details on the performance characteristics of Configuration M-4 including comparison of operation on Jet A and ERBS fuel and the effect of fuel injection through two as opposed to all four fuel injectors. At the idle condition the use of ERBS rather than Jet A fuel is shown to lead to small increases in the carbon monoxide and unburned hydrocarbon emissions that cause the combustion efficiency to be reduced by fractions of a percentage point. While the introduction of ERBS fuel leads to no significant change in the lean blowout fuel air ratio in the two injector injection Mode B it produced some improvement in this parameter when operating in the injection Mode A. Comparison of the performance at idle with the two different fuel injection modes indicates a preference for the two injector Mode B in that the idle combustion efficiency is nearly a full percentage point higher and the lean blowout fuel air ratio is close to the goal level. However, these advantages must be tempered against the need to stage the fuel system to operate in the B Mode at idle. The simplicity of a single pipe type fuel system provides considerable incentive to improve the performance of the combustor in fuel injection Mode A.

TABLE 7-14
EFFECT OF FUEL COMPOSITION ON THE PERFORMANCE
OF CONFIGURATION M-4 OF THE MARK IV COMBUSTOR

Fuel	Jet A	ERBS
Idle - Fuel Injection Mode A		
Carbon Monoxide EI gm/kg	58.3	68.4
THC EI gm/kg	13.2	16.5
Combustion Efficiency (%)	97.0	96.5
Lean Blowout F/A	0.0066	0.0057
SAE Smoke Number	6	18
Idle - Fuel Injection Mode B		
Carbon Monoxide EI gm/kg	53.5	59.1
THC EI gm/kg	8.7	10.1
Combustion Efficiency (%)	97.7	97.4
Lean Blowout F/A	0.0034	0.0035
SAE Smoke Number	12	23
Approach - Fuel Injection Mode A		
Combustion Efficiency (%)	99.6	99.8
SAE Smoke Number	9	16
Cruise - Fuel Injection Mode A		
Fuel/Air Ratio	0.0157	0.0149
Liner Temperature °K (°F)		
Avg. Primary Zone	864 (1097)	858 (1085)
Maximum	941 (1235)	932 (1219)
SAE Smoke Number	32	42
Takeoff - Fuel Injection Mode A		
Fuel/Air Ratio	0.0149	0.0150
Liner Temperature °K (°F)		
Avg. Primary Zone	876 (1118)	909 (1178)
Maximum	944 (1241)	973 (1292)
SAE Smoke Number	20	35
Location Max Liner Temp. at Cruise/Takeoff	Inner Liner Panel 2 Behind Air Module	

At the high power levels, i.e. cruise and takeoff, the liner temperature data display some anomalies not encountered in prior configurations. While the location of maximum liner temperature is the same at both operating conditions and with both fuels, the magnitude of the temperature increase associated with the Jet A to ERBS change is of the order of 28°K (50°F) which is substantially larger than encountered in previous tests.

The smoke output from Configuration M-4 also appears to be very sensitive to fuel composition. Use of ERBS fuel produced as much as two and threefold increases in Smoke Number at low power levels and significantly higher smoke output at the high power levels as well.

The results of the comparative evaluation of Configurations M-2, M-3 and M-4 established a distinct preference for partial blocking of the swirler centertube. The 65 percent restriction of the centertube assessed in Configuration M-4 was incorporated in subsequent Mark IV combustor configurations through Configuration M-10.

7.5.3 Pilot Swirler Airflow Capacity

The effect of variation in the airflow into the pilot zone through the pilot stage swirlers on the air admission modules was investigated in Configuration M-5. This configuration differed from the previously tested Configuration M-4 in that the turning angle of the swirl vanes in the primary airflow passage of the air admission modules was increased from 60° to 75° off the axial direction. This effectively restricted the flow capacity of the primary airflow passages, reducing the flow from 24.3% of the combustor air in Configuration M-4 to 17.1%. With reference to the nominal airflow distribution of Figure 4-16, the diverted air entered the combustor primarily through the secondary swirlers. Increasing the swirl angle and reducing the airflow in the primary airflow passage was expected to produce richer mixtures and stronger recirculation in the primary combustion zone adjacent to the combustor bulkhead. This scheme was pursued in an attempt to improve low power combustion efficiency and stability.

Table 7-15 presents a summary of the results of the evaluation of Configuration M-5, including both a comparison of its performance when operating on Jet A and ERBS fuel and a comparison with the previously reported Configuration M-4 with the smaller 60° primary air passage swirl angle. The results indicate that the emissions characteristics followed the anticipated fuel sensitivity trends. The carbon monoxide and unburned hydrocarbon emissions at idle were higher when operated in either the A or B fuel injection mode with ERBS fuel than with Jet A fuel. The idle emissions output from Configuration M-5 are also higher than those produced by Configuration M-4 with the difference being primarily in the carbon monoxide levels. While this would suggest that increasing the primary air swirl angle had an adverse effect on low power performance, the data on lean stability limits indicate significant reduction in the lean blowout fuel air ratio when operating on all four fuel injectors in Mode A. This result is of particular significance because successful evolution of the Mark IV for operation in a single pipe fuel system configuration would require adequate lean stability in the same injector mode employed at high power levels.

TABLE 7-15
EFFECT OF PRIMARY SWIRLER ANGLE AND AIRFLOW
ON THE PERFORMANCE OF THE MARK IV COMBUSTOR

Configuration	M-5	M-5	M-4
Primary Swirler			
Angle - degrees	75	75	60
Airflow - $\%W_{AB}$	17.1	17.1	24.3
Fuel	Jet A	ERBS	ERBS
Idle - Fuel Injection Mode A			
Carbon Monoxide EI gm/kg	72.6	84.2	68.4
THC EI gm/kg	15.5	19.1	16.5
Combustion Efficiency (%)	96.5	95.8	96.5
Lean Blowout F/A	0.0036	0.0035	0.0057
SAE Smoke Number	19	37	18
Idle - Fuel Injection Mode B			
Carbon Monoxide EI gm/kg	67.1	81.4	59.1
THC EI gm/kg	18.5	25.5	10.1
Combustion Efficiency (%)	96.3	95.1	97.4
Lean Blowout F/A	0.0036	0.0032	0.0035
SAE Smoke Number	36	35	23
Approach - Fuel Injection Mode A			
Combustion Efficiecy	99.7	99.8	99.8
SAE Smoke Number	10	36	16
Cruise - Fuel Injection Mode A			
Fuel/Air Ratio	0.0169	0.0160	0.0149
Liner Temperature °K (°F)			
Avg. Primary Zone	840 (1054)	848 (1067)	858 (1085)
Maximum	945 (1242)	962 (1273)	932 (1219)
Location of Maximum Liner Temperature*	Fuel Injector 1	Fuel Injector 1	Air Module
SAE Smoke Number	11	41	42
Takeoff - Fuel Injector Mode A			
Fuel/Air Ratio	0.0160	0.0162	0.0150
Liner Temperature °K (°F)			
Avg. Primary Zone	866 (1100)	890 (1143)	909 (1178)
Maximum	933 (1221)	965 (1279)	973 (1292)
Location of Maximum Liner Temperature	Air Module	Air Module	Air Module
SAE Smoke Number	20	41	35

*Maximum liner temperature occurred on inner liner panel 2 downstream of component indicated.

The smoke output from Configuration M-5 was higher than that from Configuration M-4 at idle and approach power levels - probably as a consequence of the richer mixtures in the primary combustion zone. At higher power levels, the effect of primary zone swirler flow capacity on smoke output is negligible. However, the substitution of ERBS for Jet A in Configuration M-5 led to significant increases; by factors of two to four; in the smoke output at all power levels. The sensitivity of liner temperatures in the primary zone to fuel composition also appears to be very pronounced in Configuration M-5. At the takeoff condition where the combustor operated on both fuels at essentially the same fuel air ratio, the use of ERBS rather than Jet A fuel produced an increase of more than 22°K (40°F) in average liner temperature. When the differences in fuel air ratio in the test conditions at cruise are recognized, the listed metal temperatures imply that the sensitivity to fuel composition is also pronounced at this operating condition as well.

7.5.4 Swirler Vane Angle Distribution

Configuration M-6 was defined to investigate the effect of the radial distribution of vane angle in the secondary swirler in the air admission module through comparison with the results of the evaluation of Configuration M-5. While the swirler vanes in each configuration had a nominal metal surface turning angle of 40° off the axial direction, the swirler used in Configuration M-5 and all previously tested configurations had essentially a free vortex angle distribution in which the tangential velocity of the discharge air varied inversely with the radius from the centerline of the air admission module. Conversely, the swirlers used in Configuration M-6 incorporated vanes in which the turning angle increased linearly with radius. For the same nominal swirl angle, this difference in vane geometry led to tangential velocity component magnitudes at the outermost radius of the swirler discharge jet which were about twice those produced by the swirlers with free vortex type vane geometry. Increasing the angular momentum of the flow at the periphery of the secondary jet was expected to accelerate its spreading and enhance the confinement of the primary combustion zone to improve combustion efficiency in that region. The incorporation of the linear angle variation vanes in Configuration M-6 produced an increase in the flow capacity of the secondary swirler at about 3.5 percent of the combustor airflow. About half of this additional flow was diverted from the primary swirler passage which enrichened the primary zone slightly.

Table 7-16 presents a summary of the results of the evaluation of Configuration M-6 including both a comparison of its performance when operating on Jet A and ERBS fuel and a comparison with the previously reported Configuration M-5 with the free vortex secondary swirler vane angle distribution. The results indicate that the emissions characteristics followed the anticipated fuel sensitivity trends. The carbon monoxide and unburned hydrocarbon emissions at idle were higher when operated with ERBS fuel than with Jet A fuel. The idle emissions output from Configuration M-6 are also much higher than those produced by Configuration M-5 and lead to a reduction of three percent in combustion efficiency while operating on ERBS fuel. The lean stability characteristics also are sensitive to fuel composition. The low lean blowout fuel air ratio observed in Configuration M-5 in fuel injection Mode A was continued in Configuration M-6 when operated on ERBS fuel. However, when this configuration was operated on Jet A fuel the stability limit was considerably higher and representative of the levels encountered in Mode A operation of test configurations prior to M-5.

TABLE 7-16
EFFECT OF SECONDARY SWIRLER VANE ANGLE DISTRIBUTION
ON THE PERFORMANCE OF THE MARK IV COMBUSTOR

Configuration	M-6	M-6	M-5
Secondary Swirler			
Mean Angle - degrees	40	40	40
Angle Distribution	Linear	Linear	Free Vortex
Fuel	Jet A	ERBS	ERBS
Idle - Fuel Injection Mode A			
Carbon Monoxide EI gm/kg	79.3	106.9	84.2
THC EI gm/kg	22.5 -	45.9	19.1
Combustion Efficiency (%)	95.5	92.8	95.8
Lean Blowout F/A	0.0052	0.0035	0.0035
SAE Smoke Number	12	22	37
Idle - Fuel Injection Mode B			
Carbon Monoxide EI gm/kg	-	-	81.4
THC EI gm/kg	-	-	25.5
Combustion Efficiency (%)	-	-	95.1
Lean Blowout F/A	-	-	0.0032
SAE Smoke Number	-	-	35
Approach - Fuel Injection Mode A			
Combustion Efficiecy	99.9	99.9	99.8
SAE Smoke Number	5	20	36
Cruise - Fuel Injection Mode A			
Fuel/Air Ratio	0.0152	0.0155	0.0160
Liner Temperature °K (°F)			
Avg. Primary Zone	866 (1100)	889 (1142)	853 (1077)
Maximum	971 (1289)	1037 (1408)	962 (1273)
Location of Maximum Liner Temperature*	Fuel Injector 1	Fuel Injector 1	Fuel Injector 1
SAE Smoke Number	8	21	41
Takeoff - Fuel Injector Mode A			
Fuel/Air Ratio	0.0168	0.0168	0.0162
Liner Temperature °K (°F)			
Avg. Primary Zone	899 (1159)	931 (1217)	890 (1143)
Maximum	960 (1270)	1066 (1460)	965 (1279)
Location of Maximum Liner Temperature	Fuel Injector 1	Fuel Injector 1	Air Module
SAE Smoke Number	17	15	41

*Maximum liner temperature occurred on inner liner panel 2 downstream of component indicated.

Configuration M-6 produced substantial improvements in the smoke output characteristics of the combustor. When operated on ERBS fuel, the SAE Smoke Number was of the order of half that observed from Configuration M-5 at all power levels. However, the combustor continued to show a high sensitivity of smoke output to fuel composition. With the exception of the simulated takeoff condition, the smoke number was two to four times higher when operated on ERBS rather than Jet A fuel.

This configuration also exhibited high liner temperatures at high power levels. At both the cruise and takeoff operating conditions, the average liner temperature in the primary combustion zone was about 39°K (70°F) higher than in Configuration M-5. Comparison of liner temperature data, both average primary zone and local maximum, also indicate a strong sensitivity to fuel composition. With changes in the maximum local temperature of more than 55°K (100°F) when ERBS is substituted for Jet A fuel, it appears that the change in heat load is caused by more than just differences in radiant heat transfer from more luminous combustion products, and an alteration in local fuel air ratios due to changes in fuel spray characteristics with the different fuels must be suspected.

In conclusion, it appears that while the use of the secondary air swirler vanes with a linearly increasing rather than free vortex turning angle distribution did lead to significant reductions in smoke output from the Mark IV combustor, it had an overall adverse effect on combustor performance. The emissions and hence combustion efficiency deteriorated at the idle operating condition, and liner temperatures were increased substantially at high power levels. Evidently the increased mixing at the interface between expanding secondary airjet and the primary combustion zone interfered with the structure or stability of the flow in the latter.

With the completion of testing Configuration M-6, the initial element of the evaluation of the Mark IV combustor in the intermediate pressure Jet Burner Test Stand at United Technologies Research Center was concluded. The advanced technology segmented liner described in Section 4.3.3 was installed in the Mark IV combustor sector and the remaining configurations of this concept; Configuration M-7 through M-13 were evaluated in the Pratt & Whitney high pressure combustor test facility where they could be operated at simulated high power levels at higher pressure and with non-vitiated inlet air. Configuration M-7 was selected to identify the basic performance and fuel sensitivity of the Mark IV combustor because it represented the accumulative evolution of the concept through the initial element of the program. The results of the evaluation of this configuration; which incorporated the aerothermal features of Configuration M-5 with the addition of the advanced technology segmented liner; were discussed in Section 7.4.

7.5.5 Pilot Zone Flow Deflectors

One of the most significant results of the evaluation of Configuration M-7 was the level of the low power emissions of carbon monoxide and unburned hydrocarbons. While the idle emissions characteristics of Configuration M-7 are deficient of the program goals and expectations for the Mark IV combustor concept, they are substantially improved relative to Configuration M-5. When operating on ERBS fuel the carbon monoxide emissions were reduced by a factor of three and the unburned hydrocarbons were less than half those observed in the evaluation of Configuration M-5. Evidently, the interaction of the pilot zone liner cooling air flow with the recirculating combustion products in that zone has a significant effect on the progress of combustion. While the quantity of cooling air was identical, the discharge of the cooling air from the segments of the advanced technology liner must have interacted more favorably with the combustion gas flow structure than that eminating from

louvers in the earlier configurations. However, the low power emissions were still substantially above the program goals and it was suspected that ejector action by the secondary air jet in the air admissions modules might be entraining incompletely reacted combustion products from the pilot combustion zone and quenching them in the cool inlet air. To inhibit this action Configuration M-9 incorporated deflectors or trip rings on the outside diameter of the secondary swirler tubes in the air admission modules as shown on Figure 4-16. The rings were intended not only to interrupt ejector action caused by the secondary swirler discharge jet but also to deflect the airflow from the primary swirler into that zone. The trip rings were 6.4 mm (0.25 inches) in radial height and were installed 24.7 mm (0.90 inches) upstream of the end of the secondary swirler tube. While the intent had been to maintain Configuration M-9 identical to Configuration M-7 in all other respects it was necessary to assemble this configuration with the secondary swirlers from Configuration M-6 having a linear vane angle distribution. As will be discussed in Section 7.5.6, the swirlers with the free vortex vane angle distribution used in Configuration M-7 and most other prior configurations were damaged during a hot shut down of the rig and were not available until later in the program.

Table 7-17 presents a comparison of the performance of Configuration M-9 with that of Configuration M-7 when both were operating on ERBS fuel in fuel injector Mode A at all operating conditions. At the idle condition the combination of the linear secondary swirler air angle distribution and the fence on that tube in Configuration M-9 led to a significant gain in lean combustion stability, but a deterioration in carbon monoxide and unburned hydrocarbon emissions that reduced the combustion efficiency by more than one percent. However, this reduction must be weighed against the change from free vortex to linear secondary swirler vane angle distribution which when introduced between Configuration M-5 and M-6 produced a loss in idle combustion efficiency of three percent without compromising the lean blowout fuel air ratio.

The changes incorporated in Configuration M-9 also cause a very pronounced increase in idle smoke output that also continued to be evident at the approach operating condition. At the higher power cruise and takeoff operating conditions the smoke output is substantially lower than either Configuration M-7 at the correspondingly operating conditions or its own low power smoke output characteristics. This reversal of the smoke output characteristics has been evident in tests of some prior configurations of the Mark IV concept.

It is also evident that the changes incorporated in Configuration M-9 had an adverse effect on the heat load in the primary zone of the combustor relative to Configuration M-7. The average and maximum liner temperature in this zone increased by the order of 55°K and 165°K (100°F and 300°F) respectively, with the peak temperature region shifting from downstream of one fuel nozzle on the outer liner to the corresponding position behind the adjacent injector. This increase could have been caused by increased convective heat transfer to the liner segments in this area because of more pronounced gas impingement effects caused by the deflection of the primary swirler discharge flow by the ring.

TABLE 7-17
EFFECT OF SWIRLER TUBE RINGS ON MARK IV
COMBUSTOR PERFORMANCE WITH ERBS FUEL

Configuration	M-7	M-9
Secondary Swirler Angle	Free Vortex	Linear
Rings on Secondary Swirler	No	Yes
Idle		
Carbon Monoxide EI gm/kg	27.0	44.4
THC EI gm/kg	8.3	16.0
Combustion Efficiency (%)	98.4	97.1
Lean Blowout F/A	0.0043	0.0028
SAE Smoke Number	12	33
Approach		
Combustion Efficiency	99.8	99.9
SAE Smoke Number	8	54
Cruise		
Fuel/Air Ratio	0.0192	0.0186
Liner Temperature °K (°F)		
Avg Primary Zone	959 (1268)	1013 (1365)
Maximum	1057 (1443)	1220 (1737)
Location of Maximum Liner Temperature	Fuel Injector 3	Fuel Injector 4
SAE Smoke Number	69	13
Takeoff		
Fuel/Air Ratio	0.0235	0.0169
Liner Temperature °K (°F)		
Avg Primary Zone	953 (1256)	1050 (1432)
Maximum	1109 (1537)	1264 (1817)
Location of Maximum Liner Temperature	Fuel Injector 3	Fuel Injector 4
SAE Smoke Number	83	5

7.5.6 Alternative Single Pipe Fuel Injector Systems

As the evaluation of the Mark IV combustor progressed it became evident that the fundamental concept of using a single pipe fuel system to produce a staged fuel injection effect was not being achieved. Other approaches to fuel injection had been under study and two of these were evaluated in Configuration M-8 and M-10.

Configuration M-8 incorporated a unique airblast fuel injector concept. As described in Section 4.3.3 and shown on Figure 4-24 this approach involved use of two flat spray fuel injectors that protruded through the bulkhead into the pilot combustion zone. The injector body has a rectangular cross section airflow path with fuel being filmed on the inner radius side of a central plate from which it is atomized by the airflow on either side of the plate at the discharge to form a fan shaped spray approximately parallel to the combustor bulkhead. The injectors were installed in locations 1 and 3 so as to direct the fuel spray radially between the secondary swirler tubes in the same direction as the induced rotation caused by the air entering through the primary swirlers in the air admission modules. As the combustor power level is increased from idle to cruise and takeoff, the momentum of the air passing

through the injector increases more rapidly than that of the fuel film. This was expected to improve atomization and cause part of the fuel laden air jet discharging from the injector to follow a trajectory that is directed further downstream, as shown in Figure 4-24. This variation in bulk trajectory with power level is consistent with the intent of the Mark IV single pipe-dual combustion zone concept.

Configuration M-10 incorporated a variation of the basic conical spray aerating fuel injectors that had been used in prior Configurations M-2 through M-7 and M-9. These "High Airflow" injectors had been found reasonably effective in dispersing fuel in the pilot zone of the combustor at idle fuel flows but were not capable of producing the transition to a downstream directed spray at high flow rates. By removing the swirl vanes from the inner passage of "High Airflow" injectors, the airflow capacity of the injector was increased an additional 24 percent and the spray angle reduced to 50° to 55°. In Configuration M-10 two of the four "High Airflow" bulkhead injectors were replaced with these "Reduced Spray Angle" injectors. With reference to Figure 4-23 the "High Airflow" injectors were installed in locations 1 and 3 because the vortical motion induced by the primary air swirlers would draw the fuel from these injectors between the secondary air swirler tubes promoting its retention in the pilot combustion zone. The "Reduced Spray Angle" injectors were installed in locations 2 and 4 where the higher momentum spray could be more effectively directed downstream. The combustor was operated only in the A injection mode of Figure 4-23, i.e, all four injectors receiving an equal fuel flow with no attempts to bias the fuel flow from one type of injector to the other as combustor fuel air ratio was changed.

Table 7-18 shows a comparison of the performance of Configurations M-8 and M-10, incorporating the two alternate fuel system approaches, with that of Configuration M-7. The results indicate that the use of the flat spray fuel injectors in Configuration M-8 did produce the intended improvement in idle emissions characteristics. Carbon monoxide emission output was reduced by an additional ten percent from an already low level, while unburned hydrocarbon emissions were reduced more than five-fold and were below the program goal level. In combination, these improvements produced a combustion efficiency at idle in excess of 99%, making this the first configuration of the Mark IV combustor to achieve this goal level at idle.

Use of the flat spray injectors also led to significant improvement in the combustion stability with the lean blowout fuel air ratio at the idle operating condition being a barely detectable 0.0010. The smoke output of the combustor at both the idle and the approach conditions is shown to be higher than that of Configuration M-7. The higher output must be attributed to the richer mixture strengths created in the primary recirculation zone in the front end of the combustor with the flat spray fuel injectors concentrating the spray in this region.

At the high power levels, i.e. cruise, climb and takeoff, it was anticipated that the dynamics of the fuel-aerating air interaction in the flat spray fuel injector would shift the direction of the fuel spray further downstream in the combustor to avoid excessively rich mixtures in the primary zone. Based on the measured smoke output shown in Table 7-18 at takeoff and particularly the cruise operating condition, it would appear that this shift was

TABLE 7-18

EFFECT OF ALTERNATE FUEL INJECTORS ON
PERFORMANCE OF THE MARK IV COMBUSTOR WITH ERBS FUEL

Configuration	M-7	M-8	M-10
Secondary Swirler Angle	Free Vortex	Free Vortex	Linear
Fuel Injectors	Four Wide Spray Angle	Two Flat Spray	Two Wide and Two Narrow Spray Angle
Idle			
Carbon Monoxide EI gm/kg	27.0	24.2	54.1
THC EI gm/kg	8.3	1.6	30.5
Combustion Efficiency (%)	98.4	99.2	95.2
Lean Blowout F/A	0.0043	0.0010	0.0043
SAE Smoke Number	12	23	8
Approach			
Combustion Efficiency	99.8	99.9	99.9
SAE Smoke Number	8	34	19
Cruise			
Fuel/Air Ratio	0.0192	0.0206	0.0198
Liner Temperature °K(°F)			
Avg Primary Zone	959 (1268)	1037 (1409)	1032 (1399)
Maximum	1057 (1443)	1283 (1851)	1251 (1793)
Location of Maximum Liner Temperature	Fuel Injector 3	Fuel Injector	Fuel Injector 4
SAE Smoke Number	69	11	28
Takeoff			
Fuel/Air Ratio	0.0235	0.0228	Not Acquired
Liner Temperature °K(°F)			
Avg Primary Zone	953 (1256)	1075 (1476)	
Maximum	1109 (1537)	1481 (2207)	
Location of Maximum Liner Temperature	Fuel Injector 3	Fuel Injector	
SAE Smoke Number	83	54	

occurring. However, the metal temperatures in the segmented liner panels enclosing the primary combustion zone were substantially higher than in Configuration M-7. Streak temperatures in the transverse planes of the fuel injectors were particularly high.

The combustor rig was inspected after completion of the test. Examination of the parts indicated considerable distress. Within the primary zone there was evidence of melting and burnoff of the lips of the bulkhead louvers and the corners of the liner segments. Some of the liner segments were also distorted by the heat concentration in the plane of the fuel injectors. Furthermore, the secondary swirler tubes on two of the three air admission modules had broken free and struck the combustor exit vane pack damaging the instrumentation on several of the vanes. While this appeared to be of serious consequence, a thorough review of the operation of the

instrumentation involved and the pressure and airflow distribution in the combustor over the duration of the test conclusively proved that the loss of the secondary swirler air tubes occurred during the post-test shutdown of the rig. While the tubes may have been hotter than in previous configurations, the cause of failure was traced to cracking of welds retaining the tubes to their mount sleeves and not to overheating. As a result, it could be confidently concluded that the combustion rig was in the intended aerodynamic configuration over the entire duration of the test and that the only distress that could be directly associated with the use of the flat spray fuel injectors was that caused by overheating the combustor front bulkhead and primary zone liner segments. It was this damaging of the secondary swirler tubes with the free vortex vane angle distribution that forced the use of the tubes with the linear vane angle distribution in Configuration M-9 through M-12 while the tubes were being rebuilt.

While the use of the flat spray injectors in Configuration M-8 did lead to local overtemperatures and damage to the combustor the results were encouraging in that they appeared to function as intended shifting the direction of the fuel spray with power level. However, it was also evident that refining this injector concept for further operation in the combustor rig would require substantial development of the injector proper that was beyond the scope of this program.

The data of Table 7-18 indicate that the use of the narrow spray angle fuel injectors in two of the four positions in Configuration M-10 led to deterioration in the idle emissions output relative to Configuration M-7. However, the lean blowout fuel air ratio remained the same as Configuration M-7 while the smoke output at idle was reduced. Except for the sustained lean stability, these shifts in performance might have been anticipated because the use of the narrower spray angle injectors was expected to reduce the fuel loading of the primary zone, creating a leaner local mixture for the same overall fuel air ratio. Another consideration is the use of the secondary swirlers with the linear vane angle distribution in Configuration M-10 as opposed to those with the free vortex distribution in Configuration M-7. In the two previously discussed cases where the linear vane angle distribution swirlers were used; Configuration M-6 of Section 7.5.4 and Configuration M-9 of Section 7.5.5; the combustion efficiency at idle was reduced relative to the reference configuration with the free vortex vane angle swirlers.

When Configuration M-10 was operating at the cruise condition the average liner temperatures in the primary zone increased by about 70°K (130°F) relative to Configuration M-7 a part of which may have been associated with the higher test fuel air ratio. More significantly, the peak liner temperature which occurred near the downstream end of the second liner segment increased by nearly 200°K (360°F) and shifted to a transverse position downstream of one of the narrow spray angle injectors. This shift, in combination with a substantial reduction in smoke output at cruise also implied that the use of the narrower spray angle was somewhat effective in shifting some of the fuel loading downstream in the combustor. However, the performance of the combustor remained deficient relative to the program goals and the intended functional operation of the fuel system.

7.5.7 Duplex Fuel System

While the evaluation of Configurations M-8 and M-10 did provide some response of the combustor performance that indicated an axial shift in fuel loading with power level it was obvious that the dispersion characteristics of the fuel system were not consistent with the expectations advanced in the conceptual definition of Section 4.3.1. Furthermore it was evident that the production of injectors with the desired spray variation characteristics would in itself require an extensive development effort beyond the scope and schedule of this program. Consequently, the last few configurations evaluated in the program were directed at demonstrating the potential of the Mark IV combustor. Specifically, since the fuel systems evaluated were incapable of supplying fuel to both the pilot and secondary combustion zone from a single source, a duplex or staged system was employed to provide this distribution artificially. In the last three configurations of the Mark IV combustor a small hollow spray cone pressure atomizing fuel injector was installed in the centertube of each of the three secondary swirler tubes. Operating the combustor on two "High Airflow" airblast injectors in the bulkhead provided fuel to the pilot combustion zone while the injectors in the secondary swirler tube was used at higher power levels to spray fuel into or radially across the swirling secondary air jet into the pilot discharge - secondary air juncture where the second stage of combustion was to be sustained at high power. In effect, the approach was a fallback to the staged type of fuel system that is considered an undesirable design approach for combustors operating on broadened properties fuels. However, these configurations were not considered candidates for concept evolution but rather artifacts for simulating the potential of the Mark IV concept.

A total of three configurations were evaluated with this duplex or staged type fuel system. The spray angle of the secondary fuel injectors was varied between 85° and 60° in Configurations M-11 and M-12. While the swirlers incorporated in these two configurations had the linear variation of secondary swirler vane angle, the swirler tubes with the free vortex distribution that were damaged after the evaluation of Configuration M-8 were rebuilt and were used in Configuration M-13 in conjunction with an 85° spray angle secondary fuel injector.

Each configuration was operated with all of the fuel admitted through the bulkhead mounted primary fuel injectors at the idle condition. Operation in both the primary only and the staged mode, the latter with both primary and secondary systems flowing, was investigated at approach. At higher power levels the combustor was operated in only the staged mode. During operation at the simulated cruise condition an investigation was conducted of the effect of primary to secondary fuel flow split and when the apparent optimum was found this split was maintained during the evaluation at higher power levels, i.e. climb and takeoff. Table 7-19 presents a summary of the performance of the three combustor configurations with the duplex fuel systems. For comparison purposes, the corresponding data from Configuration M-7 are also included.

The performance of the three configurations at the idle condition are comparable with the only significant deviation being slightly lower carbon monoxide and unburned hydrocarbon emissions from Configuration M-13. These lead to an increase of one percent in combustion efficiency and are attributable to the free vortex as opposed to linear vane angle distribution

swirlers. The idle emissions and combustion efficiency are deficient relative to the program goals and also when compared to the reference Configuration M-7. However, no advantage in performance was anticipated at idle with the duplex fuel systems and the installation of the secondary fuel injector in the secondary swirler blocked airflow through the centertubes. Evaluation of Configuration M-3 had indicated blockage of the centertube had significant adverse effects on idle emissions and lean stability which is consistent with the deficiencies in the performance of these configurations relative to Configuration M-7.

TABLE 7-19

PERFORMANCE OF MARK IV COMBUSTOR
WITH DUPLEX FUEL SYSTEMS WHEN OPERATING ON ERBS FUEL

Configuration	M-7	M-11	M-12	M-13
Fuel System	Four Primary Injectors	Duplex	Duplex	Duplex
Secondary Fuel Injector Spray Angle	N/A	85°	60°	85°
Secondary Air Swirler Tangential Velocity	Free Vortex	Linear	Linear	Free Vortex
Idle				
Carbon Monoxide EI gm/kg	27.0	43.8	39.6	33.9
THC EI gm/kg	8.3	17.3	20.1	12.5
Combustion Efficiency (%)	98.4	96.9	96.7	97.7
Lean Blowout F/A	0.0043	0.0052	0.003	0.004
SAE Smoke Number	12	15	19	17
Approach (Primary Only)				
Combustion Efficiency	99.8	99.8	99.6	99.8
SAE Smoke Number	8	10	11	49
Approach				
Fuel Split (Primary/Secondary)	----	50/50	60/40	50/50
Combustion Efficiency	----	95.2	95.8	97.1
SAE Smoke Number	----	<1	<1	21
Cruise				
Fuel/Air Ratio	0.0192	0.0204	0.0197	0.0208
Fuel Split (Primary/Secondary)	100/0	40/60	50/50	50/50
Liner Temperature °K(°F)				
Avg Primary Zone	959 (1268)	917 (1192)	930 (1215)	937 (1228)
Maximum	1057 (1443)	1233 (1760)	1122 (1561)	1142 (1597)
Location of Maximum Liner Temperature	Fuel Injector 3	Air Admission Module	Fuel Injector 1	Fuel Injector 1
EINOx gm/kg	18.0	12.03	9.47	11.45
SAE Smoke Number	69	<1	<1	38
Takeoff				
Fuel/Air Ratio	0.0235	0.0245	0.0238	0.0240
Fuel Split (Primary/Secondary)	100/0	40/60	50/50	50/50
Liner Temperature °K(°F)				
Avg Primary Zone	953 (1256)	939 (1231)	1079 (1484)	1007 (1353)
Maximum	1109 (1537)	1381 (2027)	1374 (2014)	1208 (1716)
Location of Maximum Liner Temperature	Fuel Injector 3	Air Admission Module	Fuel Injector 2	Fuel Injector 1
EI NOx gm/kg	27.60	20.57	16.71	16.85
SAE Smoke Number	83	<1	27	36

Operation of all three configurations with the duplex fuel systems in the primary only or unstaged mode at approach produced performance comparable to Configuration M-7 with combustion efficiencies well in excess of 99 percent but relatively high smoke output, particularly in the case of Configuration M-13. Shifting to staged operation reduced smoke output; to essentially undetectable levels in Configurations M-11 and M-12; as a result of the reduced fuel loading on the primary combustion zone. However, the combustion efficiency declined when the combustor was shifted to staged operation at approach. The majority of this deficiency, about 3.3 percent in combustor efficiency; in Configurations M-11 and M-12; was due to excessive unburned hydrocarbon emissions and was probably caused by fuel being trapped in the center of the secondary swirler air and not getting to an ignition source. Since the reduction in secondary injector spray angle would be expected to concentrate more fuel in this central region in Configuration M-12 this may have been the reason that Configuration M-12 optimized on the basis of combustion efficiency at approach at a primary to secondary fuel flow split of 60/40 whereas the other configurations incorporating the 85° spray angle secondary fuel injectors optimized at 50/50 fuel flow splits.

When the cruise operating condition was simulated, variation of the primary/secondary fuel split indicated that the combustion efficiency began to fall off if the fraction of the fuel flow to the primary system was reduced below about 30 percent of the total. The optimum fuel flow split appeared to be about 40/60 between the primary and secondary respectively, in Configuration M-11 but shifted to a richer pilot with a 50/50 split being preferred in Configurations M-12 and M-13. In the case of Configuration M-12 the bias toward less fuel flow in the secondary system was obviously also due to the reduction in spray angle of the secondary fuel injector. The similar bias to a 50/50 fuel flow split in Configuration M-13 must be attributable to the free vortex vane angle distribution in the secondary swirler. At the inner radii of the secondary swirler the tangential velocity of the air jet is high with the free vortex vane angle distribution whereas it is low with the linear vane angle distribution. Hence, the secondary fuel spray initially encountered a relatively quiescent region in Configuration M-11 but a high shear environment in Configuration M-13. The latter could have led to more rapid dissipation of the fuel droplet momentum with more concentration of the fuel in the core of the jet where it would be more susceptible to quenching effects that would inhibit complete combustion. Nevertheless, at all cited high power operating conditions the combustion efficiency was in excess of 99.5 percent.

The most significant results of the high power operation of the configurations with the duplex fuel system are the low levels of NOx emissions and smoke. Not only are the NOx emissions reduced 30 to 50 percent below those of the reference Configuration M-7 but those of Configurations M-12 and M-13 are below the program takeoff goal levels. The smoke output from all three configurations is also substantially below that of Configuration M-7. That from Configuration M-11 is below the program goals at all power levels and virtually nonexistent at high power. Likewise, the smoke from Configuration M-12 was low but exceeded the program goal somewhat at the takeoff condition. Relative to these two configurations, the performance of the third duplex fuel system configuration; Configuration M-13 was unusual because of the pronounced increased in smoke output at approach and higher power levels. This cannot be attributed solely to operation in the duplex

fuel injection mode because the smoke number was also higher (by a factor of about 5) when the combustor was operated in the unstaged (primary only) mode at approach.

These substantial overall reductions in the NOx emissions and smoke at high power indicate that the duplex fuel system was functioning as intended in establishing a secondary lean combustion zone further downstream.

At the cruise operating condition the average liner temperatures in the primary zone of the three combustor configurations with the duplex fuel system are 22 to 42°K (40 to 75°F) lower than in the reference Configuration M-7 with all fuel injected at the bulkhead. This implies that the shifting of combustion to the secondary zone has relieved the heat load on the primary zone liner. However, the situation is more complex at the takeoff operating condition. Comparison of the primary zone liner temperatures in the initial duplex fuel system configuration; Configuration M-11; with the reference Configuration M-7 indicates that the average liner temperature was reduced by 14°K (25°F). However, introducing the free vortex secondary swirler vane angle distribution in Configuration M-13 led to an increase in primary zone average liner temperature of more than 65°K (120°F) relative to Configuration M-11. Configuration M-13 had optimized at a higher primary to secondary fuel split than Configuration M-11 but this had caused only a 20°K (36°F) increase in primary zone liner temperature at cruise. Configuration M-12; which incorporated the same linear vane angle distribution in the secondary swirlers as Configuration M-11; but the narrower secondary injector spray angle; produced even larger increases in primary zone average liner temperature. This result was not to be expected because the narrower spray angle of the secondary fuel would tend to concentrate fuel toward the core of the secondary air jet delaying liner heating effects to further downstream. The levels of maximum primary zone liner temperatures are all substantially higher in the three configurations with duplex fuel systems than in the reference Configuration M-7 both at cruise and at takeoff. The location of the maximum temperature also shifts with configuration and even between simulated power levels. This suggests that the dominant heat transfer mechanism is convection associated with locally fuel rich regions. The observation of increased maximum liner temperature while the primary zone was being leaned through fuel staging could indicate that the streaks were caused by combustion gases at equivalence ratios beyond stochiometric. Leaning these streaks would lead to increased local gas temperatures with higher heat load potential.

Assessment of the combustor exit temperature distribution indicated that the use of the duplex fuel system also led to significant improvement in the radial temperature profile. As shown on Figure 7-31, the reference Configuration M-7 with all fuel injection through the front bulkhead had produced a two lobed radial temperature profile with a deficit at mid span due to the lack of fuel penetration into the core of the secondary swirler jets. When secondary fuel was introduced at the center of these jets the figure shows that the radial temperature profiles observed with Configurations M-11 and M-12 were significantly improved and close to the target profile.

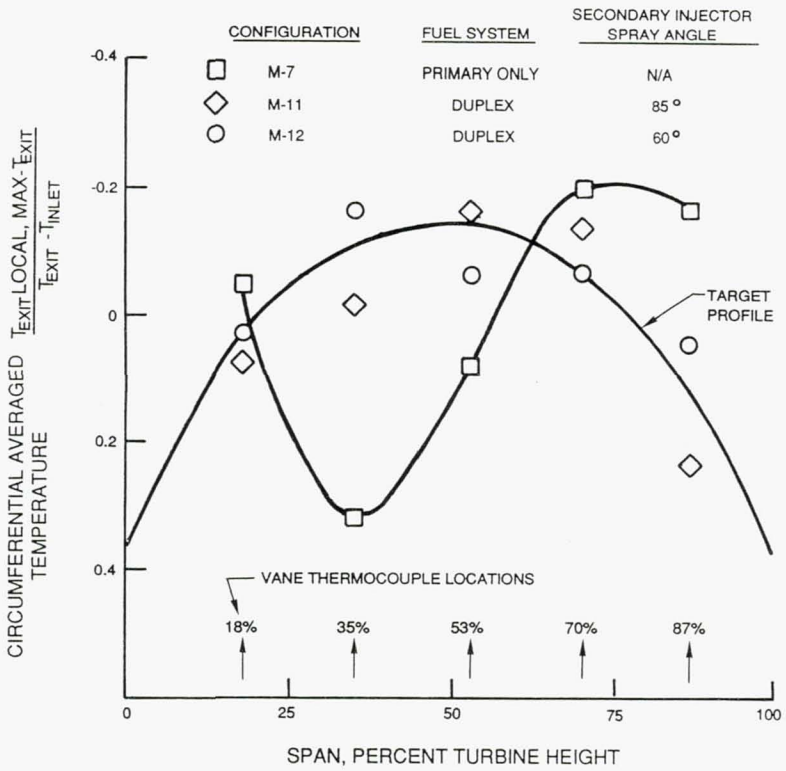

Figure 7-31 Mark IV Combustor Exit Radial Temperature Profiles with Duplex Fuel Systems.

The evaluation of Configuration M-12 also included a comprehensive evaluation of the sensitivity of the Mark IV combustor concept to fuel composition and the results are summarized in Table 7-20. Consistent but small trends are evident in the carbon monoxide emissions which increased slightly as hydrogen content decreased. Unburned hydrocarbon emissions exhibit a similar increase but in this case appear to be responding to fuel viscosity because of the decline in the emissions of this constituent when operating on the 11.8 percent hydrogen fuel blend. The lean blowout fuel air ratio is nearly invariant and appears independent of fuel composition.

Table 7-20 also lists the results at the cruise and takeoff operating conditions. The emissions of oxides of nitrogen vary in a random manner as opposed to the trend of moderate decrease in emissions index with increasing hydrogen content observed in other combustors including Configuration M-7 of the Mark IV concept. However, the NOx levels are low and the program goal is satisfied with all of the test fuels. The smoke output appears insensitive to fuel composition but does reveal the same trend of increasing smoke output as takeoff power is approached with all four test fuels. The liner metal temperatures exhibit the same random variations observed when the three duplex fuel system Configurations were evaluated only on ERBS fuel and no consistent trend with hydrogen content can be identified.

TABLE 7-20

EFFECT OF FUEL COMPOSITION ON PERFORMANCE OF CONFIGURATION M-12 OF MARK IV COMBUSTOR

Fuel Type	JET A	ERBS	Commodity Oil	11.8% H_2 Blend
Idle				
Emissions Index - gm/kg				
Carbon Monoxide	38.5	39.6	43.0	46.5
Unburned Hydrocarbon	17.9	20.1	20.2	18.7
Fuel Air Ratio At				
Lean Blowout	0.0032	0.0030	0.0030	0.0035
Approach (60/40 Fuel Split)				
Combustion Efficiency	96.6	95.8	Not	Not
SAE Smoke Number	1.5	<1	Obtained	Obtained
Cruise (50/50 Fuel Split)				
Fuel/Air Ratio	0.0193	0.0197	0.0187	0.0203
NOx Emissions Index gm/kg	10.7	10.6	19.7	11.0
SAE Smoke Number	--	<1	3	2
Liner Temperature °K(°F)				
Avg Primary Zone	982 (1309)	930 (1215)	862 (1092)	972 (1291)
Maximum	1453 (2157)	1122 (1561)	929 (1214)	1467 (2182)
Takeoff (50/50 Fuel Split)				
Fuel/Air Ratio	0.0238	0.0238	0.0246	0.0237
NOx Emissions Index gm/kg	13.0	16.7	15.0	15.5
SAE Smoke Number	28	27	29	27
Liner Temperature °K(°F)				
Avg Primary Zone	965 (1279)	1079 (1484)	1035 (1404)	1043 (1419)
Maximum	1168 (1644)	1374 (2014)	1364 (1996)	1280 (1846)

The evaluation of Configuration M-13 was also extended to include a more comprehensive evaluation of the effect of fuel composition on the lean stability characteristics of the Mark IV combustor. The results of this investigation are presented in Table 7-21. Data were obtained on the lean blowout fuel air ratio with Jet A, Experimental Referee Broad Specification Fuel (ERBS) and the commodity fuel. The evaluations were conducted at three different sets of inlet conditions corresponding to: 1) ground idle operation of the PW2037 i.e., the condition at which all idle performance has been obtained in this program, 2) conditions corresponding to a severe flight idle encountered by the PW2037 during descent, and 3) a more severe condition at the minimum possible air supply temperature and pressure in the test facility. The severity of the combustor inlet conditions is expressed in terms of the air loading parameter defined as:

TABLE 7-21

EFFECT OF FUEL COMPOSITION ON THE LEAN STABILITY
OF CONFIGURATION M-12 OF MARK IV COMBUSTOR

Fuel Type	JET A	ERBS	Commodity Oil
Ground Idle			
$T_{T\ in.}$ = 469°K (386°F)			
$P_{T\ in.}$ = 0.41MPa (59.7 psia)			
$W_{ab}^{T\ in.}$ = 1.48 kg/sec (3.25 lb/sec)			
Air Loading Parameter = 0.96			
Fuel Air Ratio at Lean Blowout	0.0031 0.0030	0.0040 0.0030	0.0038 0.0035
Minimum Flight Idle			
$T_{T\ in.}$ = 439°K (332°F)			
$P_{T\ in.}$ = 0.26MPa (37.6 psia)			
$W_{ab}^{T\ in.}$ = 0.95 kg/sec (2.1 lb/sec)			
Air Loading Parameter = 1.59			
Fuel Air Ratio at Lean Blowout	0.0033	0.0045	0.0050
Sub Idle			
$T_{T\ in.}$ = 343°K (160°F)			
$P_{T\ in.}$ = 0.19MPa (27.2 psia)			
$W_{ab}^{T\ in.}$ = 1.09 kg/sec (2.4 lb/sec)			
Air Loading Parameter = 4.44			
Fuel Air Ratio at Lean Blowout	0.0068	0.0096	0.0080

$$ALP = \frac{0.2318\ WAB}{P_{T\ in}^{1.8}\ V\ \exp(T_{Tin}/303)} \qquad (8)$$

where:

W_{ab} = burner airflow - kg/sec

$P_{T\ in}$ = burner inlet total pressure (atm)

V = volume of combustor - m^3

$T_{T\ in}$ = burner inlet total temperature - °K

The air loading parameter is a measure of the rate of heat release demanded of the combustor to that obtainable at the specific inlet conditions with higher magnitudes indicating more severe conditions where it is more difficult to sustain combustion. The data of Table 7-21 are consistent with this definition in that the lean blowout fuel air ratio increases with progressive increase of the air loading parameter. The test sequence had included a fourth test condition at the same inlet total pressure and temperature as the sub idle condition of Table 7-21 but at a higher airflow

where the loading parameter would have been about eight; however, the combustor would not operate stably at any reasonable fuel air ratio at that condition. The effect of fuel composition on lean stability is also evident in the data of Table 7-21 with a general trend of higher blowout fuel air ratio with increasing fuel viscosity and/or volatility. The sensitivity of the blowout fuel air ratio to fuel composition also appears to increase with increased combustor air loading.

7.5.8 Status of the Mark IV Combustor Concept

The results presented in Sections 7.4 and 7.5 provide an indication of the viability of the Mark IV combustor concept for accommodating broadened properties fuels. This concept was evolved through a process of refining and optimization of its aerothermal features while its performance was improved toward the program goals. The results of the evaluation of Configuration M-7 indicated that the liner temperatures exhibited only modest sensitivity to fuel hydrogen content. This configuration incorporated an advanced technology liner construction that required only moderate cooling flow levels relative to the reference PW2037 combustor. However, the location and intensity of the maximum temperature on the liner varied considerably between configurations implying that the dominant heat transfer mode at these locations was convective. The low power emissions characteristics of the combustor were improved with the evolution of the Mark IV concept to Configuration M-7 but remained deficient relative to the program goals. The incorporation of the advanced technology liner construction in Configuration led to the singular greatest improvement in low power emissions with the combustor meeting the program goal when operating on Jet A fuel but becoming deficient when ERBS fuel was introduced. Unburned hydrocarbon emissions at idle were high, exceeding the program goal by a factor of three. While the program goal for lean combustion stability was marginally satisfied, the high unburned hydrocarbon emissions precluded meeting the program goal for combustion efficiency at idle.

At power levels above idle the combustion efficiency did exceed the program goal of 99 percent but the performance was not indicative of the intended dual zone mode of combustion. Emissions of oxides of nitrogen and smoke, while demonstrating the anticipated decline with increasing fuel hydrogen content, were high relative to both expectations and the program goals. The combustion exit temperature distribution also indicated that combustion was being restricted to the areas near the liners of the combustor and that the gas temperature in the midspan regions, comprising the air from the secondary swirlers, was low. It was evident that the fundamental concept of using a single pipe fuel system to produce a staged fuel injection effect was not being achieved. While several variations of the single pipe fuel system were evaluated it became evident that the production of injectors with the desired spray variation characteristics would in itself require an extensive development effort beyond the scope of this program. Consequently, the final configurations evaluated were directed at demonstrating the long range potential of the Mark IV combustor. Since the single pipe fuel system as conceived at the time was incapable of supplying fuel to both the pilot and secondary zone from a single source, a staged fuel system was employed to provide this distribution artificially. When operated in this mode the high power performance was enhanced significantly with the program goals for smoke and oxides of nitrogen emissions being achieved and the combustor exit average radial temperature profile becoming close to the target profile.

SECTION 8.0

CONCLUDING REMARKS

The results of Phase II of the Broad Specification Fuel Combustion Technology Program have demonstrated that the use of Experimental Referee Broad Specification (ERBS) fuel rather than Jet A fuel can have a significant impact on the operation of conventional single stage combustors. While the PW2037 engine combustor selected as a reference for this phase was capable of achieving most of the relevant program goals while operating on ERBS fuel, increased liner temperatures caused by increased radiant heat load would be an obstacle in accommodating broadened properties fuel. Reductions in liner life of up to 15 percent are projected with the use of ERBS rather than Jet A in the PW2037 combustor.

The two advanced technology combustors evaluated in the Phase II program, as well as the reference PW2037 combustor, incorporate single pipe fuel systems which avoid stagnating fuel in nonoperational system components. This could be a major aspect in selection of a combustor concept for use with broadened properties fuels because of their potential for deteriorated thermal stability. The results of the evaluations conducted in this program indicate that both the variable geometry and the Mark IV combustor concepts have the long range potential for accommodating to use of broadened properties fuels while achieving realistic requirements for emissions, durability and operability. However, both of these advanced technology combustors will require refinement at the conceptual level and substantial additional development to evolve them to technical maturity. Furthermore, the technical risks associated with the development and use of these complex combustor concepts are large. If these advanced technology combustors were required solely for the purpose of accommodating a particular broadened properties fuel, the costs and risks involved would become major factors in a cost-benefit analysis of the acceptability of that fuel.

NOMENCLATURE

A	Flow Area cm^2 (in^2)
C_D	Discharge Coefficient
CO	Carbon Monoxide
EI	Emission Index gm/kg
F/A	Fuel to Air Ratio
g_c	Gravitational Constant m/sec^2 (ft/sec^2)
H	Humidity gm/kg
NO_x	Oxides of Nitrogen
P_S	Static Pressure MPa (psia)
P_T	Total Pressure MPa (psia)
THC	Total Unburned Hydrocarbons
T_f	Flame Temperature °K (°F)
T_T	Total Temperature °K (°F)
V	Volume m^3 (ft^3)
V_{ref}	Velocity at a Cross Section of the Burner in the Absence of Combustion m/sec (ft/sec)
W_A	Airflow kg/sec (lb/sec)
W_{AB}	Burner Airflow kg/sec (lb/sec)
W_F	Burner Fuel Flow kg/sec (lb/sec)
ηc	Combustion Efficiency

APPENDICES

APPENDIX A
COMBUSTOR AIR ADMISSION GEOMETRY

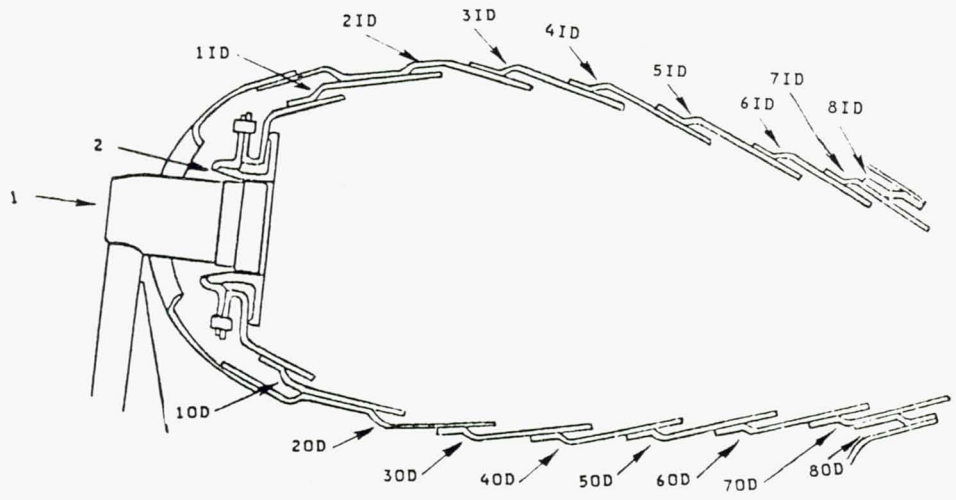

	BASE BURNER HOOD	AREA* CM^2	AREA* IN^2
1	FUEL NOZZLE	4.79	0.742
2	INSERT & DOME COOLING	2.92	0.452

*ACD

BYPASS AIR	AREA CM^2	AREA IN^2
OD TURBINE COOLING AIR	3.65	0.565
ID TURBINE COOLING AIR	5.02	0.778
ENDWALL COOLING AIR	6.04	0.936
ENDWALL SEALS AIR	5.29	0.820
OD BURNER LINER LEAKAGE	0.81	0.125
ID BURNER LINER LEAKAGE	0.81	0.125

LINER COOLING					
INNER LINER			OUTER LINER		
LOUVER	AREA CM^2	AREA IN^2	LOUVER	AREA CM^2	AREA IN^2
1 ID	2.114	.3276	1 OD	2.114	.3276
2 ID	2.960	.4588	2 OD	3.133	.4856
3 ID	2.627	.4072	3 OD	2.736	.4240
4 ID	2.114	.3276	4 OD	2.521	.3908
5 ID	1.943	.3012	5 OD	2.114	.3276
6 ID	1.788	.2772	6 OD	1.639	.2540
7 ID	2.114	.3276	7 OD	1.961	.3040
8 ID	1.678	.2600	8 OD	1.647	.2552

LOUVER NUMBER	AIR TYPE	PENTRATIONS				
		NUMBER	TYPE	SIZE CM	SIZE IN	SPACING
3 OD	DILUTION	8	SHARP EDGE	1.229D	0.484D	IN LINE
5 OD	DILUTION	8	SHARP EDGE	1.389D	0.547D	BETWEEN
3 ID	DILUTION	8	SHARP EDGE	1.229D	0.484D	IN LINE
5 ID	DILUTION	8	SHARP EDGE	1.389D	0.547D	BETWEEN

Figure A-1 Combustor Air Admission Geometry for Configuration V-1.

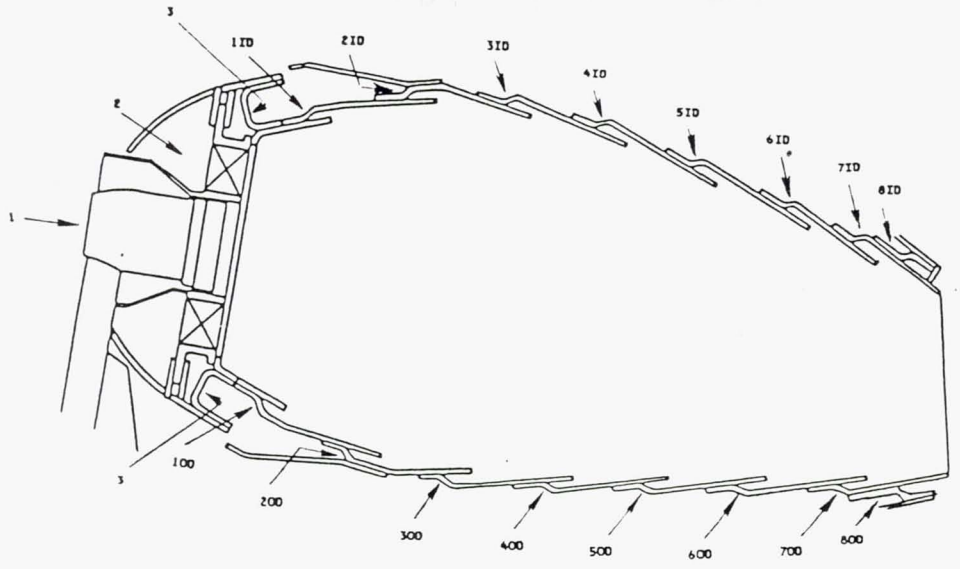

	VARIABLE GEOMETRY HOOD	AREA* CM^2	AREA* IN^2
1	FUEL NOZZLE	4.79	0.742
2	SWIRLER (VALVE OPEN)	27.12	4.212
	SWIRLER (VALVE CLOSED)	3.86	0.598
3	DOME COOLING	2.35	0.364

*ACD

BYPASS AIR	AREA CM^2	AREA IN^2
OD TURBINE COOLING AIR	3.65	0.565
ID TURBINE COOLING AIR	5.02	0.778
ENDWALL COOLING AIR	6.04	0.936
ENDWALL SEALS AIR	5.29	0.820
OD BURNER LINER LEAKAGE	0.81	0.125
ID BURNER LINER LEAKAGE	0.81	0.125

LINER COOLING					
INNER LINER			OUTER LINER		
LOUVER	AREA CM^2	AREA IN^2	LOUVER	AREA CM^2	AREA IN^2
1 ID	2.114	.3276	1 OD	2.114	.3276
2 ID	2.960	.4588	2 OD	3.133	.4856
3 ID	2.627	.4072	3 OD	2.736	.4240
4 ID	2.114	.3276	4 OD	2.521	.3908
5 ID	1.943	.3012	5 OD	2.114	.3276
6 ID	1.788	.2772	6 OD	1.639	.2540
7 ID	2.114	.3276	7 OD	1.961	.3040
8 ID	1.678	.2600	8 OD	1.647	.2552

LOUVER NUMBER	AIR TYPE	PENTRATIONS				
		NUMBER	TYPE	SIZE CM	SIZE IN	SPACING
5 OD	DILUTION	8	SHARP EDGE	1.346D	0.530D	BETWEEN
5 ID	DILUTION	8	SHARP EDGE	1.346D	0.530D	BETWEEN

Figure A-2 Combustor Air Admission Geometry for Configuration V-2, V-3, V-4.

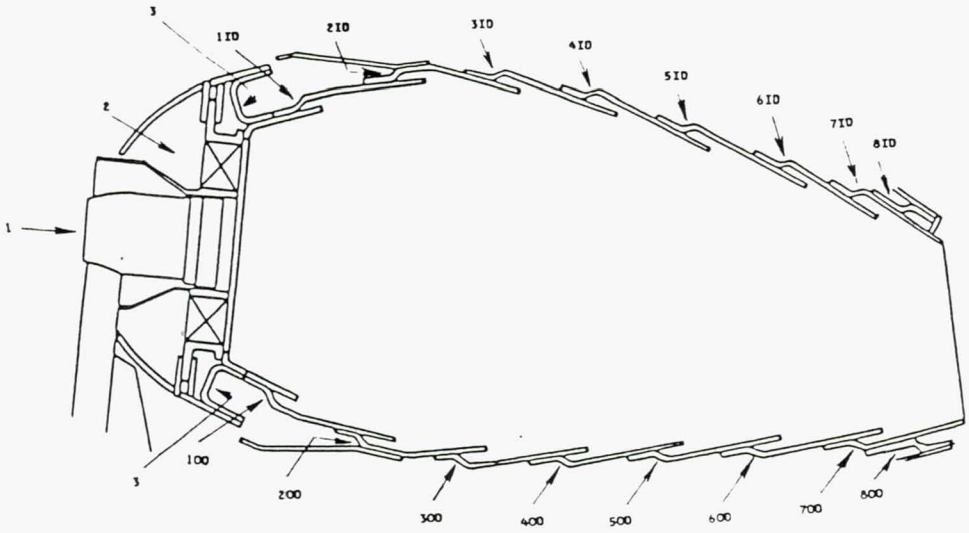

	VARIABLE GEOMETRY HOOD	AREA* CM²	AREA* IN²
1	FUEL NOZZLE	4.79	0.742
2	SWIRLER (VALVE OPEN)	27.12	4.212
	SWIRLER (VALVE CLOSED)	3.86	0.598
3	DOME COOLING	2.35	0.364

*ACD

BYPASS AIR	AREA CM²	AREA IN²
OD TURBINE COOLING AIR	3.65	0.565
ID TURBINE COOLING AIR	5.02	0.778
ENDWALL COOLING AIR	6.04	0.936
ENDWALL SEALS AIR	5.29	0.820
OD BURNER LINER LEAKAGE	0.81	0.125
ID BURNER LINER LEAKAGE	0.81	0.125

LINER COOLING					
INNER LINER			OUTER LINER		
LOUVER	AREA CM²	AREA IN²	LOUVER	AREA CM²	AREA IN²
1 ID	2.114	.3276	1 OD	2.114	.3276
2 ID	2.960	.4588	2 OD	3.133	.4856
3 ID	2.627	.4072	3 OD	2.736	.4240
4 ID	2.114	.3276	4 OD	2.521	.3908
5 ID	1.943	.3012	5 OD	2.114	.3276
6 ID	1.788	.2772	6 OD	1.639	.2540
7 ID	2.114	.3276	7 OD	1.961	.3040
8 ID	1.678	.2600	8 OD	1.647	.2552

LOUVER NUMBER	AIR TYPE	PENTRATIONS				
		NUMBER	TYPE	SIZE CM	SIZE IN	SPACING
3 OD	DILUTION	7	SHARP EDGE	1.229D	0.484D	IN LINE
3 ID	DILUTION	8	SHARP EDGE	1.229D	0.484D	IN LINE
5 ID	DILUTION	8	SHARP EDGE	1.346D	0.530D	BETWEEN

Figure A-3 Combustor Air Admission Geometry for Configuration V-5, V-5A, V-6, V-7.

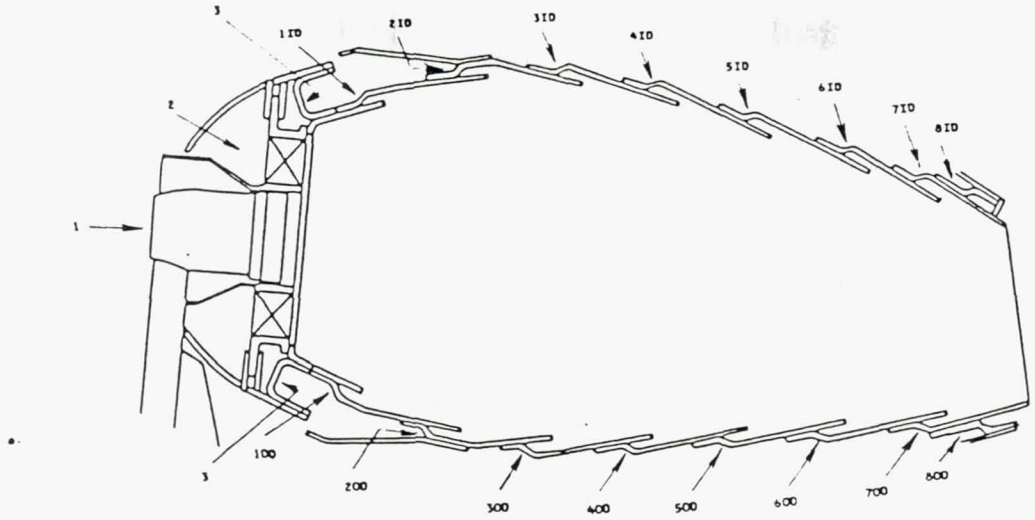

VARIABLE GEOMETRY HOOD	AREA* CM²	AREA* IN²
1 FUEL NOZZLE	4.79	0.742
2 SWIRLER (VALVE OPEN)	27.12	4.212
SWIRLER (VALVE CLOSED)	3.86	0.598
3 DOME COOLING	2.35	0.364

*ACD

BYPASS AIR	AREA CM²	AREA IN²
OD TURBINE COOLING AIR	3.65	0.565
ID TURBINE COOLING AIR	5.02	0.778
ENDWALL COOLING AIR	6.04	0.936
ENDWALL SEALS AIR	5.29	0.820
OD BURNER LINER LEAKAGE	0.81	0.125
ID BURNER LINER LEAKAGE	0.81	0.125

LINER COOLING					
INNER LINER			OUTER LINER		
LOUVER	AREA CM²	AREA IN²	LOUVER	AREA CM²	AREA IN²
1 ID	2.114	.3276	1 OD	2.114	.3276
2 ID	2.960	.4588	2 OD	3.133	.4856
3 ID	2.627	.4072	3 OD	2.736	.4240
4 ID	2.114	.3276	4 OD	2.521	.3908
5 ID	1.943	.3012	5 OD	2.114	.3276
6 ID	1.788	.2772	6 OD	1.639	.2540
7 ID	2.114	.3276	7 OD	1.961	.3040
8 ID	1.678	.2600	8 OD	1.647	.2552

LOUVER NUMBER	AIR TYPE	PENTRATIONS				
		NUMBER	TYPE	SIZE CM	SIZE IN	SPACING
2 OD	DILUTION	7	SHARP EDGE	1.229D	0.484D	IN LINE
2 ID	DILUTION	8	SHARP EDGE	1.229D	0.484D	IN LINE
5 ID	DILUTION	8	SHARP EDGE	1.346D	0.530D	BETWEEN

Figure A-4 Combustor Air Admission Geometry for Configuration V-8.

C-3

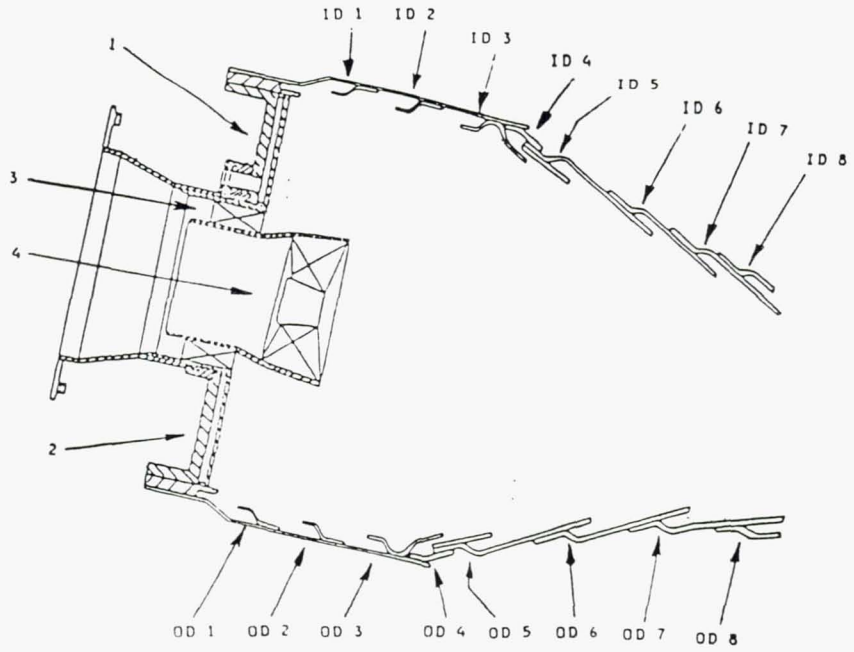

	FRONT END FLOW	AREA* CM^2	AREA* IN^2
1	FUEL NOZZLE	1.68	0.261
2	BULKHEAD COOLING	4.17	0.646
3	PRIMARY SWIRLER	13.68	2.121
4	SECONDARY SWIRLER	31.63	4.902

*ACD

BYPASS AIR	AREA CM^2	AREA IN^2
OD TURBINE COOLING AIR	13.18	2.043
ID TURBINE COOLING AIR	14.28	2.124
ENDWALL COOLING AIR	9.05	1.403
ENDWALL BYPASS AIR	13.59	2.107

LINER COOLING					
INNER LINER			OUTER LINER		
LOUVER	AREA CM^2	AREA IN^2	LOUVER	AREA CM^2	AREA IN^2
1 ID	1.148	.1780	1 OD	1.148	.1780
2 ID	1.148	.1780	2 OD	1.148	.1780
3 ID	1.148	.1780	3 OD	1.148	.1780
4 ID	1.148	.1780	4 OD	1.148	.1780
5 ID	1.595	.2473	5 OD	1.595	.2473
6 ID	1.379	.2138	6 OD	1.379	.2138
7 ID	1.265	.1961	7 OD	1.265	.1961
8 ID	0.712	.1103	8 OD	0.712	.1103

Figure A-5 Combustor Air Admission Geometry for M-1.

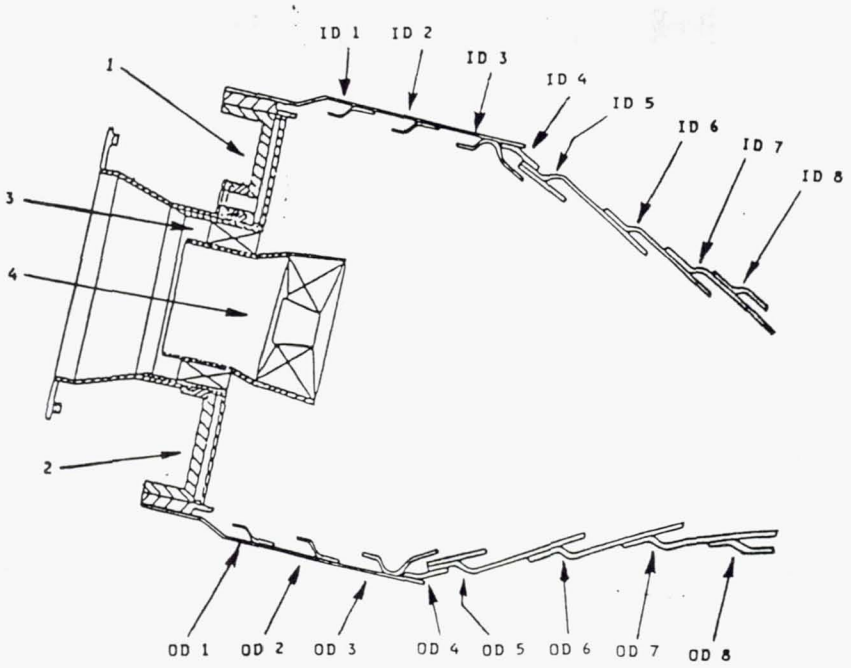

	FRONT END FLOW	AREA* CM²	AREA* IN²
1	FUEL NOZZLE	2.71	0.420
2	BULKHEAD COOLING	4.17	0.646
3	PRIMARY SWIRLER	13.68	2.121
4	SECONDARY SWIRLER	31.63	4.902

*ACD

BYPASS AIR	AREA CM²	AREA IN²
OD TURBINE COOLING AIR	13.18	2.043
ID TURBINE COOLING AIR	14.28	2.124
ENDWALL COOLING AIR	9.05	1.403
ENDWALL BYPASS AIR	13.59	2.107

LINER COOLING					
INNER LINER			OUTER LINER		
LOUVER	AREA CM²	AREA IN²	LOUVER	AREA CM²	AREA IN²
1 ID	1.148	.1780	1 OD	1.148	.1780
2 ID	1.148	.1780	2 OD	1.148	.1780
3 ID	1.148	.1780	3 OD	1.148	.1780
4 ID	1.148	.1780	4 OD	1.148	.1780
5 ID	1.595	.2473	5 OD	1.595	.2473
6 ID	1.379	.2138	6 OD	1.379	.2138
7 ID	1.265	.1961	7 OD	1.265	.1961
8 ID	0.712	.1103	8 OD	0.712	.1103

Figure A-6 Combustor Air Admission Geometry for Configuration M-2.

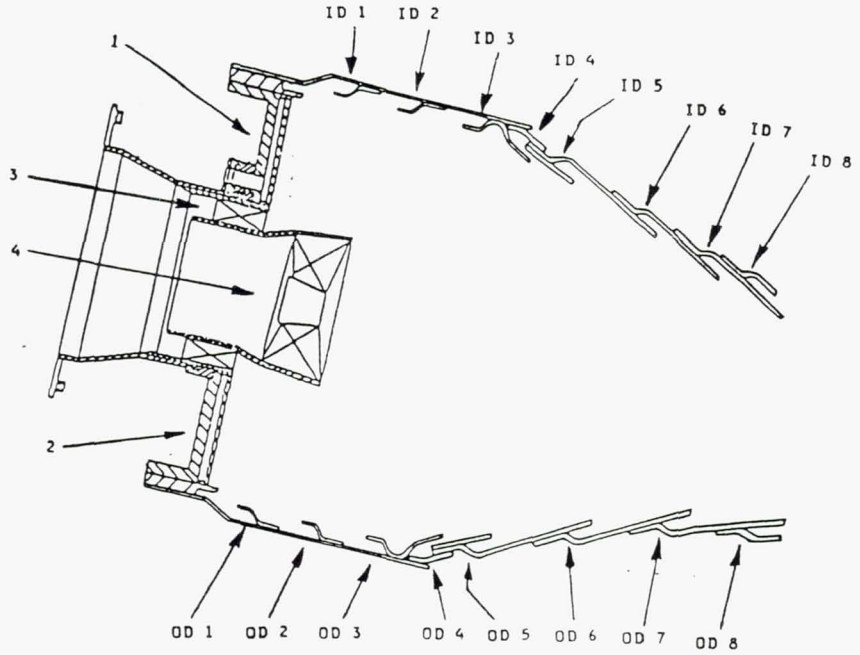

FRONT END FLOW	AREA* CM²	AREA* IN²
1 FUEL NOZZLE	2.71	0.420
2 BULKHEAD COOLING	2.10	0.325
3 PRIMARY SWIRLER	13.01	2.016
4 SECONDARY SWIRLER	29.69	4.602

*ACD

BYPASS AIR	AREA CM²	AREA IN²
OD TURBINE COOLING AIR	13.18	2.043
ID TURBINE COOLING AIR	14.28	2.124
ENDWALL COOLING AIR	9.05	1.403
ENDWALL BYPASS AIR	13.59	2.107

LINER COOLING					
INNER LINER			OUTER LINER		
LOUVER	AREA CM²	AREA IN²	LOUVER	AREA CM²	AREA IN²
1 ID	1.148	.1780	1 OD	1.148	.1780
2 ID	1.148	.1780	2 OD	1.148	.1780
3 ID	1.148	.1780	3 OD	1.148	.1780
4 ID	1.148	.1780	4 OD	1.148	.1780
5 ID	1.595	.2473	5 OD	1.595	.2473
6 ID	1.379	.2138	6 OD	1.379	.2138
7 ID	1.265	.1961	7 OD	1.265	.1961
8 ID	0.712	.1103	8 OD	0.712	.1103

Figure A-7 Combustor Air Admission Geometry for Configuration M-4.

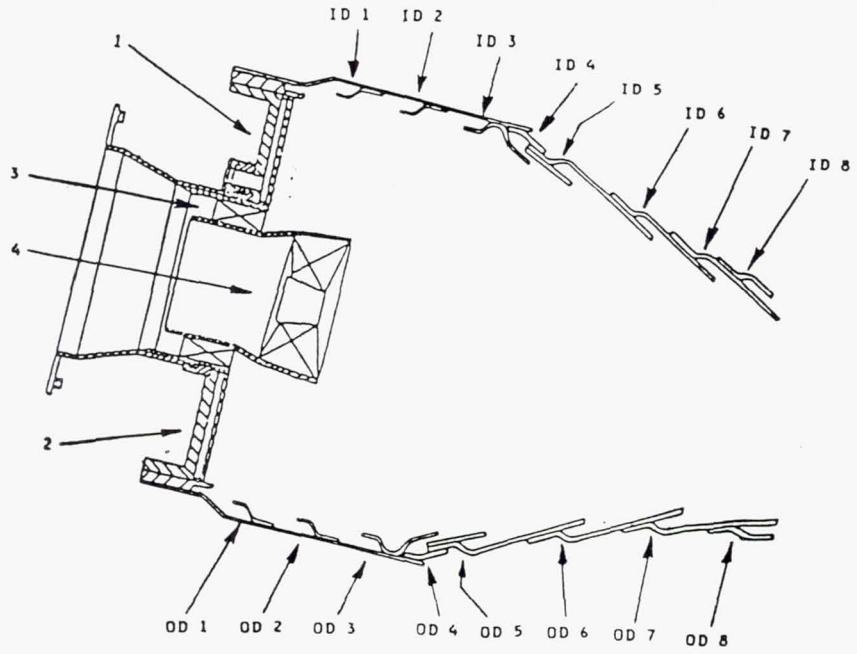

	FRONT END FLOW	AREA* CM^2	AREA* IN^2
1	FUEL NOZZLE	2.71	0.420
2	BULKHEAD COOLING	2.10	0.325
3	PRIMARY SWIRLER	9.19	1.425
4	SECONDARY SWIRLER	29.69	4.602

*ACD

BYPASS AIR	AREA CM^2	AREA IN^2
OD TURBINE COOLING AIR	13.18	2.043
ID TURBINE COOLING AIR	14.28	2.124
ENDWALL COOLING AIR	9.05	1.403
ENDWALL BYPASS AIR	13.59	2.107

LINER COOLING					
INNER LINER			OUTER LINER		
LOUVER	AREA CM^2	AREA IN^2	LOUVER	AREA CM^2	AREA IN^2
1 ID	1.148	.1780	1 OD	1.148	.1780
2 ID	1.148	.1780	2 OD	1.148	.1780
3 ID	1.148	.1780	3 OD	1.148	.1780
4 ID	1.148	.1780	4 OD	1.148	.1780
5 ID	1.595	.2473	5 OD	1.595	.2473
6 ID	1.379	.2138	6 OD	1.379	.2138
7 ID	1.265	.1961	7 OD	1.265	.1961
8 ID	0.712	.1103	8 OD	0.712	.1103

Figure A-8 Combustor Air Admission Geometry for Configuration M-5.

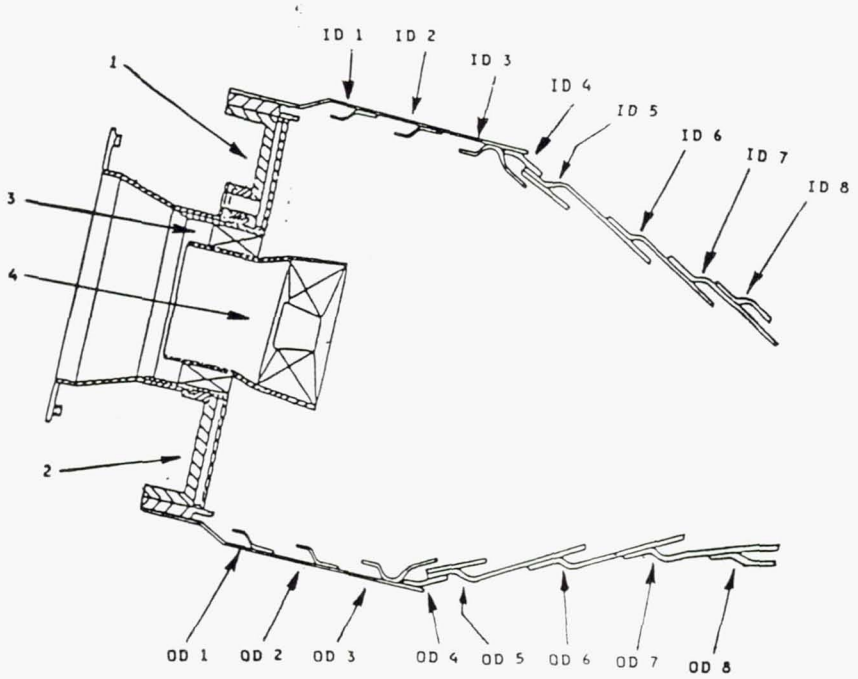

	FRONT END FLOW	AREA* CM²	AREA* IN²
1	FUEL NOZZLE	2.71	0.420
2	BULKHEAD COOLING	2.10	0.325
3	PRIMARY SWIRLER	9.19	1.425
4	SECONDARY SWIRLER	34.32	5.319

*ACD

BYPASS AIR	AREA CM²	AREA IN²
OD TURBINE COOLING AIR	13.18	2.043
ID TURBINE COOLING AIR	14.28	2.124
ENDWALL COOLING AIR	9.05	1.403
ENDWALL BYPASS AIR	13.59	2.107

LINER COOLING					
INNER LINER			OUTER LINER		
LOUVER	AREA CM²	AREA IN²	LOUVER	AREA CM²	AREA IN²
1 ID	1.148	.1780	1 OD	1.148	.1780
2 ID	1.148	.1780	2 OD	1.148	.1780
3 ID	1.148	.1780	3 OD	1.148	.1780
4 ID	1.148	.1780	4 OD	1.148	.1780
5 ID	1.595	.2473	5 OD	1.595	.2473
6 ID	1.379	.2138	6 OD	1.379	.2138
7 ID	1.265	.1961	7 OD	1.265	.1961
8 ID	0.712	.1103	8 OD	0.712	.1103

Figure A-9 Combustor Air Admission Geometry for Configuration M-6.

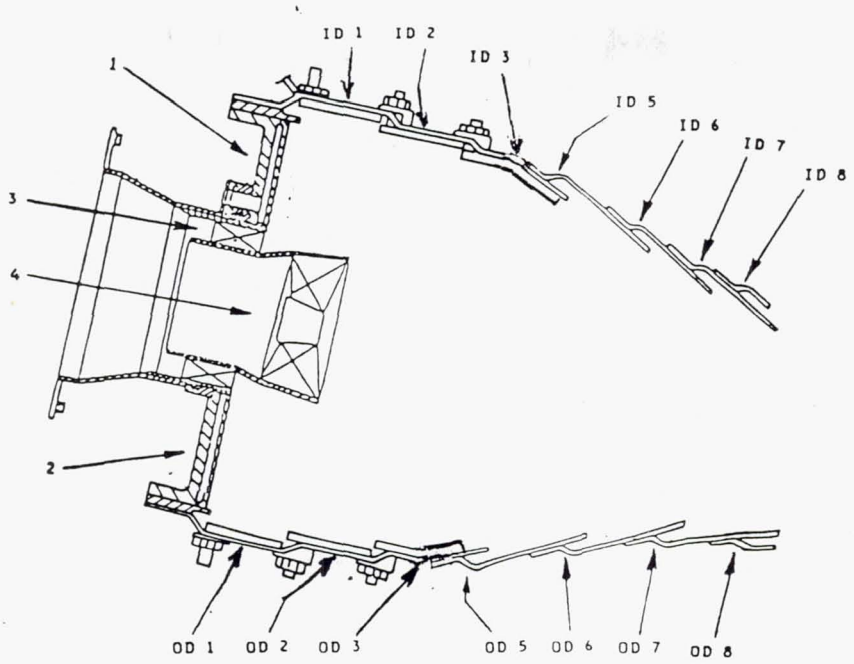

FRONT END FLOW	AREA* CM²	AREA* IN²
1 FUEL NOZZLE	2.71	0.420
2 BULKHEAD COOLING	2.10	0.325
3 PRIMARY SWIRLER	9.19	1.425
4 SECONDARY SWIRLER	29.69	4.602

*ACD

BYPASS AIR	AREA CM²	AREA IN²
OD TURBINE COOLING AIR	13.18	2.043
ID TURBINE COOLING AIR	14.28	2.124
ENDWALL COOLING AIR	9.05	1.403
ENDWALL BYPASS AIR	13.59	2.107

LINER COOLING					
INNER LINER			OUTER LINER		
LOUVER	AREA CM²	AREA IN²	LOUVER	AREA CM²	AREA IN²
1 ID*	0.92	.139	1 OD*	0.92	.139
2 ID*	0.92	.139	2 OD*	0.92	.139
3 ID*	0.92	.139	3 OD*	0.92	.139
5 ID	1.595	.2473	5 OD	1.595	.2473
6 ID	1.379	.2138	6 OD	1.379	.2138
7 ID	1.265	.1961	7 OD	1.265	.1961
8 ID	0.712	.1103	8 OD	0.712	.1103

*ACD

Figure A-10 Combustor Air Admission Geometry for Configurations M-7 and M-8.

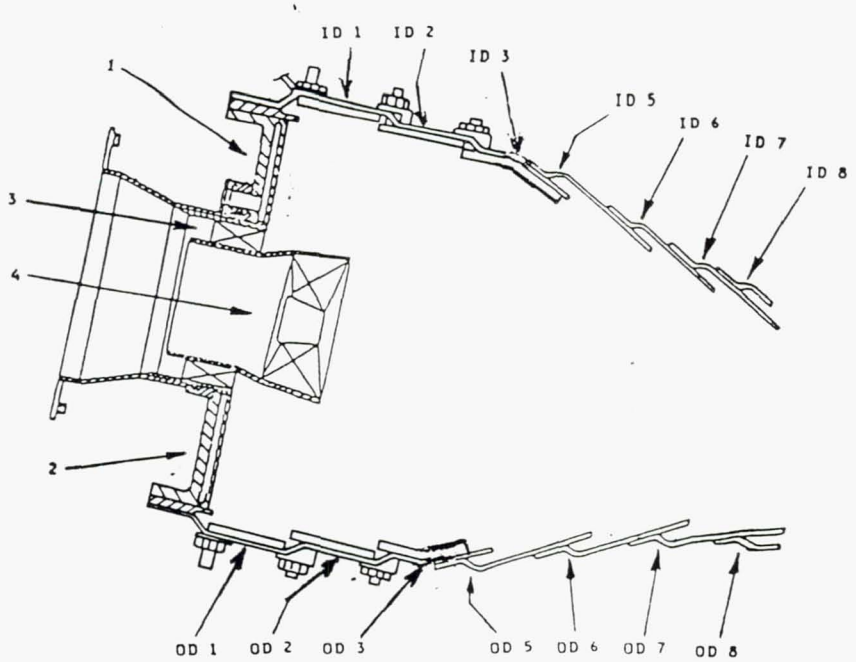

	FRONT END FLOW	AREA* CM²	AREA* IN²
1	FUEL NOZZLE	2.94	0.462
2	BULKHEAD COOLING	2.10	0.325
3	PRIMARY SWIRLER	9.19	1.425
4	SECONDARY SWIRLER	32.30	5.030

*ACD

BYPASS AIR	AREA CM²	AREA IN²
OD TURBINE COOLING AIR	13.18	2.043
ID TURBINE COOLING AIR	14.28	2.124
ENDWALL COOLING AIR	9.05	1.403
ENDWALL BYPASS AIR	13.59	2.107

LINER COOLING					
INNER LINER			OUTER LINER		
LOUVER	AREA CM²	AREA IN²	LOUVER	AREA CM²	AREA IN²
1 ID*	0.92	.139	1 OD*	0.92	.139
2 ID*	0.92	.139	2 OD*	0.92	.139
3 ID*	0.92	.139	3 OD*	0.92	.139
5 ID	1.595	.2473	5 OD	1.595	.2473
6 ID	1.379	.2138	6 OD	1.379	.2138
7 ID	1.265	.1961	7 OD	1.265	.1961
8 ID	0.712	.1103	8 OD	0.712	.1103

*ACD

Figure A-11 Combustor Air Admission Geometry for Configuration M-9.

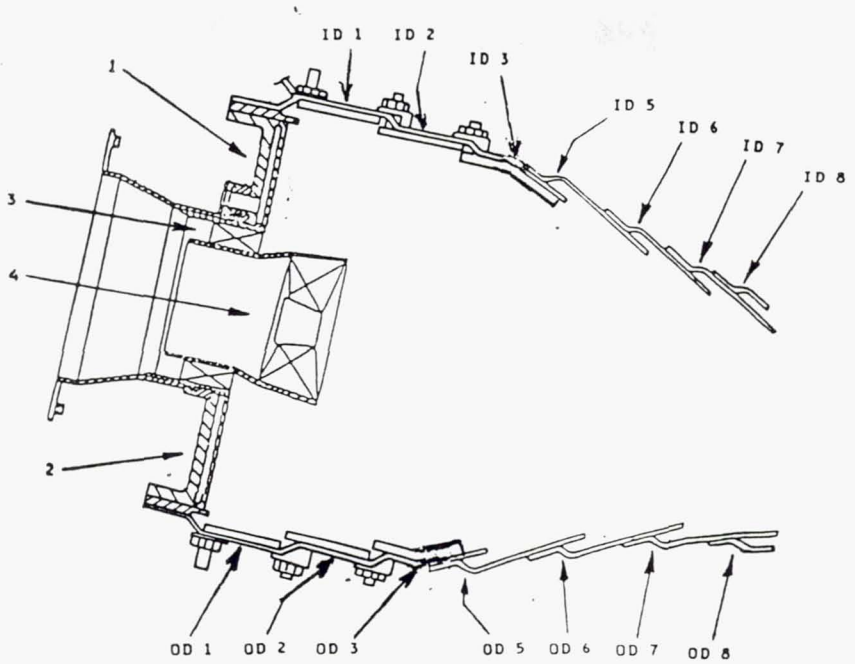

FRONT END FLOW		AREA* CM²	AREA* IN²
1	FUEL NOZZLE	2.71	0.420
2	BULKHEAD COOLING	2.10	0.325
3	PRIMARY SWIRLER	9.19	1.425
4	SECONDARY SWIRLER	32.30	5.030

*ACD

BYPASS AIR	AREA CM²	AREA IN²
OD TURBINE COOLING AIR	13.18	2.043
ID TURBINE COOLING AIR	14.28	2.124
ENDWALL COOLING AIR	9.05	1.403
ENDWALL BYPASS AIR	13.59	2.107

LINER COOLING					
INNER LINER			OUTER LINER		
LOUVER	AREA CM²	AREA IN²	LOUVER	AREA CM²	AREA IN²
1 ID*	0.92	.139	1 OD*	0.92	.139
2 ID*	0.92	.139	2 OD*	0.92	.139
3 ID*	0.92	.139	3 OD*	0.92	.139
5 ID	1.595	.2473	5 OD	1.595	.2473
6 ID	1.379	.2138	6 OD	1.379	.2138
7 ID	1.265	.1961	7 OD	1.265	.1961
8 ID	0.712	.1103	8 OD	0.712	.1103

*ACD

Figure A-12 Combustor Air Admission Geometry for Configuration M-10.

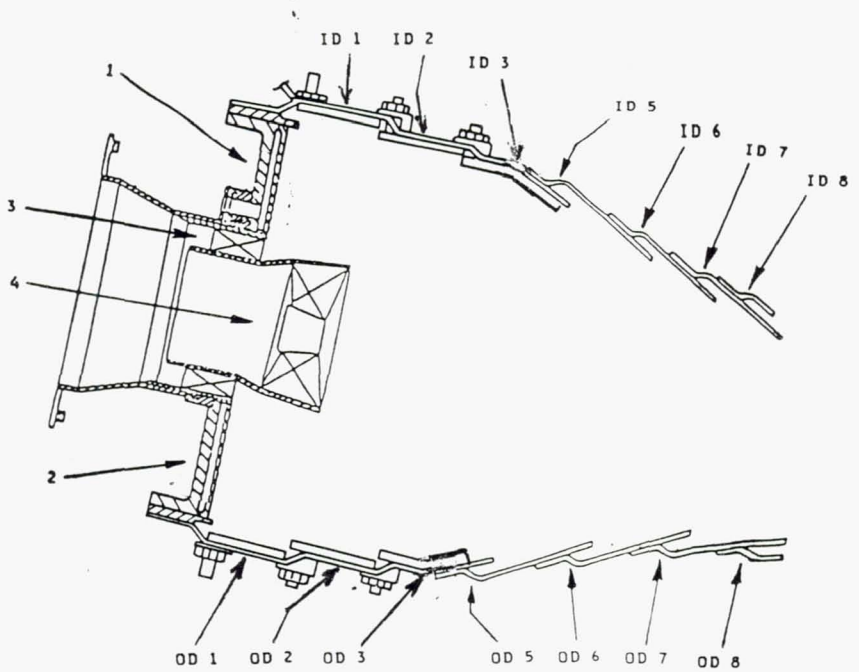

	FRONT END FLOW	AREA* CM²	AREA* IN²
1	FUEL NOZZLE	1.35	0.210
2	BULKHEAD COOLING	2.10	0.325
3	PRIMARY SWIRLER	9.19	1.425
4	SECONDARY SWIRLER	29.40	4.570

*ACD

BYPASS AIR	AREA CM²	AREA IN²
OD TURBINE COOLING AIR	13.18	2.043
ID TURBINE COOLING AIR	14.28	2.124
ENDWALL COOLING AIR	9.05	1.403
ENDWALL BYPASS AIR	13.59	2.107

LINER COOLING					
INNER LINER			OUTER LINER		
LOUVER	AREA CM²	AREA IN²	LOUVER	AREA CM²	AREA IN²
1 ID*	0.92	.139	1 OD*	0.92	.139
2 ID*	0.92	.139	2 OD*	0.92	.139
3 ID*	0.92	.139	3 OD*	0.92	.139
5 ID	1.595	.2473	5 OD	1.595	.2473
6 ID	1.379	.2138	6 OD	1.379	.2138
7 ID	1.265	.1961	7 OD	1.265	.1961
8 ID	0.712	.1103	8 OD	0.712	.1103

*ACD

Figure A-13 Combustor Air Admission Geometry for Configurations M-11 and M-12.

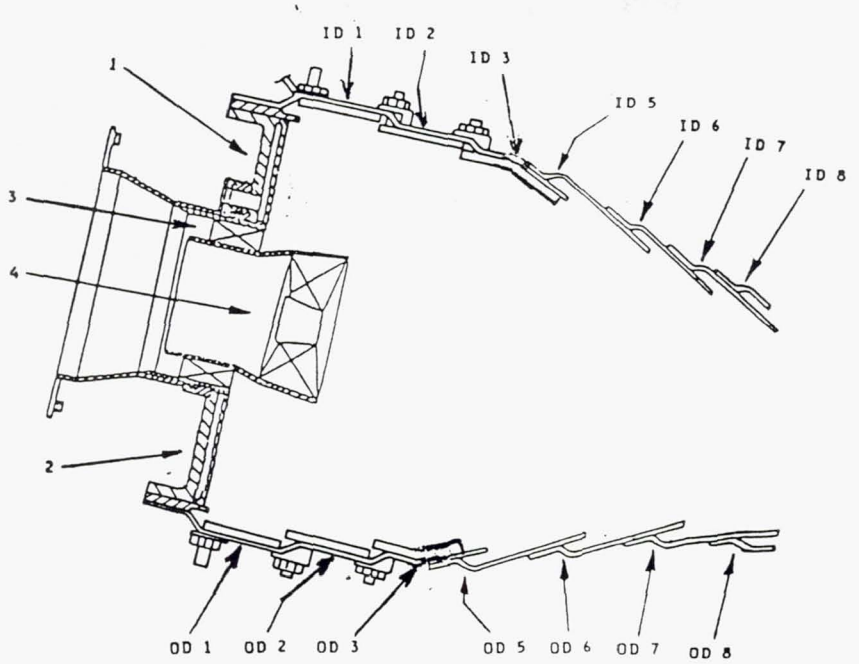

	FRONT END FLOW	AREA* CM²	AREA* IN²
1	FUEL NOZZLE	1.35	0.210
2	BULKHEAD COOLING	2.10	0.325
3	PRIMARY SWIRLER	9.19	1.425
4	SECONDARY SWIRLER	26.71	4.140

*ACD

BYPASS AIR	AREA CM²	AREA IN²
OD TURBINE COOLING AIR	13.18	2.043
ID TURBINE COOLING AIR	14.28	2.124
ENDWALL COOLING AIR	9.05	1.403
ENDWALL BYPASS AIR	13.59	2.107

LINER COOLING					
INNER LINER			OUTER LINER		
LOUVER	AREA CM²	AREA IN²	LOUVER	AREA CM²	AREA IN²
1 ID*	0.92	.139	1 OD*	0.92	.139
2 ID*	0.92	.139	2 OD*	0.92	.139
3 ID*	0.92	.139	3 OD*	0.92	.139
5 ID	1.595	.2473	5 OD	1.595	.2473
6 ID	1.379	.2138	6 OD	1.379	.2138
7 ID	1.265	.1961	7 OD	1.265	.1961
8 ID	0.712	.1103	8 OD	0.712	.1103

*ACD

Figure A-14 Combustor Air Admission Geometry for Configuration M-13.

APPENDIX B
FUEL INJECTOR SPRAY EVALUATION

Fuel atomization and spray characterization tests were conducted on the three aerated injectors that were used in the baseline PW2037 (V-1) and the variable geometry combustor configurations V-2 to V-8 that were evaluated during this program. Figure B-1 is a schematic diagram of the air and fuel supply systems in the test facility. The test injector was installed in a plenum box, and ambient temperature air was supplied to the plenum to provide airflow through the aerating air passages of the injector. The supply pressure in the plenum was adjusted to match the air velocity occurring in these passages at the appropriate engine operating condition. For injector evaluations at the cold start condition, the fuel was cooled with a liquid nitrogen bath cooler.

Each injector was tested on three fuels: Jet A, Experimental Referee Broad Specification Fuel (ERBS) and a No. 2 Diesel fuel. The properties of these fuels, as determined by laboratory analysis, are listed in Table B-1.

While not used in the remainder of the program, the diesel fuel had been selected as the third test fuel because it had a viscosity level considerably above ERBS which would provide a reasonably wide range of atomization properties. The No. 2 commodity fuel used in some of the high pressure combustor tests had not yet been procured when these tests were conducted.

TABLE B-1
PROPERTIES OF TEST FUELS FOR FUEL INJECTOR EVALUATION

	Fuel		
	Jet A	ERBS	Diesel
Specific Gravity 289/289°K (60/60°F)	0.8109	0.8408	0.8509
Viscosity - centistokes			
at 299°K (80°F)	1.67	2.16	3.30
at 250°K (-10°F)	5.32	8.54	--
at 269°K (25°F)	--	--	7.86
Surface Tension - dynes/cm			
at 297°K (75°F)	28.9	29.4	30.7
Aromatic Content - % volume	19.7	31.9	39.4
Hydrogen Content - % weight	13.77	12.92	12.92

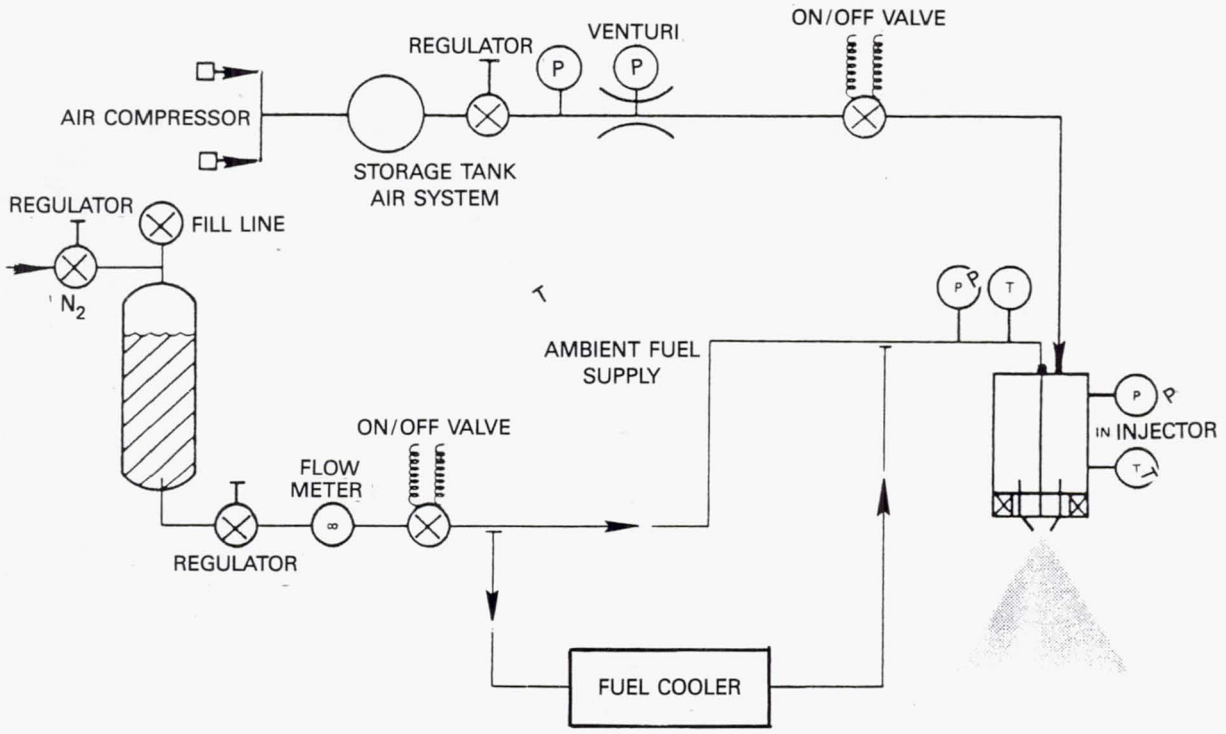

Figure B-1 Schematic Diagram of Air and Fuel Supply to Fuel Injector Test Facility

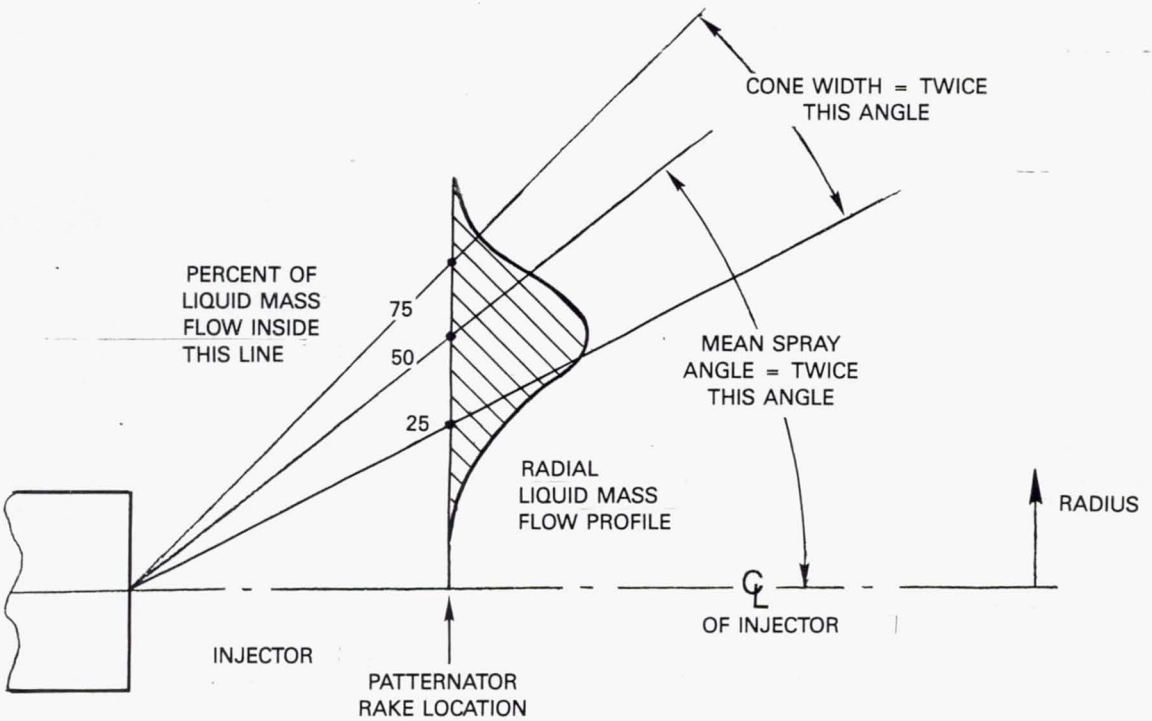

Figure B-2 Definition of Spray Angles

The tests were conducted at simulated idle, takeoff and cold starting conditions of the PW2037 engine, the latter with 250°K (-10°F) fuel temperature. Data were obtained at aerating air velocities that corresponded to the air pressure drop across the fuel injector with the variable geometry valves on the combustor in the closed position for the simulated idle and cold starting conditions. At the simulated takeoff condition, this velocity was adjusted to be representative of operation of the variable geometry combustor with the hood valves open. Fuel injector B was the prototype of the injector that eventually became the Bill of Material for the PW2037 engine combustor. This injector was also evaluated with aerating air velocities corresponding to the pressure drop characteristics of the fixed geometry PW2037 type combustor to support evaluation of the results of the test of combustor configuration V-1.

The injector evaluation consisted of acquisition of data on the droplet size distribution, spray angle and spray quality. Spray angle data was obtained with a twenty tube patternator rake positioned 7.9 cm (3.125 inches) downstream of the injector face. In the case of Injector A, which had a wider spray angle, patternator data was also obtained with the rake 5.4 cm (2.125 inches) from the nozzle face. As shown on Figure B -2, two parameters of interest were obtained from the patternator data:

Mean Spray Angle - the angle including 50 percent of the total volume flow of the spray as measured from the injector centerline.

Spray Band Width - the double angle between rays subtending 25 percent and 75 percent of the total volume flow of the spray.

Droplet size distribution in the spray was obtained with a Malvern particle size analyzer with the laser beam intersecting the spray at a plane 4.1 cm (1.625 inches) from the injector face. Two characteristic drop sizes are of interest:

Sauter Mean Diameter - the single droplet size with the same surface area to volume ratio as the entire spray.

Peak Density Diameter - the droplet size with the greatest mass fraction of the spray.

Droplet size distribution may be characterized by the Rosin - Rammler distribution function:

$$R = \exp(-ax)^n$$

where R is the fraction of the spray having droplet sizes greater than X and a and n are constants. The exponent n is a measure of the uniformity of droplet distribution with higher values of n being indicative of greater uniformity.

The two spray angle parameter and two droplet sizes defined above as well as the value of the exponent giving the best fit of the experimental data to the Roxin - Rammler distribution function are listed on Tables B-2 and B-3 for each combination of injector type, fuel and simulated engine operating conditions tested.

TABLE B-2
RESULTS OF FUEL INJECTOR SPRAY EVALUATION
AT VARIABLE GEOMETRY COMBUSTOR PRESSURE DROPS

	Injector A			Injector B			Injector C		
Fuel	Jet A	ERBS	No. 2	Jet A	ERBS	No. 2	Jet A	ERBS	No. 2
CONE ANGLE (1)									
Cold Start	51.4	55.8	63.2	48.2	52.3	38.2	54.6	58.4	55.7
Idle	84.8	78.7	78.4	48.4	45.9	48.9	49.3	49.6	53.3
Takeoff	86.7	86.3	85.6	82.1	82.4	82.8	52.9	51.7	54.8
CONE WIDTH (2)									
Cold Start	32.0	23.7	18.6	19.3	20.4	15.0	13.8	21.6	16.0
Idle	9.8	23.2	23.3	19.1	19.3	19.8	16.0	17.9	19.3
Takeoff	9.1	8.2	8.9	12.7	12.4	12.0	16.0	16.1	18.7
SAUTER MEAN DIAMETER									
Cold Start	106.8	109.0	107.8	41.3	46.0	45.8	20.9	25.1	25.2
Idle	36.4	45.0	48.7	30.6	32.1	30.2	9.5	12.9	14.8
Takeoff	36.6	41.0	44.3	44.3	49.8	52.5	---	8.0	11.9
PEAK DENSITY DROPLET SIZE(3)									
Cold Start	161.0	173.7	166.5	65.0	65.3	70.0	40.6	47.8	50.3
Idle	86.0	89.5	115.5	46.0	49.0	45.0	30.0	34.5	28.3
Takeoff	98.0	119.0	105.0	105.0	102.0	100.0	<1.0	14.5	23.0
ROSIN - RAMMLER EXPONENT									
Cold Start	2.45	2.23	2.40	2.30	2.75	2.40	1.84	1.88	1.80
Idle	1.60	1.80	1.60	2.47	2.40	2.50	1.40	1.50	1.87
Takeoff	1.50	1.45	1.60	1.60	1.80	1.85	1.50	1.95	2.00

NOTE: (1) Total included angle.
(2) 50 percent of droplets in this angle.
(3) Droplet size with greatest number of droplets.

TABLE B-3
RESULTS OF FUEL INJECTOR SPRAY EVALUATION
INJECTOR B
EFFECT OF AIRSIDE PRESSURE DROP SCHEDULE

	FIXED GEOMETRY			VARIABLE GEOMETRY		
Fuel	Jet A	ERBS	No. 2	Jet A	ERBS	No. 2
CONE ANGLE (1)						
Cold Start	52.4	50.2	43.4	48.2	52.3	38.2
Idle	50.4	53.8	54.0	48.4	45.9	48.9
Takeoff	61.4	61.4	60.9	82.1	82.4	82.8
CONE WIDTH (2)						
Cold Start	18.0	17.8	32.6	19.3	20.4	15.0
Idle	21.7	21.2	20.2	19.1	19.3	19.8
Takeoff	11.9	12.5	12.3	12.7	12.4	12.0
SAUTER MEAN DIAMETER						
Cold Start	48.1	47.7	47.5	41.3	46.0	45.8
Idle	32.3	32.7	34.5	30.6	32.1	30.2
Takeoff	20.2	20.5	23.5	44.3	49.8	52.5
PEAK DENSITY DROPLET SIZE(3)						
Cold Start	73.3	67.3	71.3	65.0	65.3	70.0
Idle	50.3	51.0	53.5	46.0	49.0	45.0
Takeoff	79.5	81.0	85.7	105.0	102.0	100.0
ROSIN - RAMMLER EXPONENT						
Cold Start	2.40	2.73	2.47	2.30	2.75	2.40
Idle	2.37	2.33	2.35	2.47	2.40	2.50
Takeoff	1.30	1.30	1.37	1.60	1.80	1.85

NOTE: (1) Total included angle.
(2) 50 percent of droplets in this angle.
(3) Droplet size with greatest number of droplets.

APPENDIX C
TABULATED TEST DATA

OPERATING CONDITION	INLET PRES MPA	INLET TEMP °K	BURNER AIR KG/SEC	METER F/A RATIO	FUEL TYPE	FUEL TEMP °K	CARBON BAL F/A RATIO	CO2 %	SPEC HUMID G/KG	CORRECTED EMISSIONS — TEST MATRIX — CO EI G/KG	THC EI G/KG	NOX EI G/KG	— ENGINE TABLE — CO EI G/KG	THC EI G/KG	NOX EI G/KG	CORR COMB EFFIC	SAE SMOKE #
*********	*****	*****	******	******	*****	****	******	****	*****	******	******	******	******	******	******	******	*****
IDLE	0.443	478.4	1.856	0.0108	JET-A	302.	0.0134	2.73	1.05	10.32	0.60	4.86	10.32	0.60	4.86	99.70	32.5
IDLE	0.446	478.8	1.840	0.0139	JET-A	301.	0.0169	3.42	1.86	11.31	0.73	4.70	11.31	0.73	4.70	99.67	0.0
IDLE	0.441	478.0	1.856	0.0089	JET-A	304.	0.0112	2.29	0.73	10.92	1.30	4.48	10.92	1.30	4.48	99.61	0.0
IDLE	0.444	478.0	1.844	0.0108	ERBS	304.	0.0136	2.76	0.96	13.56	0.65	4.48	13.56	0.65	4.48	99.62	44.8
IDLE	0.445	478.0	1.839	0.0136	ERBS	301.	0.0166	3.35	1.61	15.14	0.89	4.63	15.14	0.89	4.63	99.56	0.0
IDLE	0.442	478.0	1.848	0.0091	ERBS	306.	0.0115	2.33	0.68	14.59	1.50	4.30	14.59	1.50	4.30	99.50	0.0
IDLE	0.426	478.2	2.179	0.0110	ERBS	301.	0.0138	2.80	1.50	14.70	0.45	4.70	14.70	0.45	4.70	99.60	0.0
IDLE	0.428	478.1	1.848	0.0113	11.8%	303.	0.0140	2.84	1.00	16.89	0.83	4.73	16.89	0.83	4.73	99.50	46.6
IDLE	0.430	478.5	1.860	0.0092	11.8%	304.	0.0114	2.32	0.67	16.95	2.02	4.44	16.95	2.02	4.44	99.36	0.0
IDLE	0.429	478.3	1.853	0.0114	COMM	304.	0.0144	2.91	0.94	15.67	0.88	4.88	15.67	0.88	4.88	99.53	49.4
IDLE	0.430	478.2	1.850	0.0142	COMM	304.	0.0175	3.52	1.62	16.00	1.22	5.00	16.00	1.22	5.00	99.48	0.0
IDLE	0.420	478.5	1.854	0.0096	COMM	305.	0.0121	2.45	0.67	15.90	1.49	4.86	15.90	1.49	4.86	99.44	0.0
APPROACH	1.074	601.9	3.767	0.0169	JET-A	304.	0.0207	4.20	1.18	2.44	0.02	8.77	2.44	0.02	8.77	99.94	37.8
APPROACH	1.074	603.1	3.757	0.0174	ERBS	304.	0.0210	4.24	1.16	2.49	0.02	8.84	2.49	0.02	8.84	99.94	37.6
CRUISE	1.440	745.6	4.769	0.0193	JET-A	301.	0.0220	4.45	0.96	0.73	0.11	15.69	0.73	0.11	15.69	99.97	41.0
CRUISE	1.439	746.3	4.759	0.0200	ERBS	302.	0.0215	4.36	0.99	0.82	0.01	16.36	0.82	0.01	16.36	99.98	48.8
CRUISE	1.438	746.8	4.758	0.0197	11.8%	302.	0.0210	4.25	1.00	0.86	0.01	17.67	0.86	0.01	17.67	99.98	44.3
CRUISE	1.442	745.4	4.763	0.0203	COMM	300.	0.0211	4.27	1.00	0.73	0.04	17.85	0.73	0.04	17.85	99.98	38.1
CLIMB	2.214	756.3	7.242	0.0199	JET-A	302.	0.0234	4.74	0.73	0.80	0.01	14.96	0.51	0.00	18.72	99.99	47.8
CLIMB	2.213	757.2	7.232	0.0204	ERBS	302.	0.0240	4.85	0.71	0.84	0.01	14.77	0.54	0.01	18.47	99.99	47.6
TAKEOFF	2.281	784.9	7.180	0.0193	JET-A	303.	0.0233	4.71	0.74	0.64	0.00	17.44	0.36	0.00	23.37	99.99	34.6
TAKEOFF	2.294	789.5	7.103	0.0199	ERBS	303.	0.0244	4.94	0.76	0.62	0.0	17.70	0.35	0.0	23.72	99.99	20.5
TAKEOFF	2.262	788.3	7.112	0.0179	ERBS	303.	0.0222	4.49	0.75	0.63	0.0	19.08	0.35	0.0	25.58	99.99	0.0
TAKEOFF	2.278	789.2	7.118	0.0159	ERBS	304.	0.0200	4.06	0.74	0.59	0.0	21.95	0.33	0.0	29.42	99.99	0.0
TAKEOFF	2.265	791.7	7.136	0.0205	11.8%	302.	0.0242	4.88	0.76	0.61	0.00	18.82	0.34	0.00	25.22	99.99	32.8
TAKEOFF	2.266	792.3	7.123	0.0203	COMM	302.	0.0237	4.79	0.75	0.55	0.00	18.59	0.31	0.00	24.91	99.99	22.8
TAKEOFF	2.280	787.7	6.434	0.0194	ERBS	304.	0.0240	4.85	0.81	0.50	0.0	18.77	0.28	0.0	25.16	99.99	0.0
IDLE	0.431	478.8	1.867	0.0109	JET-A	364.	0.0134	2.72	1.10	9.20	0.36	5.47	9.20	0.36	5.47	99.75	9.1
IDLE	0.434	477.7	1.867	0.0103	ERBS	367.	0.0124	2.51	0.89	11.52	0.40	5.50	11.52	0.40	5.50	99.69	16.0
IDLE	0.425	477.5	1.865	0.0082	ERBS	373.	0.0103	2.08	0.57	14.32	2.48	4.45	14.32	2.48	4.45	99.37	0.0
IDLE	0.438	478.9	1.853	0.0111	11.8%	375.	0.0139	2.82	0.96	11.17	0.33	5.32	11.17	0.33	5.32	99.70	23.1
IDLE	0.429	477.9	1.871	0.0090	11.8%	378.	0.0117	2.37	0.65	12.56	1.18	5.01	12.56	1.18	5.01	99.56	0.0
IDLE	0.440	478.6	1.858	0.0113	COMM	374.	0.0140	2.85	0.93	12.67	0.48	5.57	12.67	0.48	5.57	99.65	31.1
IDLE	0.432	478.1	1.855	0.0094	COMM	370.	0.0118	2.39	0.65	14.40	0.95	5.13	14.40	0.95	5.13	99.55	0.0

CONFIGURATION V-1

												CORRECTED EMISSIONS							
												TEST MATRIX			ENGINE TABLE				
		INLET	INLET	BURNER	METER		FUEL	CARBON BAL		SPEC	CO	THC	NOX	CO	THC	NOX	CORR	SAE
	OPERATING	PRES	TEMP	AIR	F/A	FUEL	TEMP	F/A	CO2	HUMID	EI	EI	EI	EI	EI	EI	COMB	SMOKE
BT	CONDITION	MPA	°K	KG/SEC	RATIO	TYPE	°K	RATIO	%	G/KG	G/KG	G/KG	G/KG	G/KG	G/KG	G/KG	EFFIC	#
VC	IDLE	0.433	464.8	1.796	0.0095	JET-A	289.	0.0114	2.26	0.0	53.80	3.92	3.61	53.80	3.92	3.61	98.32	0.0
VC	IDLE	0.426	451.9	1.766	0.0102	ERBS	284.	0.0118	2.33	0.0	56.95	5.11	3.51	56.95	5.11	3.51	98.05	0.8
VO	IDLE	0.439	465.2	1.906	0.0090	ERBS	291.	0.0104	1.91	0.0	89.23	75.28	2.27	89.23	75.28	2.27	89.38	3.7
VC	IDLE	0.428	459.0	1.782	0.0127	ERBS	284.	0.0144	2.85	0.0	51.87	2.87	4.47	51.87	2.87	4.47	98.44	0.0
VC	IDLE	0.427	455.0	1.804	0.0072	ERBS	285.	0.0079	1.52	0.0	95.14	11.02	2.35	95.14	11.02	2.35	96.46	0.0
VC	IDLE	0.430	457.0	1.833	0.0098	ERBS	287.	0.0113	2.23	0.0	57.05	3.94	3.53	57.05	3.94	3.53	98.20	0.0
VO	APPROACH	1.066	603.7	3.691	0.0149	JET-A	285.	0.0143	2.90	41.13	9.52	0.87	37.96	9.52	0.87	37.96	99.67	3.0
VO	APPROACH	1.060	597.9	3.745	0.0139	ERBS	283.	0.0141	2.85	40.11	12.47	1.07	38.65	12.47	1.07	38.65	99.57	4.0
VO	CRUISE	1.476	743.2	4.561	0.0225	JET-A	295.	0.0246	4.97	55.95	1.27	0.22	50.11	1.27	0.22	50.11	99.95	19.8
VO	CRUISE	1.481	735.2	4.529	0.0218	ERBS	288.	0.0239	4.83	55.26	1.48	0.28	51.40	1.48	0.28	51.40	99.94	21.0
VO	CLIMB	1.493	737.7	4.814	0.0233	JET-A	297.	0.0248	5.00	56.92	1.09	0.15	52.69	0.70	0.09	65.91	99.96	20.0
VO	CLIMB	1.465	742.4	4.780	0.0232	ERBS	289.	0.0233	4.70	57.16	1.19	0.13	55.86	0.76	0.08	69.83	99.95	19.0
VO	TAKEOFF	1.538	803.7	4.596	0.0229	JET-A	288.	0.0246	4.97	67.23	0.61	0.09	45.78	0.34	0.05	61.36	99.93	4.5
VO	TAKEOFF	1.525	776.3	4.639	0.0205	JET-A	288.	0.0224	4.53	66.22	0.66	0.14	47.37	0.37	0.08	63.49	99.97	18.7
VO	TAKEOFF	1.552	780.1	4.648	0.0221	ERBS	284.	0.0242	4.89	62.95	0.63	0.10	53.35	0.35	0.06	71.50	99.97	15.0
VO	TAKEOFF	1.521	751.7	4.700	0.0196	ERBS	285.	0.0224	4.53	62.90	0.66	0.09	53.71	0.37	0.05	71.98	99.97	0.7

CONFIGURATION V-2

												CORRECTED EMISSIONS							
												TEST MATRIX			ENGINE TABLE				
		INLET	INLET	BURNER	METER		FUEL	CARBON BAL		SPEC	CO	THC	NOX	CO	THC	NOX	CORR	SAE
	OPERATING	PRES	TEMP	AIR	F/A	FUEL	TEMP	F/A	CO2	HUMID	EI	EI	EI	EI	EI	EI	COMB	SMOKE
BT	CONDITION	MPA	°K	KG/SEC	RATIO	TYPE	°K	RATIO	%	G/KG	G/KG	G/KG	G/KG	G/KG	G/KG	G/KG	EFFIC	#
VC	IDLE	0.438	462.4	1.825	0.0086	ERBS	281.	0.0097	1.84	0.0	77.46	39.21	0.0	77.46	39.21	0.0	93.73	28.8
VC	IDLE	0.431	462.6	1.832	0.0110	ERBS	282.	0.0119	2.28	0.0	77.95	30.86	0.0	77.95	30.86	0.0	94.59	0.0
VC	IDLE	0.423	453.8	1.831	0.0062	ERBS	286.	0.0076	1.43	0.0	85.84	38.82	0.0	85.84	38.82	0.0	93.36	0.0
VO	IDLE	0.429	440.7	2.027	0.0074	ERBS	293.	0.0097	1.80	0.0	92.26	59.52	7.31	92.26	59.52	7.31	90.90	0.0
VC	IDLE	0.437	463.9	2.188	0.0088	ERBS	283.	0.0097	1.82	0.0	92.26	43.01	0.0	92.26	43.01	0.0	92.94	0.0
VC	IDLE	0.437	461.4	1.807	0.0089	ERBS	284.	0.0095	1.84	0.0	69.48	26.48	0.0	69.48	26.48	0.0	95.36	0.0
VO	APPROACH	1.103	606.1	3.780	0.0140	ERBS	284.	0.0158	3.18	40.59	23.26	1.54	35.87	23.26	1.54	35.87	99.29	36.7
VC	APPROACH	1.090	586.7	3.456	0.0141	ERBS	277.	0.0137	2.77	40.84	11.68	2.21	39.22	11.68	2.21	39.22	99.47	12.2
VO	CRUISE	1.433	717.1	4.512	0.0208	ERBS	287.	0.0226	4.53	56.32	16.33	0.14	33.49	16.33	0.14	33.49	99.60	37.1
VC	CRUISE	1.431	741.2	4.354	0.0221	ERBS	285.	0.0201	4.07	57.76	2.01	0.56	44.99	2.01	0.56	44.99	99.89	45.8
VO	CLIMB	1.492	751.6	4.640	0.0234	ERBS	288.	0.0249	5.00	61.57	12.56	0.02	33.13	8.02	0.01	41.45	99.70	0.0
VC	CLIMB	1.507	759.5	4.536	0.0237	ERBS	285.	0.0206	4.17	61.47	1.93	0.32	37.97	1.23	0.20	47.50	99.92	0.0
VO	TAKEOFF	1.509	781.7	4.844	0.0213	ERBS	289.	0.0245	4.93	65.49	8.95	0.06	33.70	4.98	0.04	45.17	99.78	24.4
VC	TAKEOFF	1.511	794.1	4.354	0.0274	ERBS	283.	0.0238	4.80	64.51	1.68	0.20	38.55	0.94	0.11	51.66	99.94	16.0
VO	TAKEOFF	1.474	796.4	4.738	0.0199	ERBS	288.	0.0228	4.60	64.20	8.35	0.04	35.43	4.65	0.02	47.49	99.79	28.9
VO	TAKEOFF	1.489	769.6	4.721	0.0172	ERBS	288.	0.0208	4.20	63.26	9.23	0.02	40.20	5.14	0.01	53.87	99.77	25.0
VC	TAKEOFF	1.539	783.1	4.393	0.0277	JET-A	292.	0.0217	4.40	63.53	0.98	0.06	40.17	0.55	0.03	53.84	99.97	26.9

CONFIGURATION V-3

BT	OPERATING CONDITION	INLET PRES MPA	INLET TEMP °K	BURNER AIR KG/SEC	METER F/A RATIO	FUEL TYPE	FUEL TEMP °K	CARBON BAL F/A RATIO	CO2 %	SPEC HUMID G/KG	CORRECTED EMISSIONS — TEST MATRIX — CO EI G/KG	THC EI G/KG	NOX EI G/KG	— ENGINE TABLE — CO EI G/KG	THC EI G/KG	NOX EI G/KG	CORR COMB EFFIC	SAE SMOKE #
**	**********	*****	*****	******	******	*****	****	******	****	*****	******	******	******	******	******	******	******	*****
VC	IDLE	0.416	449.6	1.879	0.0085	ERBS	286.	0.0095	1.82	0.0	77.95	27.60	4.70	77.95	27.60	4.70	94.79	12.1
VC	IDLE	0.418	452.4	1.921	0.0107	ERBS	287.	0.0112	2.18	0.0	62.39	23.92	4.73	62.39	23.92	4.73	95.64	0.0
VC	IDLE	0.425	458.7	1.865	0.0064	ERBS	283.	0.0076	1.43	0.0	106.22	38.92	3.53	106.22	38.92	3.53	92.90	0.0
VO	IDLE	0.432	460.2	1.801	0.0098	ERBS	294.	0.0103	1.93	20.39	90.30	46.69	8.32	90.30	46.69	8.32	92.49	0.0
VC	IDLE	0.426	455.5	2.297	0.0086	ERBS	283.	0.0091	1.73	0.0	87.08	33.81	3.60	87.08	33.81	3.60	93.97	0.0
VC	IDLE	0.411	450.4	1.906	0.0084	ERBS	289.	0.0089	1.70	0.0	74.33	27.31	4.08	74.33	27.31	4.08	94.85	0.0
VO	APPROACH	1.080	593.9	3.661	0.0144	ERBS	297.	0.0146	2.95	35.49	13.54	3.90	42.41	13.54	3.90	42.41	99.22	0.0
VC	APPROACH	1.068	587.7	3.573	0.0135	ERBS	284.	0.0132	2.69	37.97	4.70	0.29	41.57	4.70	0.29	41.57	99.85	2.2
VO	CRUISE	1.414	722.3	4.574	0.0211	ERBS	285.	0.0204	4.13	56.87	1.03	0.03	44.39	1.03	0.03	44.39	99.97	14.9
VC	CRUISE	1.416	738.4	4.290	0.0224	ERBS	282.	0.0201	4.07	55.80	1.36	0.10	32.91	1.36	0.10	32.91	99.96	16.4
VO	CLIMB	1.540	729.1	4.801	0.0218	ERBS	283.	0.0201	4.08	60.38	1.06	0.05	52.24	0.68	0.03	65.36	99.97	0.0
VC	CLIMB	1.498	741.2	4.612	0.0233	ERBS	281.	0.0211	4.27	58.15	0.69	0.07	35.61	0.44	0.05	44.55	99.97	0.0
VO	TAKEOFF	1.529	773.2	4.604	0.0205	ERBS	296.	0.0207	4.18	62.53	1.03	3.66	63.01	0.57	2.04	84.46	99.55	5.6
VC	TAKEOFF	1.520	770.6	4.535	0.0239	ERBS	281.	0.0221	4.47	63.07	0.67	0.10	42.86	0.37	0.05	57.44	99.97	16.8
VO	TAKEOFF	1.464	789.8	4.505	0.0181	ERBS	297.	0.0171	3.47	63.84	1.18	3.25	74.68	0.66	1.81	100.09	99.58	0.1
VO	TAKEOFF	1.521	776.2	4.688	0.0198	ERBS	284.	0.0197	4.00	63.96	1.07	0.04	50.33	0.60	0.02	67.46	99.97	0.1
VC	TAKEOFF	1.497	787.7	4.465	0.0253	JET-A	285.	0.0211	4.27	62.99	0.69	0.12	43.63	0.39	0.07	58.48	99.97	0.0
VC	IDLE	0.423	451.3	1.868	0.0085	JET-A	287.	0.0102	1.98	0.0	63.87	29.75	4.04	63.87	29.75	4.04	95.04	0.0
VC	APPROACH	1.075	598.9	3.564	0.0141	JET-A	286.	0.0123	2.51	38.10	5.06	0.50	46.35	5.06	0.50	46.35	99.82	0.1
VO	CRUISE	1.403	738.2	4.558	0.0219	JET-A	287.	0.0207	4.19	57.38	0.71	0.02	48.84	0.71	0.02	48.84	99.98	16.3
VO	CLIMB	1.534	734.2	4.884	0.0212	JET-A	287.	0.0201	4.07	61.78	1.38	0.23	51.22	0.88	0.14	64.08	99.94	0.0
VO	TAKEOFF	1.520	795.0	4.585	0.0206	JET-A	297.	0.0195	3.94	64.34	2.67	6.37	60.96	1.49	3.54	81.71	99.21	22.5
VO	TAKEOFF	1.494	782.4	4.577	0.0183	JET-A	299.	0.0182	3.68	64.22	1.48	5.47	74.71	0.82	3.04	100.14	99.33	0.5

CONFIGURATION V-4

BT	OPERATING CONDITION	INLET PRES MPA	INLET TEMP °K	BURNER AIR KG/SEC	METER F/A RATIO	FUEL TYPE	FUEL TEMP °K	CARBON BAL F/A RATIO	CO2 %	SPEC HUMID G/KG	CORRECTED EMISSIONS — TEST MATRIX — CO EI G/KG	THC EI G/KG	NOX EI G/KG	— ENGINE TABLE — CO EI G/KG	THC EI G/KG	NOX EI G/KG	CORR COMB EFFIC	SAE SMOKE #
**	**********	*****	*****	******	******	*****	****	******	****	*****	******	******	******	******	******	******	******	*****
VC	IDLE	0.425	438.2	1.837	0.0090	ERBS	296.	0.0110	2.13	0.0	62.01	30.37	3.93	62.01	30.37	3.93	94.95	6.4
VC	IDLE	0.424	448.0	1.847	0.0111	ERBS	297.	0.0113	2.20	0.0	62.85	23.36	6.15	62.85	23.36	6.15	95.75	0.0
VC	IDLE	0.420	480.6	1.853	0.0076	ERBS	296.	0.0093	1.75	0.0	80.06	44.57	3.21	80.06	44.57	3.21	92.77	0.0
VO	IDLE	0.438	460.8	1.901	0.0093	ERBS	290.	0.0105	1.93	22.53	96.39	66.60	5.17	96.39	66.60	5.17	90.18	0.0
VC	IDLE	0.429	467.1	2.243	0.0089	ERBS	296.	0.0109	2.10	0.0	65.98	30.98	3.74	65.98	30.98	3.74	94.84	0.0
VC	IDLE	0.424	447.0	1.870	0.0089	ERBS	295.	0.0111	2.13	0.0	66.91	31.45	3.25	66.91	31.45	3.25	94.70	0.0
VO	APPROACH	1.085	601.9	3.688	0.0144	ERBS	289.	0.0173	3.50	37.29	9.80	1.09	26.79	9.80	1.09	26.79	99.64	0.0
VC	APPROACH	1.085	584.4	3.602	0.0136	ERBS	288.	0.0172	3.50	37.10	5.34	0.24	34.80	5.34	0.24	34.80	99.85	18.9
VO	CRUISE	1.425	738.6	4.405	0.0183	ERBS	288.	0.0196	3.98	55.16	1.40	0.46	41.90	1.40	0.46	41.90	99.91	18.3
VC	CRUISE	1.388	739.2	4.407	0.0221	ERBS	288.	0.0150	3.06	57.22	0.96	0.0	58.23	0.96	0.0	58.23	99.98	22.4
VO	CLIMB	1.515	730.4	4.732	0.0183	ERBS	288.	0.0193	3.91	57.15	1.09	0.61	43.20	0.69	0.39	54.04	99.90	0.0
VC	CLIMB	1.503	721.4	4.797	0.0217	ERBS	288.	0.0219	4.44	56.65	0.67	0.0	33.71	0.43	0.0	42.17	99.98	0.0
VO	TAKEOFF	1.517	778.8	4.594	0.0189	ERBS	289.	0.0228	4.60	63.74	1.76	1.34	40.86	0.98	0.74	54.76	99.80	25.2
VC	TAKEOFF	1.528	784.5	4.547	0.0214	ERBS	287.	0.0219	4.44	63.89	0.68	0.0	27.18	0.38	0.0	36.43	99.98	9.7
VO	TAKEOFF	1.510	776.4	4.647	0.0176	ERBS	288.	0.0186	3.78	64.05	1.46	0.68	36.69	0.81	0.38	49.17	99.88	31.8
VO	TAKEOFF	1.502	770.5	4.642	0.0158	ERBS	289.	0.0195	3.94	65.09	3.24	2.12	57.11	1.80	1.18	76.55	99.67	6.5
VO	TAKEOFF	1.529	789.1	4.123	0.0178	ERBS	288.	0.0193	3.91	61.56	1.43	0.50	39.31	0.80	0.28	52.69	99.91	21.8

CONFIGURATION V-5

											CORRECTED EMISSIONS							
								CARBON			TEST MATRIX			ENGINE TABLE				
	OPERATING	INLET PRES	INLET TEMP	BURNER AIR	METER F/A	FUEL	FUEL TEMP	BAL F/A	CO2	SPEC HUMID	CO EI	THC EI	NOX EI	CO EI	THC EI	NOX EI	CORR COMB	SAE SMOKE
BT	CONDITION	MPA	°K	KG/SEC	RATIO	TYPE	°K	RATIO	%	G/KG	G/KG	G/KG	G/KG	G/KG	G/KG	G/KG	EFFIC	#
**	**********	*****	*****	******	******	*****	****	******	****	*****	******	******	******	******	******	******	******	*****
VC	IDLE	0.433	466.8	1.867	0.0087	ERBS	292.	0.0108	2.05	0.0	79.63	39.44	3.30	79.63	39.44	3.30	93.59	38.4
VC	IDLE	0.432	470.8	1.826	0.0114	ERBS	291.	0.0137	2.59	0.0	89.66	33.25	3.36	89.66	33.25	3.36	94.05	37.1
VC	IDLE	0.428	454.8	1.880	0.0070	ERBS	292.	0.0090	1.68	0.0	88.80	47.01	3.23	88.80	47.01	3.23	92.42	24.8
VC	IDLE	0.433	469.9	2.220	0.0090	ERBS	291.	0.0110	2.05	0.0	111.24	43.83	3.23	111.24	43.83	3.23	92.35	22.3
VC	IDLE	0.435	446.7	1.840	0.0089	ERBS	291.	0.0107	2.03	0.0	89.57	37.40	3.11	89.57	37.40	3.11	93.63	41.0

CONFIGURATION V-5A

											CORRECTED EMISSIONS							
								CARBON			TEST MATRIX			ENGINE TABLE				
	OPERATING	INLET PRES	INLET TEMP	BURNER AIR	METER F/A	FUEL	FUEL TEMP	BAL F/A	CO2	SPEC HUMID	CO EI	THC EI	NOX EI	CO EI	THC EI	NOX EI	CORR COMB	SAE SMOKE
BT	CONDITION	MPA	°K	KG/SEC	RATIO	TYPE	°K	RATIO	%	G/KG	G/KG	G/KG	G/KG	G/KG	G/KG	G/KG	EFFIC	#
**	**********	*****	*****	******	******	*****	****	******	****	*****	******	******	******	******	******	******	******	*****
VC	IDLE	0.427	467.5	1.881	0.0178	ERBS	292.	0.0164	3.18	0.0	36.01	37.88	4.07	36.01	37.88	4.07	94.72	15.6
VC	IDLE	0.427	466.7	1.878	0.0201	ERBS	292.	0.0180	3.59	0.0	19.67	14.08	4.67	19.67	14.08	4.67	97.89	0.0
VC	IDLE	0.426	470.2	1.878	0.0150	ERBS	293.	0.0140	2.64	0.0	69.97	48.35	3.95	69.97	48.35	3.95	92.67	0.0
VO	IDLE	0.424	450.3	1.933	0.0192	ERBS	289.	0.0196	3.68	23.42	96.50	34.09	4.49	96.50	34.09	4.49	93.69	0.0
VC	IDLE	0.434	476.5	2.227	0.0178	ERBS	291.	0.0161	3.12	0.0	44.31	30.31	3.50	44.31	30.31	3.50	95.48	0.0
VC	IDLE	0.428	453.3	1.951	0.0084	ERBS	294.	0.0167	3.23	0.0	59.07	21.99	4.28	59.07	21.99	4.28	96.04	0.0
VC	APPROACH	1.052	600.5	3.614	0.0136	ERBS	292.	0.0141	2.85	37.00	16.93	0.69	31.41	16.93	0.69	31.41	99.51	0.1
VO	CRUISE	1.398	727.1	4.680	0.0224	ERBS	291.	0.0249	5.02	55.57	0.84	0.15	38.87	0.84	0.15	38.87	99.96	4.4
VC	CRUISE	1.403	733.2	4.396	0.0220	ERBS	290.	0.0216	4.37	53.39	0.68	0.40	41.80	0.68	0.40	41.80	99.94	0.8
VO	CLIMB	1.490	762.8	4.855	0.0241	ERBS	291.	0.0242	4.89	58.04	0.60	0.14	40.66	0.38	0.09	50.87	99.97	0.0
VC	CLIMB	1.499	747.7	4.657	0.0232	ERBS	289.	0.0232	4.70	56.41	0.63	0.46	43.09	0.40	0.30	53.90	99.93	0.0
VO	TAKEOFF	1.484	788.7	4.803	0.0255	ERBS	290.	0.0248	5.00	64.49	1.09	0.26	46.73	0.60	0.14	62.64	99.94	1.6
VC	TAKEOFF	1.521	763.9	4.502	0.0265	ERBS	288.	0.0262	5.28	57.77	0.57	0.75	30.92	0.31	0.42	41.45	99.90	0.9
VO	TAKEOFF	1.494	805.9	4.668	0.0232	ERBS	290.	0.0232	4.70	64.85	0.90	0.24	41.83	0.50	0.13	56.06	99.95	3.6
VO	TAKEOFF	1.531	802.3	4.776	0.0191	ERBS	290.	0.0219	4.44	63.60	0.97	0.19	44.33	0.54	0.11	59.41	99.95	4.1
VO	TAKEOFF	1.514	795.9	4.300	0.0253	ERBS	289.	0.0262	5.28	62.50	0.56	0.04	33.60	0.31	0.02	45.03	99.98	1.6

CONFIGURATION V-6

BT	OPERATING CONDITION	INLET PRES MPA	INLET TEMP °K	BURNER AIR KG/SEC	METER F/A RATIO	FUEL TYPE	FUEL TEMP °K	CARBON BAL F/A RATIO	CO2 %	SPEC HUMID G/KG	CORRECTED EMISSIONS — TEST MATRIX — CO EI G/KG	THC EI G/KG	NOX EI G/KG	CORRECTED EMISSIONS — ENGINE TABLE — CO EI G/KG	THC EI G/KG	NOX EI G/KG	CORR COMB EFFIC	SAE SMOKE #
**	*********	*****	*****	******	******	*****	****	******	****	*****	******	******	******	******	******	******	******	*****
VC	IDLE	0.440	463.0	1.856	0.0090	ERBS	304.	0.0107	2.13	0.0	35.81	11.36	5.77	35.81	11.36	5.77	97.89	22.8
VC	IDLE	0.433	465.0	1.854	0.0113	ERBS	304.	0.0131	2.59	0.0	38.06	13.10	5.50	38.06	13.10	5.50	97.60	0.0
VC	IDLE	0.435	463.2	1.866	0.0067	ERBS	304.	0.0089	1.66	0.0	43.41	83.85	0.0	43.41	83.85	0.0	89.35	0.0
VO	IDLE	0.428	455.1	1.969	0.0100	ERBS	296.	0.0115	2.26	21.59	48.40	24.53	6.56	48.40	24.53	6.56	95.99	0.0
VC	IDLE	0.425	467.6	2.196	0.0094	ERBS	304.	0.0113	2.26	0.0	32.79	7.18	5.77	32.79	7.18	5.77	98.38	0.0
VC	IDLE	0.428	456.6	1.875	0.0089	ERBS	304.	0.0092	1.80	0.0	53.38	18.37	8.67	53.38	18.37	8.67	96.60	0.0
VO	APPROACH	1.087	604.0	3.660	0.0147	ERBS	300.	0.0118	2.40	43.29	5.38	0.22	38.68	5.38	0.22	38.68	99.85	0.0
VC	APPROACH	1.087	599.4	3.435	0.0147	ERBS	303.	0.0115	2.35	46.61	3.45	0.05	33.96	3.45	0.05	33.96	99.91	7.8
VO	CRUISE	1.424	741.3	4.541	0.0228	ERBS	298.	0.0259	5.22	55.57	1.07	0.10	32.47	1.07	0.10	32.47	99.96	46.0
VC	CRUISE	1.453	714.7	4.426	0.0217	ERBS	307.	0.0199	4.04	49.69	1.08	0.0	44.65	1.08	0.0	44.65	99.98	40.8
VO	CLIMB	1.512	732.3	4.844	0.0219	ERBS	300.	0.0242	4.89	56.51	1.13	0.22	35.67	0.72	0.14	44.62	99.95	0.0
VC	CLIMB	1.536	755.9	4.634	0.0233	ERBS	308.	0.0242	4.89	50.56	0.88	0.0	46.46	0.56	0.0	58.12	99.98	0.0
VO	CLIMB	1.572	765.5	4.759	0.0219	ERBS	304.	0.0252	5.09	62.79	1.13	0.23	43.05	0.72	0.15	53.85	99.95	30.5
VC	TAKEOFF	1.528	782.9	4.567	0.0246	ERBS	309.	0.0231	4.67	55.44	0.92	0.0	30.60	0.51	0.0	41.01	99.98	24.3
VO	TAKEOFF	1.544	793.3	4.753	0.0194	ERBS	302.	0.0222	4.50	60.56	1.25	0.22	36.94	0.70	0.12	49.51	99.95	31.7
VO	CLIMB	1.523	770.8	4.720	0.0177	ERBS	301.	0.0193	3.91	60.54	1.42	0.16	44.82	0.91	0.10	56.08	99.95	24.9
VO	CRUISE	1.460	741.3	4.456	0.0182	ERBS	301.	0.0245	4.96	47.63	1.15	0.0	42.89	1.15	0.0	42.89	99.97	27.8

CONFIGURATION V-7

BT	OPERATING CONDITION	INLET PRES MPA	INLET TEMP °K	BURNER AIR KG/SEC	METER F/A RATIO	FUEL TYPE	FUEL TEMP °K	CARBON BAL F/A RATIO	CO2 %	SPEC HUMID G/KG	CORRECTED EMISSIONS — TEST MATRIX — CO EI G/KG	THC EI G/KG	NOX EI G/KG	CORRECTED EMISSIONS — ENGINE TABLE — CO EI G/KG	THC EI G/KG	NOX EI G/KG	CORR COMB EFFIC	SAE SMOKE #
**	*********	*****	*****	******	******	*****	****	******	****	*****	******	******	******	******	******	******	******	*****
VO	IDLE	0.435	476.2	1.950	0.0093	JET-A	304.	0.0090	1.43	2.79	105.89	205.36	1.51	105.89	205.36	1.51	74.37	3.2
VO	IDLE	0.424	471.4	1.913	0.0094	ERBS	303.	0.0085	1.15	2.91	119.98	323.29	1.02	119.98	323.29	1.02	59.03	4.2
VO	IDLE	0.424	474.1	1.923	0.0097	COMM	301.	0.0076	1.00	2.90	107.52	355.54	1.10	107.52	355.54	1.10	55.20	8.7
VO	IDLE	0.433	474.6	1.937	0.0098	11.8%	300.	0.0089	1.21	2.85	104.58	333.09	1.15	104.58	333.09	1.15	58.52	8.0
VO	APPROACH	1.081	607.9	3.858	0.0127	JET-A	302.	0.0134	2.71	3.27	8.71	3.10	8.12	8.71	3.10	8.12	99.44	10.5
VO	APPROACH	1.075	607.7	3.845	0.0128	ERBS	300.	0.0132	2.68	3.27	12.06	3.12	7.90	12.06	3.12	7.90	99.35	13.1
VO	CRUISE	1.418	755.3	4.830	0.0198	JET-A	300.	0.0190	3.85	2.10	1.55	0.65	19.41	1.55	0.65	19.41	99.89	29.8
VO	CRUISE	1.420	752.3	4.864	0.0203	ERBS	300.	0.0192	3.90	2.17	1.60	0.14	21.12	1.60	0.14	21.12	99.95	32.9
VO	CRUISE	1.420	752.2	4.875	0.0208	11.8%	302.	0.0199	4.03	2.13	1.72	0.14	20.75	1.72	0.14	20.75	99.94	34.7
VO	CRUISE	1.416	751.7	4.864	0.0205	COMM	301.	0.0192	3.90	2.12	1.84	0.17	13.02	1.84	0.17	13.02	99.94	28.5
VO	CLIMB	2.345	765.6	7.788	0.0208	JET-A	306.	0.0210	4.26	2.59	0.97	0.11	20.39	0.62	0.07	25.51	99.98	45.1
VO	CLIMB	2.316	762.8	7.799	0.0213	ERBS	298.	0.0218	4.41	2.47	1.34	0.07	19.31	0.85	0.05	24.16	99.97	48.7
VO	TAKEOFF	2.372	789.5	7.318	0.0224	JET-A	300.	0.0216	4.38	2.96	0.83	0.10	21.83	0.46	0.06	29.26	99.98	33.6
VO	TAKEOFF	2.366	788.6	7.298	0.0220	ERBS	301.	0.0216	4.37	2.93	0.66	0.07	23.73	0.37	0.04	31.80	99.98	36.1
VO	TAKEOFF	2.361	788.7	7.297	0.0193	ERBS	299.	0.0196	3.98	2.94	0.70	0.06	24.33	0.39	0.03	32.61	99.98	0.0
VO	TAKEOFF	2.362	788.9	7.278	0.0170	ERBS	300.	0.0176	3.58	3.00	0.81	0.07	23.08	0.45	0.04	30.93	99.98	0.0
VO	TAKEOFF	2.361	788.4	7.325	0.0217	11.8%	301.	0.0216	4.37	3.12	0.68	0.07	25.67	0.38	0.04	34.41	99.98	35.4
VO	TAKEOFF	2.354	784.7	7.282	0.0223	COMM	302.	0.0214	4.35	2.94	0.72	0.07	23.50	0.40	0.04	31.50	99.98	33.1
VO	TAKEOFF	2.375	787.2	7.333	0.0199	JET-A	300.	0.0196	3.97	2.89	0.66	0.09	22.52	0.37	0.05	30.19	99.98	0.0
VO	TAKEOFF	2.358	785.3	7.288	0.0177	JET-A	300.	0.0177	3.60	2.96	0.71	0.11	22.04	0.39	0.06	29.54	99.98	0.0

CONFIGURATION V-8 - VALVES OPEN

											CORRECTED EMISSIONS							
											TEST MATRIX			ENGINE TABLE				
BT	OPERATING CONDITION	INLET PRES MPA	INLET TEMP °K	BURNER AIR KG/SEC	METER F/A RATIO	FUEL TYPE	FUEL TEMP °K	CARBON BAL F/A RATIO	CO2 %	SPEC HUMID G/KG	CO EI G/KG	THC EI G/KG	NOX EI G/KG	CO EI G/KG	THC EI G/KG	NOX EI G/KG	CORR COMB EFFIC	SAE SMOKE #
**	*********	*****	*****	******	******	*****	****	******	****	*****	******	******	******	******	******	******	******	*****
VC	IDLE	0.430	471.7	1.711	0.0104	JET-A	302.	0.0091	1.66	2.76	61.10	96.34	2.19	61.10	96.34	2.19	87.57	6.9
VC	IDLE	0.428	474.0	1.729	0.0120	JET-A	301.	0.0108	2.09	2.88	43.23	42.64	2.82	43.23	42.64	2.82	94.10	0.0
VC	IDLE	0.427	475.3	1.672	0.0095	JET-A	301.	0.0079	1.34	2.83	68.45	163.90	1.94	68.45	163.90	1.94	79.55	0.0
VC	IDLE	0.428	477.2	1.690	0.0104	ERBS	298.	0.0085	1.47	3.47	85.04	138.28	2.03	85.04	138.28	2.03	81.86	3.4
VC	IDLE	0.427	478.4	1.697	0.0127	ERBS	297.	0.0110	2.09	3.43	55.45	53.26	2.74	55.45	53.26	2.74	92.46	0.0
VC	IDLE	0.429	477.1	1.668	0.0098	ERBS	297.	0.0079	1.30	3.21	86.07	178.33	1.91	86.07	178.33	1.91	77.21	0.0
VC	IDLE	0.424	479.0	1.698	0.0104	11.8%	299.	0.0087	1.46	3.24	82.45	158.17	2.10	82.45	158.17	2.10	79.10	4.9
VC	IDLE	0.428	477.5	1.683	0.0105	COMM	297.	0.0078	1.31	3.37	100.85	160.42	1.95	100.85	160.42	1.95	78.70	5.0
VC	IDLE	0.427	476.9	1.677	0.0131	COMM	296.	0.0106	1.99	3.45	66.87	63.67	2.65	66.87	63.67	2.65	90.90	0.0
VC	APPROACH	1.080	608.7	3.687	0.0136	JET-A	299.	0.0120	2.44	3.55	3.49	0.70	9.10	3.49	0.70	9.10	99.84	9.2
VC	APPROACH	1.078	611.1	3.679	0.0135	ERBS	296.	0.0121	2.46	3.45	4.70	0.90	9.19	4.70	0.90	9.19	99.78	9.6
VC	CRUISE	1.428	750.8	4.632	0.0206	ERBS	295.	0.0179	3.64	3.53	0.48	0.07	18.67	0.48	0.07	18.67	99.98	16.7
VC	TAKEOFF	2.101	794.4	6.645	0.0241	JET-A	302.	0.0209	4.24	3.32	0.25	0.08	26.03	0.14	0.04	34.89	99.99	12.0
VC	TAKEOFF	2.108	788.0	6.661	0.0239	ERBS	295.	0.0203	4.12	3.55	0.34	0.08	26.00	0.19	0.05	34.85	99.99	20.1
VC	TAKEOFF	2.098	793.7	6.664	0.0239	COMM	295.	0.0206	4.18	3.32	0.26	0.14	27.69	0.14	0.08	37.11	99.98	9.5

CONFIGURATION V-8 - VALVES CLOSED

OPERATING CONDITION	INLET PRES MPA	INLET TEMP K	BURNER AIR KG/SEC	METER F/A RATIO	FUEL TYPE	FUEL TEMP K	CARBON BAL F/A RATIO	CO2 %	SPEC HUMID G/KG	CORRECTED EMISSIONS — TEST MATRIX — CO EI G/KG	THC EI G/KG	NOX EI G/KG	— ENGINE TABLE — CO EI G/KG	THC EI G/KG	NOX EI G/KG	CORR COMB EFFIC	SAE SMOKE #
*********	*****	*****	******	******	*****	****	******	****	*****	******	******	******	******	******	******	******	*****
IDLE	0.426	427.2	1.550	0.0	10	0.	0.0004	0.08	0.0	0.0	0.0	0.0	0.0	0.0	0.0	100.00	0.0
IDLE	0.432	473.4	1.543	0.0129	JET-A	299.	0.0072	1.42	0.0	48.03	15.71	0.0	48.03	15.71	0.0	97.11	14.7
IDLE	0.427	464.2	1.549	0.0091	JET-A	300.	0.0053	1.03	0.0	72.93	33.91	0.0	72.93	33.91	0.0	94.40	0.0
IDLE	0.421	429.0	1.547	0.0069	JET-A	301.	0.0042	0.79	0.0	74.46	53.76	0.0	74.46	53.76	0.0	91.98	0.0
IDLE	0.441	462.5	1.545	0.0156	JET-A	304.	0.0085	1.70	0.0	38.39	12.17	0.0	38.39	12.17	0.0	97.78	0.0
IDLE	0.435	465.7	1.548	0.0090	JET-A	305.	0.0055	1.07	0.0	54.49	28.59	0.0	54.49	28.59	0.0	95.53	1.1
IDLE	0.441	465.4	1.544	0.0113	JET-A	306.	0.0068	1.34	0.0	44.31	24.94	0.0	44.31	24.94	0.0	96.23	0.0
IDLE	0.445	448.1	1.542	0.0131	JET-A	306.	0.0078	1.55	0.0	35.69	23.77	0.0	35.69	23.77	0.0	96.58	0.0
IDLE	0.432	469.7	1.542	0.0065	JET-A	307.	0.0045	0.87	0.0	60.38	35.18	0.0	60.38	35.18	0.0	94.62	0.0
IDLE	0.429	470.6	1.540	0.0053	JET-A	306.	0.0037	0.71	0.0	65.54	48.76	0.0	65.54	48.76	0.0	92.90	0.0
IDLE	0.455	463.1	1.540	0.0155	JET-A	307.	0.0091	1.80	0.0	34.31	22.91	0.0	34.31	22.91	0.0	96.78	0.0
IDLE	0.441	475.2	1.539	0.0092	JET-A	307.	0.0044	0.87	0.0	45.57	26.08	0.0	45.57	26.08	0.0	96.07	22.2
IDLE	0.410	420.9	1.557	0.0061	JET-A	308.	0.0029	0.55	0.0	72.19	44.07	0.0	72.19	44.07	0.0	92.97	0.0
IDLE	0.427	474.8	1.548	0.0152	JET-A	309.	0.0064	1.26	0.0	45.51	23.44	0.0	45.51	23.44	0.0	96.24	0.0
IDLE	0.423	468.0	1.546	0.0132	JET-A	309.	0.0056	1.10	0.0	51.16	26.84	0.0	51.16	26.84	0.0	95.68	0.0
IDLE	0.416	438.8	1.546	0.0109	JET-A	309.	0.0050	0.99	0.0	46.88	30.05	0.0	46.88	30.05	0.0	95.33	0.0
IDLE	0.424	456.7	2.164	0.0098	JET-A	305.	0.0054	1.03	0.0	93.44	40.23	0.0	93.44	40.23	0.0	93.16	0.0
IDLE	0.427	450.2	2.163	0.0070	JET-A	306.	0.0042	0.75	0.0	98.10	99.07	0.0	98.10	99.07	0.0	86.31	0.0
IDLE	0.437	463.4	2.161	0.0098	JET-A	308.	0.0056	1.10	0.0	57.79	16.79	0.0	57.79	16.79	0.0	96.80	0.0
IDLE	0.431	462.0	2.158	0.0067	JET-A	308.	0.0043	0.83	0.0	79.45	33.78	0.0	79.45	33.78	0.0	94.32	0.0
IDLE	0.434	465.8	2.153	0.0081	JET-A	309.	0.0042	0.79	0.0	75.75	68.03	0.0	75.75	68.03	0.0	90.56	0.0
IDLE	0.421	425.9	1.600	0.0089	ERBS	297.	0.0066	1.26	0.0	72.81	35.83	0.0	72.81	35.83	0.0	94.00	2.6
IDLE	0.425	447.3	1.594	0.0111	ERBS	296.	0.0075	1.46	0.0	58.42	23.03	0.0	58.42	23.03	0.0	95.91	0.0
IDLE	0.430	463.5	1.591	0.0129	ERBS	295.	0.0089	1.75	0.0	44.38	17.14	0.0	44.38	17.14	0.0	96.96	0.0
IDLE	0.419	470.7	1.585	0.0093	ERBS	294.	0.0077	1.50	0.0	50.05	23.63	0.0	50.05	23.63	0.0	95.98	26.3
IDLE	0.422	436.0	1.583	0.0116	ERBS	294.	0.0097	1.90	0.0	42.52	20.61	0.0	42.52	20.61	0.0	96.54	0.0
IDLE	0.426	467.8	1.580	0.0130	ERBS	294.	0.0091	1.80	0.0	37.41	21.41	0.0	37.41	21.41	0.0	96.60	0.0
IDLE	0.424	455.1	1.580	0.0130	ERBS	293.	0.0067	1.26	0.0	57.90	57.99	0.0	57.90	57.99	0.0	91.78	0.0
IDLE	0.420	460.4	1.577	0.0117	ERBS	293.	0.0059	1.15	0.0	48.96	31.76	0.0	48.96	31.76	0.0	95.05	0.0
IDLE	0.416	464.6	1.576	0.0096	ERBS	293.	0.0053	1.03	0.0	53.61	35.79	0.0	53.61	35.79	0.0	94.39	37.4
IDLE	0.427	444.8	1.603	0.0079	ERBS	295.	0.0050	0.95	0.0	82.06	53.59	0.0	82.06	53.59	0.0	91.79	0.0
IDLE	0.419	441.5	1.605	0.0071	ERBS	294.	0.0053	1.03	0.0	62.92	32.92	0.0	62.92	32.92	0.0	94.56	0.0
APPROACH	1.094	592.1	3.319	0.0109	JET-A	304.	0.0074	1.50	0.0	13.42	0.70	0.0	13.42	0.70	0.0	99.61	0.0
APPROACH	1.115	596.6	3.336	0.0135	JET-A	304.	0.0083	1.70	0.0	6.06	0.0	0.0	6.06	0.0	0.0	99.86	0.0
APPROACH	1.119	599.2	3.383	0.0132	JET-A	302.	0.0076	1.55	0.0	5.34	0.73	0.0	5.34	0.73	0.0	99.80	24.8
APPROACH	1.094	574.6	3.395	0.0096	JET-A	301.	0.0062	1.28	0.0	5.37	0.30	0.0	5.37	0.30	0.0	99.84	0.0
APPROACH	1.108	588.1	3.377	0.0129	JET-A	301.	0.0085	1.75	0.0	5.27	0.20	0.0	5.27	0.20	0.0	99.86	42.4
APPROACH	1.062	594.2	3.448	0.0122	ERBS	298.	0.0060	1.22	0.0	8.01	0.0	0.0	8.01	0.0	0.0	99.81	14.3
APPROACH	1.053	575.0	3.454	0.0099	ERBS	295.	0.0058	1.18	0.0	4.11	0.0	0.0	4.11	0.0	0.0	99.90	28.2

CONFIGURATION M-1

OPERATING CONDITION	INLET PRES MPA	INLET TEMP K	BURNER AIR KG/SEC	METER F/A RATIO	FUEL TYPE	FUEL TEMP K	CARBON BAL F/A RATIO	CO2 %	SPEC HUMID G/KG	CORRECTED EMISSIONS — TEST MATRIX — CO EI G/KG	THC EI G/KG	NOX EI G/KG	CORRECTED EMISSIONS — ENGINE TABLE — CO EI G/KG	THC EI G/KG	NOX EI G/KG	CORR COMB EFFIC	SAE SMOKE #
*********	*****	*****	******	******	*****	****	******	****	*****	******	******	******	******	******	******	******	*****
IDLE	0.593	300.9	2.794	0.0	10	0.	0.0	0.0	0.0	0.0	0.0	0.0	0.0	0.0	0.0	100.00	0.0
IDLE	0.426	472.1	1.545	0.0122	JET-A	304.	0.0088	1.70	0.0	56.52	35.46	0.0	56.52	35.46	0.0	94.60	0.0
IDLE	0.431	474.5	1.558	0.0145	JET-A	305.	0.0108	2.10	0.0	54.23	27.73	0.0	54.23	27.73	0.0	95.59	0.0
IDLE	0.427	473.1	1.571	0.0097	JET-A	305.	0.0061	1.15	0.0	76.97	61.04	0.0	76.97	61.04	0.0	91.20	9.5
IDLE	0.430	475.1	1.598	0.0079	JET-A	305.	0.0052	0.95	0.0	91.49	76.89	0.0	91.49	76.89	0.0	89.11	0.0
IDLE	0.427	474.3	1.559	0.0099	JET-A	305.	0.0072	1.38	0.0	76.25	36.26	0.0	76.25	36.26	0.0	94.05	17.5
IDLE	0.422	474.0	1.525	0.0126	JET-A	306.	0.0091	1.75	0.0	68.86	28.59	0.0	68.86	28.59	0.0	95.05	0.0
IDLE	0.433	473.2	1.538	0.0144	JET-A	306.	0.0111	2.15	0.0	67.76	23.03	0.0	67.76	23.03	0.0	95.83	0.0
IDLE	0.426	476.4	1.529	0.0139	ERBS	308.	0.0126	2.45	0.0	69.61	14.03	0.0	69.61	14.03	0.0	96.71	0.0
IDLE	0.427	474.5	1.533	0.0121	ERBS	308.	0.0108	2.10	0.0	78.26	17.04	0.0	78.26	17.04	0.0	96.15	0.0
IDLE	0.427	475.0	1.532	0.0099	ERBS	308.	0.0083	1.60	0.0	85.56	24.48	0.0	85.56	24.48	0.0	95.11	20.2
IDLE	0.433	476.8	1.571	0.0082	ERBS	309.	0.0076	1.46	0.0	77.24	29.81	0.0	77.24	29.81	0.0	94.76	0.0
IDLE	0.432	476.6	1.565	0.0122	ERBS	309.	0.0070	1.34	0.0	91.64	21.45	0.0	91.64	21.45	0.0	95.38	0.0
IDLE	0.429	475.3	1.541	0.0102	ERBS	308.	0.0054	1.03	0.0	106.92	32.50	0.0	106.92	32.50	0.0	93.70	32.6
IDLE	0.430	476.1	1.560	0.0085	ERBS	308.	0.0043	0.79	0.0	129.28	47.74	0.0	129.28	47.74	0.0	91.41	0.0
APPROACH	1.085	602.6	3.396	0.0134	JET-A	303.	0.0074	1.50	0.0	25.51	7.12	0.0	25.51	7.12	0.0	98.59	13.6
APPROACH	1.078	604.8	3.404	0.0140	ERBS	304.	0.0099	2.00	0.0	28.49	5.61	0.0	28.49	5.61	0.0	98.67	38.3
APPROACH	1.090	607.1	3.380	0.0108	ERBS	303.	0.0098	2.00	0.0	12.95	1.33	0.0	12.95	1.33	0.0	99.54	0.0
APPROACH	1.101	602.4	3.372	0.0132	JET-A	303.	0.0118	2.40	0.0	13.64	0.66	0.0	13.64	0.66	0.0	99.61	26.5
APPROACH	1.062	601.0	3.373	0.0175	JET-A	303.	0.0161	3.26	0.0	9.70	0.31	0.0	9.70	0.31	0.0	99.73	45.6
APPROACH	1.068	599.0	3.432	0.0108	ERBS	301.	0.0104	2.10	0.0	21.06	1.49	0.0	21.06	1.49	0.0	99.32	50.3
CRUISE	1.438	744.3	3.902	0.0195	ERBS	307.	0.0135	2.75	0.0	6.06	0.0	0.0	6.06	0.0	0.0	99.86	44.4
CRUISE	1.433	745.0	3.875	0.0199	JET-A	310.	0.0140	2.85	0.0	3.55	0.0	0.0	3.55	0.0	0.0	99.92	16.4
CRUISE	1.454	740.2	3.932	0.0138	JET-A	309.	0.0132	2.70	0.0	2.90	0.0	0.0	2.90	0.0	0.0	99.93	14.7
CLIMB	1.471	752.0	4.133	0.0199	ERBS	308.	0.0137	2.80	0.0	4.84	0.0	0.0	3.09	0.0	0.0	99.88	14.7
TAKEOFF	1.526	783.7	4.179	0.0182	JET-A	309.	0.0118	2.40	0.0	10.77	0.0	0.0	5.99	0.0	0.0	99.75	24.2
TAKEOFF	1.550	784.2	4.129	0.0217	JET-A	310.	0.0145	2.95	0.0	2.07	0.0	0.0	1.15	0.0	0.0	99.95	38.3
TAKEOFF	1.534	782.7	4.088	0.0217	ERBS	309.	0.0150	3.06	0.0	1.58	0.0	0.0	0.88	0.0	0.0	99.96	33.7
TAKEOFF	1.532	785.8	4.148	0.0139	JET-A	310.	0.0122	2.50	0.0	2.61	0.0	0.0	1.45	0.0	0.0	99.94	33.0

CONFIGURATION M-2

OPERATING CONDITION	INLET PRES MPA	INLET TEMP °K	BURNER AIR KG/SEC	METER F/A RATIO	FUEL TYPE	FUEL TEMP °K	CARBON BAL F/A RATIO	CO2 %	SPEC HUMID G/KG	CORRECTED EMISSIONS — TEST MATRIX — CO EI G/KG	TEST MATRIX THC EI G/KG	TEST MATRIX NOX EI G/KG	ENGINE TABLE CO EI G/KG	ENGINE TABLE THC EI G/KG	ENGINE TABLE NOX EI G/KG	CORR COMB EFFIC	SAE SMOKE #
IDLE	0.635	298.3	2.600	0.0	10	0.	0.0	0.0	0.0	0.0	0.0	0.0	0.0	0.0	0.0	100.00	0.0
IDLE	0.425	471.5	1.515	0.0095	JET-A	301.	0.0047	0.83	0.0	111.87	92.77	0.0	111.87	92.77	0.0	86.68	6.0
IDLE	0.425	471.6	1.519	0.0119	JET-A	301.	0.0060	1.10	0.0	91.83	61.31	0.0	91.83	61.31	0.0	90.76	0.0
IDLE	0.428	471.1	1.517	0.0136	JET-A	301.	0.0075	1.42	0.0	77.43	43.33	0.0	77.43	43.33	0.0	93.23	0.0
IDLE	0.419	474.2	1.502	0.0094	ERBS	301.	0.0046	0.83	0.0	105.35	86.15	0.0	105.35	86.15	0.0	87.18	0.0
IDLE	0.428	473.3	1.496	0.0136	ERBS	300.	0.0071	1.34	0.0	81.54	45.63	0.0	81.54	45.63	0.0	92.74	0.0
APPROACH	1.084	604.3	3.373	0.0122	JET-A	300.	0.0049	0.95	0.0	76.75	32.87	0.0	76.75	32.87	0.0	94.45	6.0
APPROACH	1.086	601.8	3.353	0.0145	JET-A	300.	0.0066	1.30	0.0	52.74	15.72	0.0	52.74	15.72	0.0	96.98	0.0
APPROACH	1.072	603.0	3.362	0.0168	JET-A	300.	0.0073	1.46	0.0	38.47	9.09	0.0	38.47	9.09	0.0	98.04	4.3
APPROACH	1.080	602.7	3.352	0.0185	JET-A	300.	0.0090	1.80	0.0	31.68	5.56	0.0	31.68	5.56	0.0	98.62	5.4
APPROACH	1.081	600.9	3.249	0.0131	ERBS	300.	0.0053	1.03	0.0	71.55	22.19	0.0	71.55	22.19	0.0	95.71	9.0
CRUISE	1.405	668.6	4.190	0.0125	ERBS	305.	0.0071	1.46	0.0	2.04	2.39	0.0	2.04	2.39	0.0	99.67	2.0
CLIMB	1.483	756.8	4.041	0.0137	ERBS	308.	0.0090	1.85	0.0	2.85	0.16	0.0	1.82	0.10	0.0	99.91	0.0
TAKEOFF	1.525	766.8	4.092	0.0144	JET-A	306.	0.0098	2.00	0.0	2.91	0.26	0.0	1.62	0.14	0.0	99.90	3.0
TAKEOFF	1.549	766.2	4.044	0.0129	ERBS	307.	0.0088	1.80	0.0	3.17	0.0	0.0	1.77	0.0	0.0	99.93	9.0
TAKEOFF	1.543	780.7	4.052	0.0117	ERBS	308.	0.0078	1.60	0.0	3.43	0.0	0.0	1.91	0.0	0.0	99.92	8.0

CONFIGURATION M-3

OPERATING CONDITION	INLET PRES MPA	INLET TEMP °K	BURNER AIR KG/SEC	METER F/A RATIO	FUEL TYPE	FUEL TEMP °K	CARBON BAL F/A RATIO	CO2 %	SPEC HUMID G/KG	CORRECTED EMISSIONS — TEST MATRIX — CO EI G/KG	TEST MATRIX THC EI G/KG	TEST MATRIX NOX EI G/KG	ENGINE TABLE CO EI G/KG	ENGINE TABLE THC EI G/KG	ENGINE TABLE NOX EI G/KG	CORR COMB EFFIC	SAE SMOKE #
IDLE	0.432	473.0	1.589	0.0091	JET-A	304.	0.0079	1.55	0.0	60.54	14.33	0.0	60.54	14.33	0.0	96.98	0.0
IDLE	0.433	473.3	1.589	0.0091	JET-A	304.	0.0079	1.55	0.0	60.66	14.36	0.0	60.66	14.36	0.0	96.98	6.0
IDLE	0.438	472.0	1.588	0.0117	JET-A	305.	0.0093	1.85	0.0	51.94	8.30	0.0	51.94	8.30	0.0	97.89	0.0
IDLE	0.434	470.7	1.593	0.0142	JET-A	305.	0.0115	2.30	0.0	44.00	5.42	0.0	44.00	5.42	0.0	98.38	0.0
IDLE	0.424	472.3	1.595	0.0092	JET-A	306.	0.0086	1.70	0.0	54.63	9.05	0.0	54.63	9.05	0.0	97.68	12.0
IDLE	0.430	472.7	1.594	0.0114	JET-A	306.	0.0111	2.20	0.0	47.95	6.88	0.0	47.95	6.88	0.0	98.11	0.0
IDLE	0.432	472.4	1.596	0.0139	JET-A	306.	0.0131	2.60	0.0	43.00	5.44	0.0	43.00	5.44	0.0	98.40	0.0
IDLE	0.423	473.1	1.598	0.0076	JET-A	307.	0.0070	1.38	0.0	62.25	12.21	0.0	62.25	12.21	0.0	97.12	0.0
IDLE	0.426	471.3	1.594	0.0097	ERBS	307.	0.0073	1.42	0.0	68.34	16.46	0.0	68.34	16.46	0.0	96.45	18.0
IDLE	0.432	471.6	1.594	0.0141	ERBS	307.	0.0111	2.20	0.0	48.13	7.93	0.0	48.13	7.93	0.0	97.96	0.0
IDLE	0.426	471.8	1.594	0.0094	ERBS	307.	0.0089	1.75	0.0	59.10	10.05	0.0	59.10	10.05	0.0	97.42	23.0
IDLE	0.432	472.0	1.594	0.0140	ERBS	307.	0.0131	2.60	0.0	48.94	6.70	0.0	48.94	6.70	0.0	98.08	0.0
IDLE	0.430	471.4	1.926	0.0090	JET-A	308.	0.0065	1.26	0.0	84.79	22.30	0.0	84.79	22.30	0.0	95.50	0.0
IDLE	0.437	471.5	1.926	0.0114	JET-A	308.	0.0088	1.75	0.0	57.80	7.12	0.0	57.80	7.12	0.0	97.89	0.0
APPROACH	1.070	601.7	3.403	0.0123	JET-A	304.	0.0098	2.00	0.0	12.73	0.56	0.0	12.73	0.56	0.0	99.64	9.0
APPROACH	1.081	603.2	3.386	0.0148	JET-A	303.	0.0113	2.30	0.0	6.08	0.05	0.0	6.08	0.05	0.0	99.85	10.0
APPROACH	1.085	605.3	3.393	0.0122	ERBS	302.	0.0098	2.00	0.0	7.02	0.0	0.0	7.02	0.0	0.0	99.83	16.0
APPROACH	1.096	606.6	3.376	0.0151	ERBS	301.	0.0120	2.45	0.0	6.12	0.0	0.0	6.12	0.0	0.0	99.86	0.0
CRUISE	1.436	736.1	3.837	0.0147	ERBS	316.	0.0122	2.50	0.0	3.41	0.0	0.0	3.41	0.0	0.0	99.92	42.0
CRUISE	1.433	733.5	3.800	0.0155	JET-A	312.	0.0130	2.65	0.0	2.14	0.0	0.0	2.14	0.0	0.0	99.95	32.0
CRUISE	1.410	737.8	3.791	0.0130	JET-A	313.	0.0105	2.15	0.0	2.88	0.0	0.0	2.88	0.0	0.0	99.93	0.0
TAKEOFF	1.549	789.0	4.015	0.0147	JET-A	306.	0.0122	2.50	0.0	2.20	0.0	0.0	1.23	0.0	0.0	99.95	20.0
TAKEOFF	1.528	781.8	4.004	0.0132	JET-A	309.	0.0103	2.10	0.0	2.20	0.0	0.0	1.23	0.0	0.0	99.95	0.0
TAKEOFF	1.527	783.7	4.030	0.0125	ERBS	308.	0.0100	2.05	0.0	2.45	0.0	0.0	1.36	0.0	0.0	99.94	0.0
TAKEOFF	1.532	787.8	3.974	0.0149	ERBS	310.	0.0122	2.50	0.0	2.10	0.0	0.0	1.17	0.0	0.0	99.95	35.0

CONFIGURATION M-4

OPERATING CONDITION	INLET PRES MPA	INLET TEMP K	BURNER AIR KG/SEC	METER F/A RATIO	FUEL TYPE	FUEL TEMP K	CARBON BAL F/A RATIO	CO2 %	SPEC HUMID G/KG	CORRECTED EMISSIONS — TEST MATRIX — CO EI G/KG	THC EI G/KG	NOX EI G/KG	— ENGINE TABLE — CO EI G/KG	THC EI G/KG	NOX EI G/KG	CORR COMB EFFIC	SAE SMOKE #
IDLE	0.425	472.7	1.430	0.0100	JET-A	301.	0.0075	1.46	0.0	69.97	14.88	0.0	69.97	14.88	0.0	96.65	19.0
IDLE	0.430	477.6	1.420	0.0126	JET-A	302.	0.0099	1.95	0.0	53.65	11.12	0.0	53.65	11.12	0.0	97.49	0.0
IDLE	0.436	479.5	1.417	0.0157	JET-A	302.	0.0128	2.55	0.0	44.09	8.03	0.0	44.09	8.03	0.0	98.09	0.0
IDLE	0.420	480.6	1.380	0.0104	JET-A	304.	0.0094	1.85	0.0	60.31	16.29	0.0	60.31	16.29	0.0	96.67	36.0
IDLE	0.428	478.6	1.442	0.0147	JET-A	304.	0.0161	3.20	0.0	37.93	8.57	0.0	37.93	8.57	0.0	98.14	0.0
IDLE	0.434	475.4	1.437	0.0102	JET-A	304.	0.0071	1.38	0.0	67.23	28.25	0.0	67.23	28.25	0.0	95.27	16.0
IDLE	0.431	473.9	1.420	0.0151	JET-A	305.	0.0103	2.00	0.0	62.13	24.14	0.0	62.13	24.14	0.0	95.82	0.0
IDLE	0.418	474.5	1.425	0.0106	ERBS	306.	0.0077	1.50	0.0	76.66	16.97	0.0	76.66	16.97	0.0	96.12	37.0
IDLE	0.432	471.9	1.442	0.0147	ERBS	305.	0.0117	2.30	0.0	55.02	10.21	0.0	55.02	10.21	0.0	97.53	0.0
IDLE	0.427	473.0	1.424	0.0106	ERBS	305.	0.0093	1.80	0.0	76.57	23.11	0.0	76.57	23.11	0.0	95.49	35.0
IDLE	0.434	471.3	1.415	0.0151	ERBS	304.	0.0157	3.06	0.0	58.78	13.86	0.0	58.78	13.86	0.0	97.04	0.0
APPROACH	1.065	602.3	3.304	0.0723	JET-A	301.	0.0098	2.00	0.0	11.19	0.61	0.0	11.19	0.61	0.0	99.66	10.0
APPROACH	1.078	601.9	3.304	0.0632	JET-A	301.	0.0118	2.40	0.0	5.81	0.0	0.0	5.81	0.0	0.0	99.86	21.0
APPROACH	1.058	601.3	3.288	0.0124	ERBS	300.	0.0103	2.10	0.0	7.26	0.0	0.0	7.26	0.0	0.0	99.82	36.0
CRUISE	1.403	740.1	3.692	0.0629	JET-A	298.	0.0127	2.60	0.0	1.91	0.0	0.0	1.91	0.0	0.0	99.96	11.0
CRUISE	1.352	736.2	3.697	0.0750	ERBS	295.	0.0122	2.50	0.0	3.52	0.0	0.0	3.52	0.0	0.0	99.91	41.0
CLIMB	1.405	754.3	3.733	0.0715	ERBS	296.	0.0132	2.70	0.0	2.19	0.0	0.0	1.40	0.0	0.0	99.94	39.0
TAKEOFF	1.551	780.2	3.890	0.0651	JET-A	298.	0.0122	2.50	0.0	1.47	0.0	0.0	0.82	0.0	0.0	99.97	20.0
TAKEOFF	1.552	766.3	3.808	0.0600	ERBS	298.	0.0132	2.70	0.0	2.12	0.0	0.0	1.18	0.0	0.0	99.95	41.0

CONFIGURATION M-5

OPERATING CONDITION	INLET PRES MPA	INLET TEMP K	BURNER AIR KG/SEC	METER F/A RATIO	FUEL TYPE	FUEL TEMP K	CARBON BAL F/A RATIO	CO2 %	SPEC HUMID G/KG	CORRECTED EMISSIONS — TEST MATRIX — CO EI G/KG	THC EI G/KG	NOX EI G/KG	— ENGINE TABLE — CO EI G/KG	THC EI G/KG	NOX EI G/KG	CORR COMB EFFIC	SAE SMOKE #
IDLE	0.651	286.5	2.717	0.0	10	0.	0.0	0.0	0.0	0.0	0.0	0.0	0.0	0.0	0.0	100.00	0.0
IDLE	0.425	475.5	1.488	0.0186	JET-A	295.	0.0143	2.85	0.0	38.63	5.27	0.0	38.63	5.27	0.0	98.49	0.0
IDLE	0.428	472.6	1.484	0.0158	JET-A	296.	0.0126	2.50	0.0	44.09	7.58	0.0	44.09	7.58	0.0	98.11	0.0
IDLE	0.423	473.3	1.486	0.0126	JET-A	296.	0.0111	2.20	0.0	49.27	10.97	0.0	49.27	10.97	0.0	97.57	0.0
IDLE	0.423	474.6	1.494	0.0118	JET-A	296.	0.0102	2.00	0.0	56.57	12.55	0.0	56.57	12.55	0.0	97.22	0.0
IDLE	0.420	476.3	1.490	0.0106	JET-A	296.	0.0079	1.55	0.0	68.37	17.29	0.0	68.37	17.29	0.0	96.37	12.0
IDLE	0.431	474.6	1.485	0.0097	JET-A	296.	0.0069	1.34	0.0	80.25	22.73	0.0	80.25	22.73	0.0	95.57	0.0
IDLE	0.429	475.1	1.482	0.0089	JET-A	296.	0.0060	1.15	0.0	88.08	29.96	0.0	88.08	29.96	0.0	94.53	0.0
IDLE	0.427	474.7	1.488	0.0160	ERBS	297.	0.0148	2.90	0.0	57.58	12.16	0.0	57.58	12.16	0.0	97.22	39.0
IDLE	0.435	473.3	1.495	0.0113	ERBS	296.	0.0080	1.50	0.0	97.99	39.29	0.0	97.99	39.29	0.0	93.21	26.0
APPROACH	1.064	605.5	3.198	0.0138	JET-A	300.	0.0103	2.10	0.0	0.03	0.14	0.0	0.03	0.14	0.0	99.98	5.0
APPROACH	1.065	607.0	3.179	0.0153	JET-A	300.	0.0117	2.40	0.0	0.03	0.04	0.0	0.03	0.04	0.0	99.99	6.0
APPROACH	1.087	601.6	3.191	0.0186	JET-A	299.	0.0150	3.06	0.0	0.02	0.0	0.0	0.02	0.0	0.0	100.00	30.0
APPROACH	1.047	608.2	3.166	0.0143	ERBS	300.	0.0117	2.40	0.0	0.03	0.17	0.0	0.03	0.17	0.0	99.98	20.0
CRUISE	1.419	741.7	3.595	0.0156	JET-A	297.	0.0122	2.50	0.0	0.01	0.0	0.0	0.01	0.0	0.0	100.00	21.0
CRUISE	1.407	741.6	3.579	0.0152	JET-A	299.	0.0112	2.30	0.0	0.01	0.0	0.0	0.01	0.0	0.0	100.00	8.0
CLIMB	1.474	751.0	3.773	0.0161	ERBS	298.	0.0122	2.50	0.0	0.01	0.0	0.0	0.00	0.0	0.0	100.00	16.0
TAKEOFF	1.499	783.4	3.813	0.0168	JET-A	298.	0.0127	2.60	0.0	0.01	0.0	0.0	0.00	0.0	0.0	100.00	15.0
TAKEOFF	1.501	782.3	3.779	0.0179	JET-A	297.	0.0132	2.70	0.0	0.01	0.0	0.0	0.00	0.0	0.0	100.00	20.0
TAKEOFF	1.478	789.2	3.788	0.0135	JET-A	298.	0.0098	2.00	0.0	0.01	0.0	0.0	0.00	0.0	0.0	100.00	6.0

CONFIGURATION M-6

OPERATING CONDITION	INLET PRES MPA	INLET TEMP °K	BURNER AIR KG/SEC	METER F/A RATIO	FUEL TYPE	FUEL TEMP °K	CARBON BAL F/A RATIO	CO2 %	SPEC HUMID G/KG	CORRECTED EMISSIONS — TEST MATRIX — CO EI G/KG	THC EI G/KG	NOX EI G/KG	CORRECTED EMISSIONS — ENGINE TABLE — CO EI G/KG	THC EI G/KG	NOX EI G/KG	CORR COMB EFFIC	SAE SMOKE #
IDLE	0.431	475.1	1.450	0.0097	JET-A	300.	0.0100	2.01	5.62	17.69	7.16	4.03	17.69	7.16	4.03	98.78	12.5
IDLE	0.428	477.1	1.449	0.0119	JET-A	300.	0.0126	2.55	5.75	15.53	5.38	3.90	15.53	5.38	3.90	99.02	0.0
IDLE	0.428	474.2	1.458	0.0079	JET-A	300.	0.0079	1.60	5.65	23.20	9.83	4.13	23.20	9.83	4.13	98.33	0.0
IDLE	0.427	474.8	1.471	0.0097	ERBS	300.	0.0102	2.05	5.08	26.96	8.35	3.88	26.96	8.35	3.88	98.39	11.9
IDLE	0.428	475.1	1.471	0.0118	ERBS	300.	0.0129	2.60	5.18	24.54	6.22	3.86	24.54	6.22	3.86	98.70	0.0
IDLE	0.430	474.9	1.478	0.0079	ERBS	300.	0.0077	1.54	5.22	34.59	12.28	3.69	34.59	12.28	3.69	97.76	0.0
IDLE	0.430	475.7	1.720	0.0096	ERBS	298.	0.0098	1.98	5.18	28.18	6.26	3.82	28.18	6.26	3.82	98.61	0.0
IDLE	0.428	474.4	1.471	0.0097	11.8%	299.	0.0104	2.09	5.15	30.45	8.33	3.90	30.45	8.33	3.90	98.28	17.5
IDLE	0.432	474.5	1.465	0.0096	COMM	300.	0.0097	1.93	5.30	34.92	9.90	4.38	34.92	9.90	4.38	98.02	15.4
IDLE	0.427	474.4	1.466	0.0119	COMM	300.	0.0125	2.50	5.26	27.43	7.21	4.24	27.43	7.21	4.24	98.50	0.0
IDLE	0.426	473.9	1.466	0.0078	COMM	301.	0.0074	1.47	5.22	42.24	14.69	4.30	42.24	14.69	4.30	97.25	0.0
IDLE	0.428	475.2	1.473	0.0096	ERBS	300.	0.0097	1.96	5.07	26.19	7.41	3.96	26.19	7.41	3.96	98.52	11.9
IDLE	0.429	474.6	1.476	0.0095	ERBS	300.	0.0114	2.29	5.12	26.58	7.30	3.81	26.58	7.30	3.81	98.52	12.7
IDLE	0.429	475.0	1.477	0.0095	ERBS	300.	0.0111	2.21	5.13	28.79	9.01	3.65	28.79	9.01	3.65	98.27	12.4
APPROACH	1.081	600.9	3.245	0.0134	JET-A	300.	0.0137	2.79	6.60	2.97	0.75	8.78	2.97	0.75	8.78	99.84	9.1
APPROACH	1.080	602.9	3.249	0.0135	ERBS	300.	0.0130	2.66	6.59	2.94	0.69	9.30	2.94	0.69	9.30	99.85	7.9
CRUISE	1.419	741.1	3.682	0.0191	JET-A	297.	0.0189	3.83	6.93	1.22	0.31	18.32	1.22	0.31	18.32	99.94	68.9
CRUISE	1.425	748.9	3.667	0.0192	ERBS	294.	0.0190	3.85	6.66	2.18	0.52	17.96	2.18	0.52	17.96	99.89	69.6
CRUISE	1.420	740.2	3.668	0.0198	11.8%	301.	0.0195	3.95	6.93	2.15	0.61	18.87	2.15	0.61	18.87	99.88	77.5
CRUISE	1.411	742.2	3.665	0.0194	COMM	300.	0.0188	3.82	6.96	1.41	0.43	19.21	1.41	0.43	19.21	99.92	70.5
CLIMB	2.044	758.0	5.215	0.0218	JET-A	297.	0.0215	4.35	5.95	1.26	0.14	16.59	0.80	0.09	20.76	99.97	79.0
CLIMB	2.031	757.2	5.193	0.0219	ERBS	293.	0.0213	4.31	6.66	1.94	0.09	17.14	1.24	0.05	21.44	99.96	82.3
TAKEOFF	2.213	790.5	5.510	0.0250	JET-A	299.	0.0227	4.60	6.45	2.39	0.11	18.73	1.33	0.06	25.10	99.95	62.9
TAKEOFF	2.309	791.4	5.188	0.0235	ERBS	292.	0.0228	4.60	6.75	2.07	0.09	20.61	1.15	0.05	27.62	99.96	83.1
TAKEOFF	2.202	803.0	5.497	0.0212	ERBS	292.	0.0204	4.13	6.84	2.62	0.12	20.96	1.46	0.07	28.10	99.95	0.0
TAKEOFF	2.210	795.5	5.528	0.0168	ERBS	293.	0.0161	3.28	7.03	2.42	0.15	22.29	1.35	0.08	29.87	99.95	0.0
TAKEOFF	2.214	791.7	5.506	0.0249	11.8%	298.	0.0235	4.74	6.78	3.67	0.12	19.60	2.05	0.07	26.26	99.93	78.2
TAKEOFF	2.192	791.0	5.478	0.0246	COMM	294.	0.0224	4.53	6.44	2.21	0.11	20.37	1.23	0.06	27.30	99.95	64.7
TAKEOFF	2.194	789.6	4.930	0.0242	ERBS	294.	0.0223	4.51	6.02	2.89	0.10	14.60	1.61	0.05	19.56	99.94	0.0

CONFIGURATION M-7

OPERATING CONDITION	INLET PRES MPA	INLET TEMP °K	BURNER AIR KG/SEC	METER F/A RATIO	FUEL TYPE	FUEL TEMP °K	CARBON BAL F/A RATIO	CO2 %	SPEC HUMID G/KG	CORRECTED EMISSIONS — TEST MATRIX — CO EI G/KG	THC EI G/KG	NOX EI G/KG	CORRECTED EMISSIONS — ENGINE TABLE — CO EI G/KG	THC EI G/KG	NOX EI G/KG	CORR COMB EFFIC	SAE SMOKE #
IDLE	0.429	473.4	1.451	0.0096	JET-A	309.	0.0091	1.84	0.76	20.86	2.03	3.37	20.86	2.03	3.37	99.28	19.0
IDLE	0.429	472.5	1.453	0.0094	ERBS	309.	0.0088	1.77	0.74	24.24	1.58	3.76	24.24	1.58	3.76	99.24	22.6
IDLE	0.427	473.0	1.454	0.0117	ERBS	310.	0.0122	2.47	0.76	18.17	0.87	3.91	18.17	0.87	3.91	99.47	0.0
IDLE	0.411	473.8	1.455	0.0074	ERBS	311.	0.0077	1.55	0.75	30.49	2.00	3.57	30.49	2.00	3.57	99.01	0.0
APPROACH	1.078	610.3	3.235	0.0136	JET-A	313.	0.0179	3.64	0.49	2.93	0.08	8.38	2.93	0.08	8.38	99.92	28.7
APPROACH	1.075	612.1	3.250	0.0134	ERBS	309.	0.0179	3.62	0.48	3.92	0.03	2.72	3.92	0.03	2.72	99.90	33.9
CRUISE	1.420	735.9	3.633	0.0209	JET-A	310.	0.0227	4.59	0.42	1.49	0.03	16.80	1.49	0.03	16.80	99.96	13.8
CRUISE	1.422	740.5	3.631	0.0206	ERBS	313.	0.0226	4.57	0.43	2.10	0.03	14.29	2.10	0.03	14.29	99.95	11.3
CLIMB	1.972	757.6	5.098	0.0220	JET-A	309.	0.0218	4.42	0.34	1.21	0.08	21.82	0.78	0.05	27.30	99.97	67.0
CLIMB	1.933	755.4	5.093	0.0216	ERBS	304.	0.0222	4.49	0.33	1.50	0.08	20.21	0.96	0.05	25.28	99.96	75.8
TAKEOFF	2.041	788.4	5.143	0.0227	JET-A	305.	0.0203	4.12	0.34	0.78	0.06	22.50	0.43	0.04	30.16	99.98	54.6
TAKEOFF	2.041	792.0	5.143	0.0228	ERBS	310.	0.0208	4.23	0.34	0.96	0.06	20.90	0.54	0.04	28.01	99.98	54.1
TAKEOFF	2.038	791.9	5.138	0.0197	ERBS	311.	0.0168	3.42	0.33	0.96	0.07	22.72	0.54	0.04	30.45	99.98	0.0
TAKEOFF	2.038	789.6	5.116	0.0168	ERBS	310.	0.0163	3.32	0.34	0.79	0.07	22.54	0.44	0.04	30.22	99.98	0.0

CONFIGURATION M-8

OPERATING CONDITION	INLET PRES MPA	INLET TEMP °K	BURNER AIR KG/SEC	METER F/A RATIO	FUEL TYPE	FUEL TEMP °K	CARBON BAL F/A RATIO	CO2 %	SPEC HUMID G/KG	CORRECTED EMISSIONS — TEST MATRIX — CO EI G/KG	TEST MATRIX — THC EI G/KG	TEST MATRIX — NOX EI G/KG	CORRECTED EMISSIONS — ENGINE TABLE — CO EI G/KG	ENGINE TABLE — THC EI G/KG	ENGINE TABLE — NOX EI G/KG	CORR COMB EFFIC	SAE SMOKE #
IDLE	0.434	472.3	1.458	0.0147	JET-A	307.	0.0145	2.91	1.30	24.23	3.71	3.79	24.23	3.71	3.79	99.03	26.0
IDLE	0.436	471.4	1.462	0.0146	ERBS	308.	0.0144	2.89	1.41	26.38	4.94	3.65	26.38	4.94	3.65	98.82	33.2
IDLE	0.430	472.1	1.464	0.0176	ERBS	307.	0.0174	3.47	1.41	28.50	2.93	3.76	28.50	2.93	3.76	98.99	0.0
IDLE	0.431	471.1	1.468	0.0112	ERBS	309.	0.0104	2.06	1.45	38.35	12.34	3.26	38.35	12.34	3.26	97.67	0.0
APPROACH	1.081	601.1	3.306	0.0201	JET-A	309.	0.0184	3.73	1.03	1.99	0.04	8.38	1.99	0.04	8.38	99.95	56.0
APPROACH	1.082	606.1	3.276	0.0210	ERBS	309.	0.0194	3.94	0.96	4.38	0.10	9.12	4.38	0.10	9.12	99.83	54.0
CRUISE	1.421	737.7	3.608	0.0187	JET-A	311.	0.0163	3.31	0.84	0.67	0.02	17.99	0.67	0.02	17.99	99.98	13.4
CRUISE	1.421	738.6	3.602	0.0186	ERBS	313.	0.0162	3.31	0.87	0.74	0.02	17.99	0.74	0.02	17.99	99.98	13.4
CLIMB	1.672	750.4	4.344	0.0170	JET-A	314.	0.0148	3.02	0.89	0.49	0.05	18.85	0.32	0.03	23.58	99.98	5.3
CLIMB	1.667	751.3	4.353	0.0167	ERBS	313.	0.0144	2.94	0.82	0.61	0.02	19.43	0.39	0.01	24.31	99.99	7.3
TAKEOFF	1.728	785.8	4.329	0.0165	JET-A	314.	0.0143	2.91	0.87	0.42	0.05	21.96	0.24	0.03	29.43	99.99	4.3
TAKEOFF	1.732	786.9	4.320	0.0169	ERBS	313.	0.0144	2.94	0.95	0.52	0.05	22.21	0.29	0.03	29.77	99.98	4.9
TAKEOFF	1.727	784.6	4.197	0.0152	ERBS	316.	0.0132	2.69	0.85	0.47	0.06	22.78	0.26	0.03	30.54	99.98	0.0
TAKEOFF	1.733	785.4	4.222	0.0136	ERBS	317.	0.0115	2.35	0.86	0.56	0.06	22.35	0.31	0.04	29.96	99.98	0.0

CONFIGURATION M-9

OPERATING CONDITION	INLET PRES MPA	INLET TEMP °K	BURNER AIR KG/SEC	METER F/A RATIO	FUEL TYPE	FUEL TEMP °K	CARBON BAL F/A RATIO	CO2 %	SPEC HUMID G/KG	CORRECTED EMISSIONS — TEST MATRIX — CO EI G/KG	TEST MATRIX — THC EI G/KG	TEST MATRIX — NOX EI G/KG	CORRECTED EMISSIONS — ENGINE TABLE — CO EI G/KG	ENGINE TABLE — THC EI G/KG	ENGINE TABLE — NOX EI G/KG	CORR COMB EFFIC	SAE SMOKE #
IDLE	0.430	471.6	1.459	0.0098	JET-A	307.	0.0085	1.67	1.64	46.58	24.42	2.74	46.58	24.42	2.74	96.13	11.7
IDLE	0.433	470.8	1.456	0.0098	ERBS	307.	0.0080	1.56	1.61	51.39	25.70	2.47	51.39	25.70	2.47	95.84	8.5
IDLE	0.429	472.1	1.455	0.0111	ERBS	306.	0.0083	1.63	1.64	44.15	21.51	0.16	44.15	21.51	0.16	96.46	0.0
IDLE	0.430	471.5	1.454	0.0090	ERBS	307.	0.0067	1.28	1.68	58.59	38.48	0.08	58.59	38.48	0.08	94.15	0.0
APPROACH	1.082	600.4	3.221	0.0135	JET-A	308.	0.0116	2.36	1.17	2.73	0.77	7.49	2.73	0.77	7.49	99.85	10.0
APPROACH	1.082	602.1	3.218	0.0128	ERBS	309.	0.0106	2.16	1.20	3.94	0.40	7.38	3.94	0.40	7.38	99.86	19.0
CRUISE	1.422	734.5	3.591	0.0203	JET-A	310.	0.0170	3.46	0.97	0.94	0.02	16.86	0.94	0.02	16.86	99.98	20.4
CRUISE	1.411	735.2	3.575	0.0198	ERBS	310.	0.0165	3.36	0.99	1.12	0.04	0.21	1.12	0.04	0.21	99.97	28.3
CLIMB	1.700	748.2	4.617	0.0216	JET-A	307.	0.0186	3.79	0.79	1.06	0.04	15.45	0.67	0.02	19.33	99.97	27.1
CLIMB	1.696	748.2	4.621	0.0223	ERBS	311.	0.0188	3.82	0.79	1.15	0.04	16.03	0.73	0.03	20.05	99.97	34.6
IDLE	0.432	473.6	1.464	0.0095	ERBS	315.	0.0004	0.09	2.52	0.0	0.0	0.0	0.0	0.0	0.0	100.00	0.0

CONFIGURATION M-10

OPERATING CONDITION	INLET PRES MPA	INLET TEMP °K	BURNER AIR KG/SEC	METER F/A RATIO	FUEL TYPE	FUEL TEMP °K	CARBON BAL F/A RATIO	CO2 %	SPEC HUMID G/KG	CORRECTED EMISSIONS — TEST MATRIX — CO EI G/KG	THC EI G/KG	NOX EI G/KG	CORRECTED EMISSIONS — ENGINE TABLE — CO EI G/KG	THC EI G/KG	NOX EI G/KG	CORR COMB EFFIC	SAE SMOKE #
IDLE	0.433	473.1	1.423	0.0091	JET-A	366.	0.0080	1.59	1.18	36.59	10.56	2.76	36.59	10.56	2.76	97.96	10.2
IDLE	0.424	470.2	1.445	0.0093	ERBS	341.	0.0078	1.55	1.13	43.82	17.30	2.62	43.82	17.30	2.62	96.92	15.4
IDLE	0.430	471.7	1.453	0.0114	ERBS	356.	0.0100	1.98	1.19	48.23	13.89	2.68	48.23	13.89	2.68	97.25	0.0
IDLE	0.434	471.2	1.445	0.0070	ERBS	348.	0.0057	1.12	1.14	41.29	20.64	2.48	41.29	20.64	2.48	96.66	0.0
APPROACH	1.081	606.8	3.285	0.0133	ERBS	404.	0.0121	2.46	0.95	6.07	0.72	6.07	6.07	0.72	6.07	99.77	9.9
APPROACH	1.078	607.4	3.278	0.0137	ERBS	310.	0.0100	1.95	0.94	38.12	33.62	4.30	38.12	33.62	4.30	95.15	0.5
CRUISE	1.414	742.8	3.619	0.0202	ERBS	314.	0.0148	2.99	0.83	11.72	4.31	11.00	11.72	4.31	11.00	99.22	0.5
CRUISE	1.411	742.7	3.623	0.0204	ERBS	312.	0.0143	2.88	0.84	13.50	4.94	12.03	13.50	4.94	12.03	99.10	0.5
CRUISE	1.417	742.2	3.609	0.0201	ERBS	309.	0.0130	2.52	0.84	56.75	29.82	9.76	56.75	29.82	9.76	95.18	0.5
CRUISE	1.422	741.3	3.615	0.0204	JET-A	312.	0.0143	2.90	0.85	10.91	3.96	11.87	10.91	3.96	11.87	99.29	0.5
CLIMB	1.848	753.3	4.649	0.0228	ERBS	311.	0.0157	3.16	0.79	24.46	3.07	13.17	15.63	1.96	16.48	99.23	0.5
TAKEOFF	1.836	788.1	4.599	0.0256	JET-A	310.	0.0181	3.67	0.74	11.02	1.01	14.99	6.13	0.56	20.10	99.69	0.5
TAKEOFF	1.845	786.3	4.599	0.0245	ERBS	310.	0.0170	3.44	0.76	21.10	1.65	15.35	11.74	0.92	20.57	99.43	0.5

CONFIGURATION M-11

OPERATING CONDITION	INLET PRES MPA	INLET TEMP °K	BURNER AIR KG/SEC	METER F/A RATIO	FUEL TYPE	FUEL TEMP °K	CARBON BAL F/A RATIO	CO2 %	SPEC HUMID G/KG	CORRECTED EMISSIONS — TEST MATRIX — CO EI G/KG	THC EI G/KG	NOX EI G/KG	CORRECTED EMISSIONS — ENGINE TABLE — CO EI G/KG	THC EI G/KG	NOX EI G/KG	CORR COMB EFFIC	SAE SMOKE #
IDLE	0.426	472.2	1.455	0.0095	JET-A	365.	0.0089	1.77	1.34	38.50	17.87	2.94	38.50	17.87	2.94	97.04	8.4
IDLE	0.428	471.3	1.454	0.0116	JET-A	365.	0.0118	2.32	1.39	50.84	16.72	3.05	50.84	16.72	3.05	96.90	0.0
IDLE	0.425	471.9	1.454	0.0079	JET-A	365.	0.0073	1.45	1.38	33.33	18.74	2.96	33.33	18.74	2.96	97.06	0.0
IDLE	0.424	470.2	1.444	0.0095	ERBS	356.	0.0087	1.72	1.72	39.65	20.11	2.82	39.65	20.11	2.82	96.69	19.5
IDLE	0.433	470.6	1.444	0.0116	ERBS	353.	0.0110	2.17	1.53	45.86	21.93	2.98	45.86	21.93	2.98	96.40	0.0
IDLE	0.432	470.4	1.437	0.0080	ERBS	359.	0.0070	1.39	1.57	36.73	20.78	2.58	36.73	20.78	2.58	96.74	0.0
IDLE	0.430	471.8	1.451	0.0097	11.8%	364.	0.0088	1.74	1.39	46.49	18.72	3.03	46.49	18.72	3.03	96.68	20.1
IDLE	0.429	471.7	1.452	0.0092	COMM	363.	0.0082	1.62	1.50	43.03	20.20	2.95	43.03	20.20	2.95	96.61	18.6
IDLE	0.432	471.8	1.462	0.0136	COMM	361.	0.0110	2.17	1.51	45.20	15.55	2.81	45.20	15.55	2.81	97.12	0.0
IDLE	0.426	472.1	1.450	0.0081	COMM	364.	0.0069	1.37	1.50	40.87	21.83	2.78	40.87	21.83	2.78	96.45	0.0
APPROACH	1.077	604.9	3.274	0.0136	JET-A	395.	0.0125	2.54	0.91	7.00	1.30	4.71	7.00	1.30	4.71	99.69	8.2
APPROACH	1.082	606.4	3.289	0.0143	JET-A	331.	0.0108	2.13	0.92	24.22	24.86	4.80	24.22	24.86	4.80	96.58	1.4
APPROACH	1.078	606.8	3.268	0.0138	JET-A	326.	0.0098	1.92	1.00	30.49	30.24	4.62	30.49	30.24	4.62	95.80	0.5
APPROACH	1.085	604.6	3.273	0.0139	ERBS	330.	0.0102	2.01	0.87	32.32	29.18	4.80	32.32	29.18	4.80	95.84	0.5
APPROACH	1.077	607.9	3.265	0.0140	ERBS	326.	0.0094	1.85	0.96	31.33	31.51	4.68	31.33	31.51	4.68	95.56	0.5
APPROACH	1.074	603.8	3.303	0.0139	ERBS	415.	0.0129	2.62	0.93	7.90	1.82	5.78	7.90	1.82	5.78	99.60	11.3
CRUISE	1.425	730.2	3.660	0.0197	ERBS	338.	0.0160	3.23	0.91	11.27	2.90	9.47	11.27	2.90	9.47	99.40	10.8
CRUISE	1.418	737.8	3.675	0.0197	ERBS	328.	0.0136	2.76	0.90	12.23	4.97	10.64	12.23	4.97	10.64	99.13	0.6
CRUISE	1.429	736.8	3.656	0.0204	ERBS	324.	0.0125	2.51	0.95	17.74	7.61	11.69	17.74	7.61	11.69	98.70	0.5
CRUISE	1.422	739.0	3.671	0.0187	COMM	329.	0.0130	2.64	0.91	10.07	4.29	19.69	10.07	4.29	19.69	99.26	2.8
CRUISE	1.427	737.9	3.668	0.0203	11.8%	329.	0.0143	2.89	0.93	11.18	3.84	10.99	11.18	3.84	10.99	99.28	2.0
CRUISE	1.423	737.5	3.658	0.0193	JET-A	330.	0.0133	2.70	0.99	6.85	2.90	10.72	6.85	2.90	10.72	99.51	12.3
CLIMB	1.652	752.9	4.262	0.0221	JET-A	328.	0.0158	3.19	0.94	8.71	1.65	10.09	5.56	1.06	12.62	99.64	25.6
CLIMB	1.654	752.6	4.273	0.0218	ERBS	328.	0.0162	3.26	1.05	14.55	2.13	4.05	9.30	1.36	5.07	99.45	33.1
TAKEOFF	1.632	781.7	4.105	0.0238	JET-A	329.	0.0170	3.44	0.98	9.87	0.97	9.71	5.50	0.54	13.02	99.68	28.0
TAKEOFF	1.632	782.2	4.106	0.0238	ERBS	330.	0.0167	3.37	0.87	10.16	1.20	12.47	5.66	0.67	16.71	99.65	27.4
TAKEOFF	1.626	784.2	4.116	0.0237	11.8%	331.	0.0168	3.40	0.95	11.16	1.18	11.51	6.22	0.66	15.43	99.62	27.2
TAKEOFF	1.633	782.4	4.101	0.0246	COMM	328.	0.0175	3.53	0.97	10.40	0.95	11.22	5.79	0.53	15.04	99.66	28.9
TAKEOFF	1.626	784.4	4.105	0.0156	JET-A	680.	0.0099	2.02	0.87	1.04	0.12	13.63	0.58	0.07	18.26	99.96	25.3
CRUISE	1.409	738.1	3.614	0.0134	JET-A	640.	0.0086	1.77	0.88	1.21	0.11	10.02	1.21	0.11	10.02	99.96	15.0
APPROACH	1.112	603.3	3.281	0.0085	JET-A	529.	0.0057	1.16	1.03	3.20	0.63	6.43	3.20	0.63	6.43	99.86	14.2

CONFIGURATION M-12

OPERATING CONDITION	INLET PRES MPA	INLET TEMP °K	BURNER AIR KG/SEC	METER F/A RATIO	FUEL TYPE	FUEL TEMP °K	CARBON BAL F/A RATIO	CO2 %	SPEC HUMID G/KG	CORRECTED EMISSIONS — TEST MATRIX — CO EI G/KG	THC EI G/KG	NOX EI G/KG	— ENGINE TABLE — CO EI G/KG	THC EI G/KG	NOX EI G/KG	CORR COMB EFFIC	SAE SMOKE #
*********	*****	*****	******	******	*****	****	******	****	*****	******	******	******	******	******	******	******	*****
IDLE	0.428	465.7	1.488	0.0094	JET-A	425.	0.0082	1.64	1.91	35.26	11.60	2.94	35.26	11.60	2.94	97.85	23.7
IDLE	0.427	467.8	1.537	0.0091	ERBS	424.	0.0080	1.59	1.82	34.18	12.90	3.04	34.18	12.90	3.04	97.68	16.7
IDLE	0.432	466.8	1.475	0.0117	ERBS	423.	0.0099	1.97	1.85	32.21	10.31	3.11	32.21	10.31	3.11	98.05	0.0
IDLE	0.431	469.3	1.590	0.0072	ERBS	423.	0.0065	1.28	1.80	38.45	20.01	2.88	38.45	20.01	2.88	96.78	0.0
APPROACH	1.091	602.1	3.322	0.0133	ERBS	393.	0.0122	2.48	1.08	5.56	0.66	5.91	5.56	0.66	5.91	99.79	48.9
APPROACH	1.085	603.1	3.377	0.0143	ERBS	316.	0.0108	2.14	1.06	27.81	19.47	4.70	27.81	19.47	4.70	97.08	20.8
APPROACH	1.076	603.2	3.407	0.0138	ERBS	320.	0.0111	2.23	1.06	16.29	7.56	4.71	16.29	7.56	4.71	98.72	38.8
CRUISE	1.425	737.9	3.663	0.0208	ERBS	322.	0.0153	3.10	1.02	6.63	1.29	11.45	6.63	1.29	11.45	99.69	38.5
CRUISE	1.415	736.9	3.618	0.0211	ERBS	325.	0.0169	3.43	0.94	5.01	0.83	9.81	5.01	0.83	9.81	99.78	52.8
CRUISE	1.414	740.1	3.641	0.0210	JET-A	322.	0.0153	3.12	1.11	4.03	1.09	11.60	4.03	1.09	11.60	99.78	32.1
CLIMB	1.716	747.1	4.392	0.0233	ERBS	322.	0.0169	3.42	1.04	8.38	1.27	11.52	5.36	0.81	14.41	99.69	34.9
TAKEOFF	1.749	780.3	4.251	0.0267	JET-A	322.	0.0201	4.07	1.08	6.33	0.60	13.27	3.52	0.34	17.79	99.81	31.0
TAKEOFF	1.767	779.5	4.386	0.0240	ERBS	322.	0.0174	3.51	1.05	9.04	0.88	12.57	5.03	0.49	16.85	99.73	36.0

CONFIGURATION M-13

REFERENCES

1. R. Roberts, A. Peduzzi, and G. E. Vitti, "Experimental Clean Combustor Program, Phase II, Alternate Fuels Addendum," NASA CR-134970, July 1976.

2. C. C. Gleason and D. W. Bahr, "Experimental Clean Combustor Program, Alternate Fuels Addendum, Phase II Final Report," NASA CR-134972, January 1976.

3. J. P. Longwell, Editor, "Jet Aircraft Hydrocarbon Fuels Technology," Proceedings of Workshop held at NASA Lewis June 7-9, 1977, NASA Conference Publication 2033, 1978.

4. R. P. Lohmann, E. J. Szetela, A. Vranos, "Analytical Evaluation of the Impact of Broad Specification Fuels on High Bypass Turbofan Combustors," NASA CR-159454, December 1978.

5. R. P. Lohmann, R. A. Jeroszko, "Broad Specification Fuels Combustion Technology Program, Phase I," NASA CR-168180, July 1983.

6. J. S. Fear, "The NASA Broad Specification Fuels Combustion Technology Program - An Assessment of Phase I Test Results," American Society of Mechanical Engineers Paper 83JPGC-GT-16, September 1983.

7. R. P. Lohmann, J. S. Fear, "NASA Broad Specification Fuels Combustion Technology Program - Pratt and Whitney Aircraft Phase I Results and Status," AIAA Paper 82-1088, 18th Joint Propulsion Conference, June 1982.

8. R. Roberts, A. Peduzzi, G. E. Vitti, "Experimental Clean Combustor Program, Phase I, Final Report," NASA CR-134756, October 1975.

9. R. Roberts, A. Peduzzi, G. E. Vitti, "Experimental Clean Combustor Program, Phase II, Final Report," NASA CR-134969, November 1976.

10. R. Roberts, A. Fiorentino, W. Greene, "Experimental Clean Combustor Program, Phase III, Final Report," NASA CR-135253, October 1977.

11. D. J. Dubiel, W. Greene, C. V. Sundt, S. Tanrikut, M. H. Zeisser, "Energy Efficient Engine Sector Combustor Rig Test Program Technology Report," NASA CR-167913, September 1982.

12. W. Greene, S. Tanrikut, D. Sokolowski, "Development and Operating Characteristics of an Advanced Two Stage Combustor," American Institute of Aeronautics and Astronautics Paper 82-0191, 1982.

13. A. J. Fiorentino, W. Greene, J. Kim, "Lean Premixed Prevaporized Fuel Combustor Conceptual Design Study," NASA CR-159647, August 1979.

14. T. R. Clements and R. R. Kazmar, "Variable Geometry Combustor Development," Air Force Aeropropulsion Laboratory Report AFWAL-TR-80-2102, October 1980.

15. S. J. Markowski, B. V. Johnson, R. L. Marshall, "Combustion Experiments with a New Burner Air Distribution Concept," American Society of Mechanical Engineers Paper 83-GT-31, 1983.

16. B. V. Johnson, S. J. Markowski, H. M. Craig, "Cold Flow and Combustion Experiments with a New Burner Air Distribution Concept," American Society of Mechanical Engineers 30th International Gas Turbine Conference, March 1985.

17. Environmental Protection Agency, "Control of Air Pollution from Aircraft and Aircraft Engines," Federal Register 40 CFR Part 87 (43 FR 12615), March 24, 1978.

18. Environmental Protection Agency, "Control of Air Pollution from Aircraft and Aircraft Engines," Federal Register 40 CFR 87 Vol. 47, No. 251, December 30, 1982.

19. International Civil Aviation Organization, "International Standard for Aircraft Emissions," Annex 16, Vol. II, 1981.

20. Moffat, R. J., Hunn, B. D. and Ayers, J. F., "Development of a Transpiration Radiometer," Transactions of Instrument Society of America, Vol 4, 1971.

21. Atkinson, W. H., Cyr, M. A. and Strange, R. R., "Development of Advanced High Temperature Heat Flux Sensors - Phase II Xerification Testing", NASA CR-174973, August 1985.

22. Federal Register, Vol. 38, No. 136, July 17, 1973.

23. Odgers, J. and Kretschmer, D., "Considerations of the use of Vitiated Preheat", AIAA Journal of Energy, Vol 4, No. 6, pp. 260-265, 1980.

DISTRIBUTION LIST

CR - 191066

I. NASA		Copies
2.	NASA Lewis Research Center 21000 Brookpark Road Cleveland, OH 44135	
	Attn: Report Control Office MS 60-1	1
	Technology Utilization Office MS 7-3	1
	P. L. Burstadt MS 100-5	1
	J. E. Bolander MS 500-305	1
	Library MS 60-3	1
	R. W. Niedzwiecki MS 77-10	1
	E. J. Mularz MS 5-11	1
	AFSC Liaison Office MS 501-3	1
	Propulsion Directorate, USARTL MS 77-12	1
	Project Manager, J. S. Fear MS 100-5	40
2.	NASA Headquarters Attn: RS/Director, Subsonic Transportation Division 600 Independence Avenue, S. W. Washington, DC 20546	
	NASA Scientific & Technical Information Facility Attn: Accessioning Department P. O.. Box 8757 Baltimore/Washington International Airport MD 21240	25

II. OTHER GOVERNMENT AGENCIES	Copies
1. Air Force Office of Scientific Research Attn: J. Tischkoff Bolling AFB Washington, DC 20332	1
2. Sverdrup Corp. Attn: Library Arnold Air Force Station, TN 37389	1
3. Chief Army Research Office Attn: D. Mann P. O. Box 12211 Research Triangle Park, NC 27709	1
*4. Commander U. S. Army Aviation R&D Command Attn: DRDAV-EQP (L. Bell) 4300 Goodfellow Blvd. St. Louis, MO 63120	1
5. Commander U. S. Army Fuels & Lubricants Research Lab. Southwest Research Institute Attn: C. Moses P. O. Drawer 28510 San Antonio, TX 78284	1
6. Defense Documentation Center Cameron Station 5010 Duke Street Alexandria, VA 22314	1
*7. Director, Applied Tech. Laboratory Attn: DAVDL-ATL-AT (R. Bolton) U. S. Army Research & Tech. Lab. (AVRADCOM) Ft. Eustis, VA 23604	1
8. Environmental Protection Agency Attn: Library Mail Drop 65 Research Triangle Park, NC 27111	1
*9. Environmental Protection Agency Attn: W. Lanier Mail Drop 65 Research Triangle Park, NC 27111	1
10. FAA Headquarters Attn: N. Krull 800 Independence Avenue SW Washington, DC 20591	1

Other Government Agencies (Cont'd)

11. FAA Headquarters — 1
    Attn: Library
    2100 Second Street, SW
    Washington, DC 20591

*12. Jet Propulsion Laboratory — 1
    Attn: M. Clayton MS 125-224
    4800 Oak Grove Drive
    Pasadena, CA 91103

*13. Sandia Laboratories — 1
    Attn: D. Hartley
    Combustion Sciences Department
    Livermore, CA 94055

14. Naval Air Propulsion Center — 1
    Attn: S. Clouser PE-42
    P. O. Box 7176
    Trenton, NJ 08628

15. Naval Air Propulsion Center — 1
    Attn: P. Karpovich PE-71
    P. O. Box 7176
    Trenton, NJ 08628

16. Naval Air Propulsion Center — 1
    Attn: R. Kamin PE-71
    P. O. Box 7176
    Trenton, NJ 08628

17. Wright-Patterson Air Force Base — 1
    Attn: E. Graber AFWAL/NASA-PO
    Wright-Patterson AFB, OH 45433

18. Wright-Patterson Air Force Base — 1
    Attn: T. Jackson AFWAL/POSF
    Wright-Patterson AFB, OH 45433

*19. Wright-Patterson Air Force Base — 1
    Attn: J. Petty AFWAL/TBC
    Wright-Patterson AFB, OH 45433

20. Wright-Patterson Air Force Base — 1
    Attn: C. Martel AFWAL/POSF
    Wright-Patterson AFB, OH 45433

*21. FAA/NAFEC — 1
    Attn: W. Westfield, ANA-310
    Atlantic City, NJ 08405

*22. United States Air Force — 1
    Attn: Major J. Slankas/AFESC/RDVC
    Tyndall Air Force Base, FL 32403

III. UNIVERSITIES	Copies
1. Purdue University Attn: Prof. A. H. Lefebvre School of Mechanical Engineering West Lafayette, IN 47907	1
2. Department of Mechanical Engineering Attn: Prof. J. Odgers Laval University Quebec, CANADA Gik 7Pa	1
3. University of California Attn: Prof. R. F. Sawyer Mechanical and Environmental Eng. Berkley, CA 94720	1
4. University of California Attn: Prof. G. S. Samuelson Department of Mechanical Engineering Irvine, CA 92717	1
5. University of California Attn: Prof. W. Sirignano Mechanical and Environmental Eng. Irvine, CA 92717	1
6. University of California - San Diego Attn: Prof. P. Libby Dept. of Applied Mechanics and Engineering Sciences Mail Code B-010 La Jolla, CA 92093	1
7. University of California - Berkley Attn: Prof. A.. K. Oppenheim Dept. of Mechanical Engineering Berkely, CA 94720	1
*8. University of Illinois at Urbana-Champaign Attn: Prof. R. A. Strehlow Dept. of Aeronautical & Astronautical Engineering 101 Transportation Building Urbana, IL 61801	1
*9. University of Michigan Attn: Prof. A. Nicholls Department of Aerospace Engineering Gas Dynamics Lab. North Campus Ann Arbor, MI 48105	1

Universities (cont'd)

*10. University of Southern California — 1
Associate Dean of Engineering
Attn: Prof. Melvin Gerstein
School of Engineering
Los Angeles, CA 90007

11. Carnegie-Mellon University — 1
Department of Mechanical Engineering
Pittsburgh, PA 15213

12. Drexel University — 1
Dept. of Mechanical Engineering and Mechanics
Philadelphia, PA 19104

13. Oklahoma State University — 1
Attn: Prof. David Lilley
Dept. of Mechanical and Aerospace Engineering
Engineering North 218
Stillwater, OK 74074

14. Vanderbilt University — 1
Attn: Prof. A. M. Mellor
Dept. of Mechanical Engineering
Nashville, TN 37235

IV. INDUSTRY	Copies
1. Avco/Lycoming Corp. Attn: N. Marachionna 550 South Main Street Stratford, CT 06497	1
2. Avco/Lycoming Corp. Attn: Library 550 South Main Street Stratford, CT 06497	1
*3. Battelle Columbus Laboratories Attn: D. Locklin 505 King Avenue Columbus, OH 43201	1
4. Battelle Columbus Laboratories Attn: Library 505 King Avenue Columbus, OH 43201	1
5. Calspan Corporation Attn: Library 4455 Genesee Street Buffalo, NY 14221	1
6. Curtiss-Wright Corporation Attn: Library One Passaic Street Woodridge, NJ 07075	1
*7. Detroit Diesel Allison Div. Attn: J. Tomlinson Department 8882, Plant 8 Speed Code U27A P. O. Box 894 Indianapolis, IN 46202	1
*8. Detroit Diesel Allison Div. Attn: R. Sullivan Speed Code U27A P. O. Box 894 Indianapolis, IN 46202	1
9. Detroit Diesel Allison Div. Attn: H. Mongia Speed Code T-01 P. O. Box 420 Indianapolis, IN 46202	1

Industry (Cont'd)

10. Detroit Diesel Allison Div. — 1
    Attn: P. Ross
    Speed Code T-01
    P. O. Box 420
    Indianapolis, IN 46202

11. Electric Power Research Institute — 1
    Attn: L. Angello
    Advanced Fossil Power Systems Dept.
    3412 Hillview Avenue
    P. O. Box 10412
    Palo Alto, CA 94303

12. Garrett Turbine Engine Company — 1
    A Division of the Garrett Corporation
    Attn: J. Sanborn
    111 S. 34th St., P. O. Box 5217
    Phoenix, AZ 85010

13. Garrett Turbine Engine Company — 1
    A Division of the Garrett Corporation
    Attn: Library
    111 S. 34th ST., P. O. Box 5217
    Phoenix, AZ 85010

14. Garrett Turbine Engine Company — 1
    A Division of the Garrett Corporation
    Attn: T. W. Bruce
    111 S. 34th St., P. O. Box 5217
    Phoenix, AZ 85010

15. General Applied Science Laboratories — 1
    Attn: G. Roffe
    Merrick and Stewart Avenue
    Westbury, NY 11590

16. Ex-Cello-O Corporation — 1
    Attn: T. Koblish
    850 Ladd Road
    Box 700
    Walled Lake, MI 48088

17. General Electric Company — 1
    Attn: L. Morton
    Main Combustor Design
    1000 Western Avenue
    Lynn, MA 24067

18. General Electric Company — 1
    Attn: Library
    Gas Turbine Engineering Department
    One River Road NO. 53-234
    Schenectady, NY 12345

Industry (Cont'd)

19. Northern Research & Engineering Corp. 1
    Attn: Library
    39 Olympia Avenue
    Woburn, MA 01801

20. Parker Hannifin Corp. 1
    Attn: H. Simmons
    17325 Euclid Avenue
    Cleveland, Oh 44112

*21. Solar Turbines Incorporated 1
    Attn: D. Rohy
    P. O. Box 80966
    San Diego, CA 92138

22. Rolls-Royce, Inc. 1
    Attn: A. Veninger
    1895 Phoenix Boulevard
    Atlanta, GA 30349

23. Teledyne CAE 1
    Attn: Library
    1330 Laskey Road
    Toledo, OH 43697

24. United Technologies Corporation 1
    Attn: H. Craig
    Pratt & Whitney Aircraft Group
    Commercial Engineering Business
    400 Main Street
    East Hartford, CT 06108

25. United Technologies Corporation 1
    Attn: R. Marshall
    Pratt & Whitney Aircraft Group
    Commercial Engineering Business
    400 Main Street
    East Hartford, CT 06108

26. United Technologies Corporation 1
    Attn: R. Lohmann
    Pratt & Whitney Aircraft Group
    Commercial Engineering Business
    400 Main Street
    East Hartford, CT 06108

27. United Technologies Corporation 1
    Attn: Library
    Pratt & Whitney Aircraft Group
    Commercial Engineering Business
    400 Main Street
    East Hartford, CT 06108

Industry (Cont'd)

28. United Technologies Corporation — 1
    Attn: A. Masters
    Pratt & Whitney
    Government Engine Business
    Box 2691
    West Palm Beach, FL 33402

29. United Technologies Corporation — 1
    Attn: T. Dubell
    Pratt & Whitney
    Government Engine Business
    Box 2691
    West Palm Beach, FL 33402

30. United Technologies Corporation — 1
    Attn: Library
    Pratt & Whitney
    Government Engine Business
    Box 2691
    West Palm Beach, FL 33402

31. United Technologies Research Center — 1
    Attn: R. Pelmas
    Aero-Thermal Tehcnology
    Silver Lane
    East Hartford, CT 06108

32. United Technologies Research Center — 1
    Attn: Library
    Silver Lane
    East Hartford, CT 06108

33. Westinghouse Electric Corporation — 1
    Attn: Library
    Gas Turbine Systems Division
    Lester Branch
    Box 9175
    Philadelphia, PA 19113

*34. Westinghouse Electric Corporation — 1
    Attn: R. Chamberlain
    Research and Development Center
    Pittsburgh, PA 15235

35. Westinghouse Electric Corporation — 1
    Attn: Library
    Research and Development Center
    Pittsburgh, PA 15235

*36. Williams International Corporation — 1
    Attn: M. Bak
    2280 West Maple
    Walled Lake, MI 48088

37. Yojna Incorporated — 1
Attn: A. Modak
22 Standish Road
Watertown, MA 02172

38. Sol-3 Resources Inc. — 1
Attn: J. Melconian
76 Reaver Road
Reading, MA 01867

39. Science Applications, Inc. — 1
Attn: R. Edelman
9760 Owensmouth Avenue
Chatsworth, CA 91311

40. General Electric Company — 1
Attn: D. Bahr K-64
Aircaraft Engine Group
Evandale, OH 45215

41. General Electric Company — 1
Attn: E. Ekstedt K-64
Aircraft Engine Group
Evandale, OH 45215

42. General Electric Company — 1
Attn: Tech. Info. Center N-64
Aircraft Engine Group
Evandale, OH 45215

43. General Electric Company — 1
Attn: W. Dodds, K-64
Aircraft Engine Group
Evandale, OH 45215

1.REPORT NO. NASA CR -	2. GOVERNMENT ACCESSION NO.	3.RECIPIENT'S CATALOG NO.
4.TITLE AND SUBTITLE Broad Specification Fuel Combustion Technology Program Phase II		5. REPORT DATE October 1990 6. PERFORMING ORG. CODE
7.AUTHOR(S) R. P. Lohmann, R. A. Jeroszko, and J. B. Kennedy		8. PERFORMING ORG. REPT. NO.
9.PERFORMING ORGANIZATION NAME AND ADDRESS UNITED TECHNOLOGIES CORPORATION Pratt & Whitney Commercial Engine Business		10. WORK UNIT NO. 11. CONTRACT OR GRANT NO. NAS3-23269
12. SPONSORING AGENCY NAME AND ADDRESS National Aeronautics and Space Administration Lewis Research Center 21000 Brookpark Road, Cleveland, Ohio 44135		13.TYPE REPT / PERIOD COVERED Contractor Report Final 14. SPONSORING AGENCY CODE

15. SUPPLEMENTARY NOTES
Project Manager, James S. Fear, Aerothermodynamics and Fuel Division, NASA Lewis Research Center.

16. ABSTRACT

An experimental evaluation of two advanced technology combustor concepts was conducted to evolve and assess their capability for operation on broadened properties fuels. The concepts were based on the results of Phase I of the Broad Specification Fuel Combustor Technology Program which indicated that combustors with variable geometry or staged combustion zones had a flexibility of operation that could facilitate operation on these fuels. Emphasis in defining these concepts included the use of single pipe as opposed to duplex or staged fuels systems to avoid the risk of coking associated with the reduction in thermal stability expected in broadened properties fuels. The first concept was a variable geometry combustor in which the airflow into the primary zone could be altered through valves on the front while the second was an outgrowth of the staged Vorbix combustor, evolved under the NASA/P&W ECCP and EEE programs, incorporating simplified fuel and air introduction. The results of the investigation, which involved the use of Experimental Referee Broad Specification (ERBS) fuel, indicated that in the form initially conceived, both of these combustor concepts were deficient in performance relative to many of the program goals for performance emissions. However, variations of both combustors were evaluated that incorporated features to simulate conceptual enhancement to demonstrate the long range potential of the combustor. In both cases, significant improvements relative to the program goals were observed.

17. KEY WORDS (SUGGESTED BY AUTHOR(S) Combustion, ERBS fuel, Turbofan Engine, Variable Geometry	18. DISTRIBUTION STATEMENT		
19. SECURITY CLASS THIS (REPT) Unclassified	20. SECURITY CLASS THIS (PAGE) Unclassified	21. NO. PGS	22. PRICE *